COO-4196-3

ENERGY CONSERVATION IN COAL CONVERSION

Selected Case Studies and Conservation Methodologies

Final Report for September 15, 1977—September 1, 1978

By
J. C. Purcupile

September 1978

Work Performed Under Contract No. EY-77-S-02-4196

Carnegie—Mellon University
Pittsburgh, Pennsylvania

U. S. DEPARTMENT OF ENERGY

DISCLAIMER

NOTICE

COO-4196-3
Distribution Category UC-89

ENERGY CONSERVATION IN COAL CONVERSION

FINAL REPORT

September 15, 1977 - September 1, 1978

Selected Case Studies and Conservation Methodologies

Principle Investigator:

J. C. Purcupile

Carnegie-Mellon University
Pittsburgh, PA 15213

September, 1978

Prepared for

THE U.S. DEPARTMENT OF ENERGY
Pittsburgh Energy Technology Center
UNDER CONTRACT NO. EY77S024196

ACKNOWLEDGEMENT

We would like to thank Bill Peters and Tom Ruppel of the Pittsburgh Energy Technology Center and T. S. Govindan of the DuPont Company for their interest and assistance in preparing these reports.

TABLE OF CONTENTS

LIST OF FIGURES

EXECUTIVE SUMMARY

INTRODUCTION

The purpose of this study is to apply the methodologies developed in the Energy Conservation in Coal Conversion August, 1977 Progress Report - Contract No. EY77S024196 - to an energy efficient, near-term coal conversion process design, and to develop additional, general techniques for studying energy conservation and utilization in coal conversion processes.

The process selected for study was the Ralph M. Parsons Company of Pasadena, California "Oil/Gas Complex, Conceptual Design/Economic Analysis" as described in R & D Report No. 114 - Interim Report No. 4, published March, 1977, ERDA Contract No. E(49-18)-1975. This process was chosen because:

1) A primary design objective was energy efficiency, which resulted in a plant thermal efficiency of 77%.
2) We had access to most of the needed data.
3) This design is included in the Department of Energy's coal synthetic fuels demonstration plant accelerated program.

Inspite of the high overall thermal efficiency of this design, our studies reveal areas where significant amounts of energy may be conserved or utilized in a more cost effective manner.

I - Coal Conversion Process Selection

A number of processes were examined as candidates for this study. The Ralph M. Parsons Oil/Gas Complex was chosen because:

1) A primary emphasis was placed on maximizing the energy efficiency of the process.
2) This design is included in the Coal Synthetic Fuels Demonstration Plant Accelerated Program.
3) We had access to the design data.

II - Method for Computing the Optimum Economic Pipe Diameter for Newtonian Fluids

A closed form relation is presented for calculating the diameter of a pipe line which yields the minimum life-cycle cost for a wide range of parameters and operating conditions.

A central consideration in the derivation of the relation is that the optimum diameter should reflect the energy costs for overcoming friction losses.

Diameters from the method presented here are compared with a relation developed by DuPont Co. The mean absolute percent difference between the two methods is less than 19%, with the method outlined here yielding larger diameters than the DuPont relation.

III - Energy Conservation Potential in Heat Recovery Techniques - A Case Study

In this study, we looked at replacing certain heat exchangers with Organic Rankine Cycles. In each case, we determined the cost of

generating power and then from this tabulation of capital investment for power generation, feasibility of replacement on a unit-by-unit basis was determined.

The results show that 18 heat exchangers reject sufficient heat to warrant ORC usage, with potential electric generation of 36 MW which is 17% of the 210 MW generated in the Oil/Gas Complex.

Cost estimates indicate the capital investment required to be approximately $1000/KW with a potential reduction to $300/KW for mass produced units.

IV - Alternate De-Ethanizer Refrigeration System to Conserve Energy - A Case Study

This study examines an alternate system to cool an ethane gas stream from the fractionator in Unit 18 of Parsons Oil/Gas Complex. This alternate will save 2.6×10^5 Btu/hr of energy or .25 short TPD of coal out of 36,000 TPD used in the Oil/Gas Complex, at an installed cost of $151,000 with an operation and maintenance cost of $7550/yr. Assuming a 20-year life, 9% interest rate on borrowed capital, and an electricity cost of $.025/KW-hr, the Life Cycle Cost (LCC) of the new system is $179,000 over a 20-year period. Using a Discounted Cash Flow Analysis the Return on Investment is 0%.

V - Feasibility Study of A Combined Combustion - Gasification Facility

This work examined the feasibility of mechanical deep cleaning of coal where the cleaned coal would be used for direct combustion and the rejected portion would be used in a coal gasification plant. To

make this feasible, the reduced thermal efficiency from gasifying "dirty coal" must be offset by the reduced energy requirement for the flue gas desulfurization system.

Our study indicated, for the coal being considered for the Parsons Oil/Gas Complex - Illinois No. 6 - the energy saved by reduced flue gas desulfurization was approximately equal to the energy lost from gasifying the dirty coal. The methodology for this study is presented in such a way that other coals - particularly a high pyritic sulfur content - could be studied.

VI - High Pressure Steam Generation from Heat Recovery Boilers

This section develops a methodology for calculating and evaluating the increased work potential possible from high pressure steam generation in waste heat boilers. This methodology is applied to the Ralph M. Parsons' commercial concept of the Oil/Gas Complex. Implementation of the proposed scheme would result in an export power increase of 7.7 MW which is a 4% increase of the 210 MW generated in the complex at a cost of $2110/KW.

VII - Combined Cycle In-Plant Electrical Power Generation

A combined cycle power generation scheme for the Oil/Gas Complex was studied as an alternate to the steam turbine power generation system to see if energy can be saved in a cost effective way. The combined cycle generates an excess of 22.2 MW of electricity or a 10.6% increase of the 210 MW generated in the Oil/Gas Complex at a cost of $610/KW. If electricity is exported at $.025/KW-hr, a rate of return on the additional capital

investment of 19% is realized. Using present state-of-the-art equipment, the combined cycle is a cost effective way to better utilize energy.

VIII - Direct Coal Fired Steam Generation in Lieu of Low Btu Gas

This section examined the feasibility of replacing the low Btu gas fired power generating system with a direct coal fired power generating system, in which 48,000 lb/hr of coal would be saved which is 1.6% of the total 36,000 TPD used in the Oil/Gas Complex. The difference in installed cost between the direct coal fired system and the gas fired power generation system is 36.4 million dollars. The rate of return on the additional capital cost for the coal-fired system is 8.21%. The life cycle cost is -4.4 million dollars over a 20-year life with capital borrowed at 9% interest.

IX - Alternate Acid Gas Removal Study

To reduce the reboiler steam required, we studied replacing the MEA (monoethanolamine) system proposed by the Ralph M. Parsons Co. with a DEA (diethanolamine) acid gas removal system. Steam consumption is reduced by 16,000 lbm/hr which is 1 % of the total steam generated in the Oil/Gas Complex or $317,000 per year. In addition, there is an annual savings of $88,000 for chemicals. The additional capital costs and operating expenses for the DEA system are negligible since the process plants are equivalent. It is therefore recommended that a DEA system replace the MEA system as Process Unit 17 of the Oil/Gas Complex.

X - The Thermodynamic Performance of Two Combined Cycle Power Plants Integrated with Two Coal Gasification Systems

Sections from a Ph.D. thesis present in summary, a thermodynamic treatment of four integrated coal gasification and combined power plants with the aim of studying the effects of component optimization, and emissions of NO_x and H_2S on cycle performance.

A combined cycle station efficiency of 36.67% results from the best plant configuration when allowable emmissions are met, and 10% of the electrical power generation is subtracted from the net work out. For a rankine cycle, the efficiency is 35%, when compared on an equal basis.

XI - Energy Conservation Potential in Shaft Power Generation and Distribution

A criteria for determining the most energy efficient horsepower break-point for using electric motors or steam turbines is developed and applied to the prime movers in the Ralph M. Parsons Co. Oil/Gas Complex. No significant amount of energy can be saved, since the electric motor turbine break-point established by Ralph M. Parsons Co. coincides with the criteria developed in this study.

XII - Basis for Fuel and Utility Costs

A common basis for fuel and utility costs is used throughout the sections in this study. FEA energy price projections for Region V (Michigan, Ohio, Indiana, Wisconsion, Minnesota, Illinois) and averaged prices from other sources are used.

XIII - Using Second Law Analysis to Pinpoint Inefficiencies in Coal Conversion Processes

A second law analysis is performed on the Fischer-Tropsch complex designed by the Ralph M. Parsons Company, to locate areas of energy inefficiency. The complex has an overall first law efficiency of 70% and a second law efficiency of 68.7%. Two areas in the complex where efficiencies could be improved are: unit 14, acid gas removal, and unit 21, sulfur recovery, which have second law efficiencies of 80.2% and 66.4% respectively. The other process units of the plant had efficiencies greater than 87%, indicating energy recovery and conservation techniques had been implemented in the design of the complex.

OIL/GAS PLANT DESCRIPTION

The Ralph M. Parsons Oil/Gas Complex is a coal conversion facility designed to use high-sulfur coal and convert it to SNG (substitute natural gas), LPGs (liquified petroleum gases), fuel oil and naphtha using hydroliquifaction technology. The industrial complex consists of a large captive coal mine that produces 47,000 tons per day (TPD) of run-of-mine coal which is supplied to a coal preparation plant, which in turn supplies 36,000 TPD of clean, washed coal with a heating value of 12,125 Btu/lb. Along with the above mentioned products, the plant produces by-products of ammonia and sulfur. All electricity and steam required for the Oil/Gas Complex are generated within the plant, therefore, the input to the plant is coal, oxygen and water. The overall material balance is shown on Figure 1 and the energy balance is shown on Figure 2. The estimated fixed capital investment is $1.25 billion; this figure is based on fourth quarter 1975 dollars.

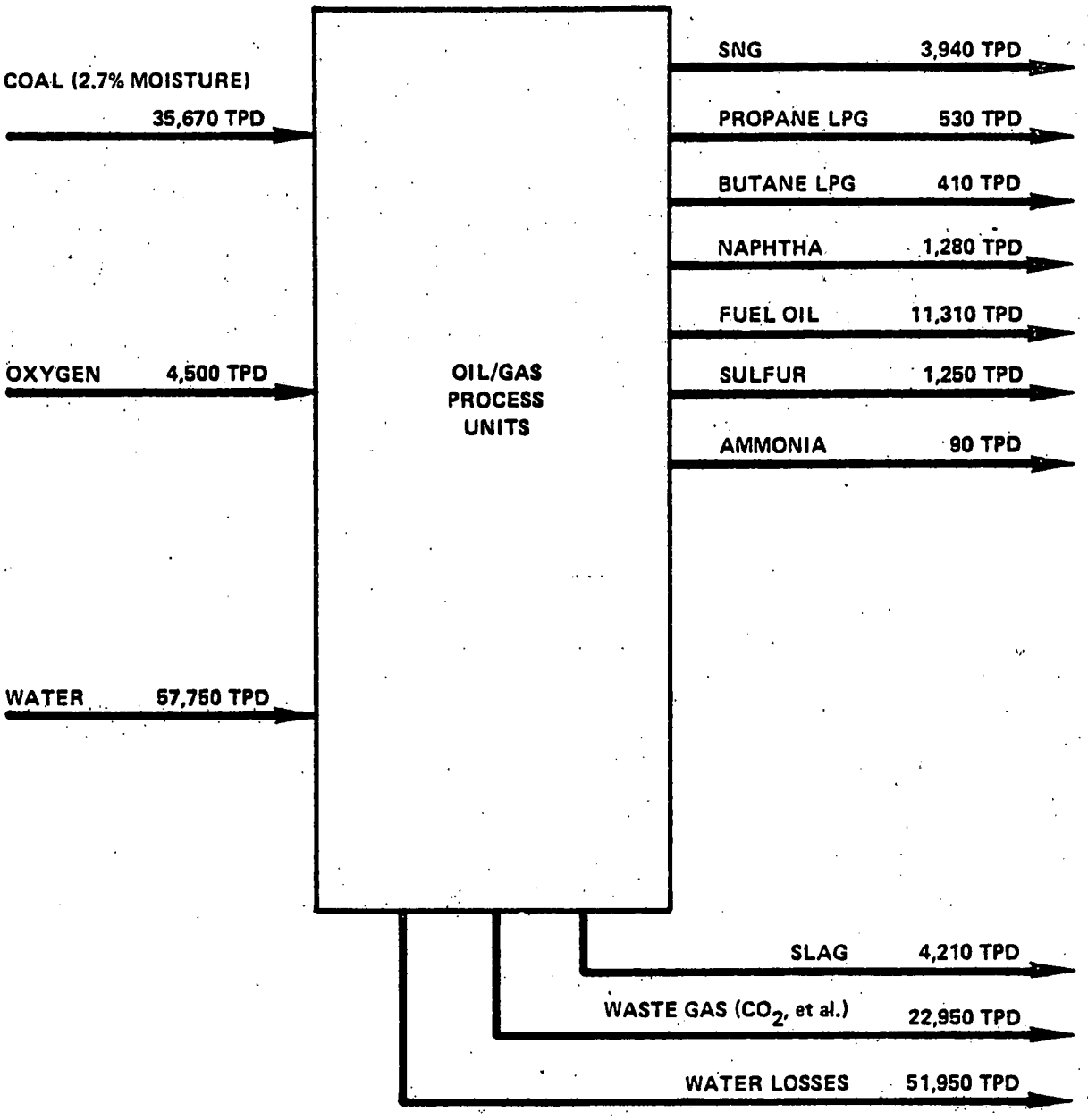

TOTAL IN = OUT 97,920 TPD

ALL FIGURES IN SHORT TONS

FIGURE 1

Overall Material Balance

Reproduced from R & D Report No. 114 - Interim Report No. 4 by The Ralph M. Parsons Company

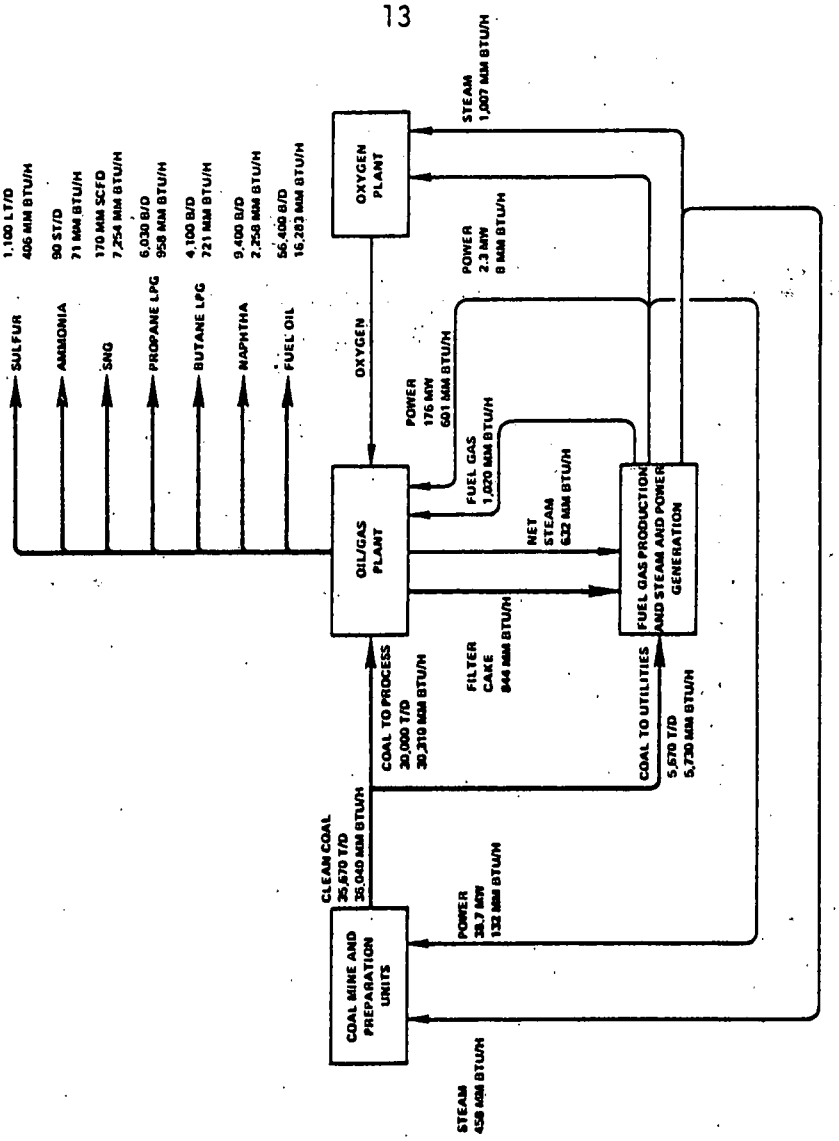

COAL ENERGY DISTRIBUTION

STREAM	MM BTU/H	% CLEAN COAL
FEEDS		
COAL TO PROCESS	30,310	84.1
COAL TO UTILITIES	5,730	15.9
TOTAL	35,040	100.0
PROCESS COAL YIELDS		
SALEABLE PRODUCTS	27,951	77.8
FILTER CAKE	844	2.3
REACTION HEATS	1,515	4.2
TOTAL	30,310	84.1

UTILITY ENERGY DISTRIBUTION

STREAM	MM BTU/H	% CLEAN COAL
INPUTS		
COAL	5,730	15.9
FILTER CAKE	844	2.3
STEAM	632	1.8
TOTAL	7,206	20.0
OUTPUTS		
TO MINING AND PREPARATION		
STEAM	458	1.3
POWER	132	0.4
TOTAL	590	1.7
TO OXYGEN PLANT		
STEAM	1,007	2.8
POWER	8	-
TOTAL	1,015	2.8
TO OIL/GAS PLANT		
POWER	601	1.7
FUEL GAS	1,020	2.8
TOTAL	1,621	4.5
LOSSES TO		
ATMOSPHERE	3,980	11.0
TOTAL	7,206	20.0

FIGURE 2

Energy Balance

Reproduced from R & D Report No. 114 - Interim Report No. 4 by the Ralph M. Parsons Company.

2 ENERGY CONSERVATION IN COAL CONVERSION

1 Coal Conversion Process Selection

R. G. McMillin

Carnegie-Mellon University
Pittsburgh, PA 15213

June, 1978

Prepared for

THE U.S. DEPARTMENT OF ENERGY
Pittsburgh Energy Technology Center
UNDER CONTRACT NO. EY77S024196

TABLE OF CONTENTS

SELECTION PROCESS

Our initial studies on energy conservation in coal conversion were performed by investigating the commercial concept design of the PETC Synthane Process. These studies developed methodologies that can be used to conserve energy in other coal conversion processes. The next step was to select another process where our methods could be applied.

The following table is a summary of the processes that we examined and the reasons listed in the remarks column were used to screen the systems. Both the Fischer Tropsch and the SRC II were acceptable systems to study and we arbitrarily chose the SRC II system for further study.

PROCESS	DEVELOPER	CLASSIFICATION	REJECTED:	REMARKS
Lurgi	Lurgi	Low btu	Yes	Powerton project in Illinois is oriented towards system integration, and of proprietary nature.
Coalcon	Coalcon Co.	Multi	Yes	Plans for a four phase project to construct a 2,600 TPD plant have been cancelled. Accelerated Program Candidate
Coalgas			Yes	In initial design stage.
Koppers-Totzek	Heinrich Koppers GmbH	Low btu	Yes	Proprietary
Koppers-Totzek	Heinrich Koppers GmbH	High btu	Yes	Proprietary
CO_2 Acceptor	Consolidated Coal Co.	High btu	Yes	Design developed for comparing various process. Energy conservation was not a design criterion.
Bi-Gas	Bituminous Coal Res.,Inc.	High btu	Yes	Energy conservation not a design criterion.
Hygas	Institute of Gas Technology	High btu	Yes	Energy conservation not a design criterion. Accelerated Program Candidate.
Fischer-Tropsch	Fischer Tropsch	Multi	Yes	Developed with energy conservation as a design criterion. Accelerated Program Candidate - see discussion.

TABLE 1

PROCESS	DEVELOPER	CLASSIFICATION	REJECTED	REMARKS
SRC II	ERDA	Multi	No	The oil/gas complex is an Accelerated Program Candiate. Developed with energy conservation as a design criterion.
Wellman-Galusha	Wellman-Galusha	High btu	Yes	No large-scale plans available.
Air Products & Chemicals	Air Products & Chemicals	Low btu	Yes	Initial design stage.
Wellman	Land O' Lakes Applied Technology	Low btu	Yes	Pilot plant.
Woodhall-Duckham	Holly Kennyshot	Low btu	Yes	Pilot plant.
Wellman-Galusha	Mason Hanger	Low btu	Yes	Pilot plant.
Stoic 2 stage	Foster-Wheeler-Univ. Minnesota (Duluth)	Low btu	Yes	Pilot plant.

TABLE 1

Processes that weren't immediately rejected because of a lack of size in the scale of the conceptual designs or lack of development were then followed-up with conversations with the process developer, sponsor, or engineering subcontractor.

The conversations with various developers led to meetings with Raymond L. Zahradnik, former Director of the Division of Coal Conversion and Utilization with ERDA. Following Dr. Zahradnik's suggestion, a meeting with Neal Cochran, who served as Senior Technical Advisor on several coal conversion conceptual design analyses, followed.

Neal Cochran provided us with documents describing the proposal for the Coal Synthetic Fuels Demonstration Plant Accelerated Program. The primary objective of the proposed Accelerated Program is to reduce the time required to achieve readiness of broad spectrum coal conversion process by increasing the level of government involvement. Developments and improvements in coal conversion processes have reached the stage where commercial-scale demonstration facilities must be constructed to establish the environmental acceptability of those processes that have the best chance of eventually achieving a competitive cost. The proposed program includes those processes indicated in the table.

The Oil/Gas Conceptual Design/Economic Analysis utilizes the SRC II process. This conceptual design developed by Ralph M. Parsons Company is for a commercial scale oil/gas coal conversion complex. The Accelerated Program chose this process as a candidate because it is capable of handling all coal ranks and does not require a reaction catalyst or a solid-liquid filtration train. Additionally, it is capable of accepting product slate modifications in response to changes in the market picture.

For these reasons, and because an extensive effort has been made to maximize the thermal efficiency of the complex, plus the ease of accessibility concerning the design, it has been selected as the process that we examined in this report.

2 ENERGY CONSERVATION IN COAL CONVERSION

1 Method for Computing the Optimum Economic Pipe Diameter for Newtonian Fluids

R. Kramek

Carnegie-Mellon University
Pittsburgh, PA 15213

June, 1978

Prepared for

THE U.S. DEPARTMENT OF ENERGY
Pittsburgh Energy Technology Center
UNDER CONTRACT NO. EY77S024196

TABLE OF CONTENTS

LIST OF TABLES

LIST OF FIGURES

ABSTRACT

A closed form relation is presented for calculating the diameter of a pipe line which yields the minimum life-cycle cost for a wide range of fluid parameters and operating conditions.

A central consideration in the derivation of the relation is that the optimum diameter should reflect the energy costs for overcoming friction losses.

Diameters from the method presented here are compared with a relation developed by DuPont Co. The mean absolute percent difference between the two methods is less than 19%, with the method outlined here yielding larger diameters than the DuPont relation. A 19% increase in diameter represents a 58% decrease in the pumping power required to overcome friction losses.

INTRODUCTION

As the cost of energy and materials continues to increase, more attention is being devoted to optimization methods in a wide range of engineering design problems. A problem amenable to optimization occurs in the selection of a pipe diameter for a flowing fluid, where increasing the pipe diameter decreases the friction losses, hence energy costs, but increases the labor and capital costs. Although a number of constraints such as erosion limitations, allowable pressure drop, process control and compressible flow may dictate the selection of the diameter in a particular situation, there are many cases where the diameter can be optimized for a given set of fluid parameters, and costs.

This section presents a method for calculating the pipe diameter which yields the minimum life cycle cost of a pipe-line for a given set of parameters. A central consideration in the development of this method was that the optimum diameter should reflect the cost of energy required for pumping the fluid. In addition, this method is quite general, and encompasses a wide range of fluid parameters, and operating conditions, since most of the methods for computing the optimum diameter found in the literature[1,2,3,4,5] were restricted to either specific flow regimes, narrow ranges of viscosities, operating temperatures, pressures, or piping materials. The significant parameters for computing the optimum economic diameter are: mass flow rate, fluid viscosity, fluid density, operating pressure, operating temperature, cost of electricity, cost of labor, return on investment, project life, percent utilization, piping material costs, and pump and motor efficiency.

Since the economics are based on a per unit length basis, the length of the piping is not in the list of parameters.

A closed form solution for the optimum economic diameter is derived and has been correlated with a software program which computes the optimum diameter as a function of the parameters above. Optimum pipe diameters for a range of parameters were compared with diameters computed from a well-known relation developed by DuPont.

DEVELOPMENT OF THE METHOD FOR COMPUTING THE OPTIMUM DIAMETER

To find the optimum diameter, it is first necessary to determine how much capital investment in increased pipe cost is justified to save a unit of power. Using the internal rate of return analysis (or discounted cash flow method), the sum of the present values of all cash flows associated with a given project plus the salvage value, is equal to the initial capital investment. This can be expressed as:

$$C = \sum_{n=1}^{N} \frac{CF_n}{(1 + i)^n} \qquad (1)$$

where:

C = capital investment, $/KW

i = rate of return, fractional

N = economic life, years

CF_n = net cash flow for any year, n, $/KW.

The factor $\frac{1}{(1 + i)^n}$ transforms each cash flow to its value at time zero.

The net cash flow for year n is defined as the savings resulting from a reduction in purchased electricity minus the operation and maintenance costs. This is expressed as:

$$CF_n = CE_n - CO_n - CM_n \qquad (2)$$

where:

CF_n = net cash flow for year n, $/KW

CE_n = cost of electricity saved for year n, \$/KW

CO_n = operating costs for year n, \$/KW

CM_n = maintenance costs for year n, \$/KW

The cost of electricity saved for year n is:

$$CE_n = CE \times U \times 8760$$

where:

CE = cost of electricity, \$/KW-hr

U = period of operation per year, fractional

We assume that the cash flows are uniform, so (1) can be written using the present worth factor, PW:

$$C = PW(CE_n - CO_n - CM_n) \tag{3}$$

It is assumed that the difference in operation and maintenance costs for an incremental change in diameter are negligible, and there is no salvage value. Therefore, (3) becomes:

$$C = PW(CE_n) \tag{4}$$

This relation is illustrated in Figure 1.

Once the justified capital investment is determined for any given operating life, return on investment, price of electricity, and utilization factor, the optimum diameter is that diameter where the ratio of the incremental pipe cost to the incremental power lost due to friction

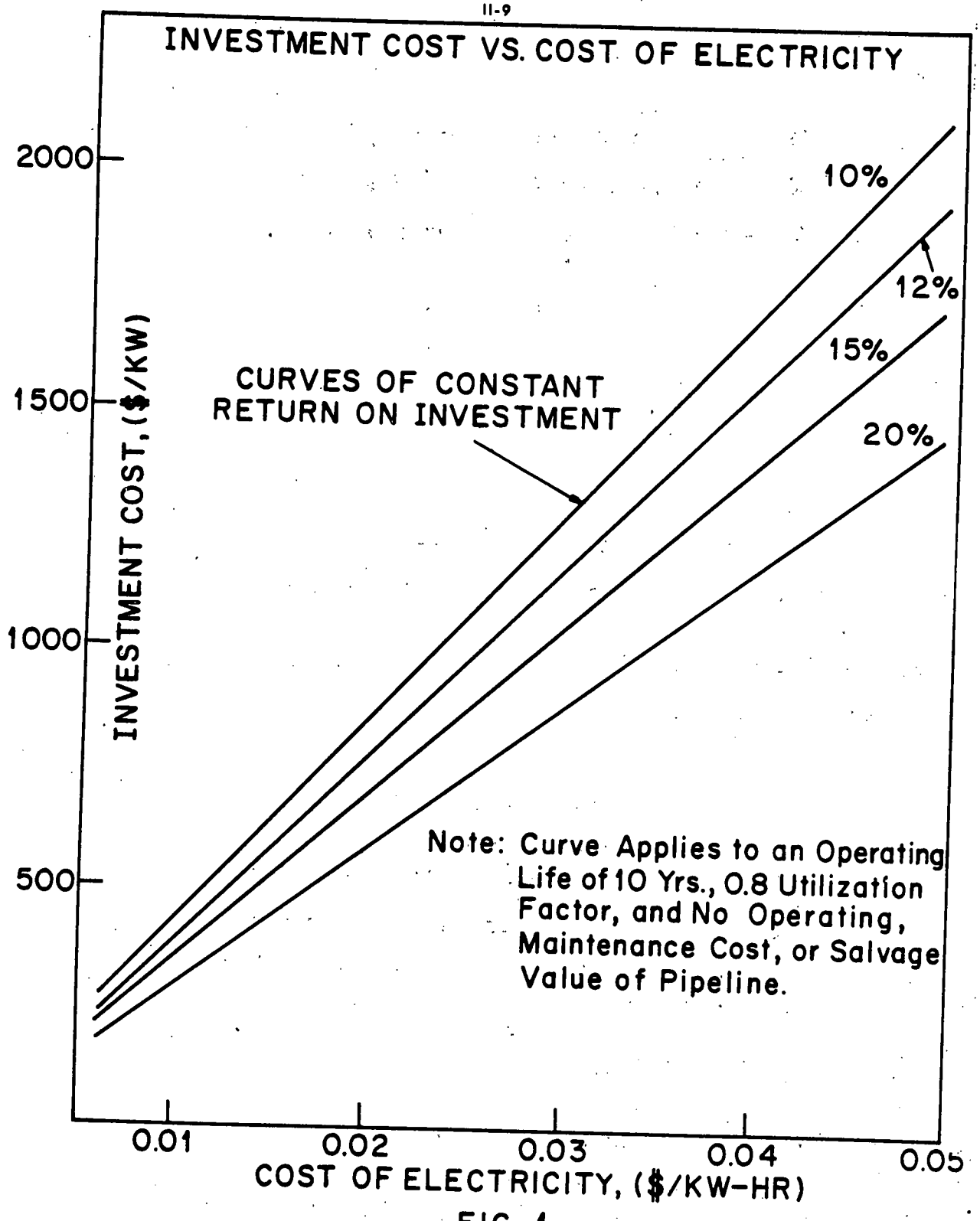
INVESTMENT COST VS. COST OF ELECTRICITY
2000
1500
1000
500
INVESTMENT COST, ($/KW)
10%
12%
15%
20%
CURVES OF CONSTANT
RETURN ON INVESTMENT
Note: Curve Applies to an Operating Life of 10 Yrs., 0.8 Utilization Factor, and No Operating, Maintenance Cost, or Salvage Value of Pipeline.
0.01
0.02
0.03
0.04
0.05
COST OF ELECTRICITY, ($/KW-HR)

FIG. 1

equals the amount of capital investment justified to save a unit of power. Mathematically,

$$C = \frac{\Delta P_c}{\Delta P_f} = \frac{\partial P_c}{\partial D} \Delta D \div \frac{\partial P_f}{\partial D} \Delta D \qquad (5)$$

where:

$\frac{\partial P_c}{\partial D} \Delta D$ is the incremental pipe cost, ΔP_c ($/Ft)

$\frac{\partial P_f}{\partial D} \Delta D$ is the incremental power loss, ΔP_f (KW/Ft)

C is the capital investment justified to save a unit of power, ($/KW)

The above expressions are illustrated graphically in Figures 2 and 3. Figure 2 depicts pumping power and pipe cost as a function of diameter. Note that the pumping power decreases inversely to the fifth power of the diameter, whereas, the pipe cost increases linearly with diameter. The ratio of incremental pipe cost to incremental pumping power is the capital investment justified to save a unit of power. A plot of the ratio of incremental pipe cost to incremental power consumption versus diameter for a flow of 6,000 gallons per minute of water is shown in Figure 3. If $100.00 can be invested to save a kilowatt, it can be seen that the optimum economic diameter is 14.5 inches, while if C = 1000 $/KW can be invested, the optimum diameter is 21 inches.

From the derivation given in Appendix A, the closed form expression relating the significant variable to the optimum diameter is:

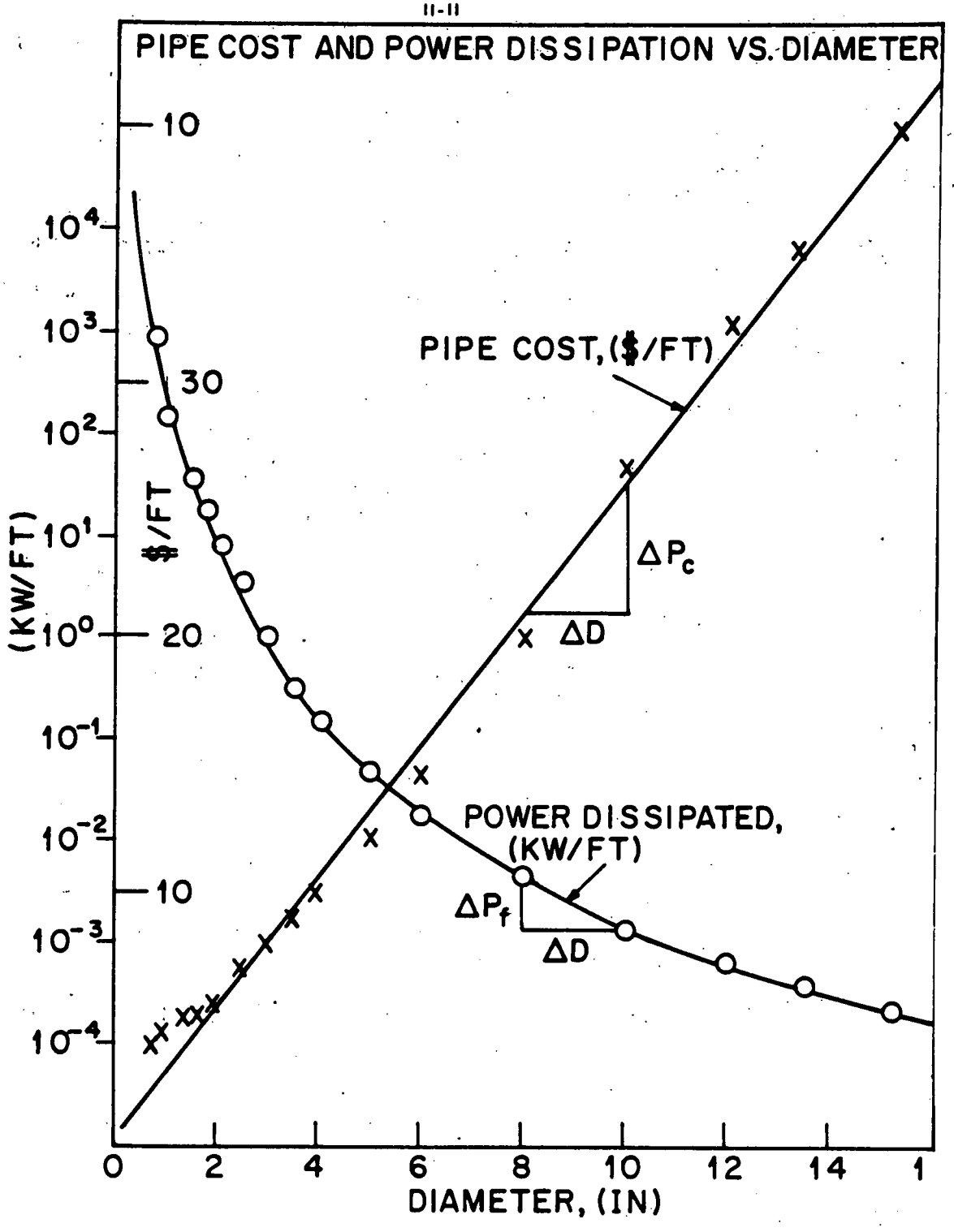
PIPE COST AND POWER DISSIPATION VS. DIAMETER
PIPE COST, ($/FT)
POWER DISSIPATED, (KW/FT)
$/FT
(KW/FT)
DIAMETER, (IN)
ΔP_c
ΔD
ΔP_f
ΔD
10
30
20
10
10^4
10^3
10^2
10^1
10^0
10^-1
10^-2
10^-3
10^-4
0
2
4
6
8
10
12
14

FIG. 2

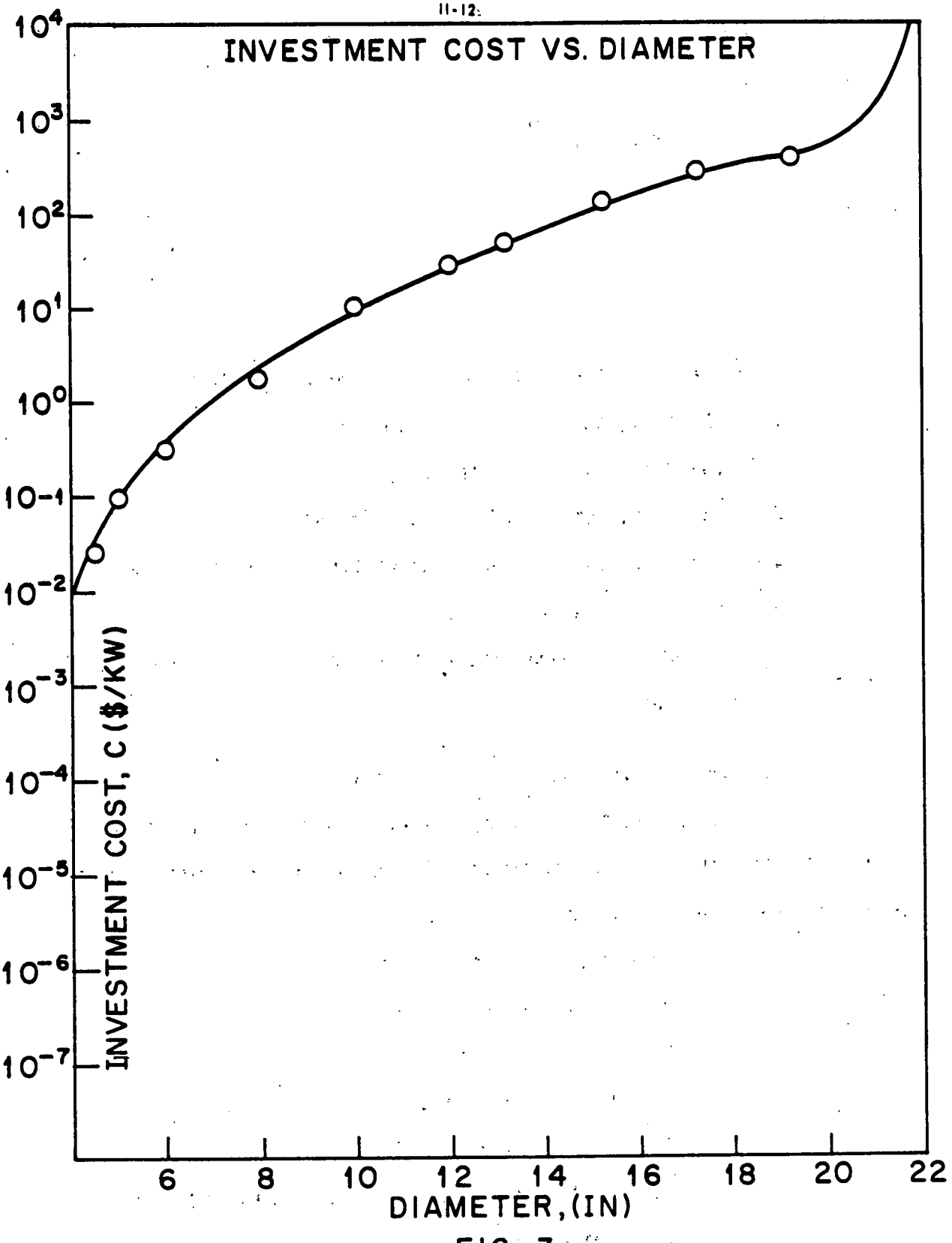
INVESTMENT COST VS. DIAMETER
INVESTMENT COST, C ($/KW)
10^{4}
10^{3}
10^{2}
10^{1}
10^{0}
10-1
10^{-2}
10^{-3}
10^{-4}
10^{-5}
10^{-6}
10^{-7}
6
8
10
12
14
16
18
20
22
DIAMETER, (IN)

FIG. 3

$$D/D_o = a_1 \gamma^{a_2}$$

where:

$$\gamma = 2.63 \times 10^{-13} \, Cfw^3/EC_p b\rho^2 \qquad (6)$$

and,

C is the capital cost to save a unit of power, \$/KW

f is the friction factor, dimensionless

w is the mass flow rate, lbm/hr

C_p is the pipe cost coefficient, \$/ft-in^2

b relates allowable stress to temperature, dimensionless

ρ is the fluid density, lbm/ft^3

E is the combined pump and motor efficiency, fractional

D_o is the unit diameter, one in.

The complete derivation of γ is given in Appendix A.

To compute the constants a_1 and a_2, a least squares linear regression of γ on D/D_o was performed. The values of D/D_o were computed by a software program with the inputs of:

1. mass flow rate
2. fluid viscosity
3. fluid density
4. operating pressure
5. cost of labor
6. capital investment to save a unit of power
7. piping material
8. pump and motor efficiency.

The program begins at an initial diameter of .5 inches and increments upwards in standard diameters, computing the incremental pipe cost and power consumed in going from one diameter to the next. When the ratio of incremental pipe cost to incremental power consumption is equal to the inputted capital cost to save a unit of power, the optimum diameter is found. A listing of the software program is given in Appendix C.

For the values of parameters in Table 1, 275 optimum diameters were computed by the software program, and the least squares linear regression yielded the constants:

$$a_1 = 2.4$$

$$a_2 = .179$$

giving the expression:

$$D/D_o = 2.4\ \gamma^{.179} \tag{7}$$

The correlation coefficient for the 275 diameters is $r = .94$

γ versus D/D_o is presented in Figure 4.

TABLE 1

PARAMETER INPUTS FOR COMPUTER RUNS

RUN 1	RUN 2
Carbon Steel	Carbon Steel
ρ = .075 lbm/ft^3	ρ = 62.5 lbm/ft^3
T = 300°F	T = 300°F
P = 500 psi	P = 500 psi
μ = .02 cp	μ = 1.0 cp
W = 1000 lbm/hr	W = 10,000 lbm/hr
10,000 lbm/hr	15,000 lbm/hr
15,000 lbm/hr	30,000 lbm/hr
30,000 lbm/hr	60,000 lbm/hr
60,000 lbm/hr	120,000 lbm/hr
C = 100 $/KW (.0025 $/KW-hr)*	250,000 lbm/hr
500 (.0126)	500,000 lbm/hr
1000 (.0253)	750,000 lbm/hr
1500 (.0379)	1,000,000 lbm/hr
2000 (.0505)	3,000,000 lbm/hr
C_L = 13.00 $/MH	4,500,000 lbm/hr
E = .7	C = 100
	500
	1000
	1500
	2000
	C_L = 13.00
	E = .7

* For the computer runs, C is related to $/KW-hr by equation (4), with 12% return on investment over a 10-year operating life, and .8 utilization factor.

TABLE 1 (cont.)

RUN 3	RUN 4	RUN 5	RUN 6
Carbon Steel	Carbon Steel	304L S.S.	Carbon Steel
ρ = 62.5 lbm/ft^3	ρ = 62.5 lbm/ft^3	ρ = 62.5 lbm/ft^3	ρ = 62.5 lbm/ft^3
T = 300°F	T = 300°F	T = 300°F	T = 700°F
P = 500 psi	P = 500 psi	P = 500 psi	P = 1000 psi
μ = 100 cp	μ = 1000 cp	μ = 1 cp	μ = 1 cp
W = same as Run 2	W = same as Run 2	W = same as Run 2	W = same as Run 2
C = same as Run 2	C = same as Run 2	C = same as Run 2	C = same as Run 2
E = .7	E = .7	E = .7	E = .7

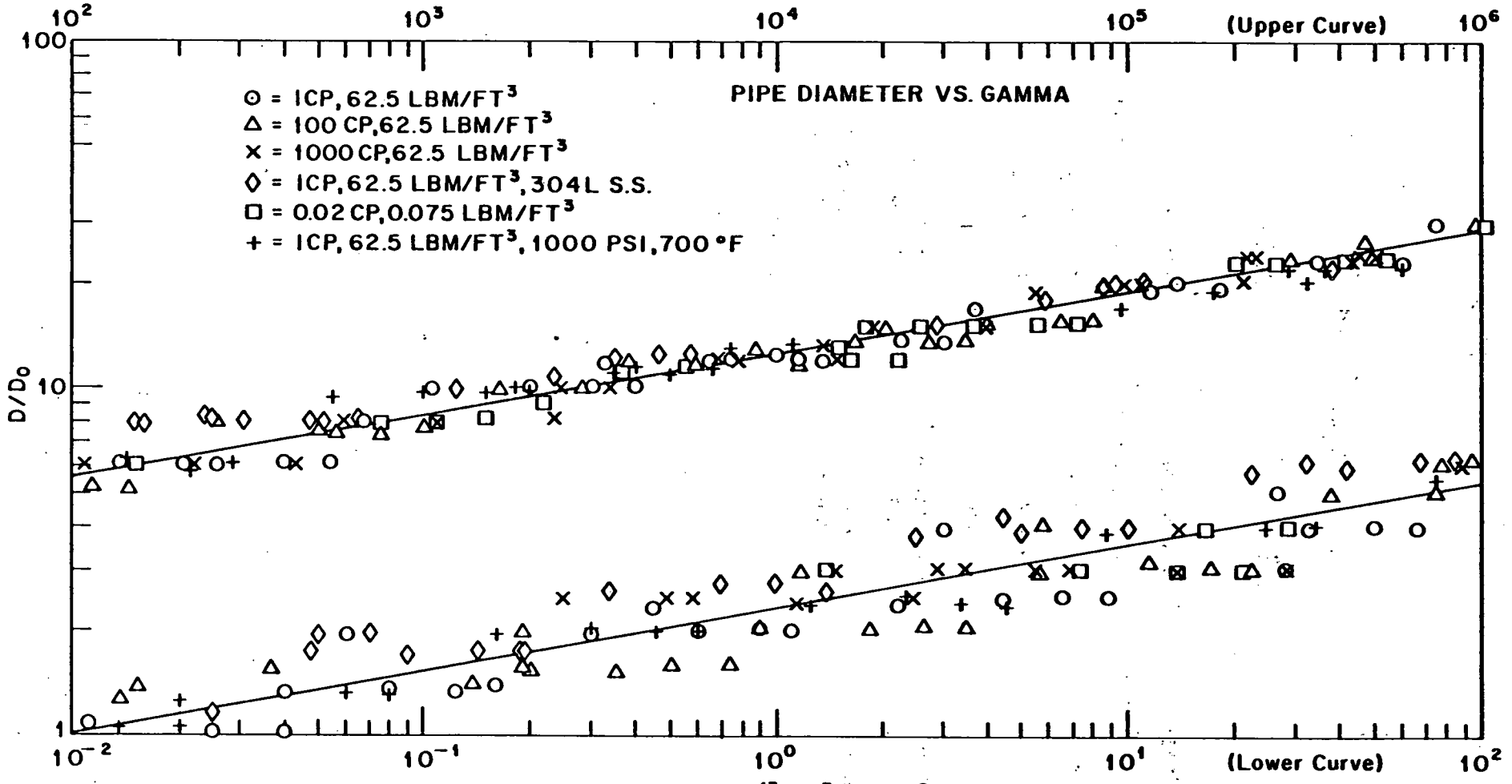
PIPE DIAMETER VS. GAMMA
⊙ = ICP, 62.5 LBM/FT³
△ = 100 CP, 62.5 LBM/FT³
× = 1000 CP, 62.5 LBM/FT³
◇ = ICP, 62.5 LBM/FT³, 304L S.S.
□ = 0.02 CP, 0.075 LBM/FT³
+ = ICP, 62.5 LBM/FT³, 1000 PSI, 700 °F
D/D₀
100
10
1
10²
10³
10⁴
10⁵
10⁶
(Upper Curve)
10⁻²
10⁻¹
10⁰
10¹
10²
(Lower Curve)
γ = 2.63 × 10⁻¹³ cfw³/ECpbρ²

FIG. 4

ASSUMPTIONS AND LIMITATIONS

The method for determining the optimum economic diameter is subject to the following assumptions and limitations.

1. The method applies to Newtonian fluids (including incompressible flow of gases).
2. The upper limits for combinations of operating temperatures and pressures are: 700°F and 1800 psi for A53 Gr. B carbon steel, and 1000°F and 2000 psi for 304 L S.S. and 316 L S.S.
3. The material and labor costs for the three piping materials were based on data from Richardson, Process Plant Construction Estimating Standards 1977-1978 Edition[6], and a least squares correlation relating material and labor costs as a function of pipe weight per foot is used in the software program for computing the optimum diameter. Figures 5 and 6 show material cost and labor cost versus weight per foot of pipe.
4. Although the software program computes the optimum economic diameter for straight runs of pipe, the method is not limited to this. To account for the material and labor cost of fittings and valves, a pipe cost constant, C_p is computed. The computation of C_p is detailed in the section: Procedure for Calculating the Optimum Diameter.

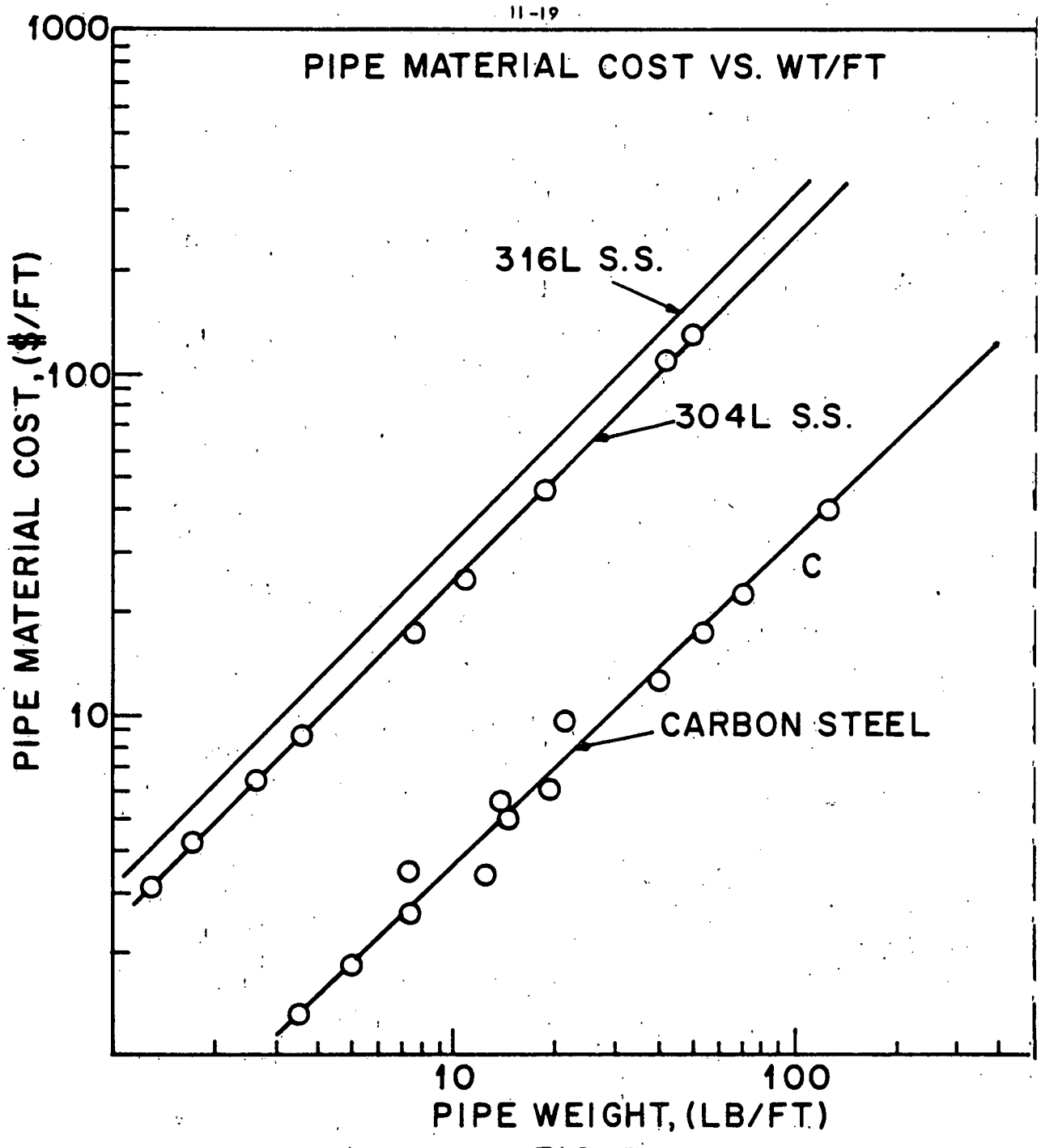
PIPE MATERIAL COST VS. WT/FT
1000
100
10
PIPE MATERIAL COST, ($/FT)
316L S.S.
304L S.S.
CARBON STEEL
10
100
PIPE WEIGHT, (LB/FT)

FIG. 5

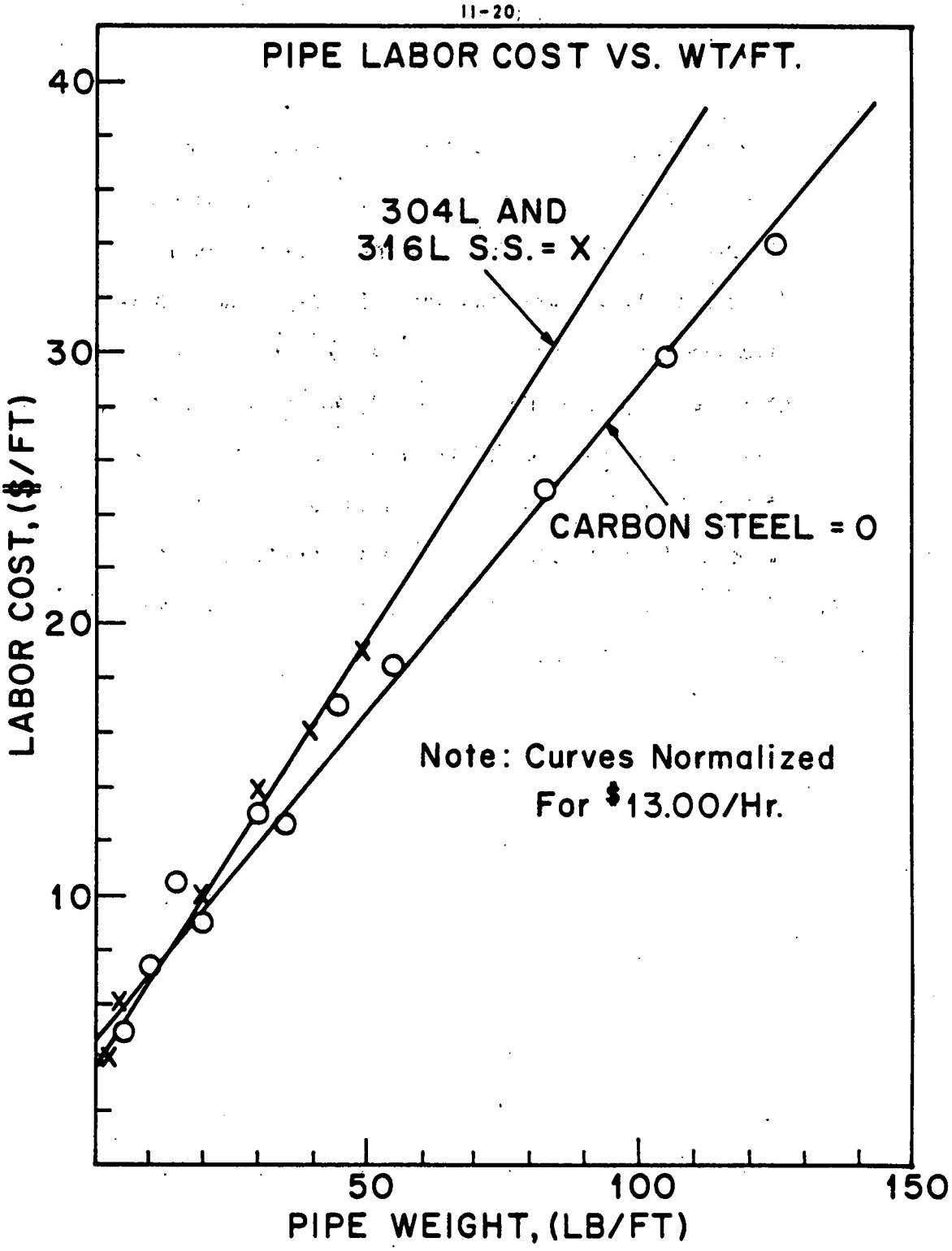
PIPE LABOR COST VS. WT/FT.
304L AND
316L S.S. = X
CARBON STEEL = 0
Note: Curves Normalized
For $13.00/Hr.
LABOR COST, ($/FT)
PIPE WEIGHT, (LB/FT)
40
30
20
10
50
100
150

FIG. 6

5. When sizing pipe, it is common practice to anticipate an increase in friction factor over the life of the pipe. To account for this the friction factor is multiplied by some constant. In the software program the friction factor is multiplied by 2, which corresponds to a value of C = 100, in the familiar William-Hazen formula for friction loss. This value of C if often used for design purposes, however, any value of f can be used in the method presented here.
6. Diameters to a maximum of thirty inches can be computed using this method.

EFFECT OF INFLATION ON THE OPTIMUM DIAMETER

By examining equation (6), it can be seen that the effect of inflation over the operative life of the pipe line would be to increase the cost of electricity, hence the capital investment to save a unit of power, C, would increase, as would the pipe cost coefficient, C_p, leaving the optimum diameter unchanged.

If the cost of electricity changes at a rate different than the material cost, the diameter would be affected as the ratio of the change in capital investment to the change in pipe cost to the .179 power.

PROCEDURE FOR CALCULATING THE OPTIMUM DIAMETER

For the parameters:

1. mass flow rate, W lbm/hr
2. fluid viscosity, μ cp
3. fluid density, ρ lbm/ft^3
4. operating pressure, P psi
5. operating temperature, T °F
6. cost of electricity, CE $/KW-hr
7. return on investment, i fractional
8. project life, N years
9. utilization factor, U fractional
10. piping material costs, C_p $/Ft-in^2
11. pump and motor efficiency, E fractional

Steps one through six outline the procedure for calculating the optimum diameter, using the relation:

$$D/D_o = 2.4\ \gamma^{.179} \qquad (7)$$

Step One: The capital investment justified to save a unit of power is calculated from equation (4), which is:

$$C = PW \times CE \times U \times 8760 \qquad (4)$$

Step Two: The quantity,

$$b = P(2(S - .6P) + P)/(S - .6P)^2 \qquad (8)$$

is computed where,

S is the allowable stress at the operating temperature, psi

P is the operating pressure, psi

This equation relates the maximum allowable stress of a given piping material to the operating temperature. Tables excerpted from the ASME pressure vessel code giving allowable stresses versus temperature for various materials are listed on pp. 6-38 to 6-41 of Perry[1].

Step Three: The pipe cost coefficient, C_p, is now computed. This coefficient depends on: (1) the piping material cost, (2) the number and cost of the various fittings and valves, and (3) the labor cost to install the pipe and all the fittings. For the commonly used piping materials, carbon steel, 304L S.S. and 316L S.S., C_p is given as:

$$C_p = .118X + .084\, C_L Y \qquad \text{for carbon steel} \qquad (9)$$

$$C_p = .208X + .162\, C_L Y \qquad \text{for 304L S.S.} \qquad (10)$$

$$C_p = .266X + .162\, C_L Y \qquad \text{for 316L S.S.} \qquad (11)$$

where:

X is the material cost per foot of 12-inch, 3/8" thickness carbon steel pipe, including the cost of fittings and valves. For 304L S.S. and 316L S.S. use 12-inch schedule 10S pipe.

Y is the man hours per foot to install the above 12-inch diameter pipe, including fittings and valves.

C_L is the cost of labor, \$/mhr

To compute X and Y, the fittings and valves in a run of pipe to be optimized are converted to the reference diameter of 12 inches. An estimating guide such as Richardson[6], can be used to determine the material and

labor costs for the various valves and fittings, all converted to the reference diameter of 12 inches.

Step Four: For materials other than carbon steel, 304L S.S. or 316L S.S., if material costs can be expressed as a multiple of carbon steel costs, it is only necessary to multiply X by this multiple. Similarly for Y. If the pipe cost is not a direct multiple of carbon steel costs in order to compute C_p, it is necessary to express the pipe cost in the form:

$$P_c = Bwt^n + C_L(Gwt + d) \qquad (12)$$

where:

P_c is the material and labor cost per foot for erecting straight pipe without fittings or valves.

wt is the pipe weight, lbm/ft

From a least squares correlation, B, n, G and d can be determined. B can be expressed as:

$$B = C_m J \qquad \text{or} \qquad C_m = B/J$$

where:

C_m is the material cost coefficient, Ft/lb

J is the material cost per foot for a straight run of 12-inch pipe of the desired material and schedule, exclusive of any fittings or valves.

Similarly:

$$G = Fk \qquad \text{or} \qquad F = G/k$$

where:

F is the labor cost coefficient, ft/lb

k is the manhours per foot to erect the 12-inch pipe above, exclusive of any fittings or valves.

From the derivation given in Appendix A, we have the result:

$$C_p = nC_mC_2X + 2C_LFC_2Y \qquad (13)$$

where:

X is the material cost per foot of the 12-inch pipe <u>including</u> all fittings and valves.

Y is the manhours per foot to erect the above pipe fittings and valves.

n is the exponent given in equation (12)

C_2 is the specific weight of the pipe, lb/ft-in^2

C_L is the labor rate, $/mh.

<u>Step Five</u>: The effect of additional head loss due to fittings and valves (over 100 feet of straight pipe) is accounted for by computing an "equivalent" friction factor, f', to be used in equation (6)

$$f' = 2f(1 + L_e/100) \qquad (14)$$

where:

f is the friction factor from the moody chart for a given Reynolds number and pipe diameter

L_e is the equivalent length in feet of pipe due to fitting and valve head loss only.

The factor of 2 was discussed under the section, Assumptions and Limitations, and is used to anticipate increasing friction factor with pipe aging.

Step Six: All the parameters needed to compute $D/D_o = 2.4\ \gamma^{.179}$ are known at this stage with the exception of f'. Since $f' = f(N_{RE}, e/D)$ for turbulent flow, D/D_o cannot be calculated explicitly. Therefore, it is necessary to assume an initial diameter. From this diameter, N_{RE} is calculated, and f is found from the Moody chart. L_e can also be computed, since L_e/D is known from the various fittings and valves. Consequently, f' can be calculated from Step Four. D/D_o can now be computed. Using this value of D, f and L_e are again found, and a new f' is calculated as before. This f' is substituted into Equation (6), and new D is calculated. From this D, the above process is repeated once more, with the resulting D being the optimum diameter. At the most, three calculations of D will be required before the solution converges within ± 3% of the optimum diameter.

Following the procedure outlined above, a numerical example is given in the following section.

CALCULATION OF THE OPTIMUM DIAMETER - AN EXAMPLE

Find the optimum economic diameter given the following parameters:

1. mass flow, W = 750,000 lbm/hr
2. fluid density, ρ = 62.5 lbm/ft^3
3. fluid viscosity, μ = 100 cp
4. operating temperature, T = 300°F
5. operating pressure, P = 300 psi
6. pump and motor efficiency, E = .7
7. utilization factor, U = .8
8. cost of electricity, CE = .038 $/KW-hr
9. return on investment, i = .12
10. operating life of 10 years
11. cost of labor, C_L = 13.55 $/hr
12. A53 Gr B carbon steel piping with the following fittings:

    5 - 90° ELS, 2 - T's, 2 gate valves (fully open),

    5 field butt-welds per 100 foot of pipe

Step One: The capital investment is calculated from Equation (4)

$$C = PW(CE \times U \times 8760)$$
$$= 5.65(.038 \times .8 \times 8760)$$
$$= 1505 \text{ \$/KW}$$

Step Two: The coefficient relating allowable stress to temperature is calculated, with information from pp. 6-38 to 6-41 of Perry[1].

$$b = P(2(S - .6P) + P)/(S - .6P)^2$$

$$= 300(2(18{,}150 - .6(300) + 300)/(18{,}150 - .6(300)^2)$$

$$= .034$$

Step Three: The pipe cost coefficient is calculated. The following table is constructed for the 12-inch, 3/8-inch wall thickness reference pipe, based on data from Richardson[6].

Item	Quan.	Material Cost	Man Hours Req'd	Le/D
90° ELS	5	5 x 86.00 = 430.00	5 x 10.6 = 53	150
T'S	2	2 x 149.00 = 248.00	2 x 10.6 = 21.2	40
300#Gate Valves	2	2 x 3119.00 = 6238.00	2 x 5 = 10	20
Pipe	100 ft.	1523.00	68.6	--
Field Welds	5	--	5 x 11.1 = 55.5	--
TOTALS		8489.00	208.3	210

Therefore,

$$X = 8489/100 = 84.9 \text{ \$/ft}$$

and,

$$Y = 208.3/100 = 2.08 \text{ mh/ft}$$

From Equation (9),

$$C_p = .118X + .084C_L Y$$

$$= .118(84.9) + .084(13.55)(2.08)$$

$$= 12.38$$

Steps Five and Six: Calculation of f' and D. Assuming an initial diameter of 6 inches yields;

$$N_{RE} = 6.32\ W/\mu D = 6.32(75{,}000)/(100)(6)$$
$$= 7{,}900,$$

and from the Moody chart, f = .034. Therefore,

$$L_e = (210)(.5) = 105 \text{ and from equation (14)}$$

$$f' = 2f(1 + L_e/100) = 2(.034)(1 + 105/100)$$
$$= .139$$

From equation (6),

$$\gamma = 2.63 \times 10^{-13}\ Cf'w^3/EC_p b\rho^2$$
$$= 2.63 \times 10^{-13}\ (1505)(.139)(750{,}000)^3/(.7)(12.38)(.034)(62.5)^2$$
$$= 2.0 \times 10^4$$

Therefore,

$$D/D_o = 2.4\ \gamma^{.179}$$
$$= 2.4\ (2.0 \times 10^4)^{.179}$$
$$= 14.14$$

The Reynolds number is now recalculated.

$$N_{RE} = 6.32(750{,}000)/(100)(14.14)$$
$$= 3352$$

and from the Moody Chart,

$$f = .042$$

$$L_e = (210)(1.17) = 247.5$$

$$f' = (2)(.042)(1 + 247.5/100)$$

$$= .292$$

Therefore,

$$\gamma = (2.63 \times 10^{-13})(1505)(.292)(750{,}000)^3/(.7)(12.38)(.034)(62.5)^2$$

$$= 4.24 \times 10^4$$

and,

$$D/D_o = 2.4(4.24 \times 10^4)^{.179}$$

$$= 16.3$$

Recalculating the Reynolds number once again,

$$N_{RE} = 2926$$

and,

$$f = .0425$$

$$L_e = 285.3$$

$$f' = .326$$

$$\gamma = 4.73 \times 10^4$$

$$D/D_o = 16.5$$

This is the optimum diameter.

CONCLUSION

The method developed here for determining the optimum diameter was compared with a relation developed by DuPont cited in Perry[1] for the range of parameters listed in computer runs one through three of Table 1. DuPont's equation and the assumptions made in the comparison are given in Appendix B. The software program computed the percent difference in diameter (where $\% \Delta D = \frac{D_Y - D_{DuPont}}{D_{DuPont}} \times 100\%$) for 135 diameters, and the results are summarized in Table 2. For each mass flow range of 1,000 - 60,000 lbm/hr listed in Table 2, five diameters were compared, and for each mass flow range of 10,000 - 4,500,000 lbm/hr, eleven diameters were compared. From Table 2 it can be seen that the mean absolute percent difference in diameters between the two methods is less than 19%, with the method presented here yielding larger diameters than the DuPont relation, for diameters over four inches. A 19% increase in diameter represents a decrease of 58% in the pumping power required to overcome friction losses.

The method for computing the optimum diameter is straight forward, and encompasses a wide range of parameters with an emphasis on the cost of energy, as evidenced by the larger diameters produced, relative to another accepted method.

TABLE 2

DIAMETER COMPARISON BETWEEN DUPONT RELATION

AND DIAMETER CALCULATED FROM GAMMA

Mass flow (lbm/hr)	Density (lbm/ft^3)	Viscosity (cp)	Energy Cost ($/KW-hr)	Max %ΔD	Mean Absolute %ΔD
1,000 - 60,000	.075	.02	.0025	- 11.1	6.8
			.0126	27	17.8
			.0253	29	15.7
			.0379	23	12.3
			.0505	19	10.6
10,000 - 4.5 MM	62.5	1.0	.0025	19	8.7
			.0126	37	11.4
			.0253	28.7	14.4
			.0379	21.8	11.5
			.0505	43	14.2
		100	.0025	22.8	10.5
			.0126	35	18.8
			.0253	37	17.6
			.0379	28.5	12.8
			.0505	23	11.6

REFERENCES

1. Robert H. Perry, Cecil H. Chilton, Chemical Engineer's Handbook (Fifth Edition), McGraw-Hill Book Co., N.Y., NY, 1973.

2. G. V. Shaw, A. W. Loomis, Cameron Hydraulic Data (14th Edition), I-R Co., Woodcliff Lake, NJ, 1970.

3. J. Michael Osborne, C. Douglas James, "Marginal Economics Applied to Pipeline Design", ASCE J. of Transp. Eng., V100 n6, Dec. 1974, pp. 1263-1275.

4. J. Michael Osborne "Marginal Economics Applied to Air Piping", ASCE J. of Environ. Eng., V 99, n TE3, Dec. 1974, pp. 637-653.

5. B. Duckham, "Finding Economic Pipe Diameters for Viscous Liquids", Process Eng., Nov. 1972, pp. 85-86.

6. Process Plant Construction Estimating Standards 1977-1978, Published by Richardson Engineering Services Inc., Solana Beach, CA.

7. L. Simpson, "Sizing Piping for Process Plants", Chem. Eng., June 17, 1968, pp. 192-214.

APPENDIX A

Derivation of Gamma

The head loss due to friction of fluid flowing in a closed conduit is given by the D' Arcy-Weisbach Equation as:

$$h_L = f\left(\frac{L}{D_1}\right)\frac{V^2}{2g} \tag{1}$$

In terms of pressure drop per unit length of pipe:

$$\frac{P_1'}{L} = P_1 = \frac{fV^2}{2gD_1}\rho \tag{2}$$

where,

$$P_1 = LBf/Ft^2 - Ft$$

For laminar flow,

$$f = 64/N_{RE} \tag{3}$$

and for transition and turbulent flow, the empirical relation,

$$\frac{1}{f} = -2\log_{10}\left(\frac{2.5}{\sqrt{f}\,N_{RE}} + \frac{e}{3.7D_1}\right) \tag{4}$$

will be used.

The power dissipated as a result of friction loss per unit length is:

$$P_f = \frac{P_f'}{L} = PVA \qquad (5)$$

The power input for a combined pump and motor efficiency, E, in terms of W and D is:

$$P_f = \frac{C_1 f w^3}{E D^5 \rho^2 g} \qquad (6)$$

As a basis for piping costs, Richardson Process Plant Construction Estimating Standards 1977-1978 was used. Using a least squares linear regression, the following correlation was obtained:

$$P_c = C_m X wt^n + C_L(FYwt + d) \qquad (7)$$

where,

C_m = .0228, n = .974, F = .01573, d = .268 (for carbon steel)

C_m = .0375, n = 1.04, F = .0303, d = .188 (for 304L S.S.)

C_m = .048, n = 1.04, F = .0303, d = .188 (for 316L S.S.)

wt = lb/ft

X = $/ft, material cost per foot of 12-inch, 3/8" wall thickness carbon steel pipe. Includes cost of pipe, fittings, and valves. For 304L S.S. and 316L S.S. use 12-inch SCH. 10S pipe.

Y = mh/ft, manhours to install 12-inch, 3/4" wall thickness carbon steel pipe, including all fittings and valves. For 304L S.S. and 316L S.S. use 12-inch, SCH 10S pipe.

C_L = $/mhr, cost of labor.

The pipe cost is a function of weight per length for a given material. This in turn is a function of operating pressure and temperature (unless special considerations require extra wall thickness for abrasion, for example). With no allowance for corrosion, the wall thickness as a function of temperature and pressure is given by the ASME pressure vessel code formula for seamless pipes as:

$$t_m = PD_o/2(S + .4P) \tag{8}$$

or in terms of inside diameter, D, this can be expressed as:

$$t_m = PD/2(s - .6P). \tag{9}$$

Since,

$$wt = c_2(D_o^2 - D^2) \tag{10}$$

and,

$$D_o = D + 2t_m. \tag{11}$$

We can combine these expressions, and the weight per length can be expressed as:

$$wt = c_2D^2b \tag{12}$$

where,

$$b = P(2(S - .6P) + P)/(S - .6P)^2. \tag{13}$$

Using the case of carbon steel as an example, and substituting (12) into (7) we have:

$$P_c = C_m X\ (C_2 D^2 b)^{.974} + C_L (FYC_2 D^2 b + d) \tag{14}$$

Computing the incremental pipe cost for a ΔD yields:

$$\Delta P_c \doteq \frac{dP_c}{dD} \Delta D = (1.948 C_m \times (C_2 b)^{.974} \times D^{.948} + 2C_L FYC_2 Db)\Delta D \tag{15}$$

where,

$$\Delta P_c = \$/ft.$$

The incremental change in the power required for this ΔD is:

$$\Delta P_f \doteq \frac{dP_f}{dD} \Delta D = - \frac{6C_1 fw^2}{ED^6 \rho^2 g} \Delta D\ . \tag{16}$$

Therefore,

$$C = \frac{\Delta P_c}{\Delta P_f} = \frac{dP_c}{dD} \Delta D \times \frac{dD}{dP_f} \frac{1}{\Delta D}$$

$$= - \frac{ED^6 \rho^2 g(1.948 C_M \times (C_2 b)^{.974} \times D^{.948} + 2C_L FYC_2 Db)}{6C_1 fw^3} \tag{17}$$

Making the approximation:

$$DbC_p \doteq Db(1.948 C_M \times C_2 + 2C_L FYC_2) \tag{18}$$

or,

$$C_p = (1.948 C_M \times C_2 + 2C_L FYC_2). \tag{19}$$

For carbon steel this becomes:

$$C_p = .118X + .084 C_L Y \tag{20}$$

For 304L S.S. this is:

$$C_p = .208X + .162C_L Y \tag{21}$$

and for 316L S.S. this is:

$$C_p = .266X + .162C_L Y \tag{22}$$

We can simplify (17) so that:

$$C = \frac{\Delta P_c}{\Delta P_f} = - EC_p\rho^2 bD^7 g/6C_1 fw^3 \ . \tag{23}$$

For any given investment cost to save a unit of power, C ($/kw), the optimum diameter is:

$$D = (C6C_1 fw^3/EC_p bg\rho^2)^{1/7} \tag{24}$$

Dividing by the unit diameter D_o, inches,

$$D/D_o = (C6C_1 fw^3/D_o^7 EC_p bg\rho^2)^{1/7} \tag{25}$$

Let:

$$C_6 = 3.83 \times 10^{-11} \text{ in}^5/\text{ft}^5 \cdot \text{hr}^3/\text{sec}^3 \cdot \text{kw-sec/ft-lbf} \cdot 6C_1/EC_p g \tag{26}$$

or:

$$C_6 = 2.63 \times 10^{-13}/EC_p \ , \ \text{kw-hr}^3\text{-in}^7/\$\text{-lbm-ft}^6 \tag{27}$$

Therefore,

$$D = f(C,f,b,w^3,\rho^2,E,C_6) \tag{28}$$

We define gamma as:

$$\gamma = 2.63 \times 10^{-13} \, Cfw^3/EC_p b\rho^2, \tag{29}$$

which is the quantity relating the significant parameters to the optimum economic diameter. The parameter groups in Table 1 were inputted to the software program, and each combination of parameters yielded an optimum diameter, and a corresponding γ. A least squares linear regression of γ on D/D_o yields:

$$D/D_o = 2.4 \, \gamma^{.179} \tag{30}$$

with a correlation coefficient r = .94.

NOMENCLATURE

h_L = head loss, ft

V = velocity, ft/sec

L = ft

P_1 = Lbf/ft^2-ft

D_1 = diameter, ft

e = relative rougness, ft

A = area, ft^2

g = 32.14 ft-lbm/sec^2-lbf

ρ = density, lbm/ft^3

f = friction factor, dimensionless

N_{re} = reynolds number, dimensionless

C_1 = scale factor, dimensionless

P_f = power per unit length, lbf/sec

P_c = pipe cost, $/ft

C_L = labor cost, $/mh

C_M = material cost coefficient, ft/lb

F = labor cost coefficient, ft/lb

n = cost exponent, dimensionless

d = cost constant, mh/ft

D_o = unit diameter, one in.

P = operating pressure, psi

S = allowable stress, psi

t_m = wall thickness, in.

D = inside diameter, in.

U = fractional operation time per year, dimensionless

C_2 = 2.667 lbm/ft-in^2

wt - pipe weight, lbm/ft

b = dimensionless

ΔP_c = $/ft

ΔP_f = lbf/sec

C = $/kw

C_p = $/ft-in^2

γ = dimensionless

E = pump and motor efficiency, fractional, dimensionless

X = material cost, $/ft

Y = labor, mh/ft

w = mass flow rate, lb/hr

APPENDIX B

DuPont Co. Optimum Diameter Relation

The parameters indicated in runs 1 through 3 of Table 1 were inputted to the DuPont formula[1] below, and the diameters calculated were compared with the diameters calculated from the γ correlation. The results of these comparisons are summarized in Table 2.

Both relations computed the optimum diameter for a straight run of schedule 40 carbon steel pipe which included five field butt-welds per hundred feet. The comparison of the two methods was made on a common basis with the parameters below assigned to the DuPont formula, and where applicable, to the γ correlation.

The formula of DuPont which is based on return on incremental investment is given as:

$$D^{4.84 + n/(1 + .794L'_e D)} = \frac{.000189YKq^{2.84}\rho^{.84}\mu^{.16}\left((1 + M)(L - \phi) + \frac{ZM}{a' + b'}\right)}{n \times E(1 + F)(Z + (a + b)(1 - \phi))} \quad (1)$$

where:

D = economic pipe diameter, ft

n = exponent in pipe cost equation ($C = XD^n$)

C = cost of pipe, $/ft

X = cost of 1 ft, of 1 ft diameter pipe

L'_e = factor for friction in fittings, in pipe diameters per unit length of pipe

M = $(a' + b')EP/(17.9KY)$ ratio of annual cost of pumping installation to annual cost of power delivered to the fluid, dimensionless

E = Combined pump and motor efficiency, dimensionless

P = installed cost of pump and motor, $/Hp

K = cost of power delivered to the motor, $/kw-hr

Y = days of operation per year (24 hr days)

ϕ = factor for taxes, dimensionless

Z = fractional annual rate of return on investment, dimensionless

F = ratio of cost of fittings plus installation cost of fittings and pipe to pipe material cost, dimensionless

a' = fractional annual depreciation on pumping installation, dimensionless

b' = fractional annual maintenance on pumping installation, dimensionless

a = fractional annual depreciation on pipe line, dimensionless

b = fractional annual maintenance on pipe line, dimensionless

q = volumetric flow rate, ft^3/sec

ρ = fluid density, lbm/ft^3

μ = fluid viscosity, cp

The values assigned to the parameters are:

n = 1.256	Y = 292
X = 14.1	ϕ = .55
$L_e' = 0$	Z = .12
E = .7	a' + b' = .4
p = 150	a + b = .2

Using a least squares correlation, the following relations were derived for material and labor costs of schedule 40 carbon steel pipe based on data from Richardson[6].

$$\text{Material cost, \$/ft} = 14.1\ D^{1.256}$$

of if D is in inches,

$$\text{\$/ft} = .62\ D^{1.256}$$

also,

$$\text{Labor cost, \$/ft} - 1.22\ D^{.78}$$

assuming labor cost = \$13.00/mhr and welding cost, \$/ft = $1.08\ D^{.78}$.

The above expressions are combined to form an expression for 1 + F which is,

$$1 + F = 1 + 3.71\ D^{-.476}$$ where, D is in.

APPENDIX C

SOFTWARE PROGRAM LISTING

```
C PROGRAM FOR OPTIMIZING PIPE SIZE FOR ANY NEWTONIAN FLUID
C
C
C       ROBERT KRAMER
C       DEPARTMENT OF MECHANICAL ENGINEERING
C       CARNEGIE-MELLON UNIVERSITY
C       PITTSBURGH PENNSYLVANIA
C
C
      REAL NRE, KNEW,KOLD, LAMBDA, MU,KWHR
      DIMENSION DNOM(30), DOUT(30), TMSTL(30), TMSS(30), CKI(15),
     2 P(10), T(10), Q(30), RHO(10), MU(10), DS(10), C(10),
     3 RHOS(10), CLABOR(10)
C NOMINAL DIAMETERS FOR STANDARD PIPE SIZES ARE:
 115  DNOM(1)=.5
      DNOM(2)=.75
      DNOM(3)=1.0
      DNOM(4)=1.25
      DNOM(5)=1.5
      DNOM(6)=2.0
      DNOM(7)=2.5
      DNOM(8)=3.0
      DNOM(9)=3.5
      DNOM(10)=4.
      DNOM(11)=5.
      DNOM(12)=6.
      DNOM(13)=8.
      DNOM(14)=10.
      DNOM(15)=12.
      DNOM(16)=14.
      DNOM(17)=16.
      DNOM(18)=18.
      DNOM(19)=20.
      DNOM(20)=24.
      DNOM(21)=30.
C OUTSIDE DIAMETERS ARE AS FOLLOWS
      DOUT(1)=.840
      DOUT(2)=1.05
      DOUT(3)=1.315
      DOUT(4)=1.66
      DOUT(5)=1.9
      DOUT(6)=2.375
      DOUT(7)=2.875
      DOUT(8)=3.5
      DOUT(9)=4.
      DOUT(10)=4.5
      DOUT(11)=5.56
      DOUT(12)=6.625
      DOUT(13)=8.625
      DOUT(14)=10.75
      DOUT(15)=12.75
      DOUT(16)=14.
      DOUT(17)=16.
      DOUT(18)=18.
```

```
      DOUT(19)=20.
      DOUT(20)=24.
      DOUT(21)=30.
C SCHEDULE 40 WALL THICKNESSES
      TMSTL(1)=.109
      TMSTL(2)=.113
      TMSTL(3)=.133
      TMSTL(4)=.14
      TMSTL(5)=.145
      TMSTL(6)=.154
      TMSTL(7)=.203
      TMSTL(8)=.216
      TMSTL(9)=.226
      TMSTL(10)=.237
      TMSTL(11)=.258
      TMSTL(12)=.28
      TMSTL(13)=.322
      TMSTL(14)=.365
      TMSTL(15)=.375
      TMSTL(16)=.375
      TMSTL(17)=.375
      TMSTL(18)=.375
      TMSTL(19)=.375
      TMSTL(20)=.375
      TMSTL(21)=.375
C THICKNESSESS FOR SS TO BE SCH 10
      TMSS(1)=.065
      TMSS(2)=.065
      TMSS(3)=.065
      TMSS(4)=.065
      TMSS(5)=.065
      TMSS(6)=.065
      TMSS(7)=.083
      TMSS(8)=.083
      TMSS(9)=.083
      TMSS(10)=.083
      TMSS(11)=.109
      TMSS(12)=.109
      TMSS(13)=.109
      TMSS(14)=.134
      TMSS(15)=.156
      TMSS(16)=.156
      TMSS(17)=.165
      TMSS(18)=.175
      TMSS(19)=.188
      TMSS(20)=.218
      TMSS(21)=.250
C THE VALUES FOR PARAMETERS TO BE USED IN DO LOOPS ARE:
      T(1)=0.
      T(2)=100.
      T(3)=300.
      T(4)=500.
```

```
      T(5)=700.
      T(6)=900.
      T(7)=1000.
      T(8)=1300.
      T(9)=1500.
      P(1)=0.
      P(2)=500.
      P(3)=1000.
      P(4)=1500.
      P(5)=1800.
      P(6)=2000.
      P(7)=2500.
      P(8)=3000.
      CLABOR(1)=2.
      CLABOR(2)=8.
      CLABOR(3)=13.
      CLABOR(4)=20.
      CLABOR(5)=50.
      CKI(1)=2.
      CKI(2)=100.
      CKI(3)=500.
      CKI(4)=1000.
      CKI(5)=1500.
      CKI(6)=2000.
      Q(1)=1000.
      Q(2)=5000.
      Q(3)=10000.
      Q(4)=15000.
      Q(5)=30000.
      Q(6)=60000.
      Q(7)=120000.
      Q(8)=250000.
      Q(9)=500000.
      Q(10)=750000.
      Q(11)=1000000.
      Q(12)=3000000.
      Q(13)=4500000.
      MU(1)=.005
      MU(2)=.01
      MU(3)=.02
      MU(4)=.05
      MU(5)=1.0
      MU(6)=5.
      MU(7)=20.
      MU(8)=100.
      MU(9)=1000.
      RHO(1)=.02
      RHO(2)=.075
      RHO(3)=.09
      RHO(4)=40.
      RHO(5)=62.5
      RHO(6)=80.
C DO LOOP INDEXES FOR INPUTTED FLOW PARAMETERS ARE:
C THE TEMPERATURE INDEXES ARE:
      NT=2
      NTF=2
```

```
      NTINC=1
C THE PRESSURE INDEXES ARE:
      NP=2
      NPF=2
      NPINC=2
C THE LABOR RATE INDEXES ARE:
      NL=3
      NLF=3
      NLINC=1
C THE INVESTMENT COST INDEXES ARE:
      NK=3
      NKF=6
      NKINC=1
C THE MASS FLOW RATE INDEXES ARE:
      NQ=3
      NQF=13
      NQINC=1
C THE VISCOSITY INDEXES ARE:
      NMU=5
      NMUF=5
      NMUINC=1
C THE FLUID DENSITY INDEXES ARE:
      NR=5
      NRF=5
      NRINC=1
      TYPE 876
C THE DO LOOPS CALCULATE THE COMBINATIONS OF THE VARIOUS
C FLUID PARAMETERS AND OPERATING CONDITIONS
      DO 877 IND1=NT,NTF,NTINC
      DO 877 IND2=NP, NPF, NPINC
      DO 877 IND3=NL, NLF, NLINC
      DO 877 IND4=NK, NKF, NKINC
      DO 877 IND5=NQ, NQF, NQINC
      DO 877 IND6=NMU, NMUF, NMUINC
      DO 877 IND7=NR, NRF, NRINC
      EFF=.5
C THE PIPE COST COEFFICIENT IS C5
      C5=3.25
      INDEX=1
      ERRNEW=0.
      TM=.1
      KWOLD=9.9E+09
      PCOLD=PCNEW
      SIGMA=0.
      HLOSS1=9.9E+09
C FOR C.S. FLAG2=1, FOR 304LS.S. FLAG2=2, FOR 316L S.S. FLAG2=3
      FLAG2=1
C THE REYNOLDS NUMBER IS CALCULATED
10    IF (INDEX.GT.21) GO TO 951
      ERROLD=ERRNEW
12    D=DOUT(INDEX)-2.0*TM
      V=.16*Q(IND5)/(RHO(IND7)*3.1416*D**2)
14    NRE=124.*D*V*RHO(IND7)/MU(IND6)
      IF (NRE.LT.2100) GO TO 31
```

```
C FRICTION FACTOR FOR TURBULENT FLOW
      RELR=.0018/D
      IT2=1
      FW=.1
 20   A=1/FW**.5
      B=-2*ALOG10(2.51*A/NRE+RELR/3.7)
      ERROR2=ABS(A)-ABS(B)
      IF (ERROR2.LT.0) GO TO 21
      IF (ERROR2.LT.0.04) GO TO 55
      FW=FW+.0001
      GO TO 20
 21   FW=FW-.0001
      IT2=IT2+1
      IF(IT2.EQ.3000) GO TO 951
      GO TO 20
C STOKES LAW FOR LAMINAR FLOW
 31   FW=64/NRE
 55   F=2*FW
C THE HEAD LOSS AND PUMPING POWER IS COMPUTED ASSUMING A PUMP MOTOR EFI
C ICIENCY OF E
 40   HLOSS=.1295*F*RHO(IND7)*V**2/D
1022  FORMAT (' FRICTION FACTOR IS:',F6.4)
      PPOW=(5.71E-05/EFF)*Q(IND5)*HLOSS/RHO(IND7)
      KWNEW=PPOW
      DELTKW=KWOLD-KWNEW
      KWOLD=KWNEW
      GO TO (81,82,83), FLAG2
C ALLOWABLE PIPE STRESSES COMPUTED BY LEAST SQUARES FIT FROM
C ASME PRESSURE VESSEL CODE. FOR CARBON STEEL PIPING:
 81   IF(T(IND1).GT.1100) TYPE 98, T(IND1)
      IF (T(IND1).GT.900) GO TO 84
      IF (T(IND1).GE.750) GO TO 89
      IF (T(IND1).GE.600) GO TO 86
      IF (T(IND1).GE.100) GO TO 87
      IF (T(IND1).LT.100)  T(IND1)=100.
      GO TO 87
 84   S=8.95E31/T(IND1)**9.52
      GO TO 80
 89   S=8.38E14/T(IND1)**3.76
      GO TO 80
 86   S=2.23E06/T(IND1)**.777
      GO TO 80
 87   S=3.9E04/T(IND1)**.139
      GO TO 80
C FOR 304 SS PIPING ALLOWABLE STRESSES ARE:
 82   IF (T(IND1).GT.1500) TYPE 98, T(IND1)
      IF (T(IND1).GT.1050) GO TO 35
      IF (T(IND1).GE.700) GO TO 36
      IF (T(IND1).GE.100) GO TO 37
      IF (T(IND1).LT.100) T(IND1)=100.
      GO TO 37
 35   S=1.735E25/T(IND1)**7.03
      GO TO 80
 36   S=6.67E05/T(IND1)**.626
      GO TO 80
 37   S=7.49E04/T(IND1)**.29
      GO TO 80
```

```
C FOR 316 SS PIPING THE ALLOWABLE STRESSES ARE:
   83    IF (T(IND1).GT.1500) TYPE 98, T(IND1)
         IF (T(IND1).GT.1100) GO TO 41
         IF (T(IND1).GE.900) GO TO 42
         IF (T(IND1).GE.100) GO TO 43
         IF (T(IND1).LT.100) T(IND1)=100.
         GO TO 43
   41    S=4.783E23/T(IND1)**6.45
         GO TO 80
   42    S=3.232E10/T(IND1)**2.13
         GO TO 80
   43    S=2.54E04/T(IND1)**.062
         GO TO 80
   98    FORMAT (' THE TEMP. IS TOO HIGH; T=',F10.2)
         GO TO (84,35,41), FLAG2
   80    TM=P(IND2)*DOUT(INDEX)/(2*(S+.4*P(IND2)))
         GO TO (75,76,76) FLAG2
   75    IF (TMSTL(INDEX).LE.TM) GO TO 6
         TM=TMSTL(INDEX)
         GO TO 6
   76    IF (TMSS(INDEX).LE.TM) GO TO 6
         TM=TMSS(INDEX)
    6    WT=2.677*((D+2*TM)**2-D**2)
         GO TO (91,92,93),FLAG2
   91    PCOST=36.56*(WT**.974)+CLABOR(IND3)*(1.95*WT+26.87)
         GO TO 200
   92    PCOST=256*(WT**.96)+CLABOR(IND3)*(1.146*WT+12.41)
        2  +CLABOR(IND3)*(4.53*D+6.4)
         GO TO 200
   93    PCOST=332.8*(WT**.96)+CLABOR(IND3)*(1.146*WT+12.41)
        2  +CLABOR(IND3)*(4.53*D+6.4)
  200    PCNEW=PCOST
         IF (ABS(ERRNEW).GT.ABS(ERROLD)) GO TO 900
         DELTPC=PCNEW-PCOLD
         PCOLD=PCNEW
         LAMBDA=DELTPC/DELTKW
         ERRNEW=LAMBDA-CKI(IND4)
         IF (ERRNEW) 4,900,5
C IF THE NEW ERROR IS NEGATIVE, INCREMENT SIZE AND GO THROUGH LOOP
C AGAIN. IF NEW ERROR IS ZERO, FINISHED. IF  NEW ERROR IS POSITIVE.
C CHECK THE ABSOLUTE VALUE OF OLD AND NEW ERROR, AND SELECT MIN ERROR.
    4    INDEX=INDEX+1
         GO TO 10
    5    IF (ABS(ERRNEW).LE.ABS(ERROLD)) GO TO 900
         INDEX=INDEX-1
         GO TO 12
  900    ALEPH=P(IND2)*(2*(S-.6*P(IND2))+P(IND2))
        2  /(S-.6*P(IND2))**2
         GAMMA=2.63E-13*CKI(IND4)*F*Q(IND5)**3
        2 /(EFF*C5*ALEPH*RHO(IND7)**2)
C DUPONT'S RELATION FOR PIPE DIAMETER BASED ON INCRE-
CMENTAL RETURN ON INVESTMENT IS CALCULATED ON AN EQUAL BASIS
```

```
C WITH PIPOP.
C THE CAPITAL OUTLAY JUSTIFIED TO SAVE A KILOWATT IS BASE
C 10 YEAR PROJECT LIFE, .8 UTILIZATION, 12% ROI, NO OPERA
C OR SALVAGE VALUE.
      KWHR=CKI(IND4)/39595.
      ALPH1=2.55*EFF*(1+(1.22*D**.785+1.1*D**.78)/(.62*
      ALPH2=4.386E-12*KWHR*Q(IND5)**2.84*MU(IND6)**.16/
      ALPH3=.45+8.61E-03*EFF/KWHR
      D1=12*(ALPH2*ALPH3/ALPH1)**.164
      DELD=(D-D1)/D1*100
      WRITE (5,878) RHO(IND7), MU(IND6), P(IND2), T(IND
     2  CKI(IND4), CLABOR(IND3), V,D, KWHR, NRE,
     3  GAMMA, F, D1, DELD
      GO TO 907
  876 FORMAT (1X,' RHO',4X,' VISC',2X,' PSI',4X,' TEMP'
     2 9X,' $/KW',2X,' $/MH',1X,' VEL.',1X' DIA',3X,'
     3  10X,' GAMMA',6X,' FF',3X,' D1',2X,' %DIFF'//)
  878 FORMAT (F7.3,1X,F8.3,1X,F6.1,1X,F6.1,1X,F9.1,
     2 4X,F7.1,1X,F6.2,1X,F5.2,1X,F5.2,1X,F7.4,1X,E12.
     3 F6.4,1X,F5.2,1X,F6.2)
  907 GO TO 877
  877 CONTINUE
      GO TO 953
  951 TYPE 952
  952 FORMAT (' TOO MANY ITERATIONS WERE REQUIRED')
      GO TO 877
  953 TYPE 954, IT2, INDEX
  954 FORMAT (' IT2=',I6, ' INDEX=',I6)
      STOP
      END
```

2 ENERGY CONSERVATION IN COAL CONVERSION

Energy Conservation Potential in Heat Recovery Techniques

A Case Study

J. D. Stas

Carnegie-Mellon University
Pittsburgh, PA 15213

June, 1978

Prepared for

THE U.S. DEPARTMENT OF ENERGY
Pittsburgh Energy Technology Center
UNDER CONTRACT NO. EY77S024196

ABSTRACT

In this study, we looked at replacing certain heat exchangers with Organic Rankine Cycles. In each case, we determined the cost of generating power and then from this tabulation of capital investment for power generation, feasibility of replacement on a unit-by-unit basis was determined.

The results show that 18 heat exchangers reject sufficient heat to warrant ORC usage, with potential electric generation of 36 MW or a 17% increase of the inplant power generation of 210 MW.

Cost estimates indicate the capital investment required to be approximately $1000/KW with a potential reduction of $300/KW for mass produced units.

Based on the results of this analysis it is recommended that ORC manufacturers be engaged to further engineer and incorporate Organic Rankine Cycles into the Oil/Gas design.

TABLE OF CONTENTS

LIST OF TABLES

LIST OF FIGURES

1. Introduction

In our initial energy study, we developed a number of methods by which energy can be conserved in inefficient coal conversion plants.[10] Currently, our objective is to apply the procedures we have learned to more near term, efficient and highly engineered plants. The commercial concept Oil/Gas Complex designed by Ralph M. Parsons Company has been selected as the next candidate to be evaluated. This design has a high thermal efficiency of 77%.[11]

The purpose of this particular study is to investigate the feasibility of replacing certain heat exchangers with an organic rankine cycle. For each case, the cost of generating electric power is to be determined and then from this tabulation of capital investment for power generation, the feasibility of replacement on a unit-by-unit basis will be determined.

2. H_x Suitability for ORC

Every heat exchanger in the Oil/Gas Complex has been evaluated for its suitability of being replaced by an organic rankine cycle to produce shaft work. As shown in Figure 1, the ORC can perform essentially the same function as a heat exchanger but the exit temperature of the second stream cannot be the same, ($T_4 \neq T_4'$) since work is extracted.

In evaluating heat exchangers, there are three reasons why a heat exchanger may be rejected as a potential candidate: (1) the exchanger's operation is important to the downstream process and therefore a temperature change in any stream cannot be afforded or (2) the incoming temperature of the process stream is too low to warrant ORC usage or (3) the unit is too small.

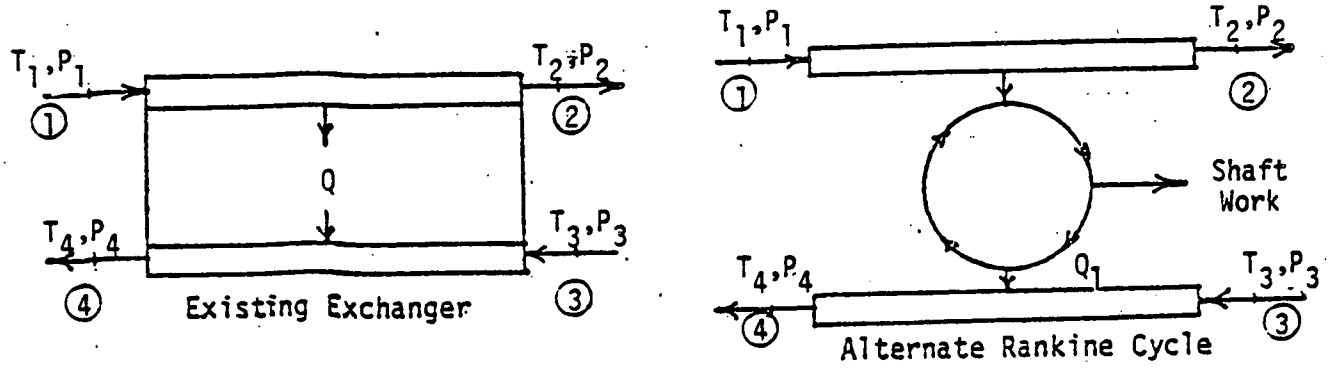

FIGURE 1.

COMPARISON OF ORC AND H_x

3. Organic Rankine Cycle

In many areas in the Oil/Gas complex, air coolers and water coolers are used to cool process streams. In some cases the coolers are used independently and in others they are used in series as shown in Figure 2A. Normally, the air cooler cools the stream to 120°F, then the water cooler cools the stream to 100°F. The inlet temperature of the air coolers vary throughout the plant from 550°F-200°F. It is these schemes which are proposed for replacement by the Rankine Cycle design in Figure 2B, in this report.

The Rankine Cycle design in Figure 2B utilizes an organic working fluid to produce shaft power through a reciprocating or turbine type expander. The air cooler and/or water cooler is replaced by the boiler of Figure 2B keeping inlet and exit states of the process stream constant. Therefore, the waste heat which was previously lost to the atmosphere is used as a heat source for the Rankine Cycle in which some of this heat is converted to mechanical energy in the expander while the remaining is rejected in the condenser to the cooling tower.

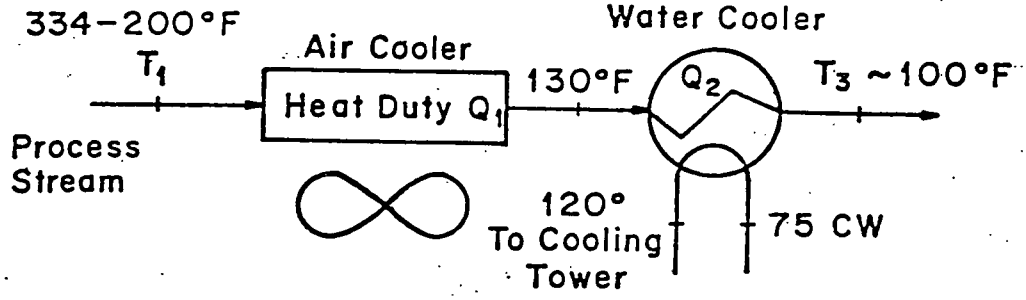

FIGURE 2A. PRESENT DESIGN

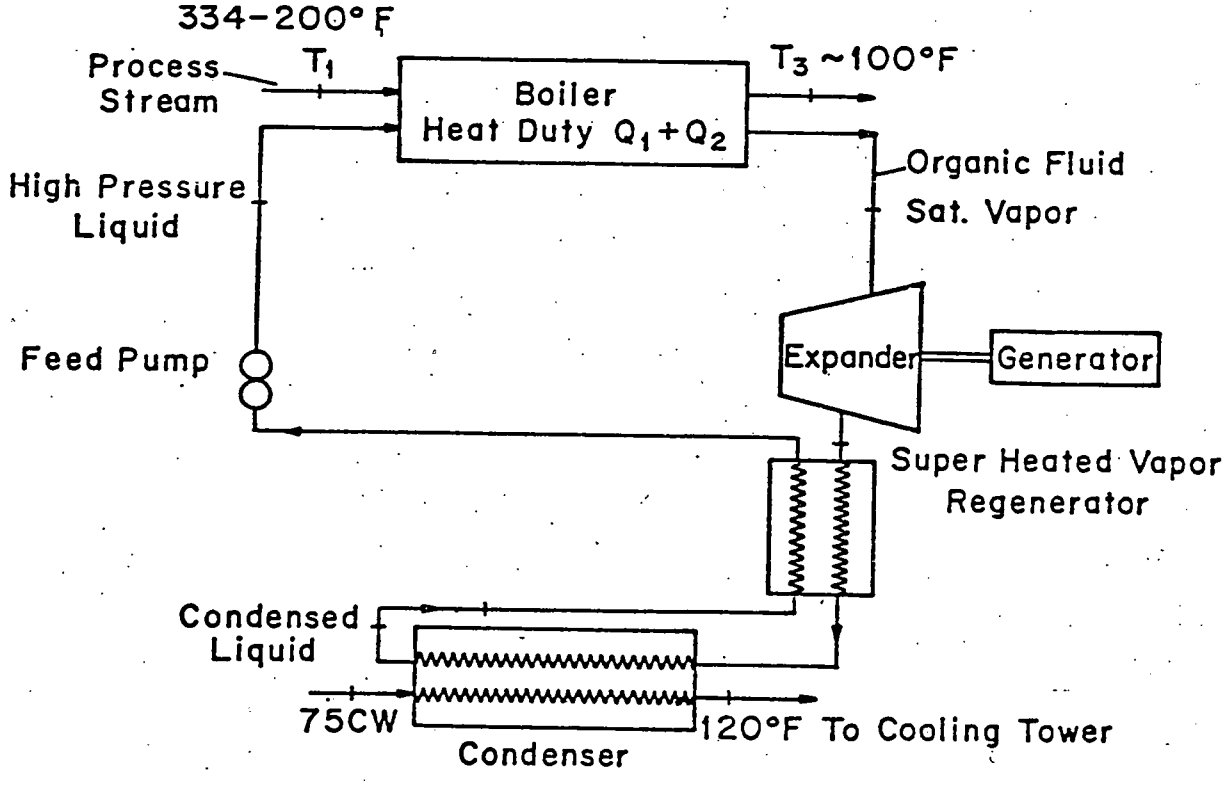

FIGURE 2B. ALTERNATIVE DESIGN ORGANIC RANKINE CYCLE

To date, only AFI Energy Systems is in a position to market Organic Rankine Cycles as low level waste heat recovery systems in the 200-400°F temperature range.[17] AFI Energy Systems is a joint venture of: Allied Chemical, Foster Wheeler and Ishikawajima Hauma (IHI) of Japan.

A demonstration 500 KW Organic Rankine Cycle system shown in Figure 3 is being constructed at the Allied Chemical facility at Claymont, Delaware and will be operating in early 1978.[8] This plant incorporates a turbine and associated technology which has been commercially applied in Japan since 1968 in a 3800 KW Organic Rankine Cycle. This system shown in Figure 4 has provided over 70,000 hours of continuous operation with no major problems.[18]

The AFI systems are being offered for sale on a turnkey, fixed price basis in four nominal sizes: 500 KW, 1000 KW, 2000 KW, and 4000 KW. Delivered costs are approximately $1000/KW.[17]

AFI's current market thrust is toward retrofitting the ORC to waste heat sources in existing plants. These systems utilize liquids or condensable vapors as a heating source. AFI feels economics are not yet justified for installation of an ORC when using gas as a heating source because of a much larger heat transfer area required in the boiler. A three-year AFI study indicated that there is a huge potential application in the following areas: chemical plants, refineries, chemical processes, and areas where there is excess process steam.[17]

Figures 5 and 6, furnished by AFI, have been used to estimate the ORC power output potential of heat exchangers with a liquid or condensable vapor as a heat source. Samples are shown in the figures.

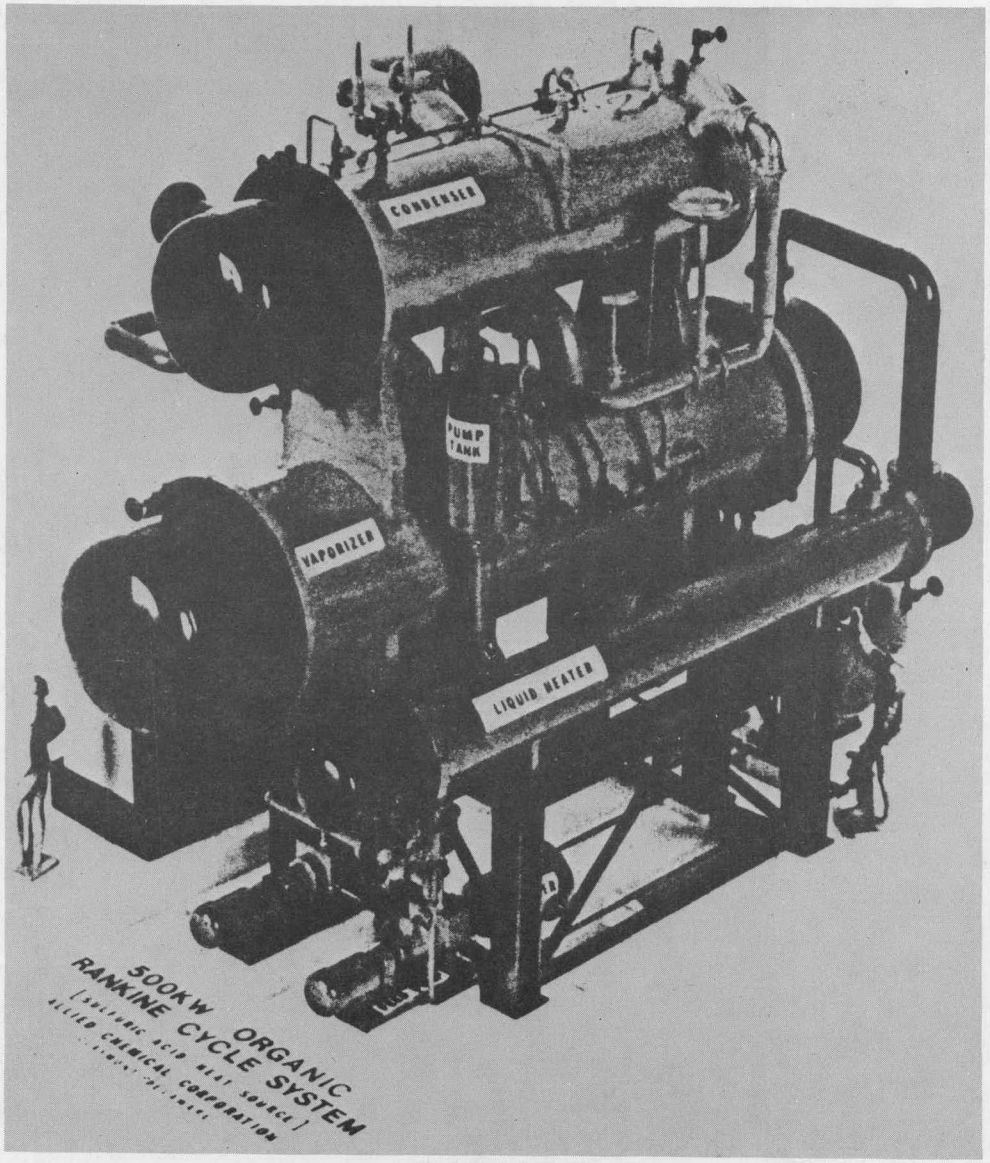
CONDENSER
PUMP TANK
VAPORIZER
LIQUID HEATER
500KW ORGANIC RANKINE CYCLE SYSTEM
[SOLTHERM ACID HEAT SOURCE]
ALLIED CHEMICAL CORPORATION

FIGURE 3

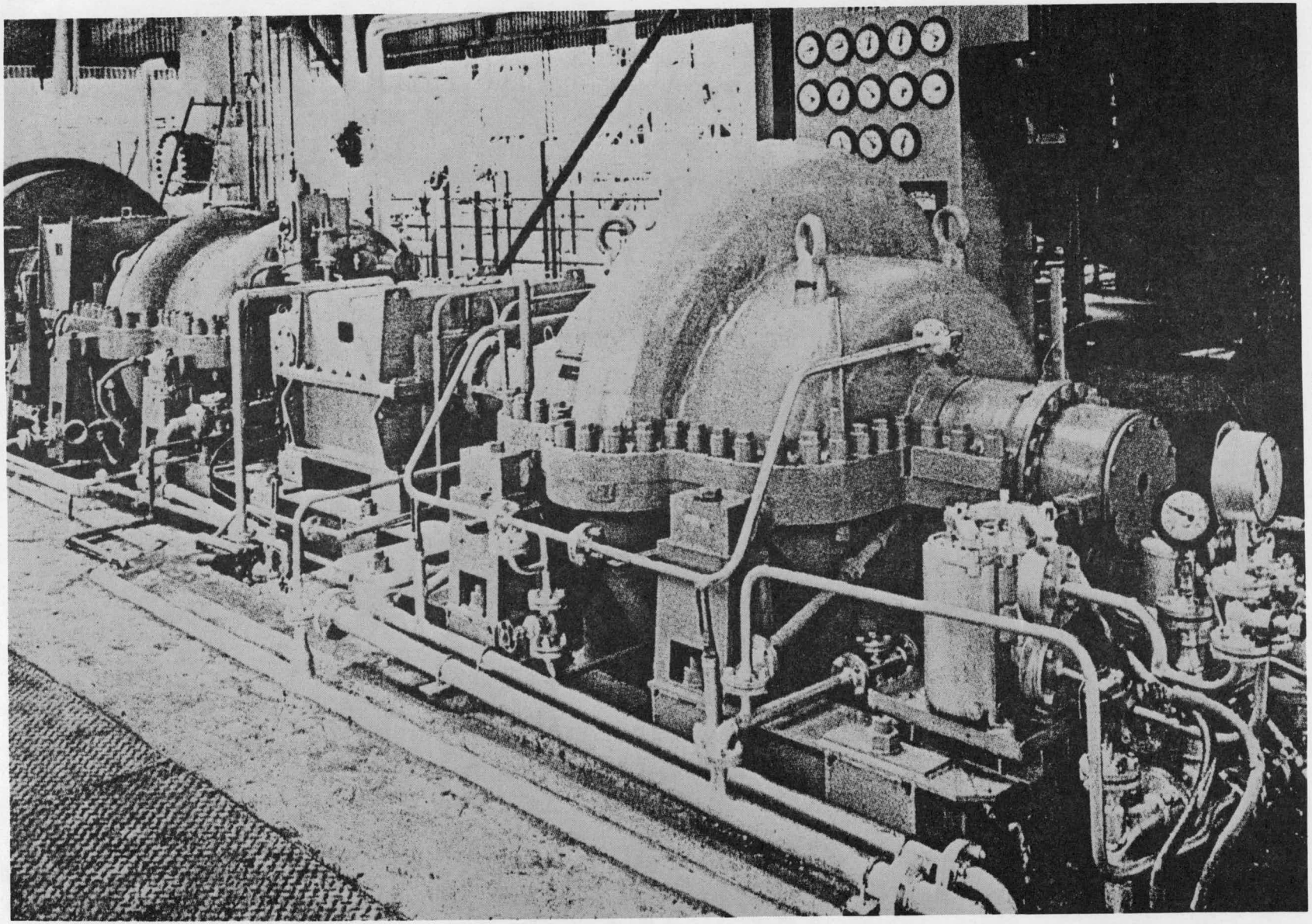

FIGURE 4

3800KW ORGANIC RANKINE CYCLE SYSTEM

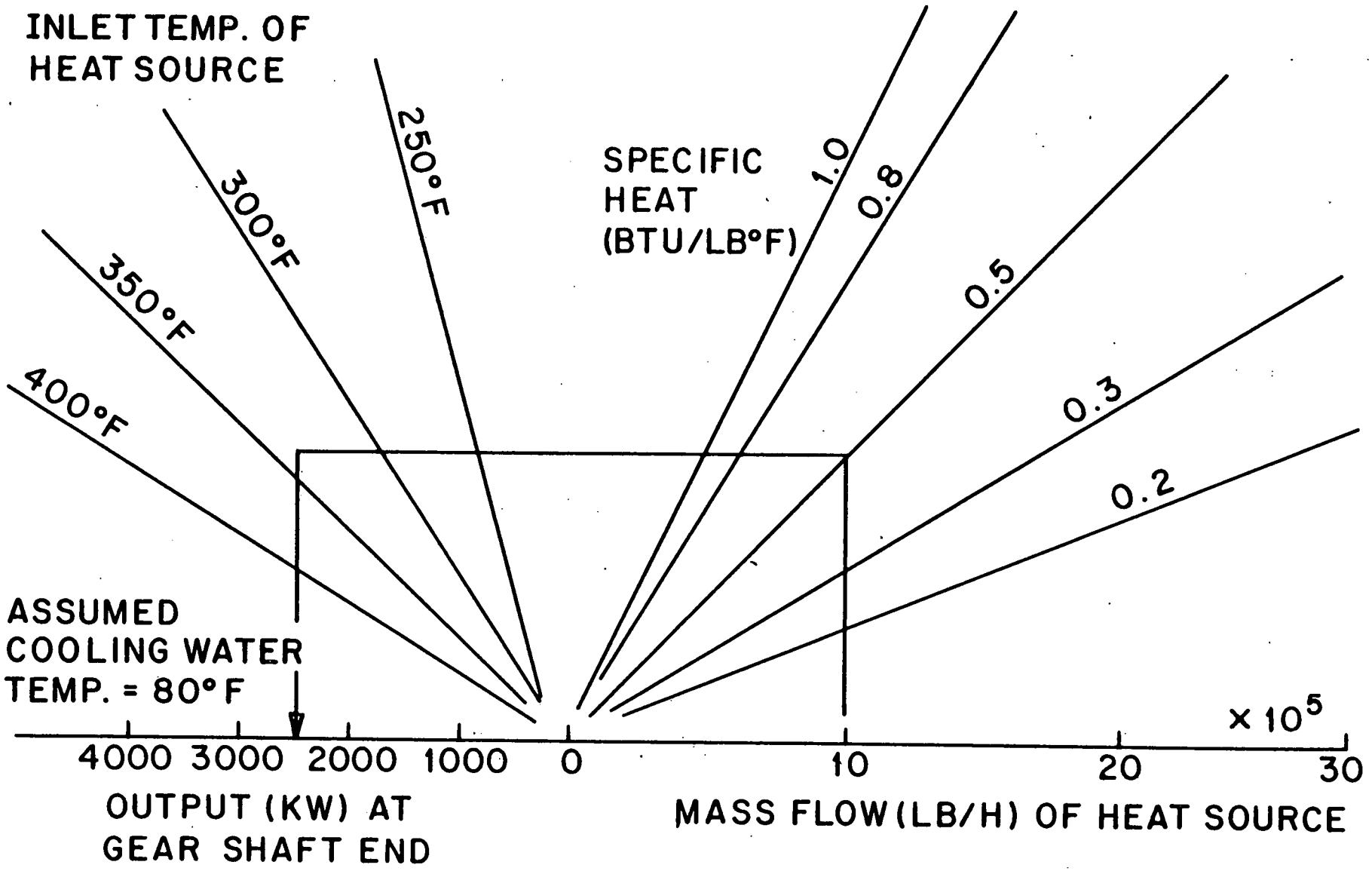

RECOVERED OUTPUT FROM LIQUID HEAT SOURCE

Fig. 5

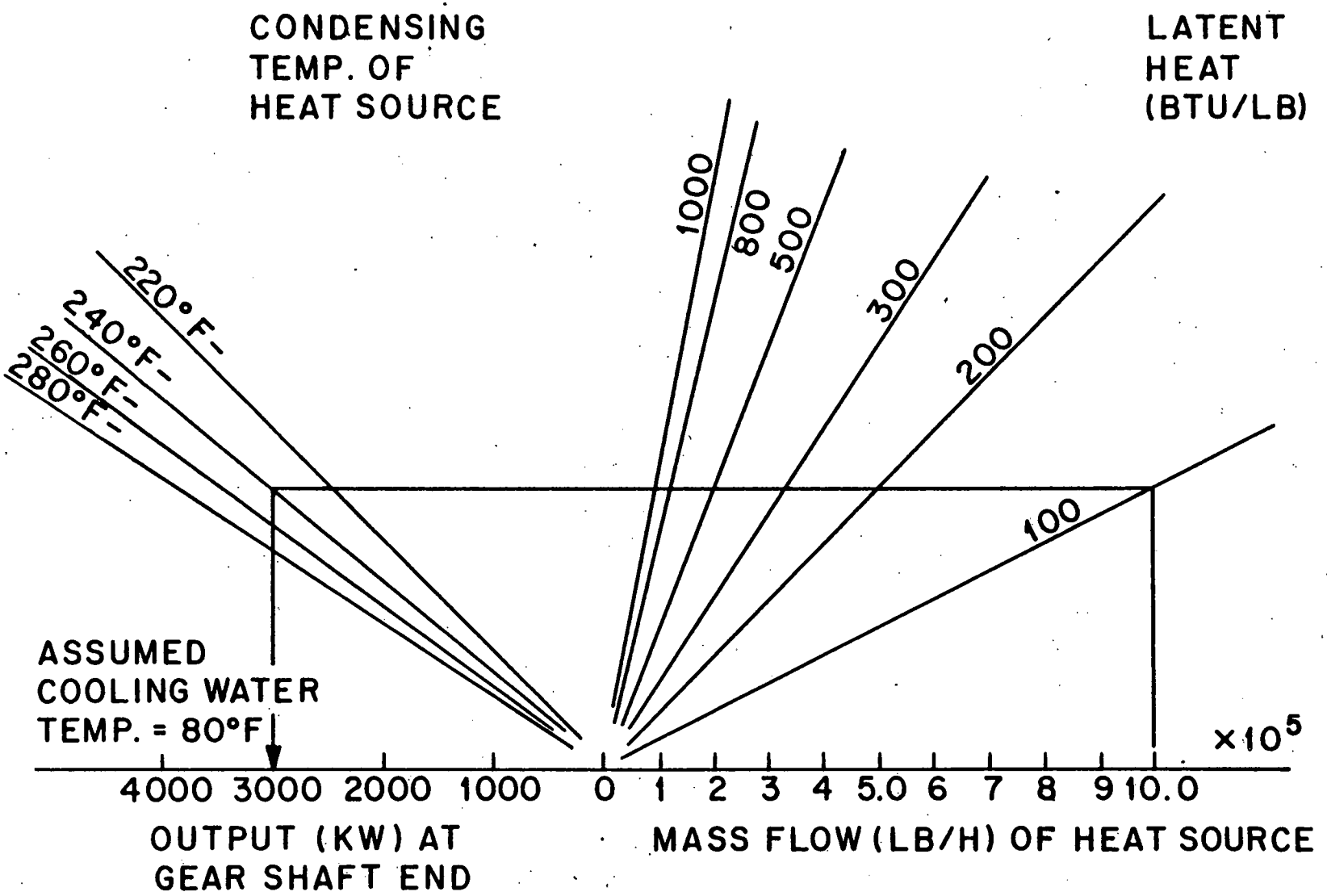

RECOVERED OUTPUT FROM CONDENSABLE HEAT SOURCE

Fig. 6

Table I shows the results of the power estimates. As can be seen in the table, this analysis indicates that 6 MW of power can be generated using AFI's hardware.

Our analysis of all heat exchangers in the Oil/Gas Complex shows that most of the rejected waste heat is removed from gas streams. Currently AFI does not market systems which can use this heat source, but this is because their market thrust is toward retrofitting in existing installations rather than application at the design stage of a new plant. When looking at the economics of the ORC in a new design, credit must be taken for the heat exchanger which would have otherwise been needed to remove the heat. This credit will make the ORC utilizing a gas heat source economically attractive.

Barber-Nichols Engineering Company (Refs. 6 and 7) has constructed a generalized curve showing the evaluation of Rankine Cycle efficiency with maximum cycle temperature for various working fluids as shown in Figure 7. It is on this curve that output power has been made for the ORC system utilizing a gas as a heat source. Sample calculations are given in Appendix A. All results are shown in Table II. The results of Table II show that by incorporating an ORC in every potential gas stream over 30 megawatts of power can be generated.

4. Cost Analysis

Only a rough figure of $1000/KW for the ORC systems has been obtained through personal conversations with a representative of Allied Chemical.[17] Installation costs have been kept at a minimum because of a modular installation approach and is estimated to be 20% of the capital

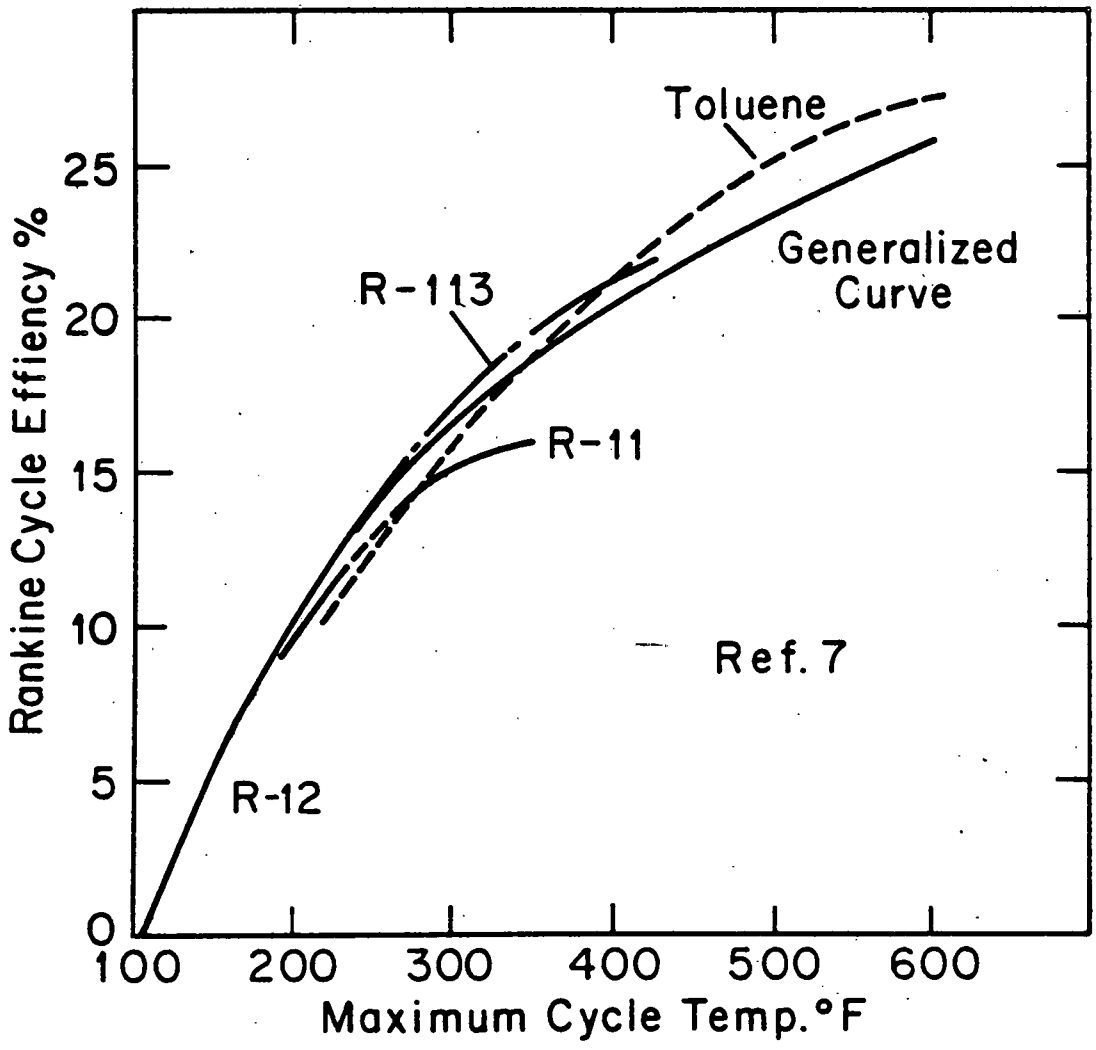

FIGURE 7. RANKINE CYCLE EFFICENCY

Table I - Output Potential-AFI Energy Systems

Item	Description	Specific Heat BTU/lb-°F	Mass Flow lb/hr	Temp. of Source °F	Output KW	Costs $/KW	Costs $
12-1301	slurry vapor condenser air	0.45	46,340	450	500	1200	600,000
12-1302	slurry vapor water condenser	0.45	44,500	260	1900	1200	2,280,000
12-1307(8)	Hp separator liquid coolers	0.41	224,740	300	500	1200	600,000
13-1301	dried vapor cooler	0.65	74,000	460	900	1200	1,080,000
14-1308	naptha air cooler	0.65	199,600	280	600	1200	720,000
14-1314	fuel oil air cooler	0.45	942,413	300	1400	1200	1,680,000
16-1307(8)	product coolers	0.57	106,500	270	500	1200	600,000
				TOTAL	6300 KW	1200	$7,560,000
				Heat Exchanger Costs --			$1,843,500
				Net Investment --			$5,716,500
				Or Installed Cost of --			$ 910/KW

Table II - Power Output-Barber and Nichols

Item	Description	Mass Flow lb/hr	Temp. of Source °F	Power Generated KW
12-1305	Hp separator vapor air cond.	605,700	300	5400
16-1303	effluent air cooler	325,350	280	900
17-1304	amine cond.	153,500	230	2500
18-1303	methanation comp. 1st stage discharge	294,300	290	1300
18-1304	methanation comp. 2nd stage intercooler	294,300	250	900
18-1308	methanation effluent air cooler	305,314	305	2200
18-1315	SNG comp. 1st stage discharge intercooler	277,295	235	800
21-1302(3)	shift gas coolers	2,019,162	260	8200
24-1307(8)	fuel gas coolers	2,213,382	300	7900
			TOTAL	30,100

★U.S. GOVERNMENT PRINTING OFFICE:1979-640-092/ 672

investment.[17] The installed cost is therefore approximately $1200/KW for systems utilizing a liquid or condensable vapor heat source. The capital investment required, shown in Table I, is 7.5 million dollars. The total replacement heat exchanger cost was found to be 1.8 million dollars. Taking the heat exchanger costs as a savings the net investment is 5.7 million dollars or $910/KW. It is assumed that the same cost will be realized with ORC's utilizing gas as a heat source when credit is taken for the replacement heat exchangers.

Figure 8 presents cost curves which were extrapolated from cost curves given in Reference 6. These curves forecast the installed costs of Rankine Cycles for production units. The costs for the Rankine system include all the components necessary to produce shaft power and, in addition, the generator and associated controls to result in electrical power generation. The additional cost to the cooling tower because of larger cooling requirements are not given in this figure.

These curves assume a 100% installation cost and a 6% escalating rate from 1976. From this figure, the installed cost of replacement Rankine Cycles was estimated based on the cycle output and maximum cycle temperature. The cost estimates are given in Table III. Sample calculations are given in Appendix B of the report.

Table III is a summary of the results of the ORC feasibility analysis for all heat exchangers in the Oil/Gas Design. This table gives the feasibility of replacement in column one and the type of feasible exchangers in column two. Column three gives the estimated power output of each replacement cycle. The estimated installed costs are given in columns four and five, column 4 is AFI's estimated costs and column 5 is

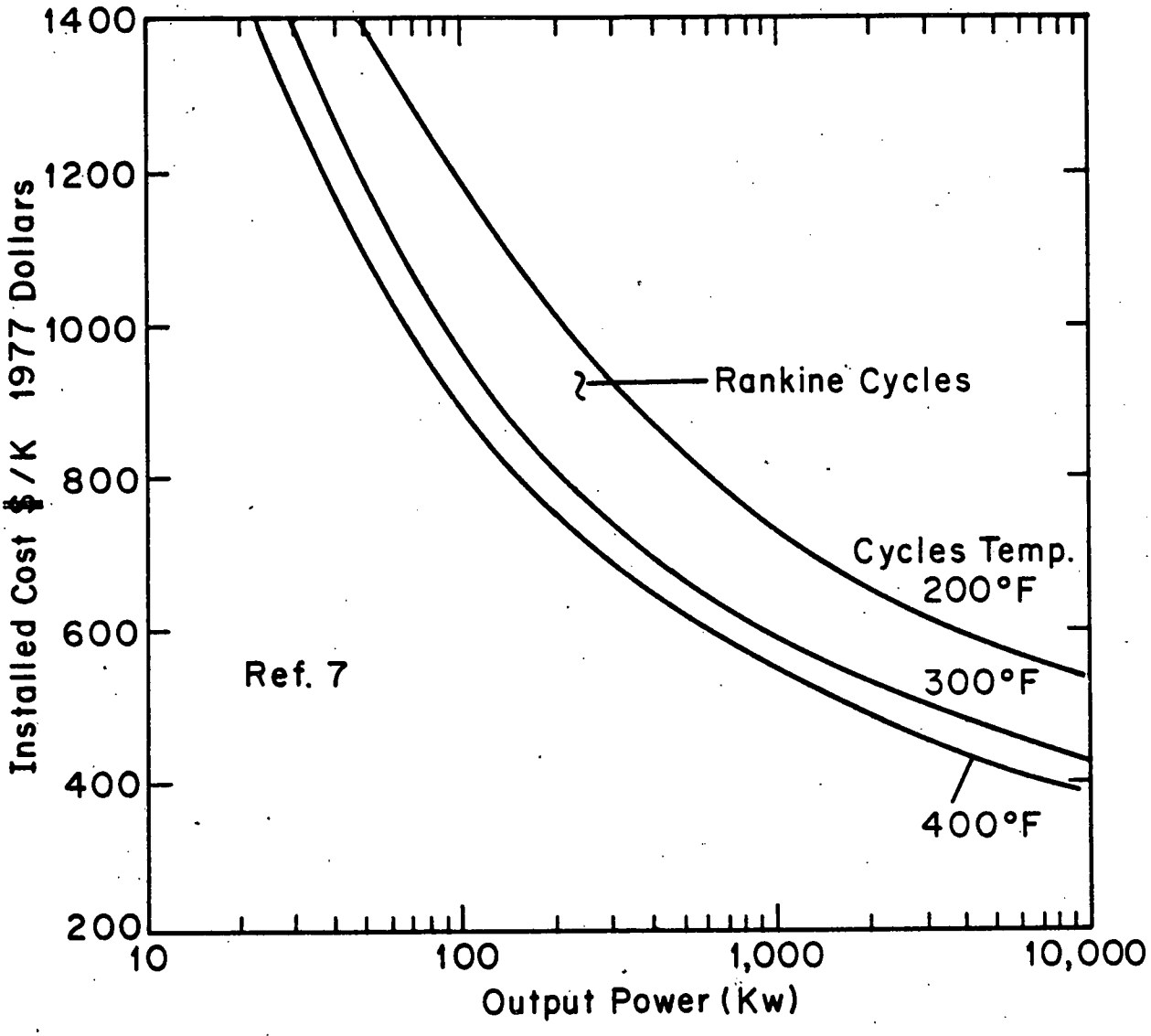

FIGURE 8. ESTIMATED INSTALLED COSTS FOR RANKINE CYCLES

Table III - Summary of ORC Analysis

Item	Description	Feasibility	Type	Power Generated KW	Installed Costs AFI ($/KW)	Installed Costs B & N	Remarks
12-1301	slurry vapor air condenser		steam-air	500	1200	725	
12-1302	slurry vapor water condenser		steam-air	1900	1200	650	
12-1310 12-1340	Hp separator slurry feed exchangers	rejected					Process Hx
12-1370		rejected					Process Hx
12-1313	Hp separator slurry OH cond. Hx	rejected					Process Hx
12-1314	Hp separator slurry steam gen.	rejected					Process Hx
12-1303	Hp separator vapor Feed Gas Hx	rejected					Process Hx
12-1304	Hp separator OH vapor steam gen.	rejected					Process Hx
12-1305	Hp separator OH vapor air condenser		gas-air	5400		500	
12-1306	Hp separator OH liq. steam gen.	rejected					Process Hx

Table III - Summary of ORC Analysis

Item	Description	Feasibility	Type	Power Generated KW	Installed Costs AFI ($/KW)	Installed Costs B & N	Remarks
12-1307	Hp separator OH liq. air cooler		Liquid-air	500	1200	625	Process Hx
12-1308	Hp separator OH liq. water cooler						+12-1307
12-1309	Hp separator OH Cond. H_2O cooler	rejected					Temp. too low
12-1315	Hp flash vapor steam generator	rejected					Process Hx
12-1316	Hp flash vapor air condenser	rejected					Output too low
12-1317	Hp flash vapor water condenser	rejected					Output too low
12-1318	1st IP flash vapor steam generator	rejected					Process Hx
12-1319	1st IP flash vapor air condenser	rejected					Output too low
12-1320	2nd IP flash vapor steam generator	rejected					Process Hx
12-1321	2nd IP flash vapor air condenser	rejected					Output too low
12-1322	LP flash vapor air condenser	rejected					Output too low
12-1324	LP vent gas condenser	rejected					Output too low

Table III - Summary of ORC Analysis

Item	Description	Feasibility	Type	Power Generated KW	Installed Costs AFI ($/KW)	Installed Costs B & N	Remarks
13-1301	Dried vapor cooler		liquid-air	900	1200	580	
13-1302	Recycle wash oil preheater	rejected					Process Hx
13-1601	Drier WHB #1	rejected					Process Hx
13-1602	Drier WHB #2	rejected					Process Hx
14-1305	Hy. Dist. PA/ Lt. Dist. Reboiler	rejected					Process Hx
14-1301	Hy. Dist. PA Feed Exchanger	rejected					Process Hx
14-1302	Hy. Dist. PA Steam generator	rejected					Process Hx
14-1307	Fract. OVHD/ Steam generator	rejected					Process Hx
14-1303	Lt. Dist. PA Steam generator	rejected					Process Hx
14-1306	Fract. Bottoms/ Hy. Dist. reboiler	rejected					Process Hx
14-1401	Main Fact. charge furnace	rejected					Process Hx
14-1304	Fract. Bottoms/ Feed exchanger	rejected					Process Hx
14-1308	NAPHTHA air cooler		liquid air	600	1200	675	

Table III - Summary of ORC Analysis

Item	Description	Feasibility	Type	Power Generated KW	Installed Costs AFI ($/KW)	Installed Costs B & N	Remarks
14-1315	ATM. Bottoms/ 600 psig steam gen.	rejected					Process Hx
14-1312	Fuel oil/150 psig steam generator	rejected					Process Hx
14-1313	Fuel oil/150 psig steam generator	rejected					Process Hx
14-1314	Fuel oil air cooler		liquid-air	1400	1200	590	
14-1309	OVHD. vapor interm. air cooler	rejected					Temp. too low
14-1310	OVHD. vapor air cooler	rejected					Temp. too low
16-1302	Charge heater	rejected					Process Hx
16-1301	Feed-effluent exchanger	rejected					Process Hx
16-1303	Effluent air cooler		gas-air	900		650	
16-1304	Stabilizer feed-bottoms exchanger	rejected					Process Hx
16-1307	Product air cooler		liquid-air	500	1200	725	
16-1304	Stabilizer OVHD air cooler	rejected					Output too low
16-1308	Product water trim cooler		liquid-H_2O				+16-1307

Table III - Summary of ORC Analysis

Item	Description	Feasibility	Type	Power Generated KW	Installed Costs AFI ($/KW) B & N	Remarks
16-1306	Stabilizer reboiler	rejected				Process Hx
19-1301	Feed effluent Hx	rejected				Process Hx
19-1302	Effluent cooler	rejected				Output too low
17-1301	Gas/Gas Hx	rejected				Process Hx
17-1302	Amine cooler	rejected				Process Hx
17-1303	Amine exchanger	rejected				Process Hx
17-1304	Amine condenser		gas-air	2500	610	
17-1305	Amine reboiler	rejected				Process Hx
17-1306	Amine reclaimer	rejected				Process Hx
18-1301	Regeneration heater	rejected				Process Hx
18-1302	Regeneration cooler	rejected				Temp. too low
18-1303	Methanation comp. 1st stage discharge		gas-H_2O	1300	620	
18-1304	Methanation comp. 2nd stage discharge intercooler		gas-H_2O	900	710	
18-1305	Methanation feed/effluent fix	rejected				Process Hx
18-1401	Methanation start-up heater	rejected				Process Hx

Table III - Summary of ORC Analysis

Item	Description	Feasibility	Type	Power Generated KW	Installed Costs AFI ($/KW)	Installed Costs B & N	Remarks
18-1306	Methanation circulating oil boiler	rejected					Process Hx
18-1308	Methanation effluent air cooler		gas-air	2200		570	
18-1311	Polish methanator feed/effluent Hx	rejected					Process Hx
18-1402	Polish methanator start-up heater	rejected					Process Hx
18-1313	Polish methanator air cooler	rejected					Output too low
18-1315	SNG compressor 1st stage discharge intercooler		gas-H_2O	800		780	
18-1316	SNG comp. 2nd stage discharge cooler	rejected					Output too low
18-1314	Deethanizer comp. 1st stage discharge intercooler	rejected					Output too low
18-1317	Deethanizer cond.	rejected					Temp. too low
18-1318	Deethanizer reboiler	rejected					Process Hx
18-1319	Depropanizer cond.	rejected					Output too low
18-1320	Depropanizer re-boiler	rejected					Process Hx

Table III - Summary of ORC Analysis

Item	Description	Feasibility	Type	Power Generated KW	Installed Costs AFI ($/KW) B & N	Remarks
18-1321	Debutanizer cond.	rejected				Temp. too low
18-1322	Debutanizer re-boiler	rejected				Process Hx
20-1301	Steam superheater	rejected				Process Hx
20-1302	Oxygen preheater	rejected				Process Hx
20-1303	Quench water air cooler	rejected				Temp. too low
20-1601	Steam boiler	rejected				Process Hx
21-1601	170 psia waste heat boiler	rejected				Process Hx
21-1301	Boiler feed water preheater	rejected				Process Hx
21-1602	40 psia waste heat boiler	rejected				Process Hx
21-1603	25 psia waste heat boiler	rejected				Process Hx
21-1302	Shift gas air cooler		gas-air	8200	520	
21-1303	Shift gas water trim cooler		gas-H_2O			+21-1302
24-1301	Quench water air cooler	rejected				Temp. too low

Table III - Summary of ORC Analysis

Item	Description	Feasibility	Type	Power Generated KW	Installed Costs AFI ($/KW)	Installed Costs B & N	Remarks
24-1302	Air/fuel gas HX #1	rejected					Process Hx
24-1303	Fuel gas-1200 psi steam generator	rejected					Process Hx
24-1304	Air/fuel gas HX #2	rejected					Process Hx
24-1305	Fuel gas-150 psi steam generator	rejected					Process Hx
24-1306	Fuel gas-25 psi steam generator	rejected					Process Hx
24-1307	Fuel gas air cooler		gas-air	7900		490	
24-1308	Fuel gas water cooler		gas-H_2O				+24-1307
26-1302	Reboiler	rejected					Process Hx
26-1351	Solution Hx	rejected					Process Hx
26-1352	Solution cooler	rejected					Process Hx
26-1353	NH_3 stripper condenser	rejected					Process Hx
26-1354	NH_3 stripper cooler	rejected					Process Hx
26-1355	NH_3 stripper reboiler	rejected					Process Hx
26-1356	NH_3 condenser	rejected					Process Hx

Table III - Summary of ORC Analysis

Item	Description	Feasibility	Type	Power Generated KW	Installed Costs AFI ($/KW)	Installed Costs B & N	Remarks
32-1311	Condenser	rejected					Process Hx
32-1312	Condenser	rejected					Process Hx
32-1313	Condenser	rejected					Process Hx
32-1315	Condenser	rejected					Process Hx
32-1316	Condenser	rejected					Temp. too low
32-1317	Condenser	rejected					Temp. too low
12-1323	LP flash vapor air condenser	rejected					Potential too low
Total 110 Hx			Total	36,400	1200	560	
18-Used			Less Hx Investment	-12,040,260	910	230	
			Plus Cooling Tower Costs	+ 2,300,000	985/KW	300/KW	

the estimated costs from Reference 7. The last column gives reasons for rejection of heat exchanger replacement.

The total results shown in page 27 of the table, indicates that 36 megawatts of power can be generated. The costs for the ORC is estimated to be around $1200/KW using AFI's data and $560/KW using the data from Reference 7. When credit is taken for the replaced heat exchangers and an adjustment made for the increased cooling tower costs the AFI estimate drops to $985/KW and $300/KW for Reference 7 costs.

Although the AFI estimates indicate the current costs of ORC for waste heat utilization, the costs from Reference 7 indicate the potential costs of the ORC given the appropriate demand. Given this range it is therefore necessary to perform a return on investment sensitivity analysis to demonstrate the potential ROI for various investment costs and selling prices.

4.1 DCF Sensitivity Analysis

A discounted cash flow analysis has been performed on varying sizes of ORC for different investment costs and electricity exporting rates and the results are shown in Figures 9 and 10. Figure 9 assumes a $.025/KW-hr exporting rate escalating 8% per year for 10 years. Figure 10 assumes a $.01/KW-hr exporting rate escalating 6% per year for 10 years. Assumptions used for the basis of this analysis are in accordance with the Gas Cost Guidelines used in the Oil/Gas Complex and are shown in Appendix B.[11]

The cost curves of Figure 8 were used as a basis for this analysis. The capital investment was taken directly from Figure 8 for curve B in Figure 9 (B and C), the most optimistic curve. The capital investment for the pessimistic outlook, curves (A and D) was assumed to be a 100%

increase in the curve of Figure 7. This analysis does take credit for replacement heat exchangers.

The expected ROI for two ORC manufacturers is also given in the figure. One is AFI at $985/KW and the other is Sundstrand Corporation, a 600 KW waste heat recovery ORC utilizing heat source temperatures above 550°F. The Sundstrand systems installed cost is $800/KW, with a mass production projection of $400/KW.

5. Discussion of ORC

The results and conclusions presented here concerning Organic Rankine Cycles are not necessarily (restricted) to coal conversion plants but can be expanded to any inudstry in which low level heat is being wasted.

By replacing air coolers and water coolers with Organic Rankine Cycles, waste heat can be utilized to produce useful electrical or shaft power. All ORC presented in this report are within the realm of technological development of Rankine Cycles. In addition to AFI Energy Systems and Sundstrand's experience, many other U.S. firms have applied considerable effort to the development of Organic Rankine Cycles for various applications. Table IV, not intended to be an all inclusive list, gives a summary of some of the companies working on ORC.

Most applications of the Organic Rankine Cycle are of a prototype nature at the present time and therefore costs are substantially higher than the estimates presented here. In some cases the costs are as high as $2000/KW-$3000/KW, but all manufacturers forecast price declines given the appropriate demand. AFI's and Sundstrand's cycles

Table IV

	Manufacturer	Type of Fluid	Type of Expander	Type of Application	Expander Inlet °F/PSIA	Rated Power Hp
1.	Aerojet-Liquid Rocket	AEF-78	Turbine	Automobile	650/1000	74.9
2.	Barber-Nichols	R-113	Turbine	Solar Cooling	200/57	2.7
3.	Barber-Nichols	R-113	Turbine	Solar Irrigation	920/221	25.0
4.	Fairchild-Hiller	FC-75	Turbine	Total Energy Plant	428/206	25.34
5.	Kinetics	R-113	Rotary	Automobile	375/355	47.0
6.	Kinetics	R-114	Rotary	Solar Cooling	200/180	7.5
7.	Ormat	MCB	Turbine	Power Pack	variable	3.0
8.	Sundstrand Aviation	CP-25	Turbine	Total Energy Plant	825/195	134.1
9.	Sundstrand Aviation	Dowtherm A	Turbine	Power Pack	700/7	8.0
10.	Sundstrand Aviation	Tolvene	Turbine	Waste Heat Recovery	550/300	900
11.	Thermo-Electron	Fluorinol 85	Turbine	Automobile	600/700	145.5
12.	Thermo-Electron	Fluorinol 85	Turbine	Gas turbine bottoming plant	600/700	
13.	Thermo-Electron	Fluorinol 85	Turbine	Diesel engine bottoming plant	600/700	1,000
14.	United Aircraft	R-113	Turbine	Solar Cooling	200-375/70-340	4.3
15.	United Aircraft	R-114	Turbine	Solar Cooling	250-275/250-400	8.0

are currently being sold at reasonable costs with satisfactory rates of return given today's electricity costs.

These efforts and the efforts of numerous other companies indicate the cost estimates presented here are certainly within the time frame necessary for use in coal conversion plants.

6. Conclusions

Based on estimates and results presented in this report, the following conclusions are drawn:

1. The Organic Rankine Cycle is an energy effective to air and water cooled systems operating at temperatures above 200°F. In the Oil/Gas Complex 36 megawatts of electricity can be produced in an energy effective manner through recovery of the waste heat of air and water coolers.
2. Incorporating Organic Rankine Cycles into coal gasification designs will generate demand to lower production costs and, therefore, enable the ORC to become cost effective in a variety of other industries where waste heat is available. On a national level the energy savings potential is incredible.

7. Recommendations

This report is a preliminary analysis which pinpoints 18 heat exchangers throughout the Oil/Gas Complex, in which the rejected heat is sufficient to generate over 36 MW of power via Organic Rankine Cycles. It is therefore recommended that current manufacturers be contacted and steps taken to further engineer and incorporate Organic Rankine Cycles into the Oil/Gas design.

8. References

1. Van Wylen, Sonntag, "Fundamentals of Classical Thermodynamics", 2nd edition, John Wiley and Sons, Inc., New York, 1973.

2. Gagiolo, Pitit, "Second Law Analysis, for Pinpointing the True Inefficiencies in Fuel Conversion Systems", Mechanical Engineering Dept., Marquette University, Milwaukee, Wisconsin 53233.

3. Morgan, D. T., Davis, V. P., Newton, C. L. and Stonehocker, V. T., "High Efficiency Diesel/Organic Rankine Cycle Combined Power Plant", ASME 75-DGP-13, April 1975.

4. Morgan, D. T., Davis, J. P., "High Efficiency Gas Turbine/Organic Rankine Cycle Combined Power Plant", ASME 74-GT-35, April 1974.

5. Steinlicht, B., "Low Level Heat Recovery Takes on Added Meaning as Fuel Costs Justify Investment", Power, April 1975.

6. Barber, R. E., "Rankine Cycle Systems for Waste Heat Recovery", Chemical Engineering, November 25, 1974.

7. Barber, R. E., "Solar Powered Organic Rankine Cycle Engines-Characteristics and Costs", 11th IECEC Proceedings, Sept., 1976-769200.

8. Lewis, G. P., Smith, R. D., Harkness, W. P., and Yamada, M., "Sulfuric Acid Plant Rankine Cycle Waste Heat Recovery", 11th IECEC Proceedings, Sept., 1976-769209.

9. DeGarmo, E. P. and Canada, J. R., "Engineering Economy", 5th Edition, The MacMillan Company, New York, 1973.

10. Popper, H., "Modern Cost Engineering Techniques", 1st Edition, McGraw-Hill Book Company, New York, 1970.

11. Oil/Gas Complex Conceptual Design/Economic Analysis, The Ralph M. Parsons Company.

12. Purcupile, J. C., "Energy Conservation in Coal Conversion", Carnegie-Mellon University, Pittsburgh, PA, 15213, August 1977.

13. Private communication with Ralph M. Parsons Company, February 1978.

14. Hittman Associates, Inc., "Assessment of the Rankine Cycle for Potential Application to Solar-Powered Cooling of Buildings", NTIS, August 1974.

15. Private communication with Mr. Michael Santucci of Sundstrand Corporation, Rockford, Illinois, February 1978.

16. Private communication with V. T. Morgon of Thermo-Electron, Waltham, Massachusetts, February 1978.

17. Private communication with J. C. Devol of AFI Energy Systems, Livingston, New Jersey, April 1978.

18. "The 3,800 KW FRON Turbine Power Generating System for Mizushima Plant of Mitsubishi Gas Chemical Company, Inc.", IHI Heavy Industries Company, Ltd., Tokyo, Japan, 1975.

Appendix A

Sample Calculations

Rankine Cycle Power Output

The High pressure Separator vapor air condenser (12-1305) is used as an example in these calculations to illustrate the method used in determining possible power output of the ORC.

Data

Heat Source Temp:	300°F
Heat Transfer:	123.3×10^6 BTU/Hr.
Mass Flow:	605,700 Lbm/Hr.

Assumptions

1. Boiler, regeneration and condenser have an effectiveness of 80%.

Sample Calculations

The heat transfer in the boiler is 123.3×10^6 BTU/Hr.

$$QB = 123.3 \times 10^6 \text{ BTU/Hr.}$$

Assuming boiler effectiveness of 80% the maximum cycle temperature is about 270°F.

$$Tmax = 270°F.$$

Using the generalized curve of Figure #7, the Rankine cycle efficiency is 15%.

$$y = 15\%$$

Multiplying the heat source from the boiler with the cycle efficiency

gives the power output of the cycle.

$$P = yQ_B = .15 \times 123.3 \times 10^6$$

$$= 18.5 \times 10^6 \text{ BTU/Hr.}$$

$$= 5{,}420 \text{ KW}$$

$$= 7{,}275 \text{ Hp}$$

Appendix B

1. Cost Analysis

The replacement rankine cycle for the air cooled system (12-1305) is used as an example for the cost analysis presented in this paper.

The installed cost of replacement rankine systems is estimated from the curves of Figure 8 using the estimated power output and cycle temperature calculated in Appendix A.

$$P_{out} = 5{,}400 \text{ KW}$$

$$T_{max} = 270°F.$$

From Figure 8 the installed cost is found to be \$500/KW

$$IC = \$500/KW$$

Since the total output possible is 5,400 KW the total installed cost is easily found.

$$(IC)_T = \$500/KW \times 5400$$

$$= \$2{,}700{,}000$$

Additional cost resulting from enlarging cooling tower capacity is estimated from data given in Reference 10.

$$\text{Cooling Tower Costs} = \$76{,}400$$

Heat exchanger costs were obtained from Reference 13.

$$\text{Hx Costs} = \$540{,}350$$

The net cost is found by adding the ORC installed cost plus the cooling tower costs minus the heat exchanger costs.

$$\text{Net Cost} = \$2{,}700{,}000 + 76{,}400 - 540{,}350$$

$$= \$2{,}236{,}050$$

$$\text{or} \quad \$415/KW$$

2. DCF - Sensitivity Analysis

A discounted cash flow analysis was performed for various capital investments and rates of electricity. The following is the assumptions used in constructing the curves of Figures 9 and 10.

All Curves

1. 20 year project life
2. Double-Declining Balance Depreciation
3. 48% federal income tax
4. $.003/KW-hr operation and maintenance costs
5. 8400 Hrs/year operating

Curve A - Pessimistic outlook

1. Capital Cost based on 100% increase of Fig. 8 with credit taken for replacement Heat Exchanger
2. Exporting rate for electric power is $.01/KW-hr escalating at a rate of 6% per year for 10 years

Curve B - Optimistic Outlook

1. Capital Cost based on Fig. 8 with credit taken for replacement Heat Exchanger
2. Exporting rate for electric power is $.025/KW-hr escalating at a rate of 8%/year for 10 years

Curve C

1. Capital Costs based on Fig. 8 with credit taken for replacement exchanger
2. Exporting rate of $.01/KW-hr escalating at a rate of 6%/year for 10 years

Curve D

1. Capital Costs based on 100% increase of Fig. 8 with credit taken for replacement exchanger
2. Exporting rate of $.025/KW-hr escalating at a rate of 8%/year for 10 years.

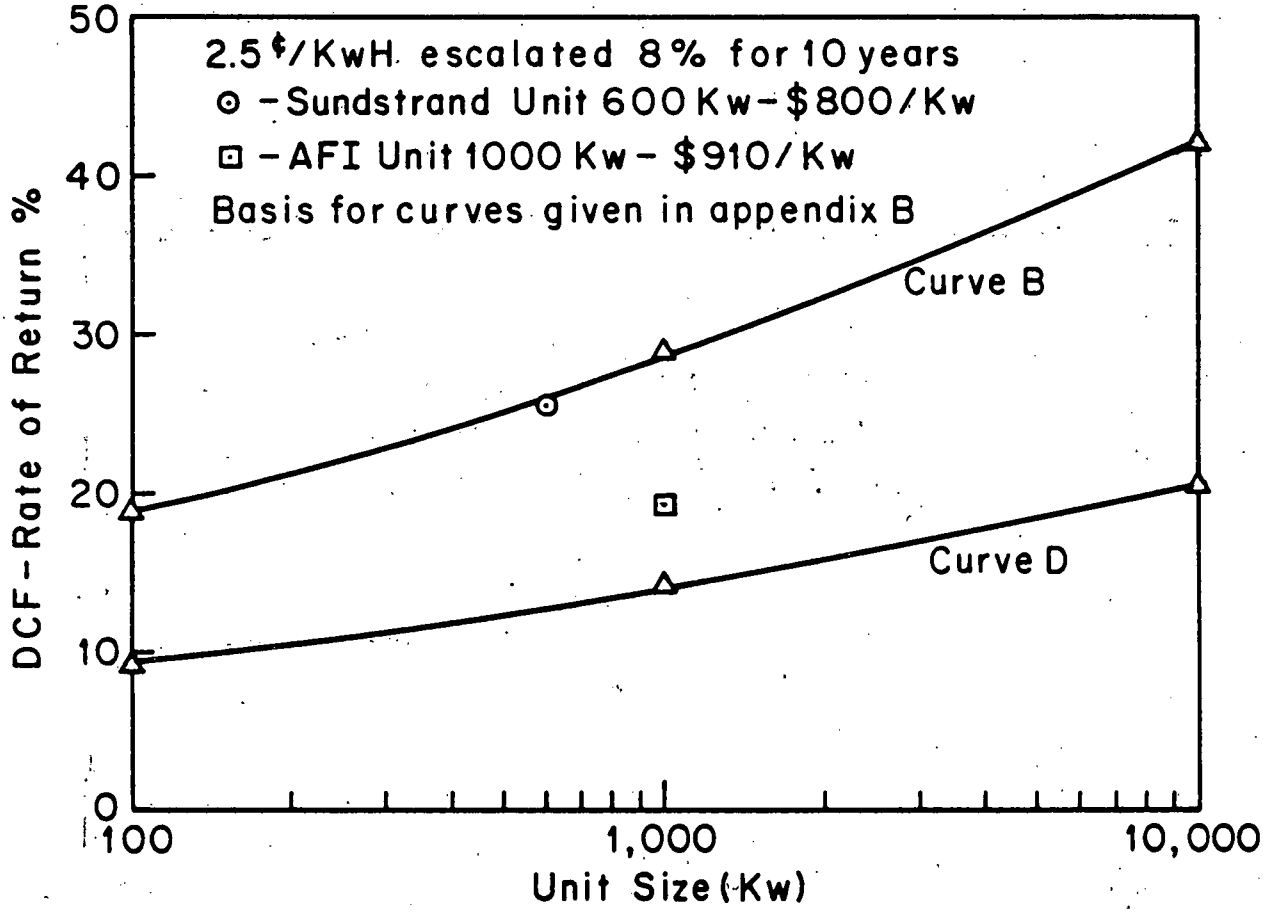

FIGURE 9. RATE OF RETURN VS CYCLE SIZE

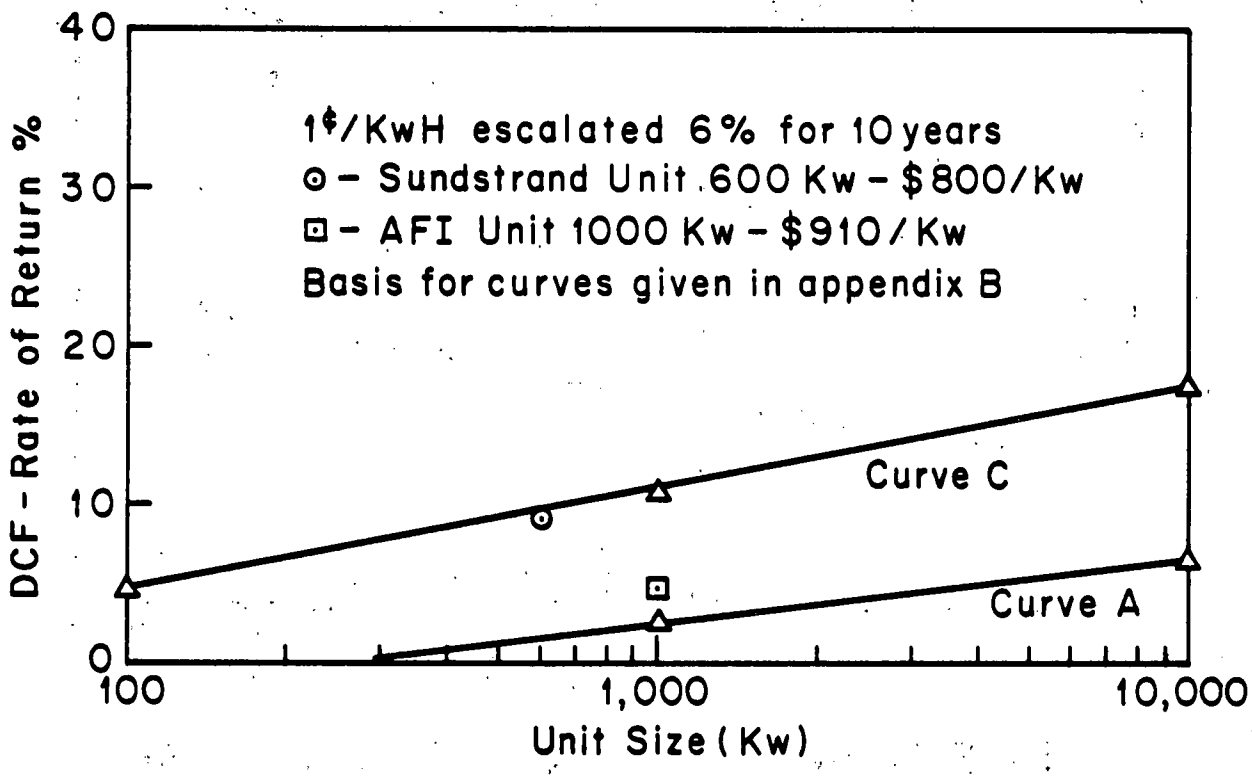

FIGURE 10. RATE OF RETURN VS CYCLE SIZE

ENERGY CONSERVATION IN COAL CONVERSION

Alternate De-Ethanizer Refrigeration System to Conserve Energy

A Case Study

L. Fucich

Carnegie-Mellon University
Pittsburgh, PA 15213

June, 1978

Prepared for

THE U.S. DEPARTMENT OF ENERGY
Pittsburgh Energy Technology Center
UNDER CONTRACT NO. EY77S024196

ABSTRACT

This study examines an alternate system to cool an ethane gas stream from the fractionator in Unit 18 of the Parsons Oil/Gas Complex. This alternate will save 2.6 x 10^5 Btu/hr of energy or .25 short TPD of coal which is a fraction of a percent of the 36,000 TPD of coal used in the Oil/Gas Complex. The installed cost of the alternate system is $151,000 with an operating and maintenance cost of $7550/yr. Assuming a 20-year life, 9% interest rate on borrowed capital, and an electricity cost of $.025/KW-hr, the Life Cycle Cost of the new system is -$179,000 over a 20-year period which shows that more money is spent installing new equipment than is realized from electricity savings. Using a Discounted Cash Flow Analysis, the Return on Investment is 0%.

ACKNOWLEDGEMENT

I would like to thank T. S. Govindan of the DuPont Company for his contributions to this study.

TABLE OF CONTENTS

INTRODUCTION

The de-ethanizer condenser (Unit 18-1317) in the Parsons Oil/Gas Complex cools an ethane gas stream from 53°F to 26°F. The cold side stream of this condenser is -40°F propane. The heated propane is piped to a storage tank, and a refrigeration unit maintains the tank at -40°F. Therefore, the heat added to the propane must be transferred from -40°F to ambient temperature (100°F) by the storage tank refrigeration unit.

The purpose of this study is to determine the energy savings resulting from a refrigeration unit to cool the ethane gas stream from 53°F to 26°F.

ENERGY SAVINGS FOR THE ALTERNATE REFRIGERATION SYSTEM

Assuming an effectiveness of .8[7] for the evaporator, the required evaporator temperature is 19°F for the alternate refrigeration system to cool the ethane stream from 53°F to the required 26°F. This results in a higher COP than the present system which must transfer heat from a -40°F reservoir. From Appendix A, the actual COP for the alternate system is 2.55 and for the required refrigeration effect of 1.3×10^6 Btu/hr (see Appendix B), 200 Hp is required[9]. The present system has a calculated COP of 1.7 and for the same refrigeration effect requires 302 Hp. Therefore, the power requirement for the alternate refrigeration system is 102 Hp or 76 KW less than the present system.

ECONOMIC ANALYSIS

The savings in electricity for a 76 KW reduction in power for the alternate system is $15,050 per year or $301,000 over 20 years assuming an electricity cost of $.025/KW-hr[10]. The installed cost of the alternate system is $151,000 and annual operating and maintenance costs are assumed to be 5% of the installed cost or $7,550. If the capital is borrowed at 9% the 20-year life cycle cost is -$179,000. The calculations and assumptions for computing the life cycle cost are given in Appendix C.

A discounted cash flow analysis was also performed. For the investment of $151,000, a rate of return of 0% is obtained. The basis for the DCF analysis are given in Appendix C.

CONCLUSIONS

For a capital investment of $151,000 and an annual operating and maintenance cost of $7,550, 601,920 KW-hrs, or $15,050 of electricity are saved annualy. This represents a 0% rate of return on investment, and a life cycle cost of -$179,000 over the 20 year life.

REFERENCES

1. "Oil/Gas Complex Conceptual Design/Economic Analysis", R & D Report No. 114 - Interim Report No. 4, The Ralph M. Parsons Company, March, 1977.

2. Van Wylen, Sonntag, "Fundamentals of Classical Thermodynamics", 2nd edition, John Wiley and Sons, Inc., New York, 1973.

3. Woods, D. R., Anderson, S. J., and Norman, S. L., "Evaluation of Capital Cost Data: Heat Exchangers", The Canadian Journal of Chemical Engineering, Vol. 54, December, 1976.

4. ASHRAE, "Thermodynamic Properties of Regrigerants", 1969.

5. Gunther, R. C., "Refrigerating, Air Conditioning, and Cold Storage", 2nd edition, Chilton Book Company, Philadelphia, 1969.

6. Conversation with Dr. J. F. Osterle, Carnegie-Mellon University, Pittsburgh, PA, June 8, 1978.

7. Holman, J. P., "Heat Transfer", Fourth edition, McGraw-Hill Book Company, New York, 1976.

8. Newnan, D. G., "Engineering Economic Analysis", Revised edition, Engineering Press, California, 1977.

9. Conversation with J. Fergurson, York Division, Borg-Warner Corp., Philadelphia, PA, June 14, 1978.

10. Section XII, Basis for Fuel and Utility Costs, Energy Conservation in Coal Conversion, June 1978.

APPENDIX A

COP Calculations

For the refrigeration effect required, 1.3×10^6 Btu/hr (from Appendix B) and the work input of 200 Hp (5.1×10^5 Btu/hr) given by reference 9, the actual COP is:

$$COP_1 = \frac{Q}{W}$$

$$= \frac{1.3 \times 10^6 \text{ Btu/hr}}{5.1 \times 10^5 \text{ Btu/hr}}$$

$$= 2.55$$

Since the only data known for the present refrigeration system is the heat load (1.3×10^6 Btu/hr), ambient temperature (100°F), and storage tank temperature (-40°F), the theoretical COP will be adjusted using a rule of thumb to arrive at a realistic value. The coefficient of performance can be written:

$$COP = \frac{T_L}{T_H - T_L}$$

To determine a realistic value of the COP, 20°F is subtracted from the low temperature reservoir or T_L = -40° - 20° = -60°F = 400°R. 20°F is added to the high temperature reservoir, T_H = 100°F + 20°F = 580°R, and to account for inefficiencies, the COP is multiplied by .75. This can be written:

$$COP_2 = .75 \left[\frac{400°R}{580°R - 400°R} \right] = 1.7.$$

APPENDIX B

Calculation of the Heat Load, Evaporator Temperature and Refrigeration Work

The mass flow of the gas stream to be cooled , the components, and the entering and exiting temperature and pressure are tabulated below. With this information the heat load or refrigeration effect can be calculated. From the first law of thermodynamics:

$$Q = \dot{m}_1 (\Delta h_1) + \dot{m}_2 (\Delta h_2) + \dot{m}_3 (\Delta h_3)$$

where:

Q = refrigerating effect (Btu/hr)

$\dot{m}$ = mass flow (lb/hr)

Δh = change in enthalpy (Btu/lb)

The following table shows the components of the gas stream, their percent composition, respective mass flows, h_1, h_2, Δh and Q from each component[5].

CHEMICAL COMPONENTS	PERCENT COMPOSITION	MASS FLOW ($\dot{m}$) lb/hr	ENTHALPY (h_1) Btu/lb	ENTHALPY (h_2) Btu/lb	Δh $h_1 - h_2$	$Q = \dot{m}(\Delta h)$ Btu/hr
Methane (CH_4)	5.6%	5,849	- 1544.3	- 1558.9	14.6	85,395
Ethane (C_2H_6)	66 %	68,934	- 844.9	- 856.8	11.9	820,315
Propane (C_3H_8)	28.4%	29,245	53.7	40.4	13.3	388,959
TOTAL HEAT REJECTED						1,294,669

Enthalpies are based on the following temperatures and pressures:[4]

$$T_1 = 53°F \; ; \; P_1 = 216 \text{ psia}$$
$$T_2 = 26°F \; ; \; P_2 = 211 \text{ psia}$$

The refrigeration effect required is:

$$Q = 1.3 \times 10^6 \text{ Btu/hr.}$$

Evaporator Temperature Calculation

Assuming the effectiveness of the evaporatorto be $\varepsilon = .8$, we have:

$$\varepsilon = \frac{T_1 - T_2}{T_1 - T_L}$$

$$.8 = \frac{53°F - 26°F}{53°F - T_L}$$

or $T_L = 19°F$.

Refrigeration Work Required

Using the values of COP determined in Appendix A the work load of the present refrigeration unit can be determined by using the definition of COP.

$$W = \frac{1.3 \times 10^6 \text{ Btu/hr}}{1.7} = 7.7 \times 10^5 \text{ Btu/hr}$$

$$\doteq 302 \text{ Hp.}$$

For the alternate system the work input is given as 5.1×10^5 Btu/hr[9]. The energy saved by installing the alternate system is:

$$7.7 \times 10^5 \text{ Btu/hr} - 5.1 \times 10^5 \text{ Btu/hr} = 2.6 \times 10^5 \text{ Btu/hr (76 KW)}$$

Assuming the coal used in the Oil/Gas Complex has a heating value of 12,125 Btu/lb[1], this presents a saving in coal consumption of:

$$\frac{2.6 \times 10^5 \text{ Btu/hr}}{12{,}125 \text{ Btu/hr}} (24 \text{ hr/day}) = 515 \text{ lb/day} \simeq 1/4 \text{ short ton/day (TPD).}$$

This is only a fraction of a percent of the 36,000 TPD[1] used in the entire complex.

APPENDIX C

Economic Calculations

Life Cycle Cost

The electricity cost savings over 20 years, with 330 full stream days/yr[1], and assuming electricity costs $.025/KW-hr is:[10]

$$(20\ yr)(2.6 \times 10^{5}\ Btu/hr)(2.928 \times 10^{-4}\ KW\text{-}hr/Btu) \times$$
$$(330\ day/yr)(24\ hr/day)(\$.025/KW\text{-}hr) = \$301,467$$

Savings = $301,000.

The cost of equipment, installation, operation, and maintenance for the alternate refrigeration system is based on the following assumptions:

1) Interest rate on borrowed money is 9%.
2) 20-year life with no salvage value[1].
3) Installation is 40% of equipment cost[3].
4) Operational and maintenance is 5% of installed cost.

The following lists give design specifications and equipment costs of the de-ethanizer condenser to be removed and the new refrigeration system to be installed.

De-ethanizer Condenser

Item number: 18-1317[1]

Heat Load: 1.3×10^{6} Btu/hr

Surface Area: 1,230 ft^2 [1]

Installation Cost: $24,000[1]

Alternate Refrigeration System

Heat Load: 1.3×10^6 Btu/hr (110 tons)

Power requirement: 200 Hp[9]

COP: 2.55

Evaporator Temp.: 19°F

Ambient Temp.: 100°F

Equipment Cost: $125,000[9]

The total installed cost of equipment with credit taken for the existing condenser is:

$$\$125,000(1.4) - \$24,000 = \$151,000$$

If this money is borrowed at 9% interest, the uniform annual payments for the loan using the Capital Recovery Factor (CRF) are:[8]

$$\$151,000(.1095) = \$16,535/yr$$

Annual operation and maintenance cost is:

$$\$151,000(.05) = \$7550/yr.$$

The total cost of installation, maintenance and operation is:

$$\$16,535 + \$7550 = \$24,085/yr$$

Therefore, the total cost over 20 years is:

$$\$480,000.$$

The Life Cycle Cost (LCC) is the total saving - the total costs, or in this case:

$$\$301,000 - \$480,000 = -\$179,000.$$

Discounted Cash Flow Analysis

With a cost of electricity of $.025/KW-hr, capital cost of $151,000, net cash flow of $7,523, and the assumptions below, the rate of return on investment can be calculated.

Assumptions:

1) 20 year project life
2) 16 year SYD depreciation (sum-of-year-digits)
3) 0% tax rate since the revenues result in a decrease in electricity use
4) No investment tax credit
5) 100% equity

The discounted cash flow formula is given as:

$$C_o = \sum_{n=1}^{N} \frac{C_n}{(1+r)^n}$$

where:

C_o is the capital cost

C_n is the annual net cash flow

N is the project life

r is the rate of return

For this problem we have:

C_o = $151,000

C_n = Annual revenues from savings in electricity - annual operation and maintenance costs

= $15,073 - $7,550

= $7,523

N = 20

Solving for the rate of return, r by interpolating, we get:

r = -.04% or r = 0%

2 ENERGY CONSERVATION IN COAL CONVERSION

1 Feasibility Study of a Combined Combustion-Gasification Facility

Keith R. Knestaut

Carnegie-Mellon University
Pittsburgh, PA 15213

June, 1978

Prepared for

THE U.S. DEPARTMENT OF ENERGY
Pittsburgh Energy Technology Center
UNDER CONTRACT NO. EY77S024196

ABSTRACT

This work examines the feasibility of mechanical deep cleaning of coal where the cleaned coal would be used for direct combustion and the rejected portion would be used in a coal gasification plant. To make this feasible, the reduced thermal efficiency from gasifying "dirty coal" must be offset by the reduced energy requirement for the flue gas desulfurization system.

Our study indicated, for the coal being considered for the Parsons Oil/Gas Complex - Illinois No. 6 - the energy saved by reduced flue gas desulfurization was approximately equal to the energy lost from gasifying the dirty coal. The methodology for this study is presented in such a way that other coals - particularly a high paritic sulfur content - could be studied.

Table of Contents

List of Figures

List of Tables

Introduction

The purpose of this investigation was to examine the feasibility of deep mechanical cleaning of coal prior to combustion. The rejected fraction of coal would be directed to a gasification process. We believe that energy could be saved by employing this concept in commercial sized gasification designs. The concept was applied to the Oil/Gas Complex designed by Ralph M. Parsons Company[1]. Quantitative results from this specific case were obtained to test our hypothesis.

We had hoped that the clean fraction of coal could be fired without additional clean-up of stack gases. This would alleviate the problem of meeting increasingly stringent emission standards[5]. The sulfur would be concentrated in the rejected (or dirty) coal feed to the gasifier, and eventually be reduced to elemental sulfur.

The overall energy efficiency of the proposed design was evaluated. Consideration was given to the reduced efficiency of gasifying "dirty" coal as well as the increased efficiency of directly combusting a portion of the coal.

The Proposed System

The addition of a deep cleaning and boiler system is the major alteration required in the proposed design. A sketch of the design is provided in Figure 1. The details of each of the processes involved will be discussed.

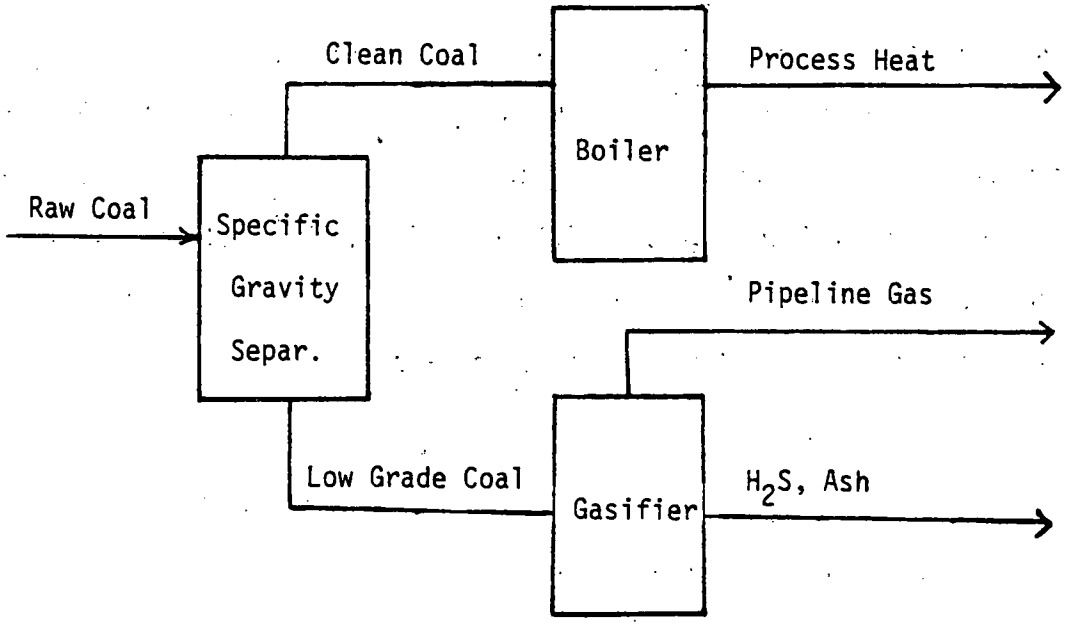

Figure 1

SCHEMATIC OF PROPOSED SYSTEM

The Deep Cleaning Unit

Deep cleaning involves the mechanical separation of raw coal to obtain a high grade coal (low sulfur and ash content). This procedure has been impractical for conventional uses because of the low recovery rate of clean coal. However, no real penalty for low recovery rates exist in this application since the remaining coal is directed to a gasifier rather than being discarded.

The deep cleaning is done by Specific Gravity Separation to deep clean the raw coal. This Specific Gravity Separation was chosen because of the availability of washability data. This method is also one of the best in terms of the quality of the clean coal recovered [2,3]. Studies performed by the Bureau of Mines[4], indicate that the degree of washability is a function of the specific gravity of the float medium

used. As the specific gravity of separation decreases, so will the pyritic sulfur, ash, and the recovery rate of clean coal.

As the crushed coal enters the separation vessel, the heavier particles containing pyritic sulfur (spec. grav. = 5.1) will sink. The lighter clean coal (spec. grav. = 1.2) will float. The clean coal is screened off the top of the liquid, to be fired in a conventional boiler. The dirty fraction is used as feed for the gasifier.

The Clean Coal Boiler

A conventional boiler is used in the proposed design to burn the recovered coal. Because the sulfur content in the clean coal has been reduced, less energy is required for flue gas desulfurization to meet the EPA emission standards[5].

The Gasifier

The design of the gasifier was based on the Bituminous Coal Research work on the Bi-Gas pilot plant at Homer City, Pennsylvania. The operating parameters (pressure, temperature and flowrate) specified in the Parson's Report on the Oil/Gas Complex were used in this study.

Since the reduced concentration of fixed carbon, decreases the product yield, conversion efficiency of the gasification reaction is reduced by using "dirty" coal.

Procedure

The proposed design was evaluated on the basis of its overall energy efficiency. The overall energy efficiency is calculated as the energy ultimately derived from the system divided by the heating value of the coal feed to the system. The coal type used throughout the analysis was "Illinois No. 6" because the Oil/Gas Complex was designed to process this coal type[2]. The specific analysis for this coal is shown in Table 1. The fraction of coal recovered from the specific gravity separation, and the composition of the "clean" and "dirty" splits are computed by extrapolating washability data compiled by the Bureau of Mines[9]. Figures 2 through 5 were generated from this data and relate the coal recovery rate to the sulfur, ash, carbon content, and heating value of the clean coal.

At a specified recovery rate the composition of the clean coal is set, and can be obtained from the curves. A mass balance is done to obtain the composition of the dirty coal. These newly determined compositions are used in the subsequent efficiency calculations.

The clean coal heating value is obtained from Figure 5. This enhanced heating value is used in all boiler calculations. A boiler efficiency of 85% is assumed in the calculation of the clean coal contribution to the total energy output. The treatment of the stack gases by FGD entails an energy penalty of 8% of the heating value of the feed coal[6]. This penalty is applied in proportion to the percentage of stack gas requiring treatment to meet EPA emission standards. This percentage is found by comparing the EPA standard of 1.2 lbs SO_2

Table 1

Proximate Analysis of Illinois No. 6 Coal

Item	Wt %
Moisture	2.7
Ash	11.8
Volatile Matter	39.7
Fixed Carbon	45.8
	100.00

Ultimate Analysis of Illinois No. 6 Coal

Element	Wt %
C	70.69
H	4.98
N	1.35
O	8.19
S	3.51
Trace Minerals*	11.28
	100.00

*A detailed analysis of all trace components is shown in Appendix B.

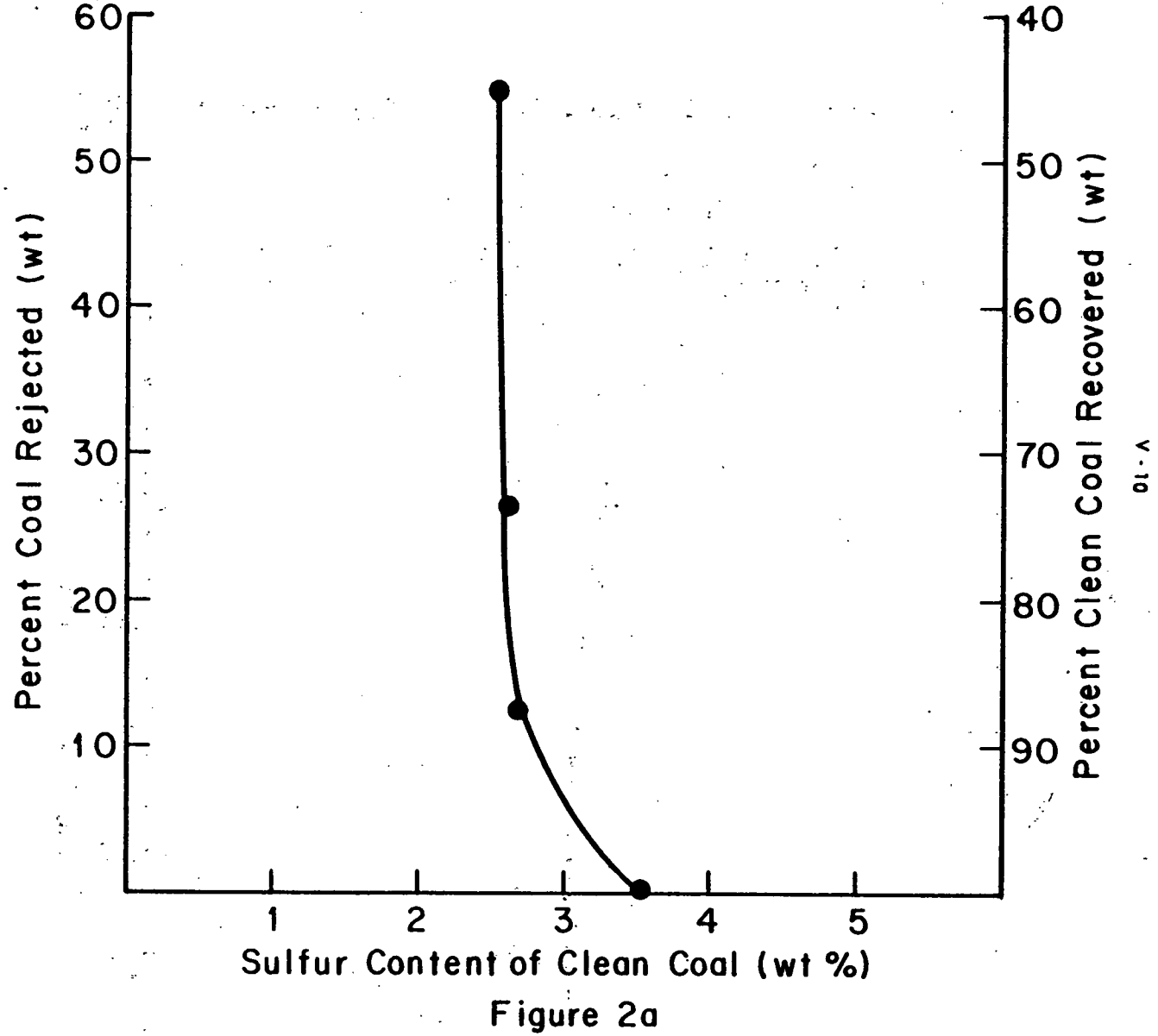

Figure 2a

Sulfur Content vs Coal Recovery During Clean-up

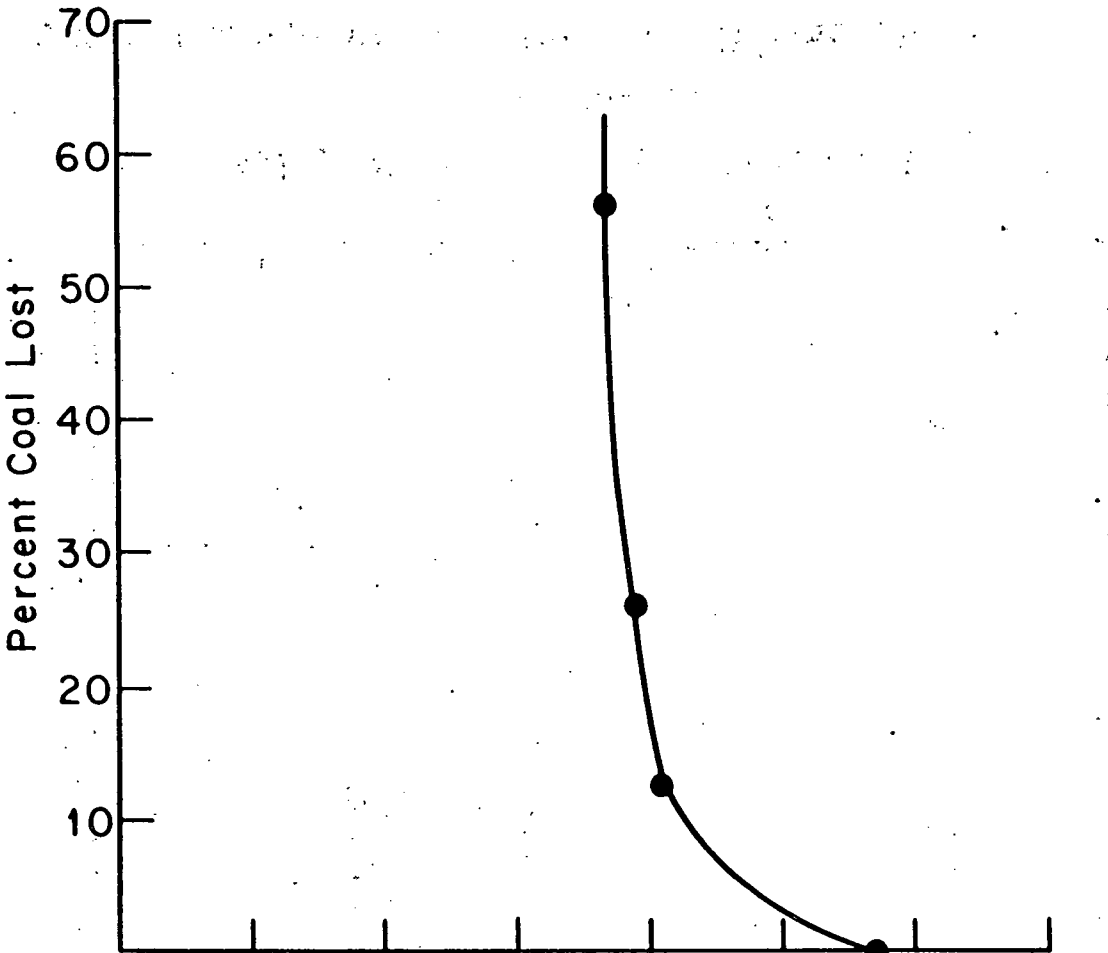

Figure 2b

Emissions vs Mass Losses of Coal During Clean-up

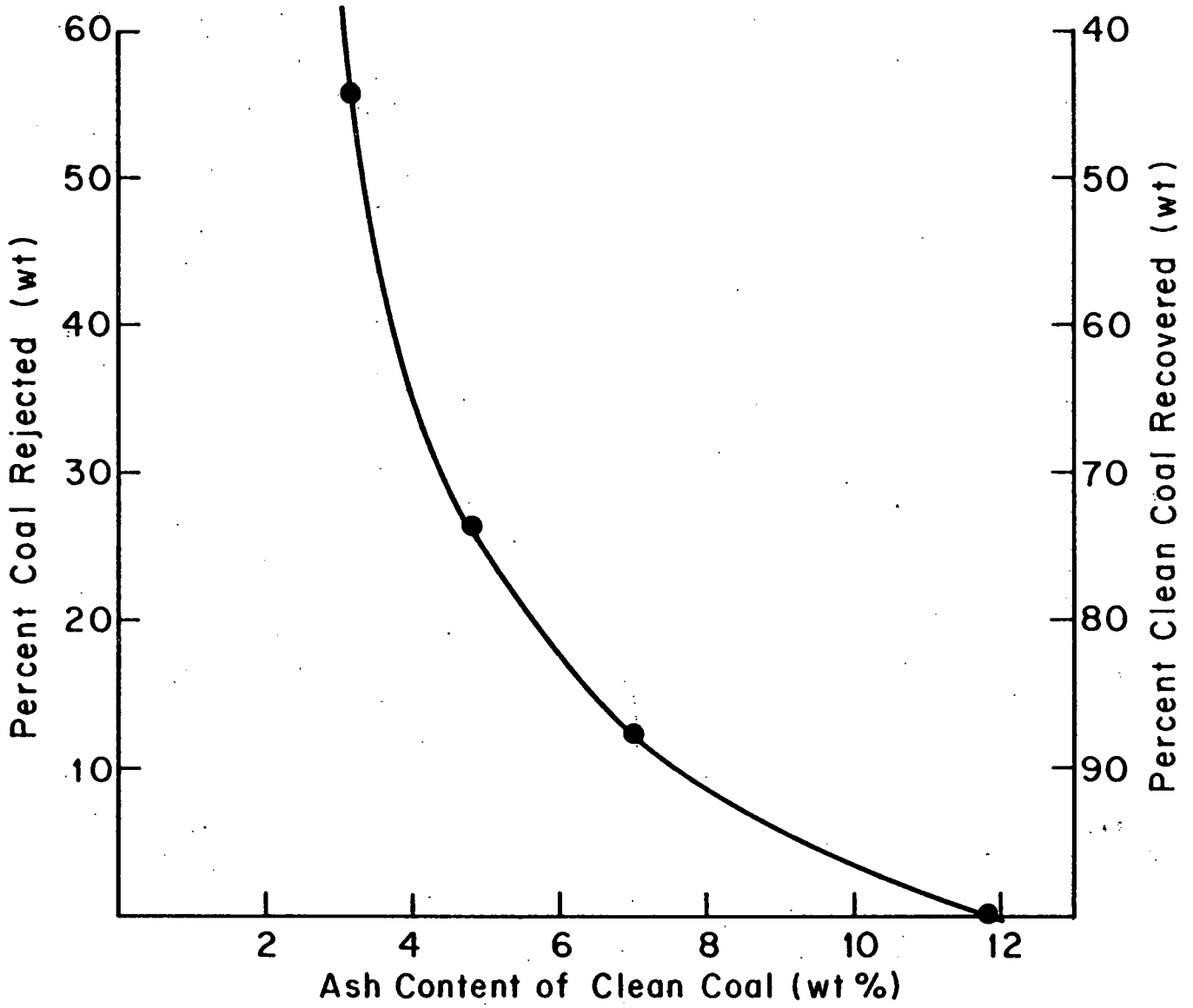

Figure 3

Ash Content vs Coal Recovery

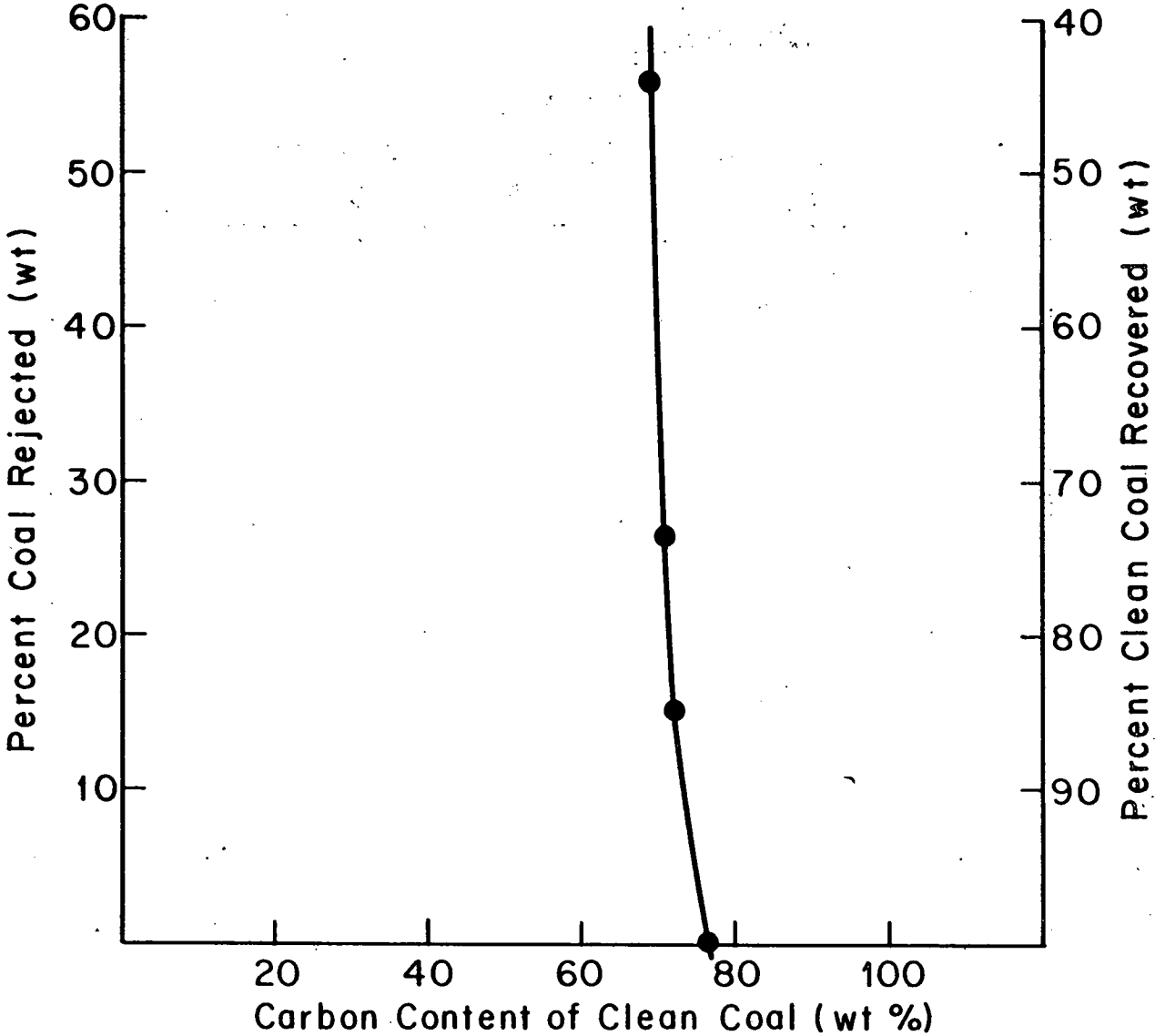

Figure 4

Carbon Content vs Coal Recovery

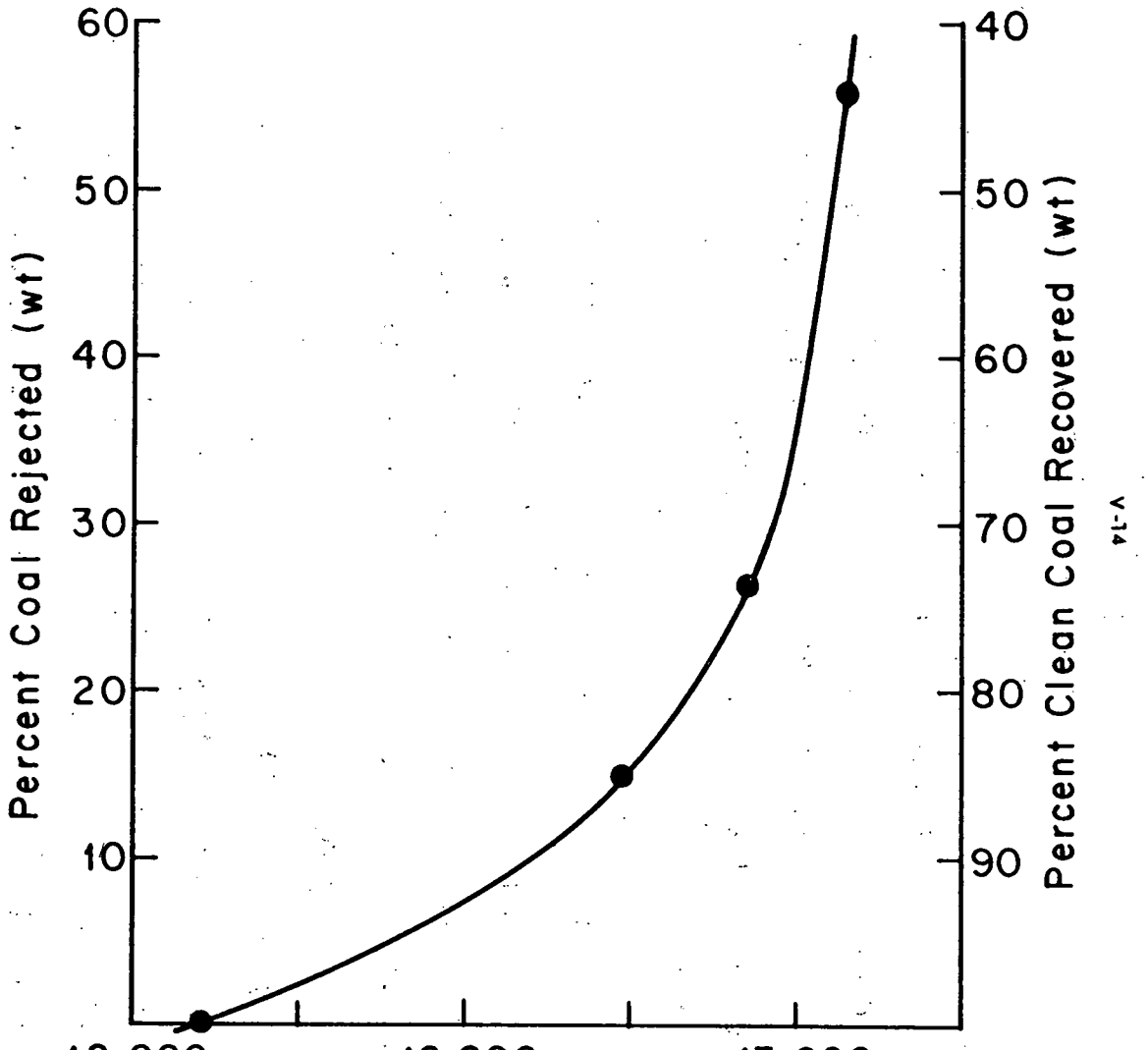

Figure 5

Higher Heating Value vs Coal Recovery

per MMBtu with the content of SO_2 in the stack gases. The specific amount of treatment was found in accordance with reference 7. (See sample calculations for details, Appendix A.) The following equation is used in determining the boiler unit's contribution to the production of useful energy.

Boiler Energy = HHV (.85 - .08 [fraction FGD Treatment])

The effect of gasifying dirty coal was also considered in this analysis. With the aid of the computer program: "Equilibrium Model of Gasification", the efficiency of the gasifier, operating at 1700°F and 1000 psi with the dirty coal was obtained(8).

The summation of the energy generated from the boiler and the energy content of the gasifier product is made. This total energy from the system is divided by the heating value of the original coal input, yielding the overall energy efficiency.

The entire procedure was iterated from several recovery rates.

Results and Discussion

The overall energy efficiency over a range of coal recovery rates has been calculated for the proposed combustion/gasification system. Figure 6 summarized these results. No significant variation in efficiency exists among various recovery rates. The energy penalty of FGD had some influence on the results. A larger impact was felt from computed values for gasifier efficiency. These were higher and more stable at various feed compositions than originally believed.

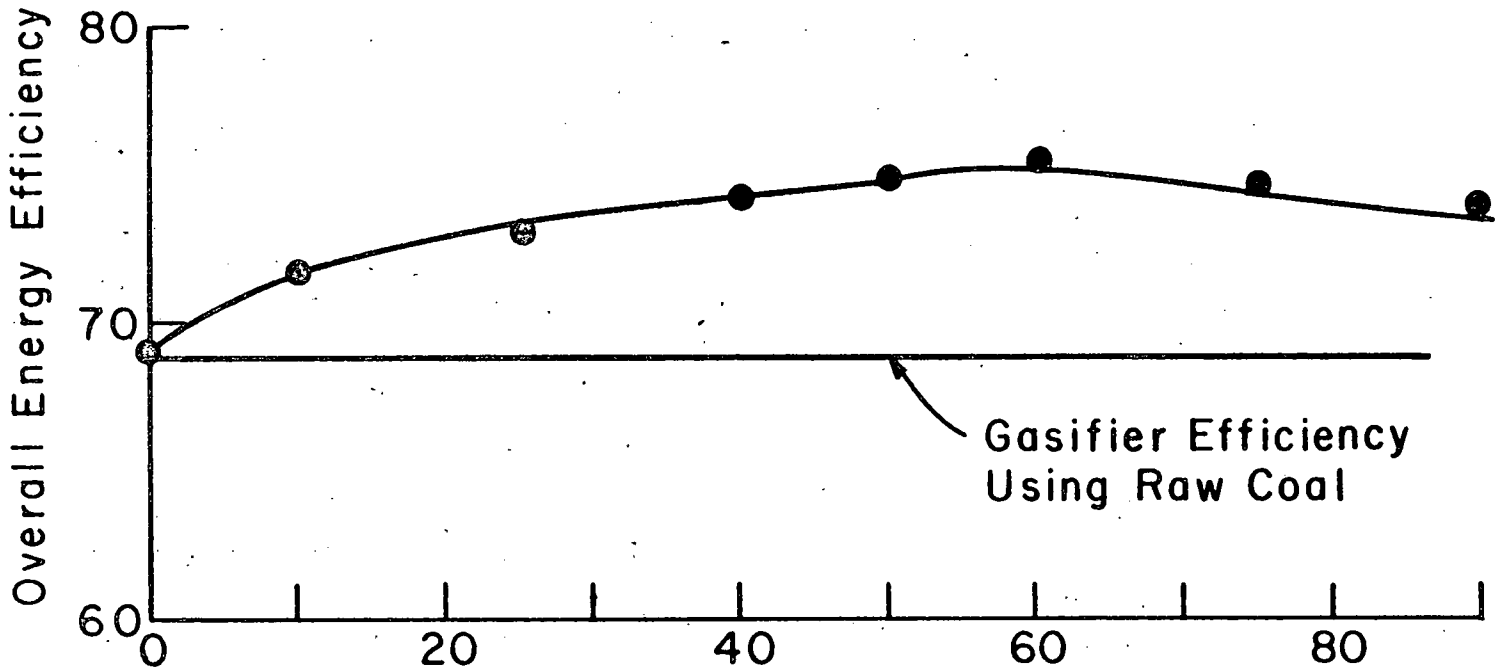

Figure 6

System Efficiency vs Coal Recovery

Figure 7 is a curve summarizing the effect of recovery rate (i.e., degree of cleaning) on the gasifier efficiency. The graph indicates that the gasification efficiency is insensitive to change in coal composition. This situation is rationalized if one observes the changing rate of steam and oxygen injection. The computer program used is an equilibrium model that optimizes these parameters for given feed compositions. Therefore, the gasification efficiency tends to be inelastic with respect to feed composition.

The efficiency for gasifying raw coal (69%), is not significantly different from direct combustion efficiency (78 - 85%). Consequently, even at the optimal recovery rate (i.e., degree of cleaning), the system efficiency has no great advantage over the present gasification system. The optimal recovery rate is represented as the relative maxima in Figure 6. It is observed that 73% is not vastly different from the raw coal gasification efficiency of 69%, when one recognizes that error of approximately 10% is inherent in this study. Therefore, installation of the proposed system can not be recommended for commercial gasification projects.

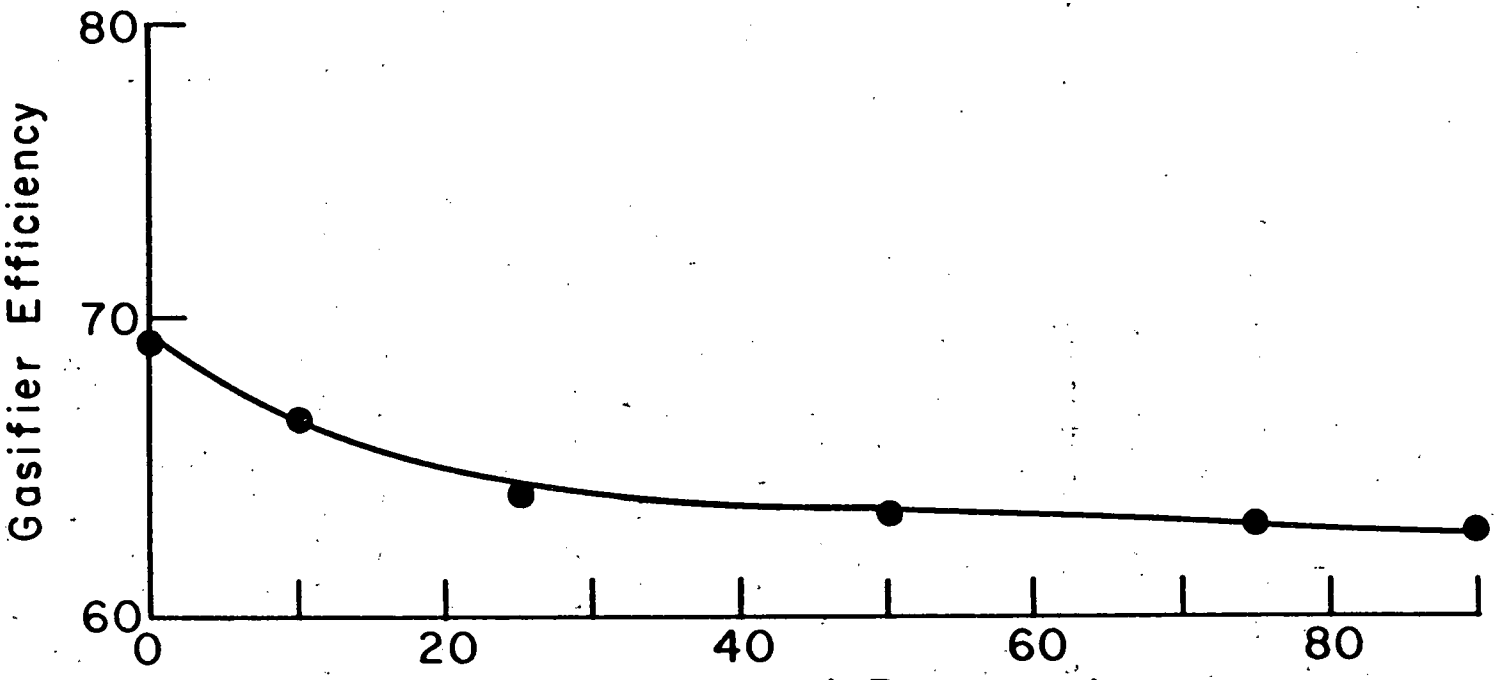

Figure 7

Gasifier Efficiency vs Coal Recovery

Accuracy and Sensitivity

Several sources of error can be identified within this study. Numerous assumptions and approximations were made. For convenience, these are listed below. The impact they have on the results of this investigation is considered as part of a sensitivity analysis which follows in Table 2.

1) Direct fired boiler efficiency of 85%.
2) Flue Gas Desulfurization energy requirements are 8% of the heat input to the boiler.
3) Energy required for coal grinding is negligible.
4) Gasification reaction approaches equilibrium conversion rate.
5) Downstream processing steps treating the gasifier effluent were unaffected.

Recognizing these limitations, an error of $\pm$ 10% can be expected in these calculations. It should be noted that Illinois No. 6 coal was used as a basis throughout this study. Other coal types may have characteristics that would alter the evaluation. Beneficial characteristics include ease of washability, high fixed carbon composition, and low sulfur and ash content.

The gasification program used to discern gasifier efficiency is an equilibrium model.[8] It does not exactly convey continuous operation results. The disparity here was believed to be small, however the surprisingly high gasifier efficiencies predicted by the model deserve some scrutiny. It is this factor which forced the retraction of the original

TABLE 2

Percent Efficiency Change for
a 10% Change of an Individual Parameter

Parameter Name [10% Change]	Value	Change in System Efficiency
Boiler Efficiency	85%	1.2%
FGD Rate	8%	0.2%
Recovery Rate	60%	1.5%
Carbon Content of Gasified Coal	59%	0.4%
Gasifier Efficiency	69%	8.3%

The highest change of 8.3% on total system efficiency of 10% change in the assumed boiler efficiency indicates that this parameter has the most significant effect. On the contrary, the lowest change of .2% of the FGD energy consumption shows the negative sensitivity of this parameter.

hypothesis. Observing that the results are very sensitive to the gasifier efficiency, an error in these values could greatly influence the results of this entire evaluation.

Conclusions and Recommendations

1. The proposed combustion-gasification system should not be applied in commercial sized gasification designs.

2. Other coal types should be considered to evaluate the impact of coal characteristics on the system.

References

1. Parsons, Ralph M., "Oil/Gas Complex Conceptual Design/Economic Analysis", Prepared for Energy Research and Development Administration, Contract No. E(49-18)-1775, March 1977.

2. Ibid, p. V-2.

3. Conversation with Kenneth Miller, Pittsburgh Energy Research Center, Bruceton, Pa.

4. Cavallaro, J. A., et al., "Sulfur Reduction Potential of the Coals of the United States", U.S. Bureau of Mines RI 8118, 1976.

5. Allegheny County Health Department, "Rules and Regulations", Article XVIII, Air Pollution Control, June 1972.

6. Torstrick, R., Shawnee-Limestone-Lime Scrubbing Process, Summary Description Report, TVA, 1976.

7. Carnahan, D. R., Energy Conservation in Flue Gas Desulfurization Systems, December 1976, p. V-64.

8. Kabadi, J. N., Gasifier Equilibrium Model, Prepared for U.S. Energy Research and Development Administration, Contract No. EY77S024196, August 1977.

9. Op. Cit., Cavallaro, p. 61, 314.

10. Personal communication with Dr. Kun Lee, Professor, Chemical Engineering, Carnegie-Mellon University.

11. Miller, Kenneth J., Flotation of Pyrite from Coal: Pilot Plant Study, Pittsburgh Energy Research Center, Bureau of Mines RI 7822, 1973.

APPENDIX A

Sample Calculations

Following will be a sample of the calculations required to obtain a value for the overall efficiency of the proposed system. The case of 40% recovery of clean coal in the separation unit is used below. The procedure applies at any recovery rate.

1. Recovery rate of 40% is chosen.
2. From Figures 2 through 5 the composition of the clean coal is determined.

S - 2.5%

Ash - 3.1%

C - 67%

Heating Value - 13,650 BTU/lb

3. By mass balance the composition of the dirty coal is calculated. Initially the raw coal composition is given as:

S - 3.5%

Ash - 11.8%

C - 70.7%

HV - 12,172 BTU/lb

Choosing a basis of 100 lbs of raw coal, the dirty coal composition is easily derived.

$$S: \quad \frac{.035 - .025(.40)}{.60} = .04$$

$$Ash: \quad \frac{.118 - .031(.40)}{.60} = .18$$

$$C: \quad \frac{.707 - .67(.40)}{.60} = .73$$

And via energy balance

$$HV: \quad \frac{12,172 - 13,650(.40)}{.60} = 11,187$$

4. The boiler calculation is done assuming 85% efficiency and penalty of 8% for stack gas clean up. The amount of gas needing treatment must first be determined. From Figure 2b the coal directly fired at 40% recovery does not meet EPA emission standards. The amount of gas treated is calculated by:

$$STD = \frac{SO_2(1 - xn_s)}{Q \text{ Boiler}}$$

where x = fraction of flue gas treated

STD = SO_2 emission regulation $lb/10^6$ BTU (1.2)

n_s = scrubber efficiency (80%)

SO_2 = lb of SO_2 in

5. The contribution to total energy from the boiler is found by the equation:

Boiler Energy = HHV (.85 - 0.8 [% FGD Treatment])

In this case

Boiler Energy = 13,650 (.85 - .08[.45])

= 11,111

6. The contribution from the gasifier is computed by multiplying the given gasifier efficiency by the heating value of the dirty coal feed.

11,187 x .66 = 7384

7. Overall Energy Efficiency

$$\frac{(11,111).40 + 7384(.60)}{12,172} = 73\%$$

ENERGY CONSERVATION IN COAL CONVERSION

High Pressure Steam Generation From Heat Recovery Boilers

R. G. McMillin

Carnegie-Mellon University
Pittsburgh, PA 15213

June, 1978

Prepared for

THE U.S. DEPARTMENT OF ENERGY
Pittsburgh Energy Technology Center
UNDER CONTRACT NO. EY77S04196

ABSTRACT

This report develops a methodology for calculating and evaluating the increased work potential possible from high pressure steam generation in waste heat boilers. This methodology is applied to the Ralph M. Parsons commercial concept of the Oil/Gas Complex. Implementation of the proposed scheme would result in an export power increase of 7.7 MW which is a 4% increase of the 210 MW generated by the Oil/Gas Complex at a cost of $2110/KW.

ACKNOWLEDGEMENT

I would like to thank T. S. Govindan of the DuPont Company for his valuable assistance in the preparation of this report.

TABLE OF CONTENTS

LIST OF FIGURES

LIST OF TABLES

Introduction

This report develops a methodology for calculating and evaluating the increased work potential possible from high pressure steam generation in waste heat boilers. The methodology is applied to the Ralph M. Parsons commercial concept of the Oil/Gas Complex[1].

Operating steam generators at higher pressures than steam users allows for work to be extracted by depressurization. Topping turbines can be used to bring the pressure down from the generation pressure level to the user pressure level. However, higher boiler operating pressures and additional turbines require a higher capital investment.

Method of Approach

Use of a steam balance format simplifies the approach (Fig. 1). Headers were drawn to represent all steam generation and user pressure levels and condensate. Steam generators were drawn above the corresponding headers, while users are drawn below these headers. Generators and users are labeled with their corresponding equipment numbers and steam mass flow rates. Heat exchanger gas mass flow rates are shown, as well as the gas inlet and exit temperatures.

Heat exchangers are then evaluated on an individual basis to determine if steam at the next highest incremental pressure can be generated. The results calculated (Appendix A) are shown in Table 1.

Two approaches are used to determine if higher pressure steam can be generated. The first approach is to hold the heat transfer constant, and evaluate the effect on the steam mass flow rate and the

STEAM UTILITY FLOW SHEET FOR THE R. PARSONS OIL GAS COMPLEX

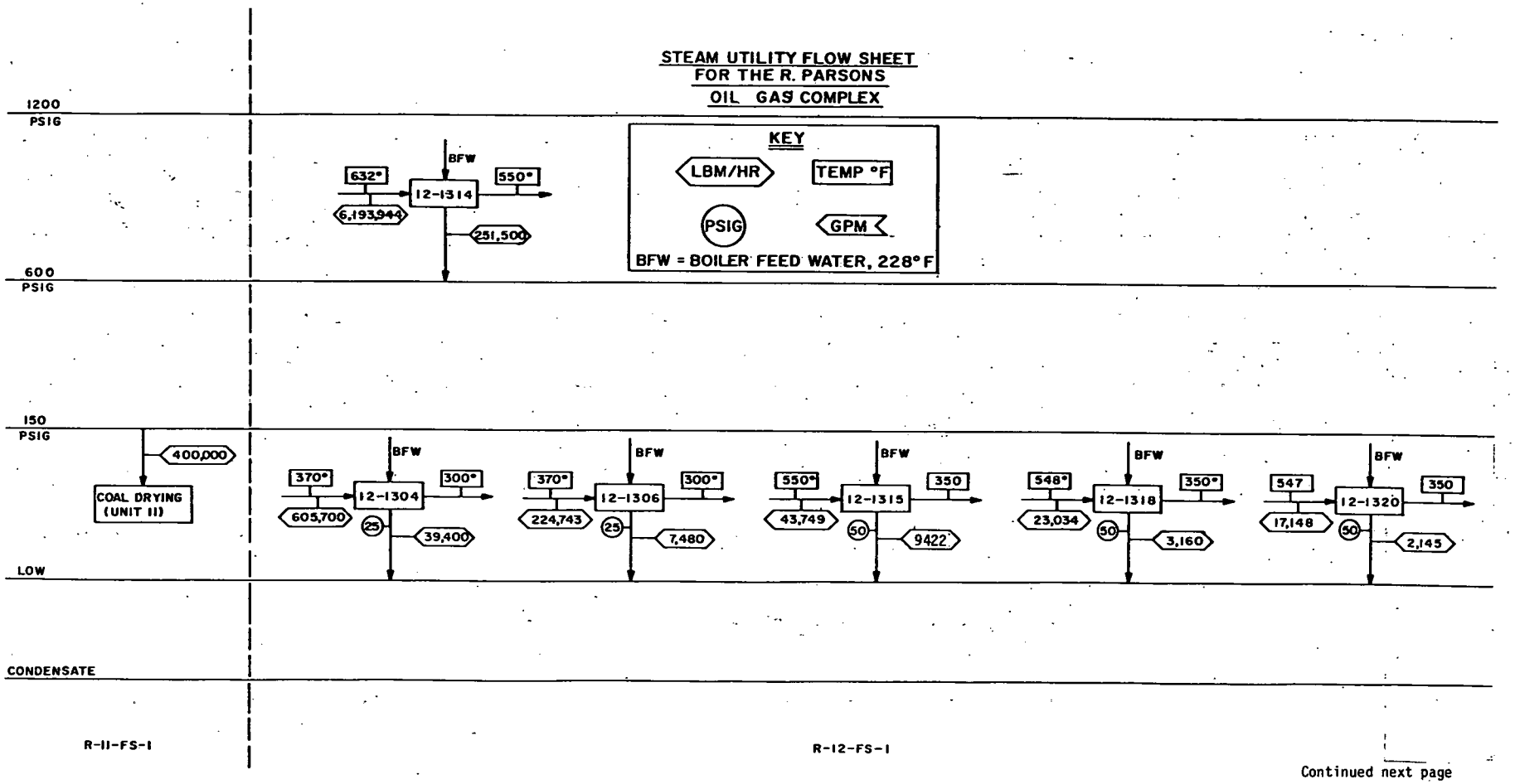

Continued next page

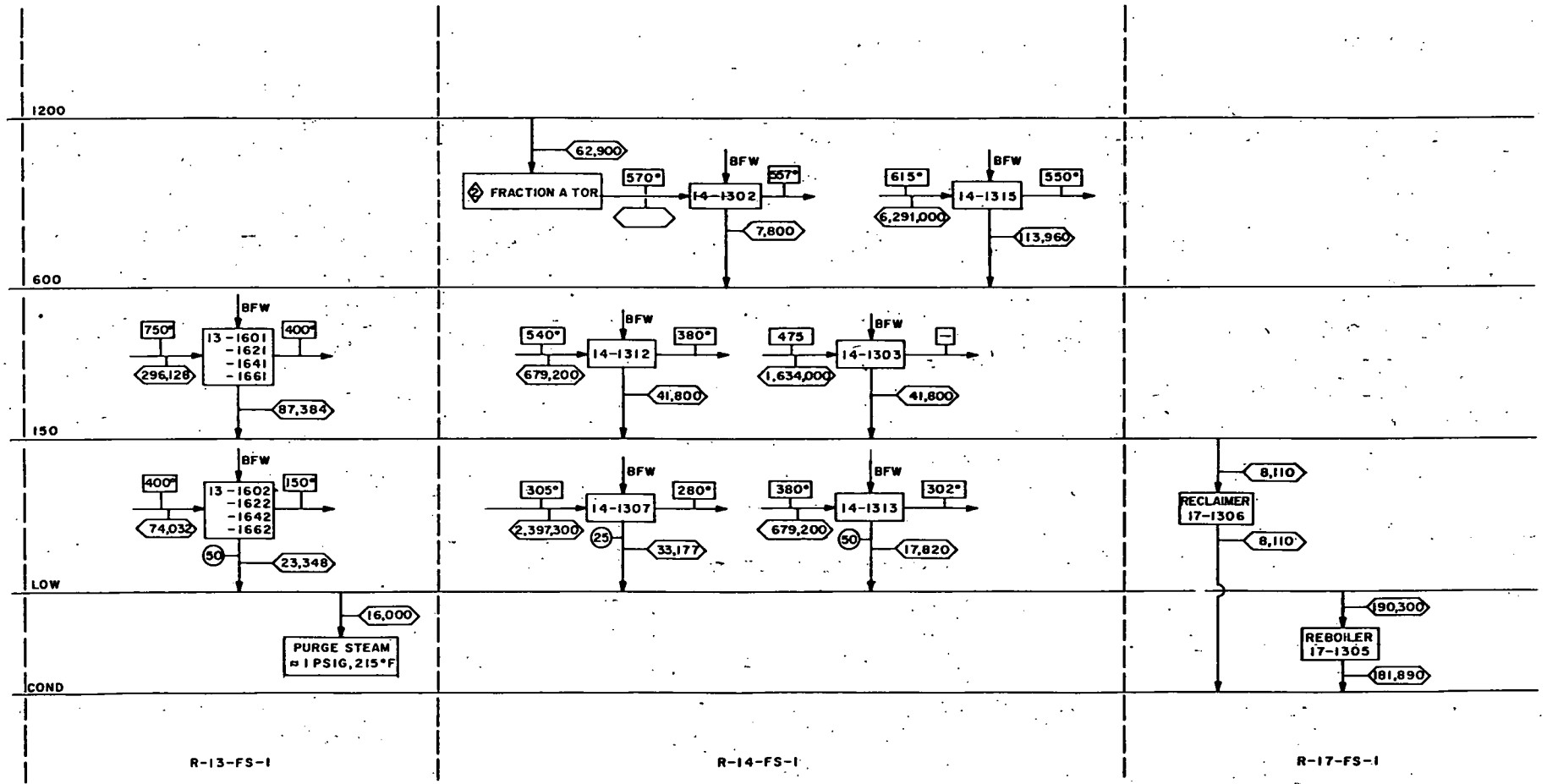

Continued next page

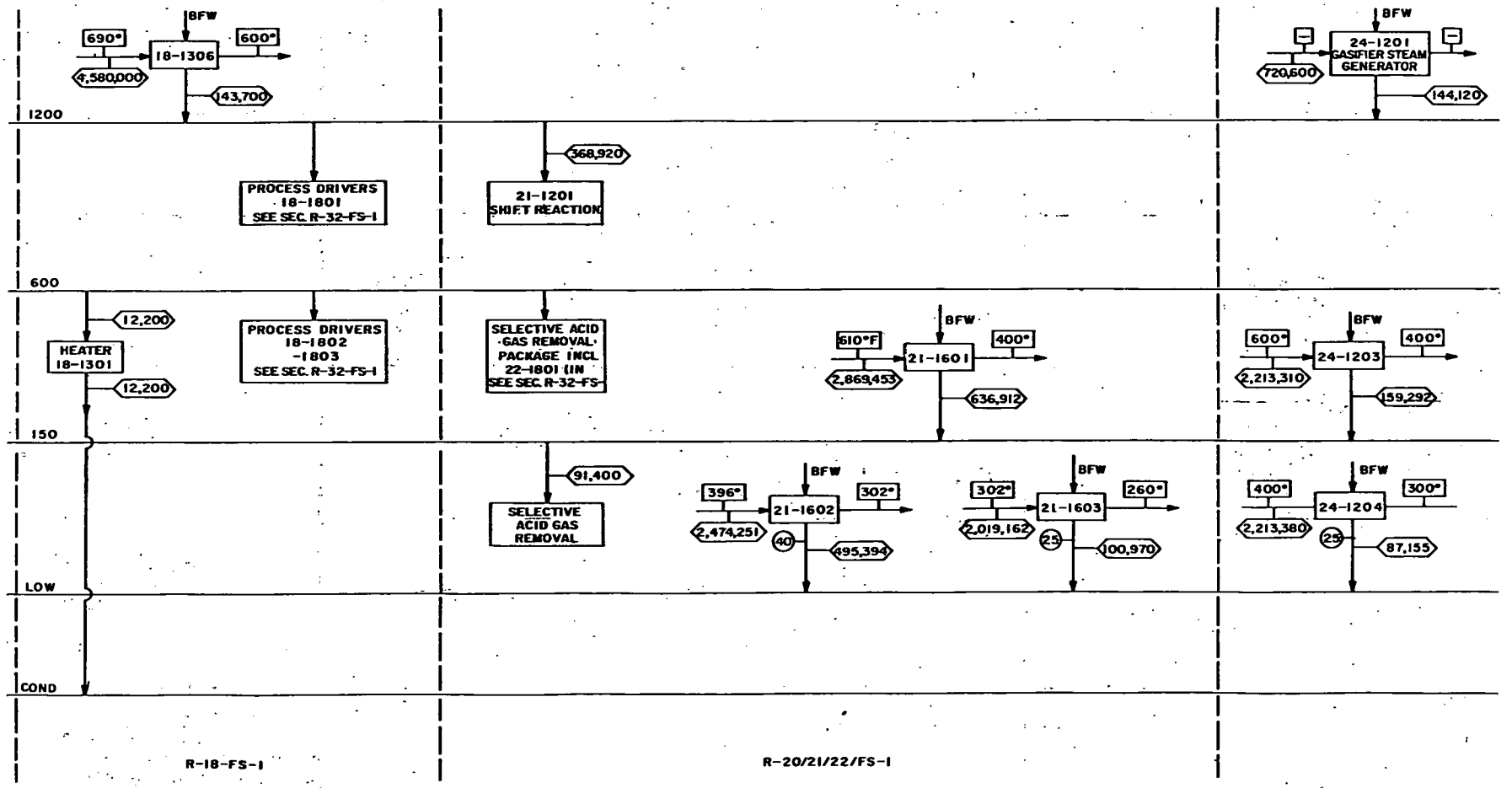

Continued next page

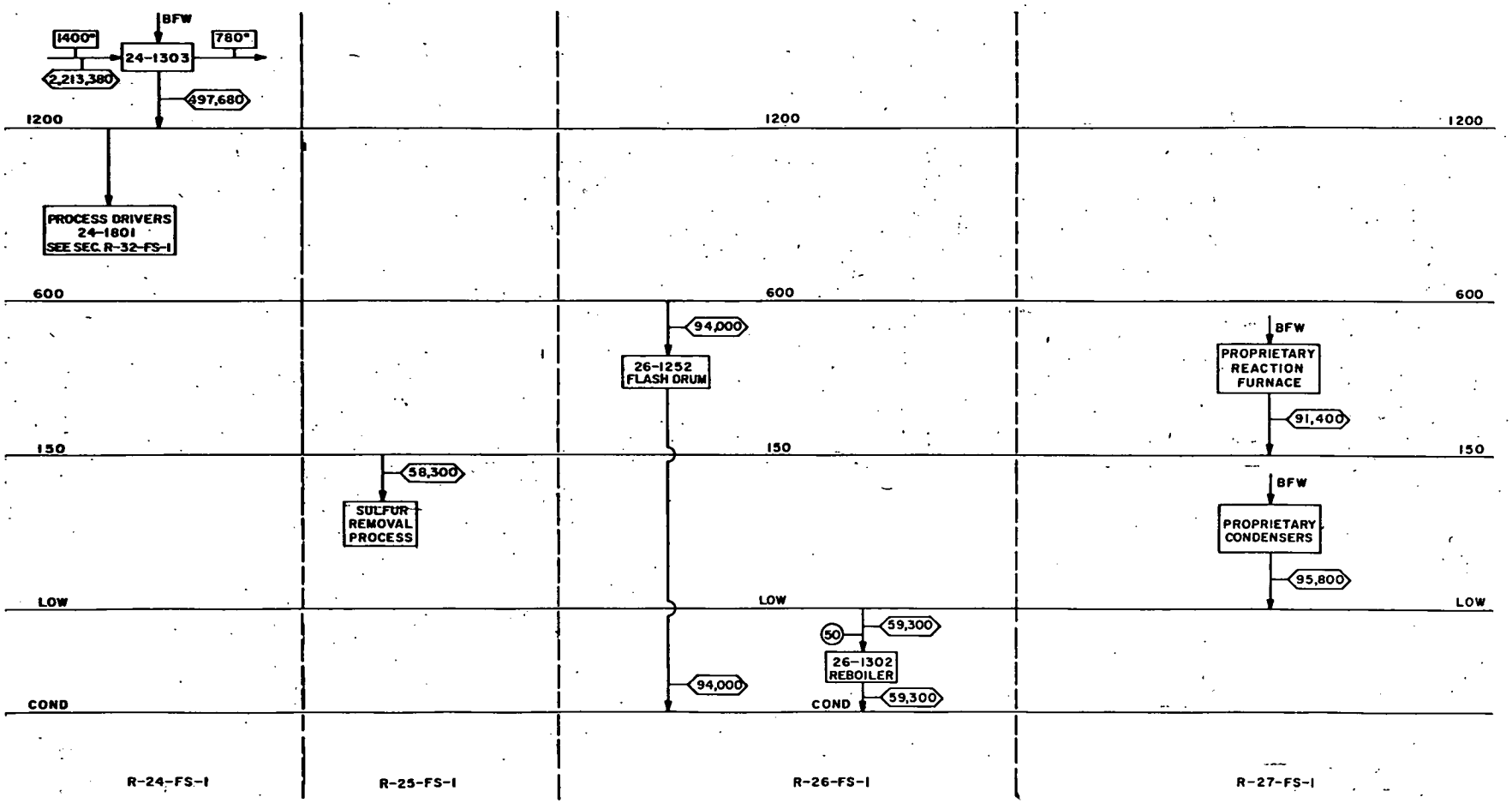

Continued next page

FIG. I
STEAM UTILITY FLOW SHEET FOR
THE R. PARSONS OIL/GAS COMPLEX

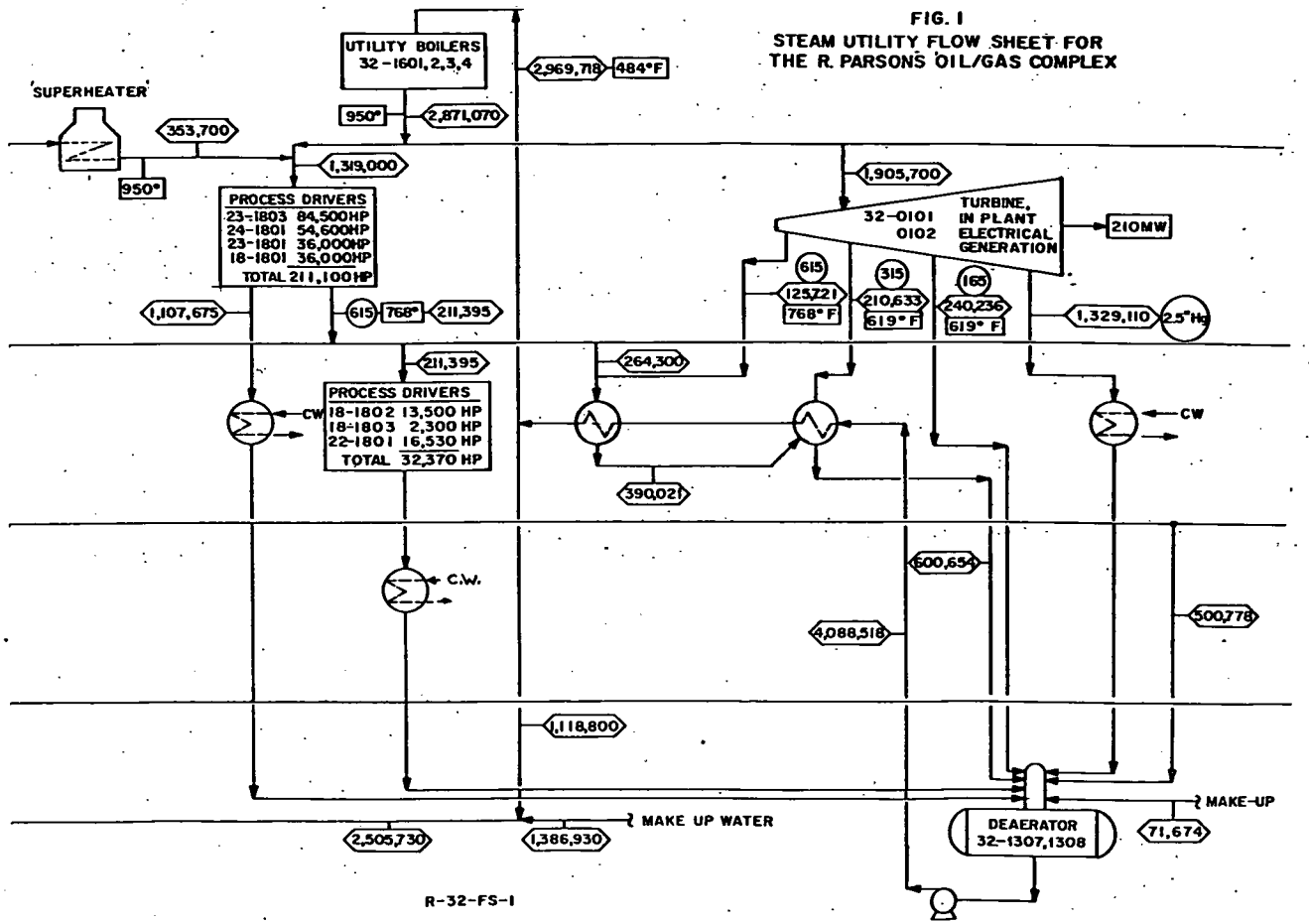

	existing							increased pressure (q_t = const.)						increased pressure (ΔT_p = 50°)						
Item #	P_s PSIG	$\dot{m}_s$ lb/hr	ΔT_p °F	U_B Btu/hr.ft²°F	A_{tot} ft²	mat'l SH/T	cost $/ft²	P_s PSIG	$\dot{m}_s$ lb/hr	ΔT_p °F	A_{tot} ft²	mat'l SH/T	cost $/ft²	P_s PSIG	$\dot{m}_s$ lb/hr	Te °F	A_{tot} ft²	mat'l SH/T	cost $/ft²	remarks
12-1304	25	39,340	35.6	131	5,300	-----	-----	50	38,956	7	----	-----	-----	50	13,150	----	-----	-----	-----	ΔT_p to low; $\dot{m}_s$ to low
12-1306	25	7,464	35.6	114	1,130	-----	-----	50	7,394	7	----	-----	-----	50	2,493	----	-----	-----	-----	ΔT_p to low; $\dot{m}_s$ to low
12-1314	600	252,900	82	56.5	42,680	CS/SS	78	900	255,000	42.6	64,050	CS/SS	105	900	218,700	561	51,970	CS/SS	105	ΔT_p acceptable; $\dot{m}_s$ acceptable
								1200	258,500	12.2	----	-----	-----	1200	66,200	-----	-----	-----	-----	ΔT_p to low; $\dot{m}_s$ to low
12-1315	50	9,422	65	153	456	CS/SS	17.6	150	6,513	11.1	----	-----	-----	150	5,041	394	510	CS/SS	35.9	ΔT_p to low; $\dot{m}_s$ acceptable
								600	------	-----	----	-----	-----	600	442	------	------	-----	-----	not possible; $\dot{m}_s$ to low
12-1318	50	3,140	67	139	230	CS/CS	17.6	150	3,086	12	-----	------	------	150	2,250	396	290	CS/CS	35.9	ΔT_p to low; $\dot{m}_s$ acceptable
12-1320	50	2,141	66	97	200	CS/CS	17.6	150	2,105	10.7	------	------	------	150	1,613	395	132	CS/CS	35.9	ΔT_p to low; $\dot{m}_s$ acceptable
13-1601/21/41/51	150	21,900	83	20.6	5,400	CS/CS	35.9	600	21,726	7	------	------	------	600	18,045	416	6,550	CS/CS	-----	ΔT_p to low; $\dot{m}_s$ acceptable
								900	-----	-----	------	------	------	900	15,465	502	5,944	CS/CS	115	ΔT_p to low; $\dot{m}_s$ acceptable
13-1602/22/42/62	50	5,837	17	30	3,997	----	-----	150	-----	-----	------	------	------	150	------	-------	------	-----	----	not possible; not possible
14-1302	600	7,800	71	82.6	1,330	----	----	900	7,849	26.6	-----	------	------	900	------	-------	------	-----	-----	ΔT_p to low; not possible
14-1315	600	111,630	78	20.3	43,860	CS/CS	36	900	112,520	36.7	74,835	CS/CS	48	900	77,980	570	90,455	CS/CS	48	ΔT_p acceptable; $\dot{m}_s$ acceptable
								1200	114,000	8	-----	------	------	1200	-----	------	------	------	----	ΔT_p to low; not possible
14-1313	50	19,450	27	30	12,650	----	------	150	-------	------	-----	------	------	150	-----	------	-------	------	-----	not possible; not possible
14-1307	25	33,177	16	-----	19,940	----	------	50	-------	------	-----	------	------	50	-----	-------	------	-----	----	not possible; not possible
18-1306	1200	143,650	66	479	11,700	A285C/CS	60	1500	147,543	42	15,430	A285C/CS	------	1500	125,904	613	12,360	A285C/CS	82	ΔT_p acceptable; $\dot{m}_s$ acceptable
								1800	150,482	22	------	------	------	1800	54,370	------	-----	-----	----	ΔT_p to low; $\dot{m}_s$ to low
21-1601	150	636,912	63	565	34,488	----	-----	600	-------	----	------	------	------	600	292,460	------	------	------	-----	not possible; $\dot{m}_s$ to low
21-1602	25	495,394	38.7	134	54,220	----	------	150	-------	----	-------	------	------	150	------	------	------	-----	-----	not possible; not possible
21-1603	10	100,970	20.6	------	23,574	----	------	50	-------	----	-------	------	------	50	-------	-------	------	-----	----	not possible; not possible
24-1201	1200	144,120	-----	------	------	----	------	-----	-------	----	-------	------	------	-----	-------	------	------	------	----	lack of information
24-1303	1200	497,680	400	13.6	55,000	SA285C/SS	480	1500	504,624	364	55,560	------	------	1500	947,116	-------	------	-----	-----	ΔT_p acceptable; not possible
								2000	622,340	419	49,170	SA285C/SS	630	2000	1,079,680	------	------	-----	-----	ΔT_p acceptable; not possible
24-1305	150	159,292	63	------	38,500	-----	-----	600	-------	----	-------	------	------	600	65,860	------	-----	-----	-----	not possible; $\dot{m}_s$ to low
24-1306	25	87,155	36	18.3	61,360	-----	-----	50	84,435	9	------	------	------	50	47,325	----				ΔT_p to low; $\dot{m}_s$ to low

P_s = steam generation pressure

$\dot{m}_s$ = steam flow

ΔT_p = pinch point temperature difference

U_B = over-all heat transfer coefficient of boiler section

A_{tot} = total area of heat exchanger

mat'l = heat exchanger materials = SH/T = Shell/Tubes

Te = exit temperature of heating stream

CS = carbon steel

SS = stainless steel

TABLE I

"pinch point" temperature differential - the minimum temperature difference between the exchanger heating stream and the saturation temperature of the steam being generated. The heat exchanger area is then calculated.

In the second approach, the "pinch point" is set at 50°F, a common design point, and the effect on the steam mass flow rate, the heating stream exit temperature, and the exchanger area are found.

While considering increasing the operating pressure of the heat exchangers, two requirements were set. First, the new mass flow rate of the steam must be within - 30% of the former steam mass flow rate. Second, the "pinch point" temperature differential must be a minimum of 36°. Also, the highest incremental steam pressure possible (up to 2000 PSIG) was of course chosen. When it was possible to replace an exchanger with either scheme, the total heat transfer held constant or the "pinch point" held at 50°, it was decided to keep the heat transfer constant wherever possible. This avoids any possible complications from the heating stream outlet temperature rising excessively.

The replaced exchangers are shown in Table 2. (The exchanger costs were found as shown in Appendix B.) The total installed cost of the existing exchanger is found by multiplying the heat exchanger area by the cost per unit area. The total installed cost of the replacement exchanger is found the same way. The difference between these two costs is the "Δ installed cost". The total increased capital investment in heat exchangers, then, is found to be $12,555,020.

Table 2

Exchanger Costs

	low pressure			high pressure			
Item #	Area (ft^2)	Cost ($/ft^2$)	Cost ($)	Area (ft^2)	Cost ($/ft^2$)	Cost ($)	Δ Installed Cost
12 -1314	42,680	78	3,300,000	64,050	105	6,725,000	3,425,000
12-1315	456	17.6	8,000	510	35.9	18,300	10,300
12-1318	230	17.6	4,000	290	35.9	10,400	6,400
12-1320	200	17.6	3,520	132	35.9	4,740	1,220
13-1601/21/41/61	5400(x4)	35.9	775,000	5,944(x4)	115	2,734,000	1,959,000
14-1315	43,860	36	1,579,000	74,835	48	3,592,000	2,013,000
18-1306	11,700	60	702,000	15,430	82	1,265,000	563,000
24-1303	55,000	480	26,400,000	49,170	630	30,977,000	4,577,000

Δ Installed cost total = $12,555,000

Table 3 shows the "accounting" of the new steam balance. The column headed "lbs/hr needed" indicates the shortage of steam at the indicated pressure due to generating the steam at a higher level. The column headed "lbs/hr generated" designates the steam now generated at a higher level.

Figure 2 demonstrates how power can be generated by utilizing the higher pressure steam. The steam is expanded through a turbine and extracted at the levels required to rebalance the system. The turbine in Figure 2, however, would be prohibitive in terms of cost due to the complexity of controls in such an induction-extraction arrangement.

Figure 3 shows how the arrangement of Figure 2 can be implemented by utilizing six separate turbines. The costs for these turbines are given in Table 4. The costs for the corresponding generators is also shown. The power output of the generator was found as shown in Appendix C. Thus, the total generator output of 7760 kw cost $3,815,600 for turbine and generation equipment, and $12,555,000 represents the increase in total installed cost of the waste heat boilers (Table 2). Thus, the proposal to generate steam at a higher pressure results in a 7760 kw power increase at a cost of $16,370,000 or $2110/kw.

The steam utility flow sheet revised to show the implementation of the higher pressure waste heat boilers and additonal turbines is shown in Figure 4.

Table 3

Steam Balance

Unit #	PSIG	lbs/$_{hr}$ needed	PSIG	lbs/$_{hr}$ generated
12-1314	600	252,900	900	255,000
12-1315	50	9,422	150	5,041
12-1318	50	3,140	150	2,250
12-1320	50	2,141	150	1,613
13-1601/21/41/61	150	21,900(x4)	900	15,465(x4)
14-1315	600	111,630	900	112,520
18-1306	1200	143,650	1500	147,543
24-1303	1200	497,680	2000	522,340

A turbine operating under the following conditions would satify the above requirements:

PSIG	$\dot{m}_{in}$	m_{out}
2000	522,340	
1500	147,543	
1200		641,330
900	429,380	
600		364,530
150		78,700
50		14,703

Figure 2

STEAM BALANCE

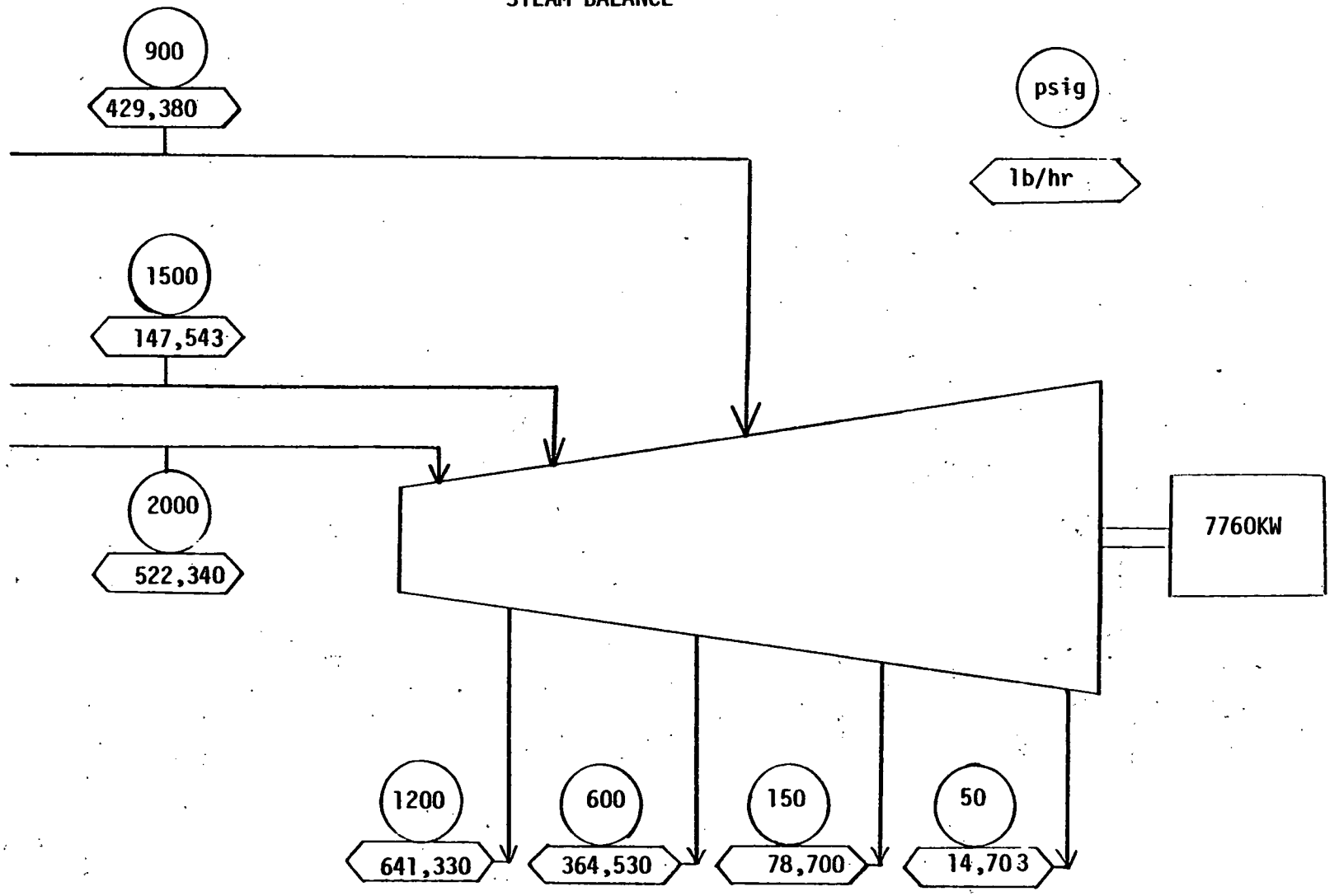

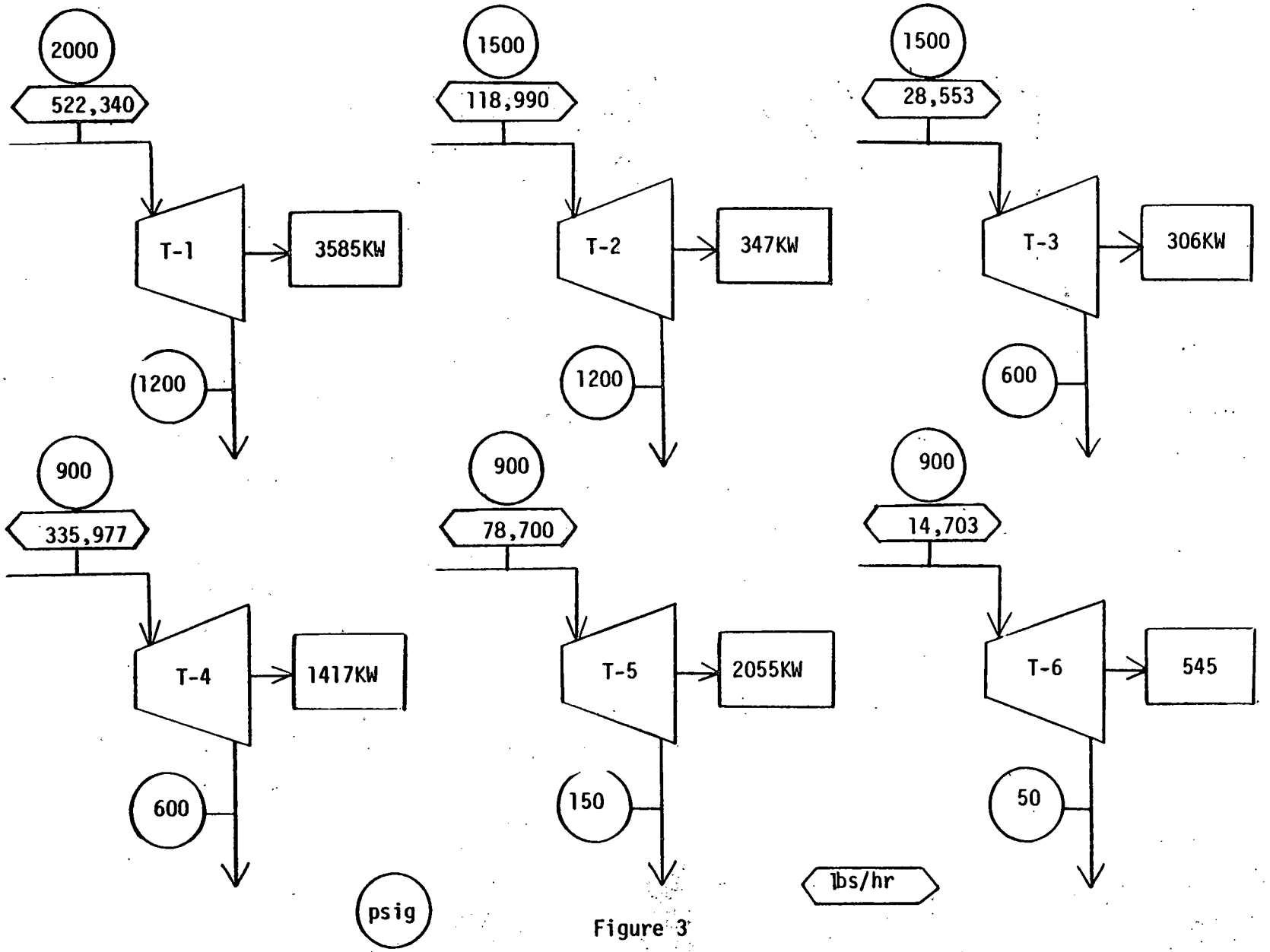

Figure 3

GENERATION SCHEME

Table 4

Turbine and Generator Costs

	HP/KW	Turbines* Installed Cost	Generators** Installed Cost
1)	4805/3585	$1,200,000	430,200
2)	465/347	525,000	41,640
3)	410/306	250,000	36,720
4)	1900/1417	425,000	170,000
5)	2755/2055	250,000	246,000
6)	730/545	175,000	65,400
Total	11,065/8255	2,825,000	990,600

Total turbine and generator installed costs = $3,815,600

Total power output = 8255 KW x 94%[8] = 7760 KW

*Appendix C

**Based on an $80/KW quote ± 10% for generators in the range shown, plus 40 - 50% for gear reduction equipment. (Reference 8.)

FIG. 4
REVISED STEAM UTILITY FLOW SHEET
FOR THE R. PARSONS OIL GAS COMPLEX

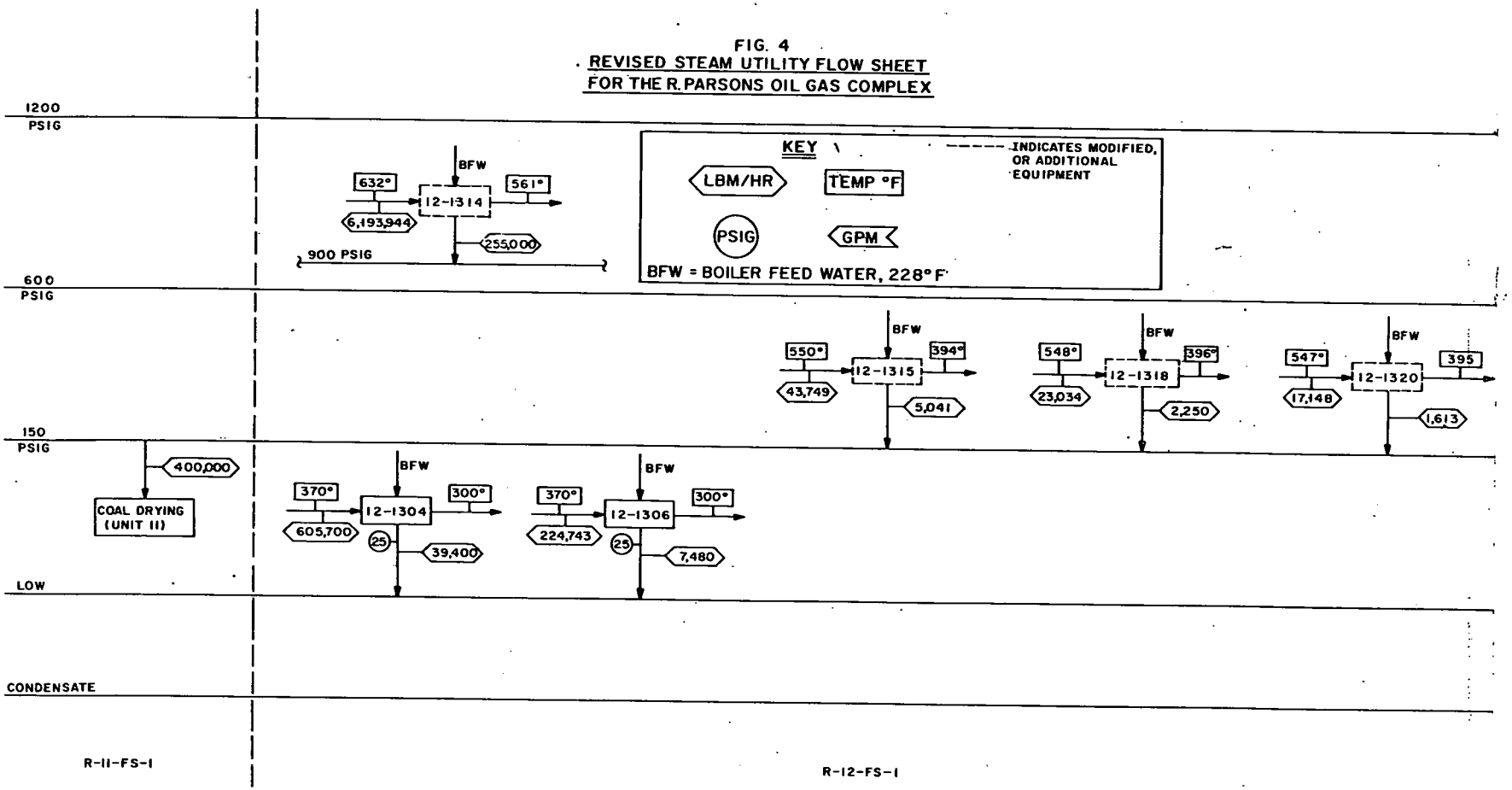

Continued next page

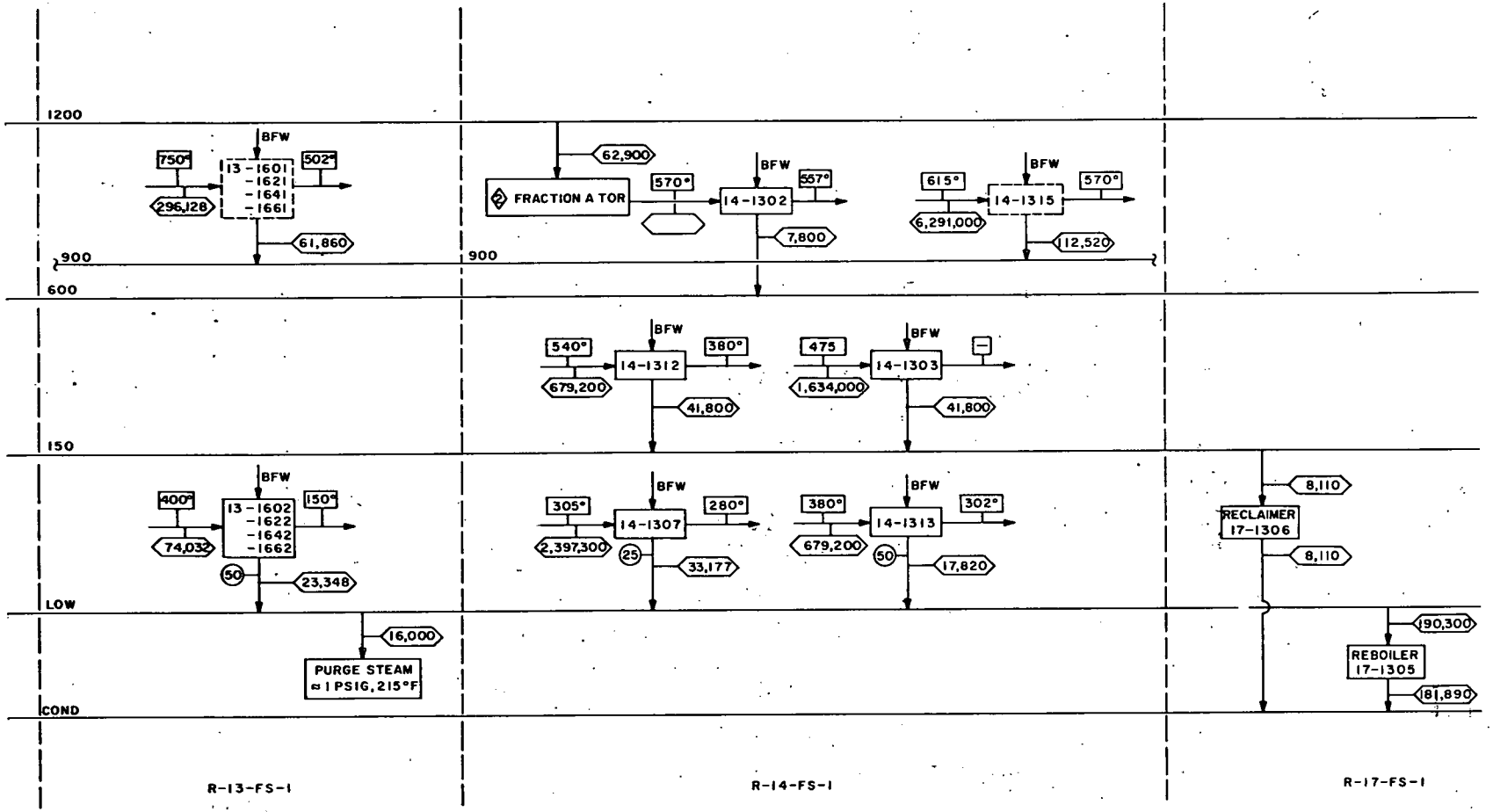

Continued next page

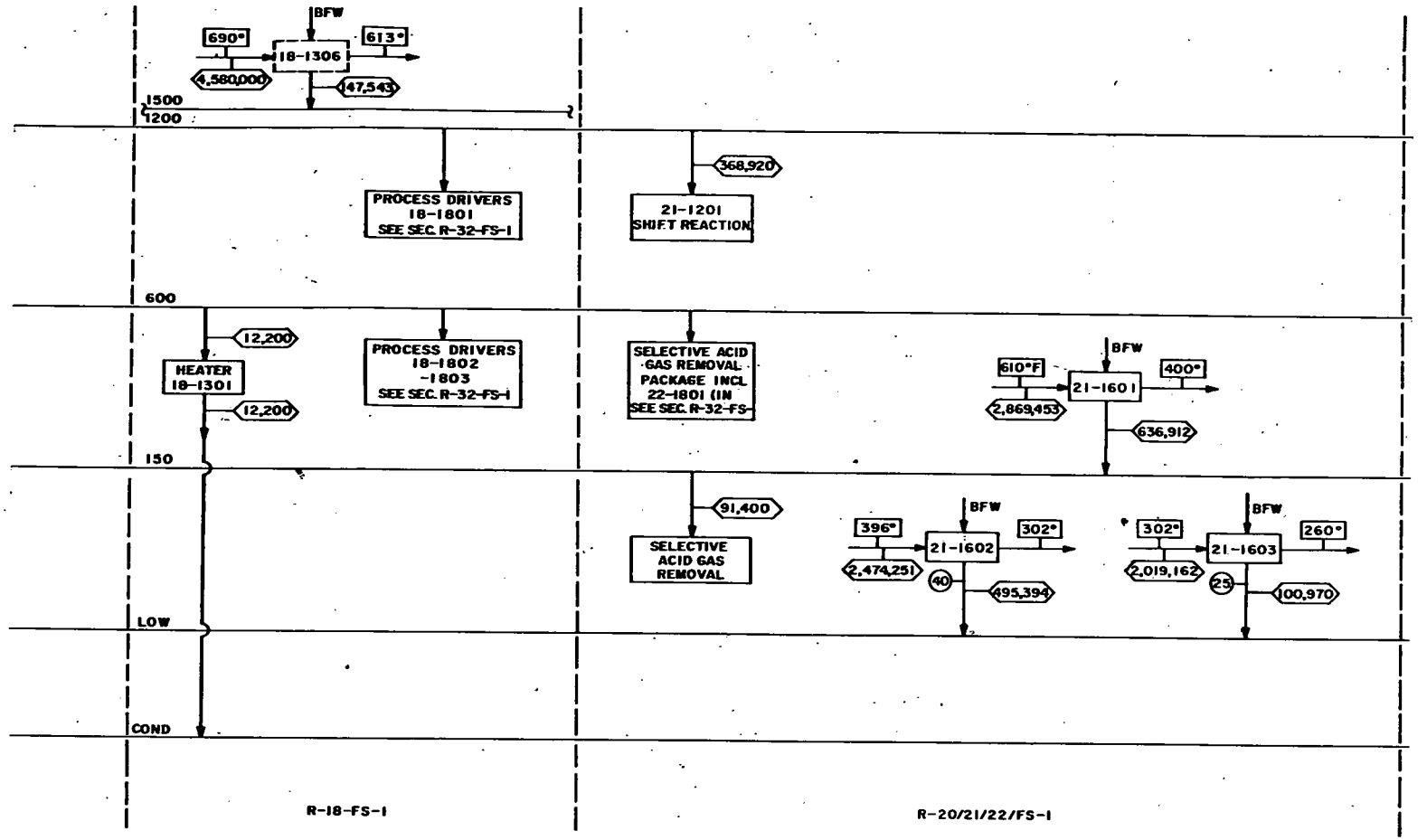

Continued next page

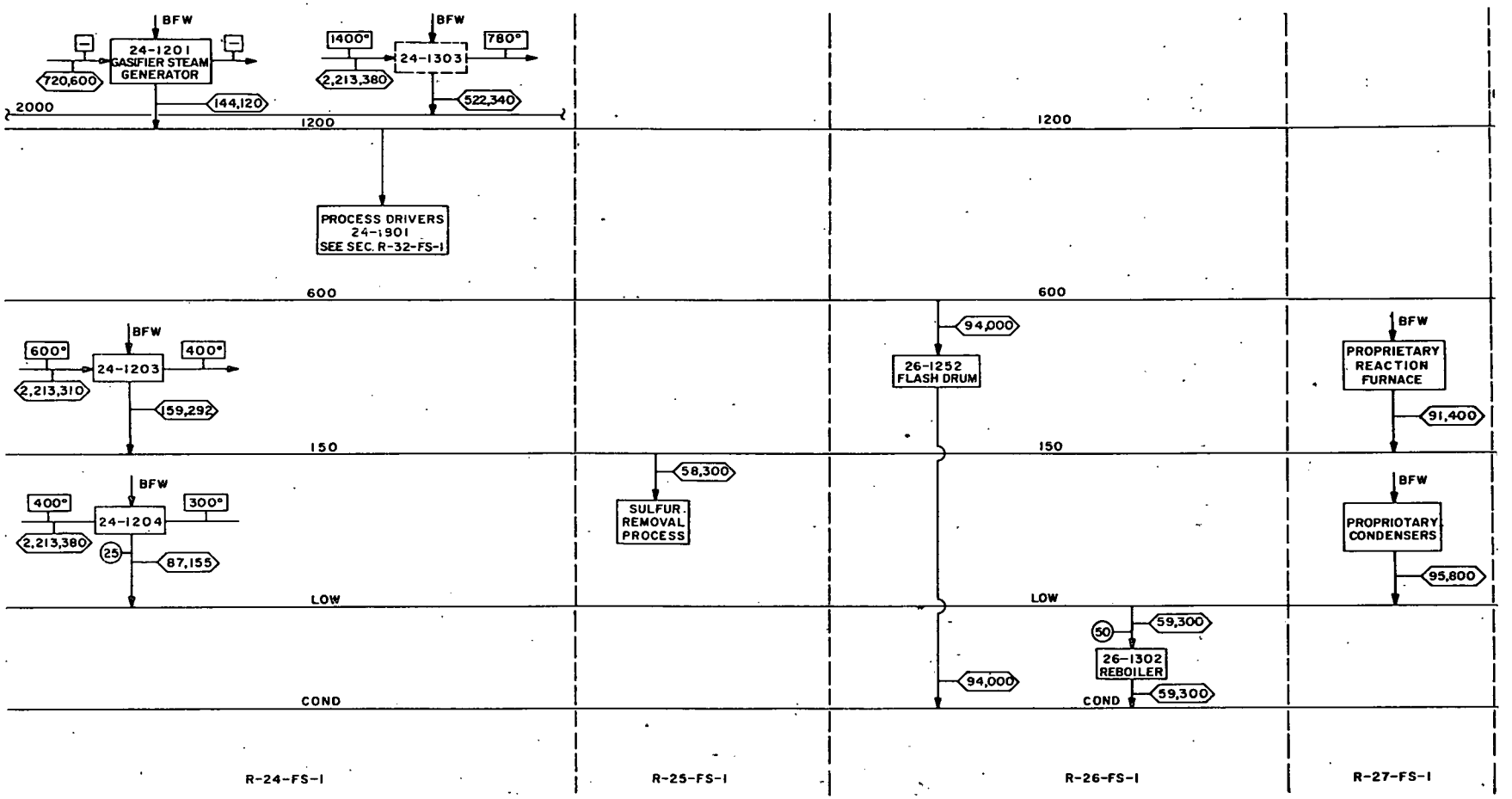

Continued next page

FIG. 4
REVISED STEAM UTILITY FLOW SHEET FOR
THE R. PARSONS OIL/GAS COMPLEX

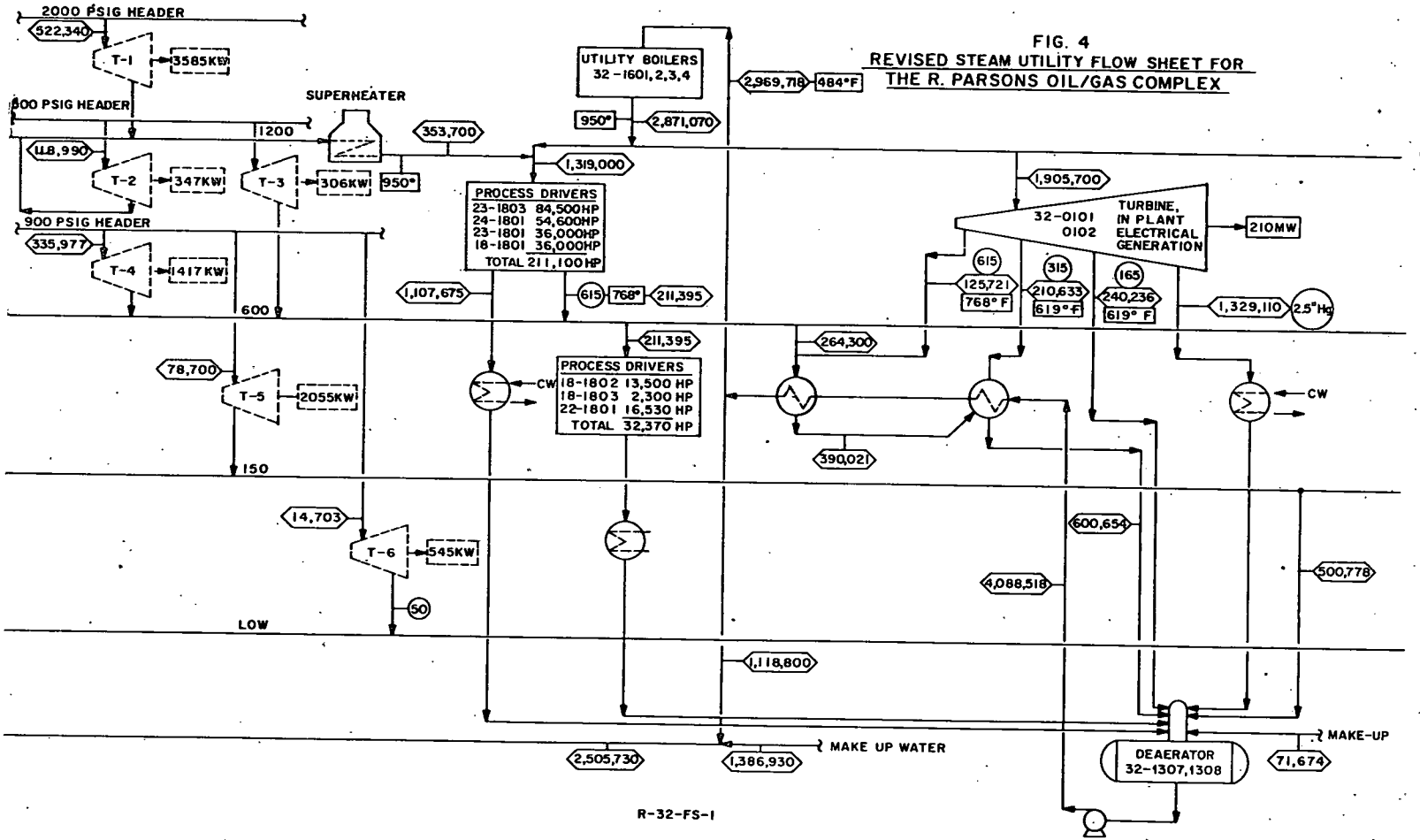

CONCLUSION

Implementation of the scheme shown in Figure II results in a 7760 KW power generation increase, at a total cost of $16,370,000.

References

1. Oil/Gas Complex Conceptual Design/Economic Analysis Oil and SNG Production R&D Report No. 114 - Interim Report No. 4 Prepared by Ralph M. Parsons Co. under contract No. E(49-18)-1775, March 1977 for Major Facility/Project Management Division of ERDA.

2. Personal communication with Daniel Whitley, Westinghouse Canada, LTD.

3. Vogt, G. A., and Walters, M.J., "Steam balance design maximizes heat recovery in refineries, plants," The Oil and Gas Journal, March 1, 1976.

4. Holman, J. P., Heat Transfer, Fourth Edition, McGraw Hill, p. 387, 1976.

5. John Zink, Process Systems Division, Tulsa, Oklahoma.

6. Personal communication with Andrew Bela , Ralph M. Parsons Co., Pasadena, California.

7. A Study of Inplant Electric Power Generation in the Chemical, Petroleum Refining, and Paper and Pulp Industries. Prepared by Thermo Electron Corp. for the Federal Energy Administration, June, 1976.

8. Personal communication with T. S. Govindan, Energy Management Consulting Division, Dupont, Wilmington, Delaware.

9. Personal communication with John Kiefer of Keystone Diesel Engine Company, Inc., Zelienople, PA.

APPENDIX A

SAMPLE CALCULATION

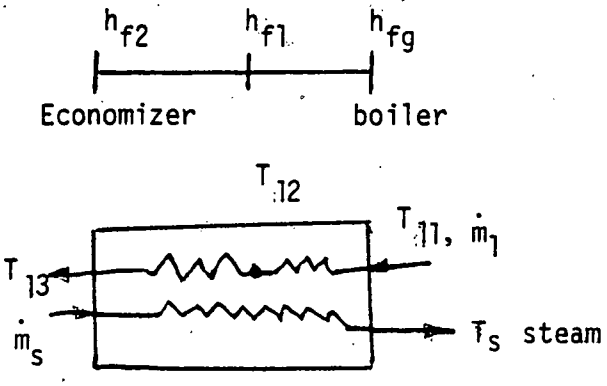

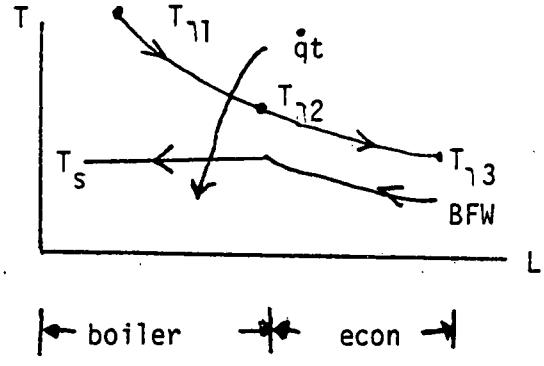

12-1314 From the flow diagram (R-12-FS-1):

T_{11} = 632°F

T_{13} = 550°F

$\dot{q}_t$ = 254.892 MM Btu/hr

$\dot{m}_1$ = 6,193,944 lb/hr

P_s = 600 PSIG

From the equipment specifications (Section 13)[1]:

$$A_{total} = 42{,}680 \text{ ft}^2$$

The following is an analysis of the existing exchanger.

From steam tables:

600 PSIG Steam: h_{fg} = 727.9 Btu/lbm

h_{f1} = 475.8

228°BFW: h_{f2} = 196.3

The mass flow of the steam is found:

$$\dot{m}_s = \frac{\dot{q}t}{h_{fg} + (h_{f1} - h_{f2})} = \frac{254.892 \times 10^6 \text{ Btu/hr}}{727.9 + 475.8 - 196.3 \text{ Btu/lbm}} = 2.53 \times 10^5 \text{ lb/hr}$$

The heat transfer in the boiler section is:

$$\dot{q}_B = \dot{m}_s h_{fg} = (2.53 \times 10^5) \text{ lb/hr} \quad (727.9) \text{ Btu/lb} = 1.84 \times 10^8 \text{ Btu/hr}$$

The heat transfer in the economizer is:

$$\dot{q}_E = \dot{m}_s (h_{f1} - h_{f2}) = (2.53 \times 10^5) \text{ lb/hr } (475.8 - 196.3) \text{ Btu/lb} = 7.08 \times 10^7 \text{ Btu/h}$$

The average specific heat of the heating stream is:

$$C_p = \frac{\dot{q}t}{\dot{m}_1 \Delta T_1} = \frac{254.892 \times 10^6 \text{ Btu/hr}}{(6,193,944) \text{ lb/hr } (632 - 550)°F} = 0.5 \text{ Btu/lb °F}$$

The temperature-length profile is:

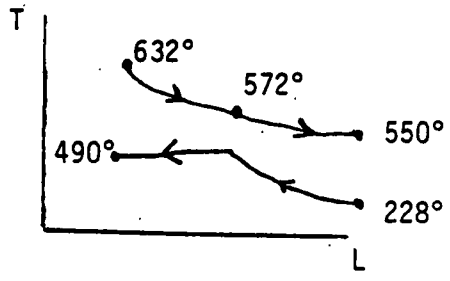

$LTD_B = 82°$

$GTD_B = 142°$

$\Rightarrow LMTD_B = 110°$

$LTD_E = 82°$

$GTD_E = 322°$

$\Rightarrow LMTD_E = 180°$

The overall heat-transfer coefficient of the economizer, U_E, was assumed to be $30 \frac{Btu}{hr \cdot ft^2 \cdot °F}$

The economizer area, then, is:

$$A_E = \frac{\dot{q}_E}{U_E \, LMTD_E} = \frac{7.08 \times 10^7 \text{ Btu/hr}}{30 \frac{Btu}{hr \cdot ft^2 \cdot °F} \, 180°F} = 13{,}103 \text{ ft}^2$$

The boiler area is:

$$A_B = A_{total} - A_E = (42{,}680 - 13{,}103) \text{ ft}^2 = 29{,}577 \text{ ft}^2$$

The overall heat-transfer coefficient of the boiler, U_B is:

$$U_B = \frac{\dot{q}_B}{A_B \, LMTD_B} = \frac{1.84 \times 10^8 \text{ Btu/hr}}{29{,}577 \text{ ft}^2 \, 110°F} = 56.5 \frac{Btu}{hr \cdot ft^2 \cdot °F}$$

This completes the analysis of the existing exchanger.

The possibility of generating 900 PSIG steam is examined, keeping $\dot{q}_t$ constant:

From the steam tables:

900 PSIG, 535°F Steam:	h_{fg}	= 665.6 Btu/lbm
	h_{f1}	= 529.8
228°F BFW:	h_{f2}	= 196.3

The mass flow of the steam is:

$$\dot{m}_s = \frac{\dot{q}t}{h_{fg} + (h_{f1} - h_{f2})} = \frac{254.892 \times 10^6 \text{ Btu/hr}}{665.6 + 529.8 - 196.3 \text{ Btu/lbm}} = 2.55 \times 10^5 \text{ lb/hr}$$

The heat transfer in the boiler is:

$$\dot{q}_B = \dot{m}_s h_{fg} = 2.55 \times 10^5 \text{ lb/hr} \quad 665.6 \text{ Btu/lb} = 1.68 \times 10^8 \text{ Btu/hr}$$

The heat transfer in the economizer is:

$$\dot{q}_E = \dot{m}_s(h_{f1} - h_{f2}) = 2.55 \times 10^5 \text{ lb/hr } (529.8 - 196.3) \text{ Btu/lb} = 8.51 \times 10^7 \text{ Btu/hr}$$

The intermediate heating stream temperature, T_{12}, is

$$T_{12} = T_{11} - \frac{\dot{q}_B}{\dot{m}_1 C_p} = 632°F - \frac{1.68 \times 10^8 \text{ Btu/hr}}{(6{,}193{,}944) \text{ lb/hr } (0.5) \text{ Btu/lb·°F}} = 578°F$$

The "pinch point" then, is:

$$\Delta T_p = T_{12} - T_{Steam} = 578° - 535° = 43°$$

The temperature length profile is:

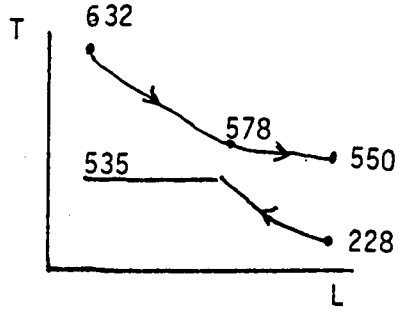

$LTD_B = 43°$

$\Rightarrow LMTD_B = 67°$

$GTD_B = 97°$

$LTD_E = 43°$

$\Rightarrow LMTD_E = 145°$

$GTD_E = 322°$

The area of the boiler, assuming U_B is constant, is:

$$A_B = \frac{\dot{q}_B}{U_B \, LMTD_B} = \frac{1.68 \times 10^8 \text{ Btu/hr}}{56.5 \dfrac{\text{Btu}}{\text{hr} \cdot \text{ft}^2 \cdot °\text{F}} \; 67°} = 44{,}485 \text{ ft}^2$$

The area of the economizer is:

$$A_E = \frac{\dot{q}_E}{U_E \, LMTD_E} = \frac{8.513 \times 10^7 \text{ Btu/hr}}{30 \dfrac{\text{Btu}}{\text{hr} \cdot \text{ft}^2 \cdot °\text{F}} \; 145°\text{F}} = 19{,}570 \text{ ft}^2$$

The total area is:

$$A_t = A_B + A_E = 44{,}485 \text{ ft}^2 + 19{,}570 \text{ ft}^2 = 64{,}055 \text{ ft}^2$$

The possibility of generating high pressure (900 PSIG) steam setting the "pinch point" at 50° is also analyzed:

Setting the "pinch point" also determines the intermediate heating stream temperature, $\bar{T}_{12}$:

$$T_{12} = T_{Steam} + 50° = 535 + 50° = 585°\text{F}$$

The heat transfer of the boiler is found:

$$q_B = (T_{11} - T_{12}) \, \dot{m}_1 \, C_p = (632 - 585)°\text{F} \; (6.19 \times 10^6) \frac{\text{lb}}{\text{hr}} \frac{(0.5) \text{ Btu}}{16°\text{F}} = 1.46 \times 10^8 \frac{\text{Btu}}{\text{hr}}$$

The mass flow of the steam is:

$$\dot{m}_s = \frac{\dot{q}_B}{h_{fg}} = \frac{1.46 \times 10^8 \text{ Btu/hr}}{665.6 \frac{\text{Btu}}{\text{lbm}}} = 2.19 \times 10^5 \text{ lb/hr}$$

The heat transfer in the economizer is:

$$\dot{q}_E = \dot{m}_s (h_{f1} - h_{f2}) = 2.19 \times 10^5 \frac{\text{lb}}{\text{hr}} (529.8 - 196.3) \frac{\text{Btu}}{\text{lb}} = 7.3 \times 10^7 \frac{\text{Btu}}{\text{hr}}$$

The exit temperature of the heating stream, T_{13}, has changed since $\dot{q}_t$ has changed. It is:

$$T_{13} = T_{12} - \frac{\dot{q}_E}{\dot{m}_g C_p} = 585°\text{F} - \frac{7.3 \times 10^7 \text{ Btu/hr}}{6{,}193{,}944 \frac{\text{lb}}{\text{hr}} \, 0.5 \frac{\text{Btu}}{\text{lb}\cdot°\text{F}}} = 561.4°\text{F}$$

The temperature-length profile is:

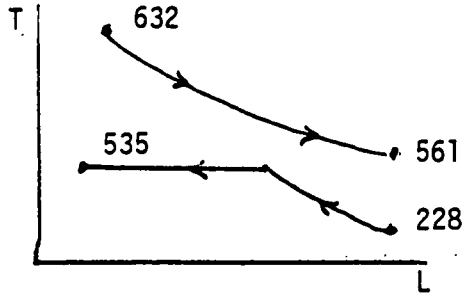

$LTD_B = 50°$

$\Rightarrow LMTD_B = 71°$

$GTD_B = 97°$

$LTD_E = 50°$

$\Rightarrow LMTD_E = 155°$

$GTD_E = 333°$

The boiler area is:

$$A_B = \frac{\dot{q}_B}{U_B \, LMTD_B} = \frac{1.455 \times 10^8 \text{ Btu/hr}}{56.5 \frac{\text{Btu}}{\text{hr} \cdot \text{ft}^2 \cdot °\text{F}} \, 71°\text{F}} = 36{,}270 \text{ ft}^2$$

The economizer area is:

$$A_E = \frac{\dot{q}_E}{U_E \, LMTD_E} = \frac{7.3 \times 10^7 \text{ Btu/hr}}{30 \dfrac{\text{Btu}}{\text{hr} \cdot \text{ft}^2 \cdot {}^\circ\text{F}} \; 155{}^\circ\text{F}} = 15{,}700 \text{ ft}^2$$

The total area, then, is:

$$A_t = A_B = A_E = 36{,}270 \text{ ft}^2 + 15{,}700 \text{ ft}^2 = 51{,}970 \text{ ft}^2$$

APPENDIX B

The installed cost of the heat exchangers in $\$/ft^2$ was found from the curves on the following two pages, Figures 5 and 6.

The Ralph Parson's factored extimates were obtained from Reference 6. The quotations from John Zink were obtained from Reference 5, and were quoted as base costs. These base costs were converted to installed costs by multiplying by a factor of 2.5 for erection, piping, site-work, etc., as described in Reference 7.

The quotations from John Zink, Inc., and Ralph Parsons on heat exchangers under 10,000 ft^2 allowed the extrapolation of the curve shown with a high level of confidence. The slope of this curve was assumed to remain the same for heat exchangers over 10,000 ft^2.

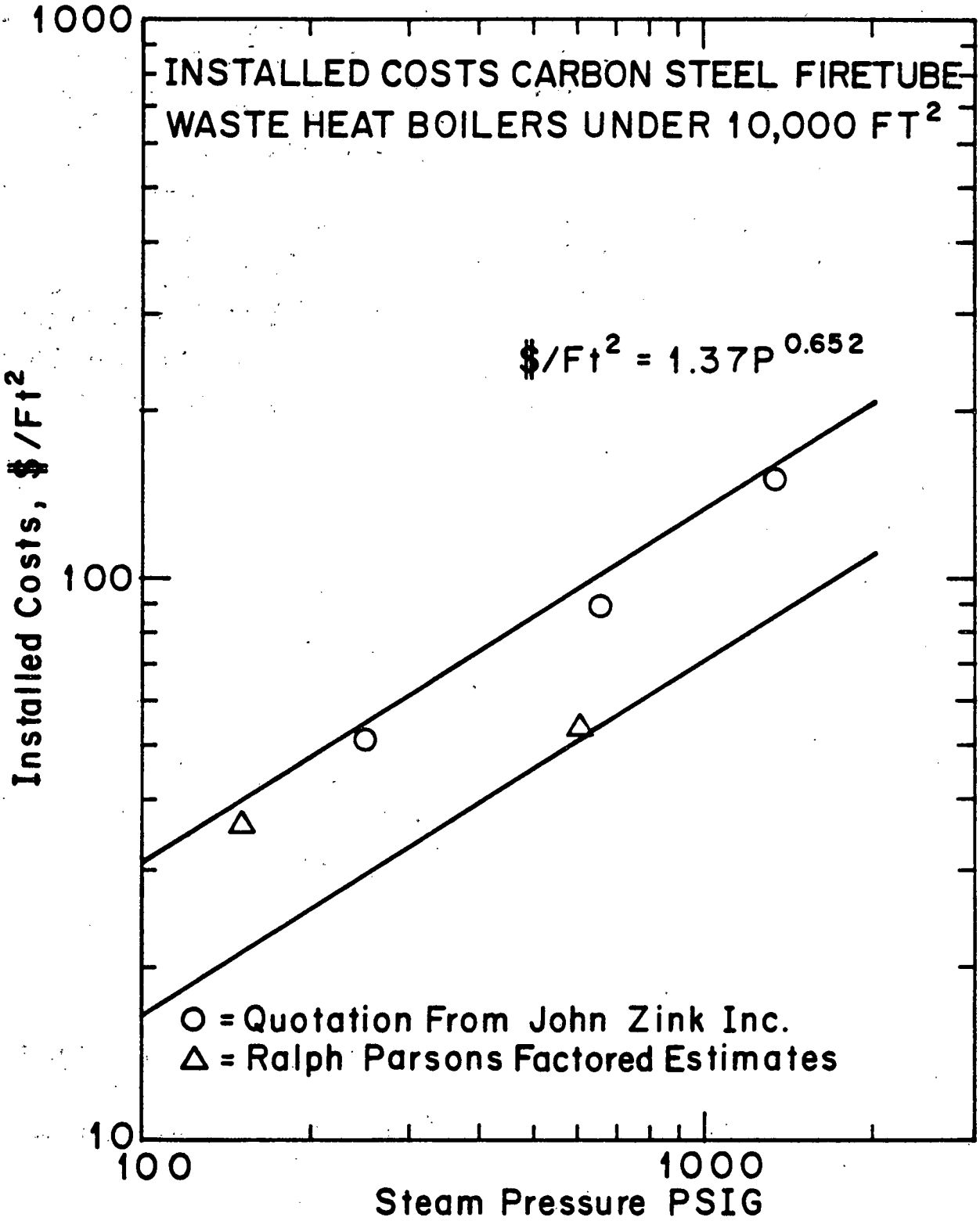
INSTALLED COSTS CARBON STEEL FIRETUBE
WASTE HEAT BOILERS UNDER 10,000 FT²
$/Ft² = 1.37P^0.652
O = Quotation From John Zink Inc.
Δ = Ralph Parsons Factored Estimates
Installed Costs, $/Ft²
1000
100
10
100
1000
Steam Pressure PSIG

FIG. 5

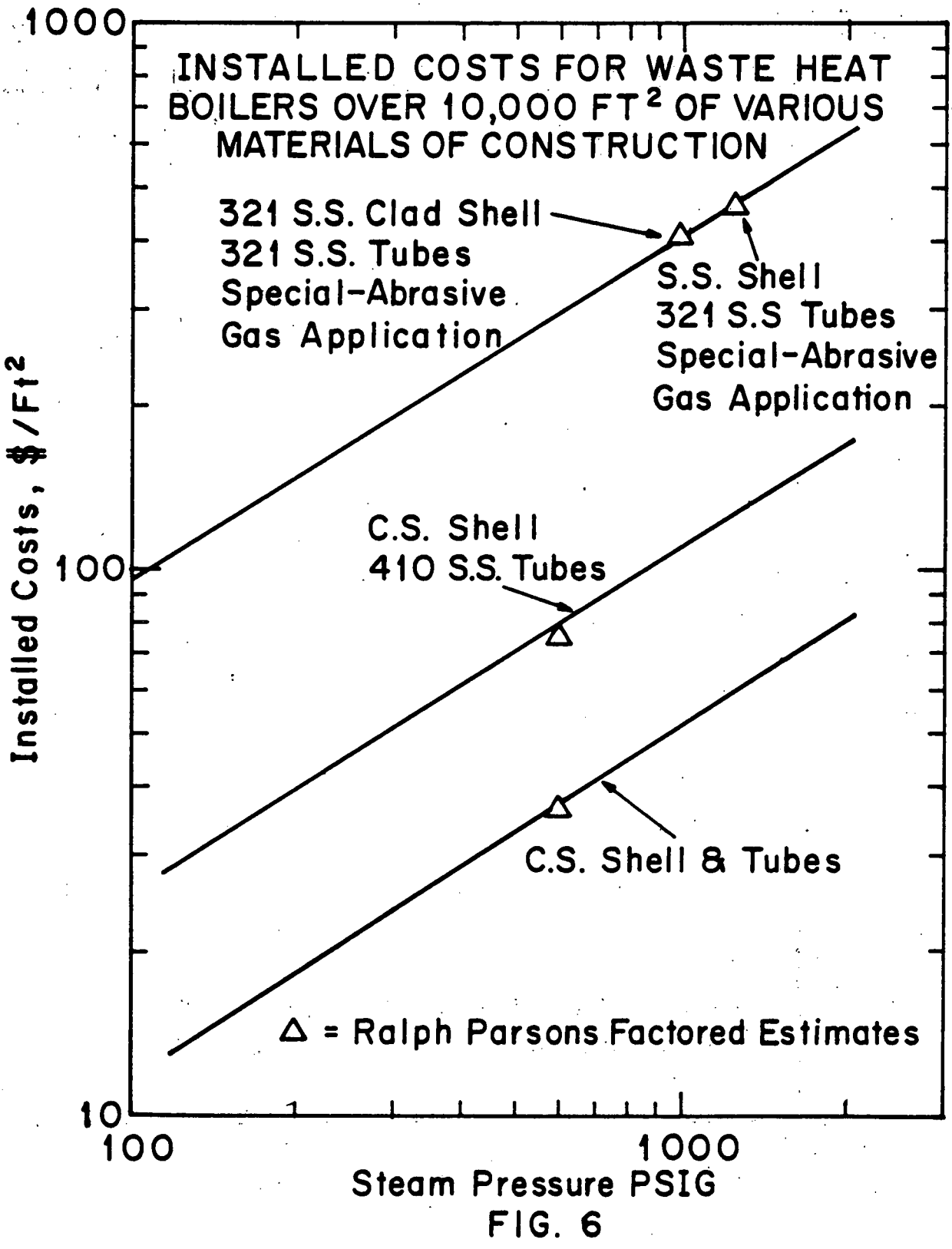
INSTALLED COSTS FOR WASTE HEAT BOILERS OVER 10,000 FT² OF VARIOUS MATERIALS OF CONSTRUCTION
321 S.S. Clad Shell
321 S.S. Tubes
Special-Abrasive
Gas Application
S.S. Shell
321 S.S Tubes
Special-Abrasive
Gas Application
C.S. Shell
410 S.S. Tubes
C.S. Shell & Tubes
△ = Ralph Parsons Factored Estimates
Installed Costs, $/Ft²
1000
100
10
100
1000
Steam Pressure PSIG

FIG. 6

APPENDIX C

The six turbines would operate under the following conditions:

Turbine	$\dot{m}$	P_{in}	P_{out}	h_1	${}_1h_{25}$	N*	P	Installed cost*
	lb/hr	PSIG	PSIG	Btu/lbm	Btu/lbm	%	HP	$
1	522,340	2000	1200	1136	1100	65	4805	1,200,000
2	118,990	1500	1200	1169	1147	45	465	525,000
3	28,553	1500	600	1164	1096	50	410	250,000
4	335,977	900	600	1196	1164	45	1900	425,000
5	78,700	900	150	1196	1054	65	2755	250,000
6	14,703	900	50	1196	986	60	730	175,000

Total HP output of turbines = 11,065 HP

h_1 = enthalpy at P_{in}

${}_1h_{25}$ = isentropic enthalpy at P_{out} with P_{in} reference

The output of turbine 1, for example was found to be:

$$P = \frac{\dot{m}\,(h_1 - {}_1h_{25})\eta}{2544\ \frac{Btu}{hp - hr}} = \frac{522{,}340\ (1136-1100)(.65)}{2544} = 4805\ HP$$

*The efficiencies (η) and costs were quoted by Westinghouse Canada, Ltd. (Ref. 2).

2 ENERGY CONSERVATION IN COAL CONVERSION

1 Combined Cycle In-Plant Electrical Power Generation

A Case Study

E. J. Mueller

Carnegie-Mellon University
Pittsburgh, PA 15213

June, 1978

Prepared for

THE U.S. DEPARTMENT OF ENERGY
Pittsburgh Energy Technology Center
UNDER CONTRACT NO. EY77S024196

ABSTRACT

A combined cycle power generation scheme for the Ralph Parsons Oil/Gas plant was studied as an alternate to the steam turbine power generation system to see if energy can be saved in a cost effective way. Using the same amount of coal as the present system, generates an excess of 22.2 megawatts of electrical power or 10.6% of the 210 MW generated in the Oil/Gas Complex at a cost of $610/KW. If electricity is exported at $.025/KW-hr the annual gross revenues are 4.3 million dollars a year. This is a 19% return on investment, using a discounted cash flow analysis. From a life cycle cost stand point, this is a total revenue of 56.5 million dollars over the 20-year life of the plant.

The combined cycle alternate, which uses present state-of-the-art equipment is a cost effective way to better utilize energy.

ACKNOWLEDGEMENTS

I would like to thank Andrew Bela of the Ralph M. Parsons Company for his valuable information and help in preparing this report.

TABLE OF CONTENTS

LIST OF TABLES

LIST OF FIGURES

INTRODUCTION

This report examines the present power generation scheme of the Ralph M. Parsons Oil/Gas Complex Conceptual Design to determine if the efficiency of the power generation system could be improved in a cost effective manner.

The alternative to the present system is a combined cycle utilizing low Btu fuel gas from the low Btu gasifier (unit 24) in a gas turbine, then using the hot exhaust gases in a heat recovery boiler to generate steam for process requirements and additional electric power generation.

The combined cycle was chosen as an alternative because (1) higher thermal efficiencies (35-45%) than straight rankine cycle efficiencies can be expected, and (2) current state-of-the-art gas turbines, heat recovery boilers and other equipment can achieve these higher efficiencies.

DESCRIPTION OF PRESENT SYSTEM

The present power and steam generation system shown in Figure 1 burns low Btu fuel gas from a low Btu gasifier (unit 24) in boilers for 1200 psig steam generation. The steam generated in this boiler is then used in the process for process steam turbine drivers, and the steam turbine generators for 210 MW of electric power production. The power generation turbines each have three extraction points, at 600 psig, 300 psig and 150 psig, for use in feedwater heaters that service the large waste heat boiler.

DESCRIPTION OF THE COMBINED CYCLE ALTERNATIVE

The combined cycle alternative must generate the same amount of steam for process use, steam turbine drivers in the process area and electric power requirements for in-plant use as the present system.

The combined cycle system shown in Figure 2 consists of a fuel gas preheater (Appendix A), two gas turbine-generators producing 112.7 megawatts each (Appendix C), one 1200 psig waste heat steam generator which uses the hot exhaust gases of the gas turbines to generate 1,508,000 lb/hr of steam (Appendix A), one each 150 and 25 psig waste heat steam generators utilizing the hot gas from the large waste heat boiler (Appendix A). The 1,508,000 lb/hr of 1200 psig steam generated in the large waste heat boiler is used for process with the balance of 131,500 lb/hr used in a steam turbine (Appendix D) for electric power generation. The turbine has one extraction point of 109,650 lb/hr of 300 psig, 619°F for feedwater heating. Because of the reduced amount of steam generated, the number of deaerators has been

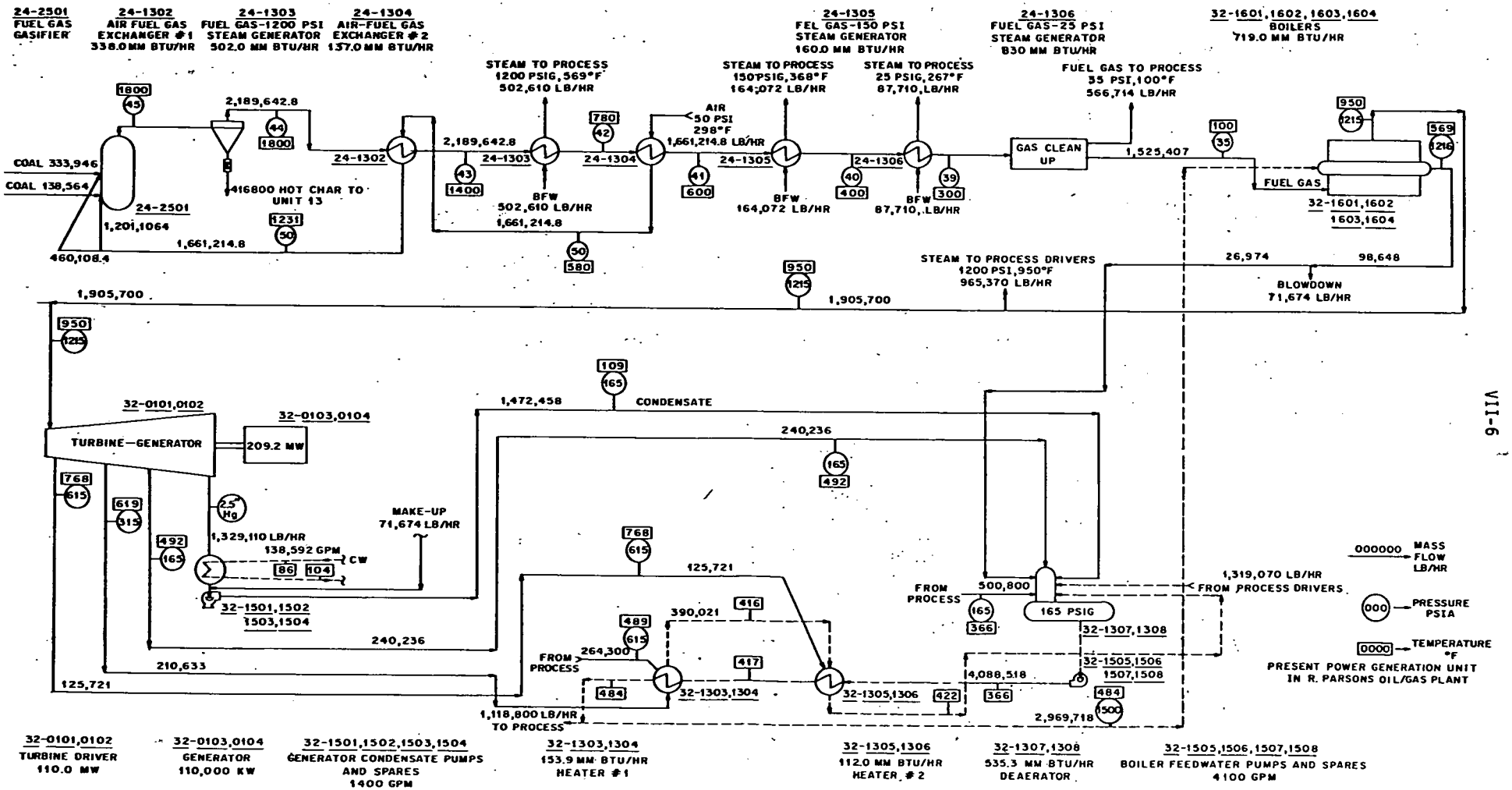

FIGURE 1 PRESENT POWER GENERATION UNIT IN R. PARSONS OIL/GAS PLANT

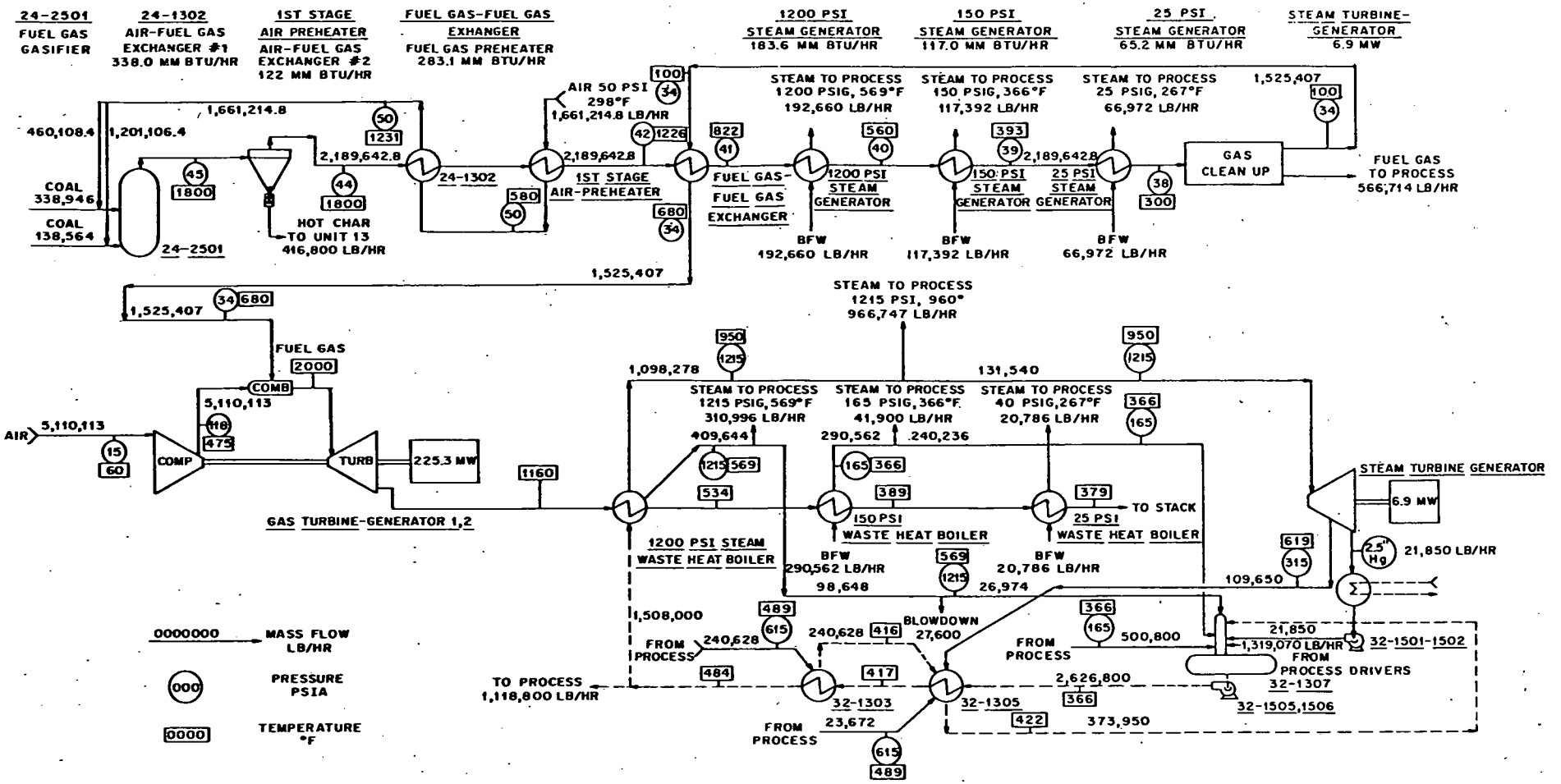

GAS-TURBINE-GENERATOR 1,2	1200 PSI STEAM WASTE HEAT BOILER	150 PSI WASTE HEAT BOILER	25 PSI WASTE HEAT BOILER	32-1501,1502 GENERATOR CONDENSATE PUMP AND SPARE	32-1505,1506 BFW PUMP AND SPARE	32-1307 DEAERATOR	32-1305 HEATER #2	32-1303 HEATER #1
112.7 MW	1247 MW BTU/HR	289.4 MW BTU/HR	19.9 MW BTU/HR	1400 GPM	4100 GPM	535.3 MW BTU/HR	112.0 MW BTU/HR	153.9 MW BTU/HR

FIGURE 2 COMBINED CYCLE ALTERNATE ELECTRIC POWER AND STEAM GENERATION SCHEME FOR THE R. PARSONS OIL/GAS COMPLEX

decreased from 2 (32-1307,08) to one (32-1307), the number of condensate pumps has been reduced from 4 (32-1501,02,03,04) to two (32-1501,02), the number of feedwater heaters has been reduced from 4 (32-1303,04,05,06) to two (32-1303,04), and the number of feedwater pumps has been decreased from 4 (32-1505,06,07,08) to 2 (32-1505,06).

ECONOMIC ANALYSIS

Installed costs shown in Table 1 for the combined cycle equipment and for the equipment in the present design are from references 1, 2,5,7,8 and calculations in the appendices. From Table 1, the installed cost of the combined cycle alternative is 99.1 million dollars while the installed cost of the present power generation unit is 85.6 million dollars, the increase in cost for the combined cycle alternative is 13.5 million dollars.

The combined cycle generates a surplus of 22.2 megawatts of electricity over and above the requirements of the plant. This is an installed cost of $610/KW. For this analysis, the electric power would be exported for revenue at a price of $ .025/KW-hr base cost and $.033/KW-hr optimistic price. These prices are given in Section XII, basis for fuel and utility costs. At $ .025/KW-hr, the gross revenue is 4.3 million dollars per year and at $.033/KW-hr the annual gross revenue is 5.7 million dollars. This assumes a 330 day operating year as specified in the Oil/Gas Conceptual Design. In addition the operating and maintenance costs for the present system and the combined cycle alternate are equal.

TABLE 1

Equipment Description and Installed Costs for the
Ralph M. Parsons Design and Combined Cycle Alternate

Equipment No. and Description		Unit Capacity	Number Req'd Parsons/Comb. Cycle	Total Installed Costs Parsons/Comb. Cycle
24-1303*	1200 psi waste heat steam generator	502 MM Btu/hr 55000 sq.ft.	1/-	$ 31,411,782
24-1304	air-fuel gas exchanger #2	137 MM Btu/hr 75440 sq.ft.	1/-	$ 3,437,323
24-1305	fuel gas 150 psi steam generator	160 MM Btu/hr 88500 sq.ft.	1/-	$ 405,817
24-1306	fuel gas 25 psi steam generator	83 MM Btu/hr 61360 sq.ft.		$ 656,989
32-1601,02,03,04	boiler	853.4 MM Btu/hr	4/-	$ 28,710,700
32-0101,02	steam turbine-generator	110.0 MW	2/-	$ 17,827,909
32-1307,08	deaerator	535.3 MM Btu/hr	2/1	$ 273,398/136,600
32-1501,02,03,04	condensate pumps and spares	1400 gpm	4/-	$ 42,472
32-1505,06,07,08	feedwater pumps and spares	4100 gpm	4/2	$ 1,389,954/69497
32-1303,04	feedwater heaters	112 MM Btu/hr	2/1	$ 694,978/347,489
32-1303,04	feedwater heaters	153.9 MM Btu/hr	2/1	$ 694,978/347,489
---	air-fuel gas exchanger	122 MM Btu/hr 15683 sq.ft.	-/1	$ 870,086
---	fuel gas-fuel gas heat exchanger	283.1 MM Btu/hr 66,222 sq.ft.	-/1	$ 3,632,278
---	1200 psi waste heat steam generator	183.6 MM Btu/hr 54384 sq.ft.	-/1	$ 29,612,088
---	150 psi waste heat steam generator	117 MM Btu/hr 82748 sq.ft.	-/1	$ 386,433
---	25 psi waste heat steam generator	65.2 MM Btu/hr 58719 sq.ft.	-/1	$ 688,744
---	gas turbine-generators	112.7 MW	-/2	$ 38,994,200
---	steam turbine-generator	6.6 MW	-/1	$ 956,440
---	1200 psi waste heat steam generator	124.7 MM Btu/hr 1,205,473 sq.ft.	-/1	$ 19,227,294
---	condensate pump and spare	45 gpm	-/2	$ 4,720
---	150 psi waste heat steam generator	289.4 MM Btu/hr 223371 sq.ft.	-/1	$ 3,562,770
---	25 psi waste heat steam generator	20 MM Btu/hr 12619 sq.ft.	-/1	$ 201,273
			TOTALS:	$ 85,546,300/ 99,037,361
				ΔCOST = 13,491,061

* Equipment number given in Reference 9.
Installed costs are from Refs. 1,2,5,7,8 and calculations in Appendices A,B,C and D.

Discounted Cash Flow Analysis

A discounted cash flow analysis was performed using the two selling prices of electricity to obtain a rate of return on the additional capital investment for the combined cycle alternate. The following bases were used:

1) 20 year project life
2) 16 year SYD depreciation
3) 52% combined state and federal income tax
4) No investment tax credit
5) 100% equity

The rate of return using $ .025/KW-hr for the price of electricity is 19% and the rate of return using $.033/KW-hr is 24.8%, each one being above the rate of return of 12% specifed by Ralph Parson's as the minimum desired rate of return on the Oil/Gas Complex[9]. The yearly tabulation of the discounted cash flow analysis is shown in Tables 2 and 3.

LIFE CYCLE COST ANALYSIS

The life cycle cost analysis assumes that 100% of the additional capital cost for the change in power generation schemes must be borrowed at 9% interest for the 20-year project life. This results in uniform annual payments of $1.48 million dollars on the loan. This cost is subtracted from the annual revenue of 4.3 million dollars to obtain a net yearly revenue of 2.82 million dollars per year, or 56.6 million dollars over the life of the plant. Using $.033/KW-hr, the net annual revenue is 4.27 million dollars per year, or 85.3 million dollars over the life of the plant.

CONCLUSION

At a cost of $610/KW, the combined cycle power generation scheme provides a minimum gross revenue of 4.3 million dollars, with a rate of return of 19% on the additional capital investment. The combined cycle alternate steam and power generation scheme is a cost effective way to generate steam and electric power in the Oil/Gas Complex using present state-of-the-art equipment.

TABLE 2

Discounted Cash Flow for

Electricity Selling Price of $.025/KW-hr

****

100 PERCENT EQUITY
9 PERCENT INTEREST

0 PERCENT TAX CREDIT ON
0 PERCENT OF INVESTMENT

THE CALCULATED RATE OF RETURN IS 19.04 PERCENT

YEAR	GROSS CASH FLOW	ANNUAL DEPREC	ANNUAL TAX	NET CASH FLOW	DISCNTD CASH FLOW
1	4305	1592	1410.76	2894.24	2516.73
2	4305	1492.5	1462.5	2842.5	2149.338
3	4305	1393	1514.24	2790.76	1834.97
4	4305	1293.5	1565.98	2739.02	1566.044
5	4305	1194	1617.72	2687.28	1336.053
6	4305	1094.5	1669.46	2635.54	1139.417
7	4305	995	1721.2	2583.8	971.3461
8	4305	895.5	1772.94	2532.06	827.7349
9	4305	796	1824.68	2480.32	705.0617
10	4305	696.5	1876.42	2428.58	600.3078
11	4305	597	1928.16	2376.84	510.8856
12	4305	497.5	1979.9	2325.1	434.5778
13	4305	398	2031.64	2273.36	369.4846
14	4305	298.5	2083.38	2221.62	313.9786
15	4305	199	2135.12	2169.88	266.6663
16	4305	99.5	2186.86	2118.14	226.3545
17	4305	0	2238.6	2066.4	192.0221
18	4305	0	2238.6	2066.4	166.9757
19	4305	0	2238.6	2066.4	145.1963
20	4305	0	2238.6	2066.4	126.2576
TOTAL	86100	13532	37735.36	48364.64	16399.4

Note: Figures are in thousands of dollars.

TABLE 3

Discounted Cash Flow for Electricity

Selling Price of $.033/KW-hr

****

100 PERCENT EQUITY
9 PERCENT INTEREST

0 PERCENT TAX CREDIT ON
0 PERCENT OF INVESTMENT

THE CALCULATED RATE OF RETURN IS 24.76 PERCENT

YEAR	GROSS CASH FLOW	ANNUAL DEPREC	ANNUAL TAX	NET CASH FLOW	DISCNTD CASH FLOW
1	5746	1592	2160.08	3585.92	3118.191
2	5746	1492.5	2211.82	3534.18	2672.348
3	5746	1393	2263.56	3482.44	2289.761
4	5746	1293.5	2315.3	3430.7	1961.514
5	5746	1194	2367.04	3378.96	1679.94
6	5746	1094.5	2418.78	3327.22	1438.449
7	5746	995	2470.52	3275.48	1231.374
8	5746	895.5	2522.26	3223.74	1053.846
9	5746	796	2574	3172	901.6804
10	5746	696.5	2625.74	3120.26	771.2805
11	5746	597	2677.48	3068.52	659.5576
12	5746	497.5	2729.22	3016.78	563.8577
13	5746	398	2780.96	2965.04	481.9019
14	5746	298.5	2832.7	2913.3	411.7328
15	5746	199	2884.44	2861.56	351.6699
16	5746	99.5	2936.18	2809.82	300.2708
17	5746	0	2987.92	2758.08	256.297
18	5746	0	2987.92	2758.08	222.867
19	5746	0	2987.92	2758.08	193.7974
20	5746	0	2987.92	2758.08	168.5195
TOTAL	114920	13532	52721.76	62198.24	20728.86

Note: Figures are in thousands of dollars.

REFERENCES

1. Ralph M. Parsons Company, Pasadena, CA.

2. D. T. Beecher, et. al., "Energy Conversion Alternatives Study, Westinghouse Phase II Final Report: Summary and Combined Gas-Steam Turbine Plant with an Integrated Low Btu Gasifier", Westinghouse Electric Corporation Research Laboratories, 1976.

3. Van Wylen and Sonntag, "Fundamentals of Classical Thermodynamics", 2nd edition, John Wiley and Sons, Inc., New York, 1973.

4. Keenan, Keyes, Hill, Moore, "Steam Tables (English Units)", John Wiley and Sons, Inc., 1969.

5. Popper, Herbert, "Modern Cost Engineering Techniques", 1st edition, McGraw-Hill Book Company, New York, 1976.

6. Holman, J. P., "Heat Transfer", McGraw-Hill Book Company, New York, 1976.

7. Thermo-Electron Corporation, Final Report: A Study of Inplant Electric Power Generation in the Chemical, Petroleum Refining and Paper and Pulp Industries".

8. P. H. Kydd, Chemical Engineering Progress, Vol. 71, No. 10, Oct 1975.

9. Oil/Gas Complex Conceptual Design/Economic Analysis R & D Report No. 114 - Interim Report No. 4, Ralph M. Parsons Company, 1977.

APPENDIX A

Heat Exchanger Area and Cost Calculations

The method for calculating heat exchanger heat transfer areas, and installed costs with examples is given below.

The heat transfer in a heat exchanger is:

$$q = \dot{m}_{fg} \times C_p \times \Delta T_{fg}$$

where:

$\dot{m}_{fg}$ = mass flow of fluid, lb/hr

C_p = constant pressure specific heat of fluid, Btu/lb-°F

ΔT_{fg} = change in temperature of the fluid, °F

The heat transferred is also:

$$q = U \times A \times \Delta T_m$$

where:

U = overall heat transfer coefficient, Btu/hr-ft^2-°F

A = area of exchanger, ft^2

ΔT_m = log mean temperature difference of the exchanger, °F

$$\Delta T_m = \frac{(GTD - LTD)}{\ln(GTD/LTD)}$$

where:

GTD = the greatest temperature difference of the fluids

LTD = the least temperature difference of the fluids.

EXAMPLE:

Calculation of Required Area for the Fuel Gas Preheater (Figure 2)

From Figure 2:

$$\dot{m}_{fg} = 2{,}189{,}643 \text{ lbm/hr}$$

$$\Delta T_{fg} = 1226°F - 822°F$$

and from reference 3,

$$C_p = .32 \text{ Btu/lb-°F.}$$

Therefore,

$$q = 2{,}189{,}643 \times .32 \text{ Btu/lb-°F} \times (1226°F - 822°F)$$

$$= 283.1 \text{ MM Btu/hr.}$$

The log-mean temperature difference is:

$$\Delta T_m = \frac{1126°F - 142°F}{\ln(1126°F/142°F)}$$

$$= 475°F$$

Using a value of 9 from reference 6 for the over-all heat transfer coefficient U we have:

$$283.1 = UA\Delta T_m$$

$$A = \frac{283.1 \times 10^6}{9 \times 475}$$

$$= 66{,}222 \text{ ft}^2$$

From reference 1, the 4th quarter, 1976 installed cost per foot for this type of exchanger is $47.54. Assuming 10% inflation, the 1978 price is:

$$\$47.54 \times (1.1)^{1.5} = \$54.85$$

Therefore, the total installed cost is:

$$C = A \times \$54.85$$
$$= 66{,}222\ ft^2 \times \$54.85/ft^2$$
$$= \$\ 3{,}632{,}278$$

The method used for calculating the required surface areas and installed costs of steam generators is similar to the heat exchanger calculations.

1200 psi Heat Recovery Boiler Calculations

From Figure 2:

$$\dot{m}_s = 1{,}098{,}278\ lb/hr$$
$$\Delta T = 950°F - 569°F$$
$$\Delta h_{SH} = 187\ Btu/lb$$

Therefore, the heat transferred in the superheater is:

$$q_{SH} = 1{,}098{,}278\ lb/hr \times 187\ Btu/lb$$
$$q_{SH} = 205\ MM\ Btu/hr$$

The log mean temperature difference between the two streams is:

$$\Delta T_m = 330°F.$$

From reference 2, U = 6 Btu/hr-°F-ft^2.

The superheater area is:

$$A_{SH} = \frac{205 \text{ MM Btu/hr}}{6 \text{ Btu/hr-°F-ft}^2 \times 330°F}$$

$$A_{SH} = 103{,}535 \text{ ft}^2$$

The heat transfer in the boiler is:

$$q_B = \dot{m} \, h_{fg}$$

where:

q_B = heat transfer in the boiler

$\dot{m}$ = mass flow of steam in boiler.

From Figure 2:

$$\dot{m} = 1{,}507{,}922 \text{ lb/hr}$$

This mass flow differs from the superheater mass flow, since some saturated steam is extracted from the boiler for process use and does not pass through the superheater.

From reference 4:

$$h_{fg} = 606 \text{ Btu/lb}$$

$$q_B = 1{,}507{,}922 \text{ lb/hr} \times 606 \text{ Btu/lb}$$

$$q_B = 913.8 \text{ MM Btu/hr}$$

From reference 2:

$$U = 6 \text{ Btu/hr-ft}^2\text{-°F}$$

and from Figure 2:

$$\Delta T_m = 163°F$$

$$A_B = 913.8 \text{ MM Btu/hr} \Big/ 6 \text{ Btu/hr-°F-ft}^2 \times 163°F$$

$$A_B = 934{,}355 \text{ ft}^2$$

where: A_B = surface area of boiler heat transfer.

The heat transfer in the economizer is:

$$q_E = \dot{m} C_p \Delta T$$

From Figure 2:

$$\dot{m} = 1{,}507{,}922 \text{ lb/hr}$$

$$\Delta T = 569°F - 484°F$$

$$q_E = 1{,}507{,}922 \text{ lb/hr} \times 1 \text{ Btu/lb-°F} \times (569°F - 484°F)$$

$$q_E = 128.2 \text{ MM Btu/hr}$$

From Figure 2:

$$\Delta T_m = 85°F$$

and from reference 2:

$$U = 9 \text{ Btu/hr-ft}^2\text{-°F}$$

$$A_E = \frac{128.2 \text{ MM Btu/hr}}{9 \text{ Btu/hr-ft}^2\text{-°F} \times 85°F}$$

$$A_E = 167{,}582 \text{ ft}^2$$

where: A_E = surface area of economizer heat transfer.

The TOTAL AREA is:

$$A_T = A_E + A_B + A_{SH}$$

$$A_T = 103,535 \text{ ft}^2 + 934,355 \text{ ft}^2 + 167,582 \text{ ft}^2$$

$$A_T = 1,205,473 \text{ ft}^2$$

Installed cost per square foot was determined from Reference 2, therefore, the cost for the boiler is:

$$C = 1,205,473 \text{ ft}^2 \times \$15.95/\text{ft}^2 = \$19,227,294$$

APPENDIX B

Electrical Power for Export

The additional electric power generated by the combined cycle alternative was claculated by subtracting the electric power requirements of the Oil/Gas plant from the total power produced by the combined cycle:

$$P_{net} = P_{cc} - P_{o/g}$$

where:

P_{net} = excess electric power

P_{cc} = electric power produced by the combined cycle

$P_{o/g}$ = electric power required by the Oil/Gas complex

Therefore:

$$P_{net} = 232.18 \text{ MW} - 210.0 \text{ MW}$$

$$P_{net} = 22.2 \text{ MW}$$

APPENDIX C

Gas Turbine-Generator Work and Cost Calculations

For a turbine inlet temperature of 2000°F, the air to fuel ratio calculated from the adiabatic flame temperature is 3.35. Therefore, the mass flow of air into the compressor is:

$$\dot{m}_a = a/f \times \dot{m}_f$$

From Figure 2, $\dot{m}_f$ = 1,525,407 lb/hr

$$\dot{m}_a = 3.35 \times 1{,}525{,}407 \text{ lb/hr}$$

$$\dot{m}_a = 5{,}110{,}113 \text{ lb/hr} - 1419 \text{ lb/s}$$

This mass flow dictates two gas turbines, since present designs are limited to mass flows of air in the 750 lb/s range[2]. So for each turbine $\dot{m}_a$ = 2,555,057 lb/hr.

Compressor power, assumine an efficiency of 87.5% is:

$$W_C = (\dot{m}_a \, C_{p_a} \, \Delta T_a)/.875$$

where:

W_C = compressor power, Btu/hr

$\dot{m}_a$ = mass flow of air = 2,555,057 lb/hr

C_{p_a} = constant pressure specific heat of air[3] = .28 Btu/lb-°F

ΔT_a = change in temperature of air through the compressor = (775°F - 60°F) (from Figure 2)

Therefore:

$$W_C = (2{,}555{,}057 \text{ lb/hr} \times .28 \text{ Btu/lb°F} \times 415°F)/.875$$

$$W_C = 339.3 \text{ MM Btu/hr}$$

The heat transferred in the combustor, assuming an efficiency of 98% is then:

$$Q_{in} = ((\dot{m}_A C_{p_a} \Delta T_a) + (\dot{m}_f C_{p_f} \Delta T_f)) / .98$$

where:

Q_{in} = heat transferred in combustion, Btu/hr

ΔT_a = change in temperature of the air = 2000°F - 475°F (from Figure 2)

$\dot{m}_f$ = mass flow of fuel gas - 762,704 lb/hr (from Figure 2)

C_{p_f} = constant pressure specific heat of fuel gas - .32 Btu/lb-°F[3]

ΔT_f = change in temperature of fuel gas = 2000°F - 680°F (from Figure 2)

$$Q_{in} = (2{,}555{,}000 \times .28 \times 1525°F) + (762{,}704 \times .32 \times 1320°F)/.98$$

$$Q_{in} = 1442 \text{ MM Btu/hr}$$

The power out of the turbine, assuming an efficiency of 87.5%[8] is:

$$W_t = (\dot{m}_p C_{p_p} \Delta T_p).875$$

where:

W_t = turbine power, Btu/hr

$\dot{m}_p$ = mass flow of products of combustion - 3,317,761 lb/hr (from Figure 2)

C_{p_p} = constant pressure specific heat of products = .30 Btu/lb-°F[3]

ΔT_p = change in temperature of products through the turbine, 2000°F - 1160°F (from Figure 2)

$$W_t = 3,317,761 \text{ lb/hr} \times .30 \text{ Btu/lb-°F} \times 840°F \times .875$$

$$W_t = 731.6 \text{ MM Btu/hr}$$

The net power out is then:

$$W_{net} = W_T - W_C$$

$$W_{net} = 731.6 \text{ MM Btu/hr} - 339.3 \text{ MM Btu/hr}$$

$$W_{net} = 392.3 \text{ MM Btu/hr}$$

The electrical power out of the generator, assuming a 98% efficiency, is:

$$P_g = .98 (W_{net})$$

$$P_g = .98(.29307 \text{ W/Btu/hr})(392.3 \text{ MM Btu/hr})$$

$$= 112.7 \text{ MW}$$

The installed cost for the gas turbine-generator set is $173/KW from Reference 7. Therefore, the total cost for two gas turbine generator sets is:

$$C_{GT} = \$173/KW \times 2 \times 112,700 \text{ KW}$$

$$= \$38,994,200$$

APPENDIX D

Calculation of Steam Turbine Work and Cost

From Figure 2, the total mass flow of steam into the turbine is 131,500 lb/hr with 109,650 lb/hr extracted at 300 psig, 619°F for the feedwater heaters. The power out of the steam turbine-generator is:

$$P_{ST} = (\dot{m}_{SE} \times \Delta h_{SE}) + (\dot{m}_{SC} \times \Delta h_{SC})$$

where:

P_{ST} = power out of steam turbine.

$\dot{m}_{SE}$ = mass flow of steam extracted at 315 psi, 619°F - 109,650lb/hr (from Figure 2)

Δh_{SE} = enthalpy change of steam extracted = 139 Btu/lb

$\dot{m}_{SC}$ = mass flow of steam condensed = 21,850 lb/hr (from Figure 2)

Δh_{SC} = enthalpy change of condensed steam = 357 Btu/lb

$$P_{ST} = (109{,}650 \text{ lb/hr} \times 139 \text{ Btu/lb}) + (21850 \text{ lb/hr} \times 357 \text{ Btu/lb})$$

$$P_{ST} = 23.0 \text{ MM Btu/hr}$$

The generator power, assuming an efficiency of 98% is:

$$P_G = .98\ (P_{ST})$$

$$P_G = .98\ (.29307 \text{ W/Btu/hr})(23.0 \text{ MM Btu/hr})$$

$$P_G = 6.6 \text{ MW}$$

An installed cost of $118.4/KW for the steam turbine-generator set is from Reference 7, and an estimate of $175,000 additional for each extraction point was supplied by Westinghouse Co.

The total installed cost is then:

$$C_{ST} = 6{,}600 \text{ KW} \times \$118.4/\text{KW} + \$175{,}000$$

$$= \$956{,}440$$

ENERGY CONSERVATION IN COAL CONVERSION

Direct Coal Fired Steam Generation in Lieu of Low Btu Gas

G. C. Cingle III

Carnegie-Mellon University
Pittsburgh, PA 15213

June, 1978

Prepared for

THE U.S. DEPARTMENT OF ENERGY
Pittsburgh Energy Technology Center
UNDER CONTRACT NO. EY77S024196

ABSTRACT

This report examines the feasibility of replacing the low Btu gas fired steam and power generating system in the Ralph M. Parsons Oil/Gas Complex with a direct coal fired steam and power generating system. The difference in capital cost between the coal fired alternate system and the fuel gas fired system is 36.4 million dollars. For a savings in coal of 586 TPD which is 1.6% of 36,000 TPD used by the Oil/Gas Complex or 6.1 million dollars annually, the rate of return on the additional capital investment is 8.21%.

ACKNOWLEDGEMENTS

I would like to thank Andrew Bela of the Ralph M. Parsons Company, T. S. Govindan of DuPont Co., George Gregorian of Westinghouse Company and George Keenan of Babcock and Wilcox for their valuable information and assistance in preparing this report.

TABLE OF CONTENTS

LIST OF FIGURES

LIST OF TABLES

INTRODUCTION

This study examines using a direct coal fired steam and electric power generation system to replace the existing low Btu gas fired steam and power generation system in the Ralph M. Parsons Oil/Gas Complex. Elimination of the gasifier train which produces fuel gas for the utility boilers results in a 17% improvement in the overall thermal efficiency of the system shown in Figure 1.

The present system is described and an alternate coal fired system which meets plant requirements for electricity, steam and fuel gas is developed to replace the present system. An economic analysis shows that a rate of return of 8.21% can be realized on the additional capital investment of 36.4 million dollars.

PRESENT SYSTEM DESCRIPTION

The existing steam and power generating system in the Ralph M. Parsons Oil/Gas Complex is shown in Figure 1. The gasifier is an air-blown, two stage slagging type, and produces 33,030 MSCF/hr of 145 Btu/SCF gas from 472,510 lb/hr of coal, 746,600 lb/hr of char-filter cake mixture and 22,277 MSCF/hr air. 23,300 MSCF/hr of this gas is burned in four utility boilers producing a total of 2,871,070 lb/hr of 1215 psi, 950°F steam while 2596 MSCF/hr of the gas is used to superheat 785,555 lb/hr of steam generated in heat recovery boilers to 950°F. The balance of the fuel gas, 7134 MSCF/hr, is used in process superheaters, gas sweetening, and sulfur tail gas processing. Of the 3,656,625 lb/hr of 1215 psia, 950°F steam produced, 341,171 lb/hr is used for the 54,600 hp gasifier air compressor, and 1,905,700 lb/hr is used for electric power

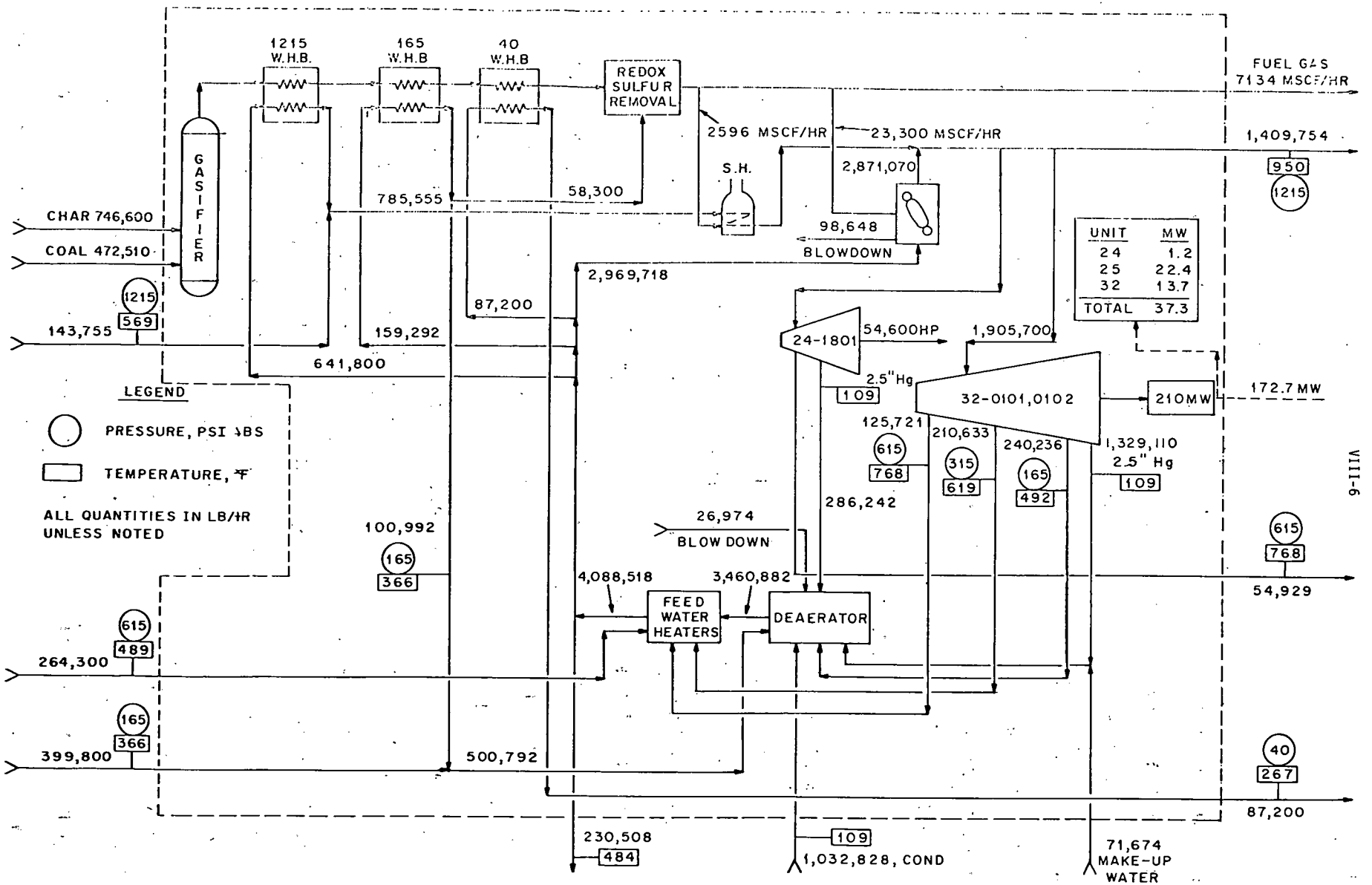

FIGURE 1 RALPH M. PARSONS OIL/GAS COMPLEX STEAM AND POWER GENERATION SYSTEM

generation in turbines 32-0101 and 32-0102 which produce a total of 210 MWE for in plant use. The remaining 1,409,754 lb/hr of 1215, 950°F steam is used for turbine process drivers throughout the plant. In addition to the 1215 psia, 950°F steam used in other areas of the plant, 54,929 lb/hr of 615 psia, 768°F steam and 87,200 lb/hr of 40 psia, 267°F steam are used in other areas of the plant.

DIRECT COAL FIRED ALTERNATE SYSTEM DESCRIPTION

The alternate direct coal fired steam and power generation system is shown in Figure 2. This system produces the same amount of steam and electric power, yet consumes 48,800 lb/yr or 586 short TPD less of coal and 325,196 lb/hr less of char-filter cake as a result of the elimination of the low Btu gasifier train and ancillary equipment. The overall thermal efficiency of the alternate steam and power generation system is 17% greater than the existing configuration (see Appendix A).

A low Btu gasifier and related equipment has been included in the alternate system to supply processes throughout the plant which require low Btu gas. This gasifier is similar to the existing gasifier except that it produces only 21.6% of the low Btu gas as the original, i.e., 7134 MSCF/hr. It has been assumed that the efficiency of the smaller gasifier is the same as the larger unit, i.e., 72.9%, where the efficiency is the Btu value of the products out divided by the total Btu value of the feed into the gasifier. Steam generation from waste heat boilers on the gasifier off-gas stream was reduced directly as the reduction in gas production, and the reduction in power required for the gasifier air compressor was direct also, resulting in a 11,794 hp turbine driver. Additional

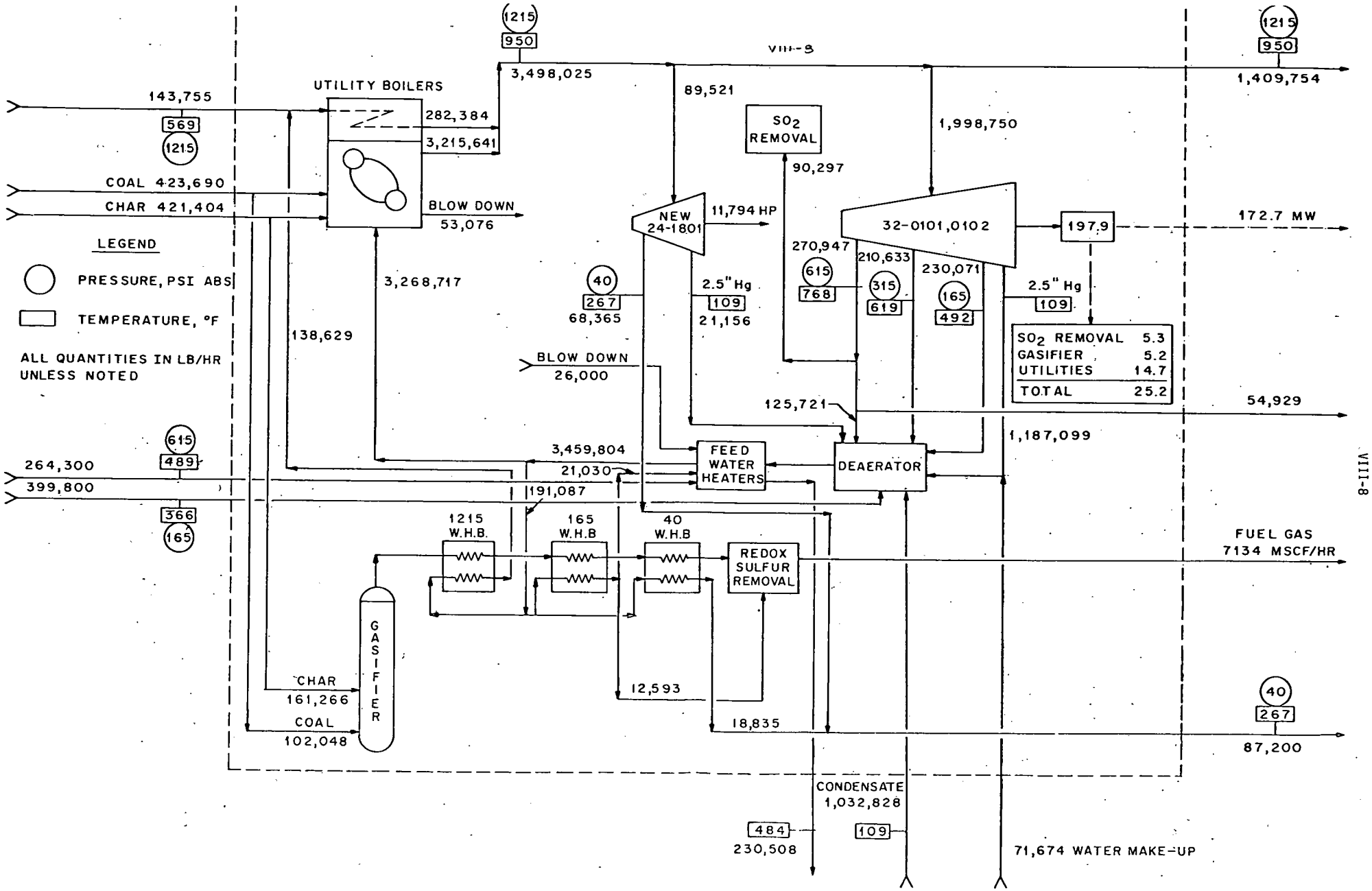

FIGURE 2 ALTERNATE DIRECT COAL FIRED STEAM AND POWER GENERATION SYSTEM

steam was required for the SO_2 scrubber system, and from Appendix B is calculated as 90,297 lb/hr at 615 psia, 768°F. The amount of 615 psia, 489°F steam required by the new redox sulfur removal system has been decreased proportionally to 12,543 lb/hr.

The electric power requirements for the alternate power generation system are:

	172.7 MW	Process
	5.2 MW	New gasifier and redox sulfur removal system
	5.3 MW	SO_2 scrubber system
	14.7 MW	Utilities, including coal fired boilers, coal and ash handling systems, electrostatic precipitators
TOTAL	197.9 MW	

It was assumed that the coal fired boilers consumed 1 MW more than equivalent gas fired boilers of the same size. The power requirements for the SO_2 scrubber system are calculated in Appendix B.

The amount of steam and electrical power required external to the two power generation systems is equal.

The amount of steam and electric power used within the alternate system is different, therefore, the steam extracted at various pressures from the large turbines 32-0101, 32-0102 and also the new gasifier air compressor turbine was adjusted to maintain the same output of steam and power from the alternate power generation system "control volume". The new coal fired boilers were sized to supply the required amount of 1215,

950°F steam, or 3,498,025 lb/hr. Turbine steam requirements and boiler calculations are given in Appendix C.

ECONOMIC ANALYSIS

The difference in the installed costs for the two power generation systems shown in Figures 1 and 2 is the installed cost of equipment added to the present system in the Oil/Gas Complex, minus the installed cost of equipment deleted, to arrive at the alternate system shown in Figure 2.

Installed costs of $25/lb-steam for coal fired boilers and $10/lb-steam for gas fired boilers were given by Babcock and Wilcox[1]. The costs include feeders, conveyors, preheaters, blowers, burners, piping, precipitators and controls. Ash removal equipment is not included in the $25/lb-steam cost and has been calculated at $1,430,000 in Appendix B. The installed cost and operating cost of the SO_2 scrubber were also calculated in Appendix B and are $36,970,000 and $2,332,600 respectively. It was assumed that the operating and maintenance costs for the original power generation system and the alternate would be equal except for the SO_2 scrubber operating and maintenance cost, above. The installed costs for the gasifier system, (unit 24), redox sulfur removal system, (unit 25), and the process steam superheaters are from reference 14, and the new gasifier system and redox system are calculated from these costs in Appendix D. Table 1 lists the equipment added or deleted, and the associated costs.

DISCOUNTED CASH FLOW ANALYSIS

The coal savings for the alternate steam and power generation system is 48,800 lb/hr. At the 1978 price of $31.53 per ton[5], the yearly gross savings for a 330 day year[14] is $6,095,600. The net yearly savings is $6,095,600 - 2,332,600 or $3,763,000. For the additional capital investment of $36,384,000, a 20 year project life, 100 per cent equity, the rate of return using a discounted cash flow analysis is 8.21%. The yearly cash flows are presented in Table 2.

LIFE CYCLE COST OF ALTERNATE SYSTEM

If the additional capital investment of $36,384,000 is borrowed at 9% interest for a period of 20 years, the life cycle cost is given by:

$$LCC = 20 \quad (R - C_{OM} - CRF \times \Delta C)$$

where

R = the annual savings in coal costs

C_{OM} = the annual operating and maintenance cost

CRF = the uniform capital recovery factor, for 20 years at 9% interest

ΔC = the additional capital investment required for the alternate system.

Therefore:

$$LCC = 20 \quad (6,095,600 - 2,332,600 - .1095 \times 36,384,000) = - \$4,421,000$$

TABLE 1

Equipment Descriptions and 1978 Installed Costs

Equipment No. and Description	Equipment Quantity Oil/Gas / Alternate	Total Installed Cost Oil/Gas / Alternate
32-1601,02,03,04 fuel gas fired boilers, 719 MMBtu/hr	4/-	28,710,000/-
Coal fired boilers*, 1048 MMBtu/hr	-/4	-/87,451,000
Ash Handling Equipment	-/1	-/ 1,430,000
Fuel gas gasifier, process unit 24**	1/-	78,071,000/-
Fuel gas gasifier, alternate system**	-/1	-/31,128,000
Redox sulfur removal, process unit 25	1/-	19,658,000/-
Redox sulfur removal, alternate system	-/1	-/ 7,838,000
32-1309,1310 process steam superheaters 112.9 MMBtu/hr	2/-	1,994,000/-
SO_2 scrubber system	-/1	-/36,970,000
		TOTAL 128,433,000/164,817,000
		ΔCOST = 36,384,000

* The coal fired boilers include conveyors, feeders, blowers, all piping, preheaters, burners, controls and electrostatic precipitators.

** The gasifier system includes feeders, char cyclones, heat exchangers, waste heat boilers, slag and dust removal equipment, precipitators, compressors, pumps and sour water removal equipment.

TABLE 2

Discounted Cash Flow for Coal Cost of $1.30/MMBtu

****

100 PERCENT EQUITY
9 PERCENT INTEREST

0 PERCENT TAX CREDIT ON
0 PERCENT OF INVESTMENT

THE CALCULATED RATE OF RETURN IS 0.21 PERCENT

YEAR	GROSS CASH FLOW	ANNUAL DEPREC	ANNUAL TAX	NET CASH FLOW	DISCNTD CASH FLOW
1	3763	4280.471	0	3763	3420.909
2	3763	4012.941	0	3763	3109.917
3	3763	3745.412	0	3763	2827.198
4	3763	3477.882	0	3763	2570.18
5	3763	3210.353	0	3763	2336.527
6	3763	2942.824	0	3763	2124.116
7	3763	2675.294	0	3763	1931.014
8	3763	2407.765	0	3763	1755.467
9	3763	2140.235	0	3763	1595.879
10	3763	1872.706	0	3763	1450.8
11	3763	1605.176	0	3763	1318.909
12	3763	1337.647	0	3763	1199.008
13	3763	1070.118	0	3763	1090.007
14	3763	802.5882	0	3763	990.9157
15	3763	535.0588	0	3763	900.8324
16	3763	267.5294	0	3763	818.9386
17	3763	0	0	3763	744.4896
18	3763	0	0	3763	676.8088
19	3763	0	0	3763	615.2807
20	3763	0	0	3763	559.3461
TOTAL	71497	32103.53	0	71497	32036.54

NET PRESENT VALUE AT A DISCOUNT RATE OF 10 PERCENT-4347.457

Note: Figures are in thousands of dollars.

CONCLUSIONS

The alternate coal fired power generation system saves 48,800 lb/hr of coal or $6,095,600 annually, at an increase in capital cost of 36.4 million dollars. This yields a rate of return of 8.21% on the capital investment.

The cost of the gasifier and redox sulfur removal system in the alternate design to supply low Btu gas for process use throughout the plant is 39 million dollars. For processes which would not require low Btu gas, the economics of the coal fired alternate would be much more attractive.

The removal of SO_2 from boiler stack gases is another major consideration in the implementation of the alternate power generation system. State-of-the-art technology in SO_2 removal from stack gases has encountered problems in meeting required emmission standards, because of equipment reliability[6]. However, given the estimated lead time of six years for construction of the Oil/Gas facility, there is a strong possibility that problems associated with SO_2 removal will have been solved, prior to start-up of the proposed plant.

REFERENCES

1. Personal communication with George Keenan, Babcock and Wilcox Co., Pittsburgh, PA.

2. Personal communication with George Gregorian, Westinghouse Corp., Calgory, Alberta.

3. Department of Mechanical Engineering, Carnegie-Mellon University, "Optimum Energy Utilization in Limestone Flue Gas Desulfurization Systems", February, 1977.

4. Thermo Electron Corporation, "Final Report: A Study of Inplant Electric Power Generation in the Chemical, Petroleum Refining and Paper and Pulp Industries".

5. Section 12 - Basis for Fuel and Utility Costs, "Energy Conservation in Coal Conversion", June, 1978.

6. Electric Power Research Institute, "EPRI Journal", April, 1978, Vol. 3, No. 3.

7. Van Wylen, Sonntag, "Fundamentals of Classical Thermodynamics", 2nd edition, John Wiley and Sons, Inc., New York, 1973.

8. Keenan, Keyes, Hill, Moore, "Steam Tables (English Units)", John Wiley and Sons, Inc., 1969.

9. McGraw-Hill, "Chemical Engineering", May 8, 1978, Vol. 85, No. 11.

10. Personal communication with Andrew Bela, Ralph Parsons Co., Pasedena, CA.

11. Newron, Donald G., "Engineering Economic Analysis", Revised edition, Engineering Press, San Jose, CA, 1977.

12. McGraw-Hill, "Chemical Engineering", April 12, 1976, Vol. 83, No. 8.

13. Popper, Herbert, "Modern Cost Engineering Techniques", 1st edition, McGraw-Hill Book Company, New York, 1970.

14. Oil/Gas Complex Conceptual Design/Economic Analysis, R & D Report No. 114 - Interim Report No.4, Ralph M. Parsons' Company, 1977.

APPENDIX A

Comparison of Overall Thermal Efficiencies Fuel Gas Steam and Power Generation System and the Direct Coal Fired Alternate System

Cycle efficiency, η is defined as:

$$\eta = \frac{W_{net}}{q_{in}}$$

where,

W_{net} = the net work out of the system

q_{in} = the net heat input to the system.

From Figures 1 and 2, it can be seen that

$$W_{net\ 1} = W_{net\ 2}$$

Therefore,

$$\frac{\eta_1}{\eta_2} = \frac{q_{in\ 2}}{q_{in\ 1}}$$

For the values of 1130.5 Btu/lb for char-filter cake[14] and 12,125 Btu/lb for the coal used[14], the heat inputs for the two systems are:

$$q_{in\ 1} = 472{,}510\ \text{lb/hr} \times 12{,}125\ \text{Btu/lb} + 746{,}600\ \text{lb/hr} \times 1130.5$$
$$= 6.57 \times 10^9\ \text{Btu/hr}$$

$$q_{in\ 2} = 423{,}690 \times 12{,}125 + 421{,}404 \times 1130.5$$
$$= 5.614 \times 10^9\ \text{Btu/hr}$$

$$\frac{n_1}{n_2} = \frac{5.614 \times 10^9}{6.57 \times 10^9}$$

$$= .854 \quad \text{or} \quad n_2 = 1.17\, n_1$$

APPENDIX B

SO_2 Scrubber Utility Requirements, Installed, and Operating Costs

An SO_2 scrubber system for a 500 MW power plant consumes 129,440 lb/hr of 615 psia steam and 7.6 MW of electricity[3]. To obtain an equivalent power generation output for the alternate system shown in Figure 2, it is assumed that the net heat out of the control volume is utilized in a Rankine Cycle with a cycle efficiency of 35%. Assuming isentropic expansion of steam through ideal turbines to a pressure of 2.5" Hg, the net total change in the enthalpy of the streams into and out of the control volume is:

$$\Delta h_{NET} = \overline{\Delta h_{OUT}} - \sum \Delta h_{IN}$$

where Δh is the isentropic change in enthalpy from the initial stream temperature and pressure to 2.5" Hg.

From Figure 2:

Δh_1 = -264,300 lb/hr (1203.2 - 820) Btu/hr

Δh_2 = -399,800 (1195.6 - 880)

Δh_3 = 1,409,754 (1470 - 920)

Δh_4 = 54,929 (1391 - 920)

Δh_5 = 87,200 (1169 - 950)

Δh_{NET} = 592.88 MMBtu/hr

$$w = \frac{\eta \times \Delta h_{NET}}{3413 \text{ Btu/hr-kw}}$$

$$= \frac{.35 \times 592.88 \times 10^6}{3413}$$

$$= 60.8 \text{ MW}$$

Assuming the fuel gas is burned in a boiler with an 85% efficiency, the work available from the fuel gas is:

$$w = \frac{7134 \times 10^3 \text{ SCF/hr} \times 145 \text{ Btu/SCF} \times .85 \times .35}{3413 \text{ Btu/hr-kw}}$$

$$= 90.2 \text{ MW}$$

The total equivalent MW output for the alternate system is:

$$w_{TOTAL} = 197.9 + 60.8 + 90.2$$

$$= 348.8 \text{ MW}$$

The 615 psia steam requirements for the SO_2 scrubber are:

$$\dot{m}_s = \left(\frac{348.8}{500}\right) \quad 129{,}440$$

$$= 90{,}297 \text{ lb/hr}$$

and the electical requirements are:

$$\left(\frac{348.8}{500}\right) \quad 7.6 = 5.3 \text{ MW}$$

SO_2 Scrubber Installed Cost and Operating Cost

Reference 3 gives the 1978 total installed cost of a 500 MW SO_2 scrubber as:

$$\$45,885,000$$

Using a .6 power law[13] the cost for a 348.8 MW scrubber is:

$$C = \$45,885,000 \left(\frac{348.8}{500}\right)^{.6}$$

$$= \$36,970,000$$

For comparison, an approximate installed SO_2 scrubber cost of \$10/lb-steam was obtained from Babcock and Wilcox[1], which is \$34,980,000 for the alternate power generation system. The two cost are within 6% of each other.

From reference 3, the 1978 annual operating costs for a 500 MW scrubber system are:

\$ 1,114,000	Limestone
2,229,700	Operating manpower and maintenance cost
\$ 3,343,700	Total annual operating and maintenance cost

Assuming a direct ratio between operating and maintenance cost and scrubber size, the cost for the alternate power system scrubber is:

$$\left(\frac{348.8}{500}\right) \quad 3,343,700 = \$2,332,600/yr$$

Ash Removal Equipment

From reference 4, a 1975 cost of $10.73/kw is given for coal and ash handling equipment for coal fired boilers. It is assumed that 1/3 of this cost is for ash handling equipment which is not included in the installed cost of $25/lb-steam for coal fired boilers. Using the Marshall and Stevens Electrical Power Industries Cost Index[9,12], the 1978 installed cost for the ash handling equipment is:

$$\left(\frac{510}{445.1}\right) \quad \$10.73 \times \frac{1}{3} = \$4.10/kw$$

The total cost for the equipment is:

$$\$4.10/kw \times 348.8 \times 10^3 kw = \$1,430,000$$

APPENDIX C

Steam Turbine and Boiler Calculations

Mass flow rates of steam from the extraction points of the new turbine are adjusted to maintain the original net steam output and power output from the power generation "control volume" shown in Figure 2. Since the original turbine and the alternate operate at nearly the same conditions it is assumed that the turbine efficiencies are equal. It is first necessary to determine the efficiency of the power generating turbine in the original system. First the Rankine Cycle steam rate, described by:

$$RCSR \frac{Lb_m}{Hp\text{-}hr} = \frac{2545 \text{ Btu/hp-hr}}{(h_1 - h_{2s}) \text{ Btu/lbm}}$$

is found by using a weighted average of the available energy described by the isentropic enthalpy drop across each extraction point. For turbines 32-0101,0102 shown in Figure 1, the Rankine Cycle steam rate can be written:

$$RCSR = \frac{2545 \text{ Btu/hp-hr}}{(1470\text{-}1375).066 + (1470\text{-}1300).111 + (1470\text{-}1242).126 + (1470\text{-}900).697}$$

$$= 5.64 \text{ lbm/hp-hr}$$

The actual steam rate, ASR is:

$$ASR = \frac{1{,}905{,}700 \text{ lbm/hr}}{210{,}000 \text{ kw} \times 1.340 \text{ hp/kw}}$$

$$= 6.77 \text{ lbm/hp-hr}$$

Therefore, the turbine efficiency is:

$$\eta_{TURB} = \frac{RCSR}{ASR} \times 100\%$$

$$= \frac{5.64}{6.77} \times 100\%$$

$$= 83.3\%$$

The new turbines have the same efficiency. From Figure 2, the output must be 197.9 MW or 265,280 hp. In addition, the required mass flows from each extraction point which yield the same steam output from the system are:

270,947 lbm/hr @ 615 psia, 768°F

210,633 lbm/hr @ 315 psia, 619°F

330,071 lbm/hr @ 165 psia, 492°F

It remains to solve for $\dot{m}$, the amount of steam condensed at 2.5" Hg. We can write:

$$RCSR = \frac{2545 \text{ Btu/hp-hr}}{95\left(\frac{270,947}{811,615+\dot{m}}\right) + 170\left(\frac{210,633}{811,615+\dot{m}}\right) + 228\left(\frac{330,071}{811,615+\dot{m}}\right) + 570\left(\frac{\dot{m}}{811,615+\dot{m}}\right)}$$

The ASR is:

$$ASR = \frac{811,615 + \dot{m}}{265,280}$$

Dividing the RCSR by ASR we have:

$$.833 = \frac{2545}{517.7 + .00215\ \dot{m}}$$

or

$$\dot{m} = 1{,}187{,}094$$

Therefore, the total steam required for the new turbines is:

$$\dot{m}_s = 1{,}187{,}094 + 811{,}651$$
$$= 1{,}998{,}750 \text{ lbm/hr}$$

A similar calculation was performed on the original 54,600 hp gasifier air compressor turbine driver, yielding a steam flow of 89,521 lb/hr for the new, 11,794 hp gasifier air compressor turbine driver.

Boiler Calculations

The amount of heat input to the boilers is:

$$q_{in} = \frac{1}{\eta_B} [\dot{m}_{SH}(h_2 - h_1) + \dot{m}_{STm}(h_2 - h_f)]$$

where:

η_B = boiler efficiency, assumed to be .8[1]

$\dot{m}_{SH}$ = amount of steam entering the boiler at 1215 psia, 569°F to be superheated to 950°F

h_2 = 1470 Btu/lbm, (1215 psia @ 950°F)

h_1 = 1183.2 Btu/lb (1215 psia @ 569°F)

h_f = 468 Btu/lb (1215 psia @ 484°F)

From Figure 2, $\dot{m}_{SH}$ = 143, 755 lbm/hr, and $\dot{m}_{STm}$ = 3,268,717 lbm/hr

Therefore:

$$q_{in} = 4.194 \times 10^9 \text{ Btu/hr}$$

In the original system, 746,600 lb/hr of a char-filter cake mixture was fed to the gasifier along with coal in a ratio of .633 coal to char-filter cake. The char-filter cake mixture consists of 329,800 lb/hr of filter-cake from the coal liquifaction process in unit 13 of the Oil/Gas Complex, and 416,800 lb/hr of char which is recovered from the gasifier off-gas and mixed with the filter-cake to aid in drying the mixture.

The gasifier in the alternate system produces .216 the amount of product gas as the original, therefore, the amount of char recovered from the product gas is:

$$416{,}800 \times .216 = 90{,}028 \text{ lb/hr}$$

The amount of char-filter cake mixture available for the alternate system is:

$$329{,}800 + 90{,}028 = 419{,}828 \text{ lb/hr.}$$

The ratio of coal to char-filter cake, .633, is maintained for the new gasifier, therefore, the amount of coal and char-filter cake required is:

$$\dot{m}_{COAL} = .216 \times 472{,}510 \text{ lbm/hr}$$

$$= 102{,}062 \text{ lbm/hr}$$

$$\dot{m}_{CHAR} = \frac{102{,}062}{.633}$$

$$= 161{,}235 \text{ lbm/hr}$$

This leaves:

$$419{,}828 - 161{,}235 = 258{,}593 \text{ lb/hr}$$

of char-filter cake for the boiler. For the char-filter cake heating value of 1130.5 Btu/lb, the amount of coal required by the boiler can be calculated.

$$q_{CHAR} = 258{,}593 \text{ lb/hr} \times 1130.5 \text{ Btu/lb}$$
$$= 2.92 \times 10^8 \text{ Btu/hr}$$

$$q_{COAL} = 4.194 \times 10^9 \text{ Btu/hr} - 2.92 \times 10^8 \text{ Btu/hr}$$
$$= 3.9 \times 10^9 \text{ Btu/hr.}$$

Therefore,

$$\dot{m}_{COAL} = \frac{3.9 \times 10^9 \text{ Btu/hr}}{12{,}125 \text{ Bru/hr}}$$
$$= 321{,}649 \text{ lb/hr.}$$

The total amount of coal required for the gasifier and the boiler is:

$$321{,}649 + 102{,}062 = 423{,}711 \text{ lb/hr}$$

The savings in coal is:

$$472{,}510 \text{ lb/hr} - 423{,}711 \text{ lb/hr} = 48{,}799 \text{ lb/hr}$$

or 586 short TPD

APPENDIX D

Gasifier and Sulfur Removal System Costs

From reference 14, the 1975 installed cost for the gasifier and associated equipment is $66,563,000. Using the Marshall and Stevens Chemical Process Industries Equipment Index[9,12], the 1978 installed cost is:

$$\frac{530.5}{452.3} \times \$66,563,000 = \$78,071,000$$

Using the same index, the 1978 installed cost for the redox sulfur removal system is:

$$\frac{530.5}{452.3} \times 16,760,000 = 19,658,000$$

Similarly, the 1978 cost for the superheaters in the original steam and power generation system is:

$$\frac{530.5}{452.3} \times 1,700,000 = \$1,994,000$$

The cost of the gasifier system for the alternate power generation system shown in Figure 2 is calculated by the .6 power law[13], which is:

$$\left(\frac{\text{Capacity A}}{\text{Capacity B}}\right)^{.6} = \frac{\text{Cost A}}{\text{Cost B}}$$

For the gasifier:

$$CG_{ALT} = 78{,}071{,}000 \left(\frac{7134 \text{ MSCF/hr}}{33{,}030 \text{ MSCF/hr}} \right)^{.6}$$

$$= \$31{,}128{,}000$$

Similarly, for the redox sulfur removal process:

$$CSR_{ALT} = \$19{,}658{,}000 \left(\frac{7134 \text{ MSCF/hr}}{33{,}030 \text{ MSCF/hr}} \right)^{.6}$$

$$= \$7{,}838{,}000$$

2 ENERGY CONSERVATION IN COAL CONVERSION

Alternate Acid Gas Removal System Study

D. A. Schatz

Carnegie-Mellon University
Pittsburgh, PA 15213

June 1978

Prepared for
THE U.S. DEPARTMENT OF ENERGY
Pittsburgh Energy Technology Center
Under Contract No. EY77S024196

ABSTRACT

To reduce the reboiler steam required, we studied replacing the MEA (monoethanolamine) system proposed by the Ralph M. Parsons Co. with a DEA (diethanolamine) acid gas removal system. Steam consumption is reduced by 16,000 lbm/hr which is 1% of the total steam generated in the Oil/Gas Complex or $317,000 per year. In addition, there is an annual savings of $88,000 for chemicals. The additional capital costs and operating expenses for the DEA system are negligible since the process plants are equivalent. It is therefore recommended that a DEA system replace the MEA system as Process Unit 17 of the Oil/Gas Complex.

ACKNOWLEDGEMENTS

I would like to thank T. S. Govindan of the DuPont Company, J. D. Crow of Graff Engineering and Bill Pierce of Dow Chemical for their time and cooperation.

TABLE OF CONTENTS

LIST OF TABLES AND FIGURES

INTRODUCTION

In the Ralph M. Parsons Oil/Gas Conceptual Design, the acid gas removal system uses MEA (monoethanolamine) to strip the dissolver gas of H_2S and CO_2. Since the MEA system has a high steam consumption, 190,300 lbm/hr, we examined the feasibility of using a DEA (diethanolamine) which uses less steam.

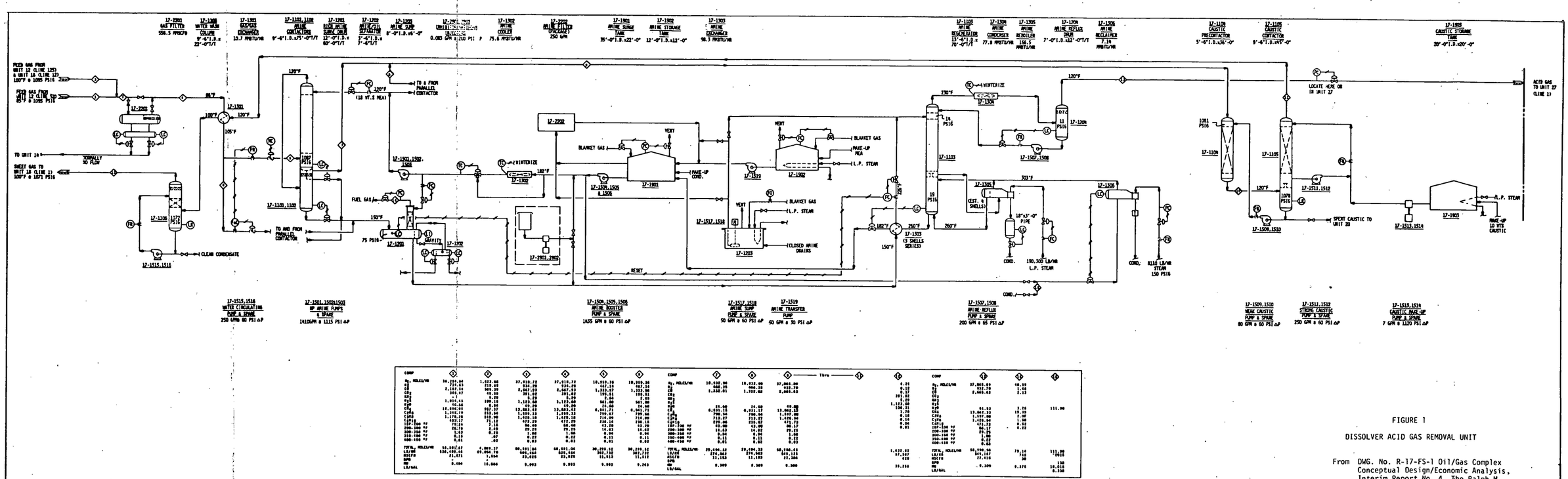

FIGURE 1

DISSOLVER ACID GAS REMOVAL UNIT

From DWG. No. R-17-FS-1 Oil/Gas Complex Conceptual Design/Economic Analysis, Interim Report No. 4, The Ralph M. Parsons Co. March 1977.

MEA PROCESS DESCRIPTION

A schematic of the system designed by Parsons is given in Figure 1. The inlet gas composition temperature and pressure is given in Table 1. Table 1 shows that the acid gas concentration is 2.495% (1.85% H_2S + .645% CO_2).

The Ralph M. Parsons design, calls for an MEA wash, followed by a caustic wash (NaOH). The reactions involved in sweetening the acid gas with aqueous MEA (RNH_2)* are:

$$2RNH_2 + H_2S \rightleftharpoons (RNH_3)_2S$$

$$(RNH_3)_2S + H_2S \rightleftharpoons 2RNH_3HS$$

$$2RNH_2 + CO_2 + H_2O \rightleftharpoons (RNH_3)_2CO_3$$

$$(RNH_3)_2CO_3 + CO_2 + H_2O \rightleftharpoons 2RNH_3HCO_3$$

$$2RNH + CO_2 \rightleftharpoons RNHCOONH_3R$$

The reactions proceed to the right at lower temperatures (in the contactors) and to the left at higher temperatures (in the stripper). Thus, at 86°F (inlet gas temp.), the amines will absorb the acid gas and form the amine salts. At a temperature of about 300°F the salts dissociate, the acid gas is liberated, and the amine is available for reuse.(2)

The caustic wash insures that the CO_2 concentration is brought to less than 5 ppm. The equations governing these reactions are:

$$2NaOH + CO_2 \rightleftharpoons Na_2CO_3 + H_2O$$

*where R = $HOCH_2CH_2$

TABLE 1

INLET STREAM COMPOSITION FROM DISSOLVER

	Moles/hr	Mole %
H_2	37,918.72	62.6
N_2	934.28	1.54
CO	2,667.93	4.4
CO_2	391.02	.645
NH_3	5.29	.009
H_2S	1,123.60	1.85
H_2O	49.20	.08
CH_4	13,883.42	22.91
C_2H_6	1,599.33	2.64
C_3H_8	1,428.18	2.36
C_4H_{10}	472.29	.78
IBP-200°F	86.40	.14
200-300°F	29.25	.05
300-350°F	1.88	.003
350-400°F	0.22	-
400-450°F	0.03	-
TOTAL	60,591.4	
lb/hr	605,464	
MSCFH	23,025	

Inlet Pressure - 1095 psig

Inlet Temp. - 86°F

$$Na_2CO_3 + H_2S \rightleftharpoons HaHS + NaHCO_3$$

The caustic is not regenerated. The NaOH make-up is approximately 6TPD.

Steam is used to reboil the rich amine solution from the Ralph M. Parsons flowsheets which specify an MEA concentration of 18% (weight) and a flowrate of ∿2850 gpm, the amine reboiler uses 190,300 lbm/hr (166.5 MMBtu/hr) of low pressure steam.

ALTERNATIVE ACID GAS REMOVAL SYSTEMS

There are other acid gas removal processes available that are more energy efficient than the amine process. Unfortunately, the partial pressure of the acid gas is too small for these processes to work efficiently[3].

DEA (diethanolamine) offers a substantial energy savings, as well as a savings in chemical costs. The mechanism by which it sweetens the gas is essentially the same as MEA, and an analagous set of reaction equations can be written[2]. The energy savings results from the lower heats of reaction of H_2S and CO_2 with DEA[2]. Thus, less steam is needed to reboil the rich amine solution. The calculated steam savings per year is 1.267×10^8 lb (see Appendix A). The savings in chemical costs result from a lower vapor pressure than that of MEA. The DEA make-up requirements are 50% lower than that of a similar MEA system[3]. The resulting savings in chemical costs are $88,180.00/yr (see Appendix B).

Another advantage of DEA is its ability to react reversibly with COS, unlike MEA, which reacts irreversibly. Thus, both amines will remove COS from the gas stream, but MEA will be deactivated, while DEA will not. COS does exist as a trace compound in the dissolver.

With minor modification, the DEA system would utilize the same parallel contactor system as the proposed MEA system. A 30% DEA solution has a slightly higher pickup rate than 18% MEA (see Figure 2) thereby cutting pumping costs slightly. Operating with the caustic wash, the 30% DEA system will bring CO_2 levels to less than 5 ppm, and H_2S levels to less than .25 grain/ccf[3].

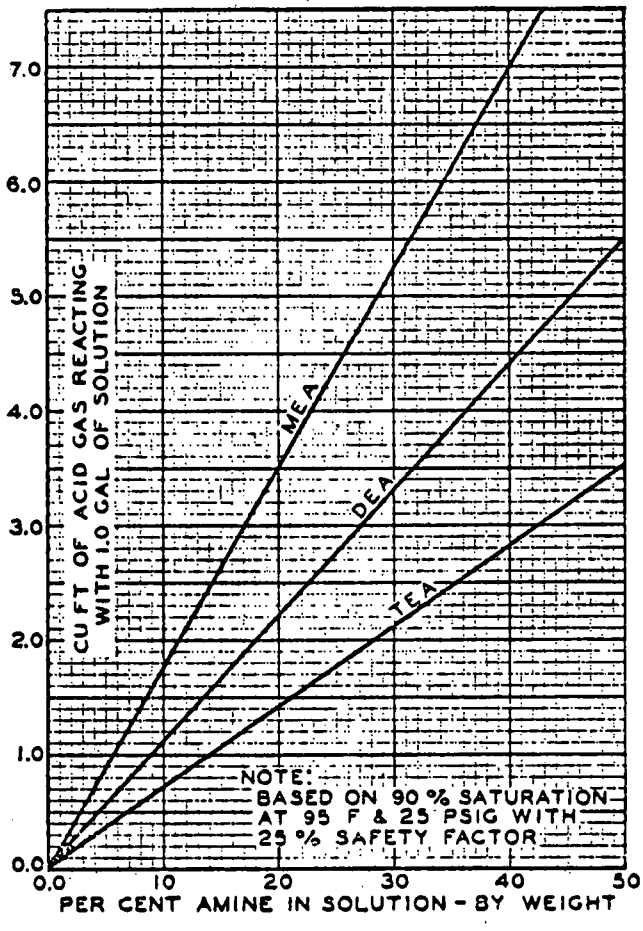

FIGURE 2

ACID GAS PICK-UP VS AMINE SOLUTION CONCENTRATION

from reference 2.

ECONOMIC COMPARISON OF DEA AND MEA

In comparing the economics of the two systems, the following assumptions will be made:

1. Process plants are considered equivalent.
2. Labor, maintenance, and startup costs are equivalent.
3. Caustic consumption is equivalent.

Therefore, the basis of comparison will rest solely on energy and amine consumption.

The annual steam savings of the DEA system is $316,760.00/yr (see Appendix A).

The annual amine make-up cost of each system is:

MEA - $180,180.00/yr

DEA - $ 92,000.00/yr (See Appendix B)

The annual DEA make-up cost is $88,180.00/yr less than the MEA make-up cost.

The cost of the initial charge of chemicals for each system is:

MEA - $117,000.00

DEA - $200,000.00 (See Appendix B)

The DEA charge is $83,000.00 more than the MEA charge.

Therefore, in the first year the savings realized by the DEA system are: $88,180 + $316,760 - $83,000 = $321,940. In subsequent years the annual saving are: $88,180 + $316,760 = $404,940. Over the twenty year life of the plant $8,015,800 is saved, in 1977 dollars.

CONCLUSIONS AND RECOMMENDATIONS

Since the DEA system meets the required plant specifications (<5 ppm CO_2, <.25 grain/ccf H_2S) and saves a significant amount of energy as well as chemicals, it should be used. There exists an additional area for energy savings in the DEA system. A step-down turbine installed between the contactor and the surge tank could supply up to 50% of the shaft power required to drive the high pressure amine pumps. This is 1200 Hp or $177,000 savings per year for electricity at .025 $/KW hr[6].

REFERENCES

1. Oil/Gas Complex, Conceptual Design/Economic Analysis. Interim Report No. 4, The Ralph M. Parsons Co., March 1977.

2. Gas Engineers Handbook. C. George Segeler, Ed.-in-Chief, The Industrial Press, New York, NY 1965.

3. Personal Communication, J.D. Crow, Graf Engineering Co., Dallas, TX.

4. Personal Communication with Bill Pierce, Dow Chemical, Inc., Midland Mich.

5. Personal Communication with John Valentine, Allied Chemical, Morristown, NJ.

6. Section XII, Basis for Fuel and Utility Costs, Energy Conservation in Coal Conversion Progress Report, June, 1978.

APPENDIX A

ENERGY SAVINGS OF DEA SYSTEM

The following assumptions will be made:

1. Specific heats of 18% MEA solution and 30% DEA solution are equivalent.
2. Flow rates of MEA and DEA are equivalent.
3. Saturated steam @ 50 psia is condensed to saturated liquid @ 50 psia in the reboiler of both the MEA and DEA systems.
4. The cost of low pressure steam is \$2.50/mlb[6].

The heats of formation of CO_2 and H_2S for the two amine systems are:

MEA - H_2S: 820 BTU/lbm

CO_2: 825 BTU/lbm

DEA - H_2S: 511 BTU/lbm

CO_2: 653 BTU/lbm

The mass flow rates of H_2S and CO_2 are:

H_2S: 38277 lbm/hr

CO_2: 17208 lbm/hr

The energy savings per year of a DEA system can be calculated as follows:

H_2S: (820-511) BTU/lbm-H_2S · 38277 $^{lbm\text{-}H_2S}/_{hr}$ · 7920 hr/yr*

$= 9.37 \times 10^{10}$ BTU/yr

CO_2: (825-653) BTU/lbm-CO_2 · 17208 $^{lbm\text{-}CO_2}/_{hr}$ · 7920 hr/yr

$= 2.34 \times 10^{10}$ BTU/yr

Total savings per year: 11.71×10^{10} BTU/yr.

*Basis - 330 Day year

From the first law of thermodynamics:

$$\dot{Q} = \dot{M} (h_1 - h_2)$$

@ 50 psia, $h_g - h_f = 924.2$ BTU/lbm.

$$\dot{Q} = 11.71 \times 10^{10} \text{ BTU/yr.}$$

Therefore, the amount of steam saved is:

$\dot{M} = \dot{Q}/(h_1 - h_2) = 11.71 \times 10^{10}/924.2 = 1.267 \times 10^{8}$ lbm/yr

which is a dollar savings of:

1.267×10^{8} lbm/yr · 1 mlb/1000 lbm · 2.50 \$/mlb

= 316,670 \$/yr

APPENDIX B

CHEMICAL COSTS FOR DEA AND MEA SYSTEMS

Assumptions:

1. Caustic consumption is the same for both the MEA and DEA systems.
2. DEA make-up is one-half MEA make-up.

Initial Charge:

MEA, 18% solution: 300,000 lbm @ .39 $/lbm[3]

$117,000.00

DEA, 30% solution: 500,000 lbm @ .40 $/lbm[3]

$200,000.00

Therefore the additional initial lost for the DEA system is:

$200,000 - $117,000 = $83,000

Annual Make-Up:

MEA solution: 462,000 lbm/yr @ .39 $/lbm

$180,180.00/yr

DEA solution: 230,000 lbm/yr @ .40 $/lbm

$92,000.00/yr

The DEA system saves:

$180,180 - $92,000 = $88,180 per year

2 ENERGY CONSERVATION IN COAL CONVERSION

Case Study: The Thermodynamic Performance of Two Combined Cycle Power Plants Integrated with Two Coal Gasification Systems

F. L. Stasa
J. F. Osterle

Carnegie-Mellon University
Pittsburgh, PA 15213

July 1978

Prepared for
THE U.S. DEPARTMENT OF ENERGY
Pittsburgh Energy Technology Center
Under Contract No. EY77S024196

PREFACE

Improving power plant efficiencies is receiving ever-increasing attention today because of the realization that our fossil fuels are in finite and dwindling supply. Most experts agree that coal is plentiful enough to warrant its use on a much wider scale for power production in order to provide a near-term solution to the energy crisis. Coal gasification provides a relatively simple (and economical) way to remove the sulfur from the coal. Moreover, the combined-cycle concept may be used to help boost overall plant performance. This study shows how these two concepts may be integrated for the production of electrical energy. Indeed, seeking the optimal plant design results in energy conservation in its most basic form.

One of the key results pertains to the design constraints provided by the federal emission standards. Without consideration of the pollution criteria, a station efficiency of 41 percent may be expected; this is equivalent to a station heat rate of only 8300 Btu/kwhr. With consideration of the criteria, the station efficiency is reduced to about 37 percent or to a heat rate of 9200 Btu/kwhr. It is readily seen that meeting the pollution criteria requires an additional 900 Btu of energy for each kilowatt-hour of electrical energy produced.

Overall performance may be improved substantially by increasing the gas turbine inlet temperature from 2000 to 2400°F. A 400°F increase in this parameter improves the station efficiency by about

5 percentage points to nearly 42 percent or by about 1100 Btu/kwhr to a station heat rate of only 8100 Btu/kwhr, with consideration of the pollution criteria.

Clearly vast amounts of energy may be conserved by improving power plant performance. Although the pollution criteria take their toll on station efficiency, the next generation of gas turbines should make this integrated gasification and combine cycle concept very attractive from an energy utilization viewpoint.

The research reported in this document was conducted by F. L. Stasa as a PhD thesis in the Mechanical Engineering Department at Carnegie-Mellon University. J. F. Osterle was his thesis adviser. The work was partially supported by the subject DOE Contract.

TABLE OF CONTENTS

TABLE OF CONTENTS
(continued)

ACKNOWLEDGEMENTS

The author is indebted to Professor J. Fletcher Osterle, who first suggested the subject area and who gave very freely of his time. The author is also grateful to Professor Albert J. Impink, Jr. of the Nuclear Science and Engineering Division, who with Professor Osterle provided much of the preliminary work which was helpful in defining the problem. The preliminary work of Dr. Aris Candris and Dr. Melvin J. Lipner is also gratefully acknowledged.

The thesis committee is complemented by Professor John C. Purcupile and Dr. Edward L. Harder, with whom it has been a pleasure to work.

The author gratefully acknowledges the support partially provided by the National Science Foundation through an Energy Fellowship and by the Department of Energy under contract number EY77S024196.

Finally, the author owes a debt of gratitude to his wife, who very expertly typed this dissertation. Her support and encouragement throughout the course of this undertaking have been instrumental in its coming to a successful conclusion.

LIST OF FIGURES

LIST OF FIGURES
(continued)

LIST OF FIGURES
(continued)

LIST OF FIGURES
(continued)

LIST OF TABLES

LIST OF TABLES
(continued)

LIST OF TABLES
(continued)

LIST OF TABLES
(continued)

ABSTRACT

Thermodynamic models of both an adiabatic and an endothermic coal gasifier integrated with either a waste heat combined cycle or a supercharged boiler combined cycle are developed and incorporated into a Fortran computer program. The adiabatic gasification process requires air and steam, while the endothermic gasification process requires only steam. The former produces a low-Btu power gas, and the latter an intermediate-Btu power gas. Most of the sulfur in the coal is removed after the gasification step in the form of hydrogen sulfide. The resulting relatively clean power gas fires the combined cycle which is composed of an open Brayton cycle and a superheated regenerative Rankine cycle without reheat. Certain components are added to each configuration in an effort to improve thermodynamic performance, with the effect of each clearly noted. Each configuration is optimized with respect to certain key operating parameters, with and without consideration of the power plant emission standards established by the federal government through the EPA. Total consumable water requirements and steam cycle heat rejection requirements are also noted. Certain key parameters, like coal composition, are varied and the effect on performance is noted.

From the results, it appears that a minimum number of feedwater heaters should be used. Intercooled air compressors are not warranted. At least one regenerator is crucial to the success of the two configurations employing adiabatic gasifiers. Without consideration of the pollution criteria, the waste heat configurations are superior to the

supercharged boiler by more than 5 percentage points on station efficiency, with 41 percent for the former and only 36 percent for the latter. All station efficiencies include a 10 percent penalty for station loads. With consideration of the criteria, the station efficiencies for each configuration are within 1 percentage point of each other when flue gas recirculation is used as a means to control the amount of nitric oxide which enters the atmosphere. With a gas turbine inlet temperature of 2000°F and with consideration of the pollution criteria, the configuration employing an adiabatic gasifier and a waste heat system is marginally the best with a station efficiency of only 37 percent. The success of power generation schemes utilizing integrated gasification and combined cycles appears to be dependent on an increased gas turbine inlet temperature; for a 400°F increase, the station efficiency improves by 5 percentage points.

CHAPTER 1

OBJECTIVES

The primary objective of this dissertation is to provide a unified and consistent thermodynamic treatment of integrated coal gasification and combined cycle power plants. Two coal gasification processes and two combined cycle concepts will be integrated to produce four possible plant configurations. The best configuration will be sought with respect to thermodynamic performance which is defined qualitatively as usable energy output compared to energy input. Later it will be seen that the station efficiency will be used to quantitatively assess the cycle performance.

Beginning with the four basic cycle configurations, certain components will be added in an effort to improve the performance. It will be instructive to take each of these potential improvements in turn and to note the effect on each configuration. The purpose of this is to see more clearly the effect of adding a particular component. We shall see that performance is not always enhanced by adding equipment usually associated with improving overall efficiency.

Having done this preliminary "optimization" with respect to components, we shall then optimize each configuration in turn, trying to seek the best configuration. In order to see more clearly the effect of meeting the federal emission standards with respect to nitrogen oxides, this optimization will be done first without consideration of the applicable criterion. From the outset, however, the criterion on sulfur dioxide will be met since one of the primary reasons for coal gasification in the first place is to provide a relatively easy way to remove

most of the sulfur from the system well before the products of combustion enter the stack. The effect on cycle performance of meeting the nitrogen oxide emission criterion via flue gas recirculation will be clearly identified.

With each configuration optimized and designed to meet the federal emission standards, other important results will be given. Among these are the consumable water requirements and steam cycle heat rejection requirements. For completeness, typical compositions of the gas leaving the gasifier and the gas leaving the combustor will also be noted.

Finally, parametric studies on some key parameters will be presented. Included in these are coal composition, regenerator effectiveness, pressure drop and component efficiencies, boiler pinch point temperature difference, and gas turbine inlet temperature.

The relevant results are presented in Chapter 5 with the conclusions and recommendations for further study in Chapter 6. It should further be noted that, as much as is feasible, off-the-shelf equipment is to be used. For example, currently available gas turbines with a peak temperature of 2000°F are used instead of advanced technologies like air- or water-cooled turbines. Consequently, it is believed that the results to be presented later are indicative of the performance that can be expected with the technology of today.

It should be noted that economic considerations are outside the scope of this dissertation. This very important facet of the design problem is necessarily outside the realm of thermodynamics, since equipment would first have to be sized. Hopefully, this disseration may provide the starting point for such an extension to this work.

CHAPTER 2

INTRODUCTION

2.1 Combined Cycles

Before describing two primary types of combined cycles, let us motivate the reason for considering combined cycles in the first place. Consider the thermodynamic cycle of a simple heat engine whose schematic is shown in Figure 2.1-1. Let us take Q_1 units of heat from a high temperature reservoir, let it be the heat source for a heat engine that operates in a cycle, and extract W_{12} net units of work. The second law of thermodynamics requires that heat be expelled from the cycle to the low temperature reservoir. Let the amount of rejected heat be Q_2. The first law of thermodynamics requires that

$$Q_1 = W_{12} + Q_2 \tag{2.1-1}$$

The cycle efficiency η is defined to be the ratio of the net work W_{12} to the heat input Q_1, or

$$\eta = \frac{W_{12}}{Q_1} \tag{2.1-2}$$

Now consider two such cycles in series, as shown in Figure 2.1-2. We shall refer to this arrangement as a combined cycle. The heat Q_1 from the high temperature reservoir drives the first heat engine which produces net work W_{12}. The amount of heat rejected to the second cycle is Q_2. In this cycle, W_{23} net units of work are produced. The second cycle then expels Q_3 units of heat to the low temperature reservoir. To make our discussion more general and closer to our observations of the real world, let us further assume that Q_ℓ units of heat are transferred directly to

the low temperature reservoir from the first engine; thus, Q_ℓ represents a heat loss. This is shown by the dashed line in Figure 2.1-2. The thermodynamic efficiencies for the first heat engine alone, the second heat engine alone, and for the two engines combined become respectively

$$\eta_1 = \frac{W_{12}}{Q_1} , \tag{2.1-3}$$

$$\eta_2 = \frac{W_{23}}{Q_2} , \tag{2.1-4}$$

and

$$\eta_{cc} = \frac{W_{12} + W_{23}}{Q_1} \tag{2.1-5}$$

If β is defined to be the ratio of the heat loss Q_ℓ to the heat input to the second cycle Q_2, we may write

$$\beta = \frac{Q_\ell}{Q_2} . \tag{2.1-6}$$

Then using Equations (2.1-3) and (2.1-4) in Equation (2.1-5), the following expression results for the combined cycle efficiency in terms of only η_1, η_2, and β:

$$\eta_{cc} = \eta_1 + \left\{\frac{1-\eta_1}{1+\beta}\right\} \eta_2 \tag{2.1-7}$$

From the definition of β, note that $\beta=0$ corresponds to no heat loss from the first heat engine. If β is infinite, then no heat is transferred to the second heat engine and the combined efficiency η_{cc} should be equal to η_1. This last observation is consistent with Equation (2.1-7).

Let us examine the implications of Equation (2.1-7). Considering the abscissa to be η_2 and the ordinate η_{cc}, Equation (2.1-7) represents a straight line with η_1 as the y-intercept and the quantity $(1-\eta_1)/(1+\beta)$ as

the slope. Clearly, the presence of β in the denominator of the expression for the slope serves to reduce η_{cc}. The best combined cycle efficiency is obtained when β is zero. When β is one, half of the heat "rejected" from the first heat engine is lost and half drives the second heat engine. Let us plot η_{cc} versus η_2 with η_1 as a parameter for these two values of β, as shown in Figure 2.1-3. In this figure, the solid lines correspond to β=0 and the dashed lines to β=1.

Consider first the case of no heat loss (β=0). From Figure 2.1-3 it may be seen that η_{cc} is always greater than both η_1 and η_2. For example, if η_1=0.25 and η_2=0.25, than η_{cc}=0.44 which represents a significant increase. A considerable amount of additional work, therefore, may be obtained by connecting two cycles in series thermodynamically. Let us now see how the presence of a heat loss affects the combined cycle efficiency.

Consider the case of a heat loss from the first heat engine to the low temperature reservoir such that Q_ℓ=Q_2 or β=1. From Figure 2.1-3 it is seen that for the example above now η_{cc}=0.34, instead of 0.44 as before. This clearly indicates that the efficiency of a combined cycle may be improved significantly over that of both the individual cycles by reducing the heat loss from the first cycle. This assumes, however, that η_1 and η_2 remain unchanged, which is unlikely. From the definition of β, it is seen that β may be decreased by reducing Q_ℓ or by increasing Q_2. Making Q_2 larger with β fixed, however, necessarily lowers η_1. Let us derive an alternate expression for η_{cc} that will prove to be more useful than Equation (2.1-7) in explaining some of the results to be shown later in Chapter 5.

An equivalent expression for η_{cc} is given by

$$\eta_{cc} = 1 - \frac{Q_\ell + Q_3}{Q_1} \tag{2.1-8}$$

and for η_2 by

$$\eta_2 = 1 - \frac{Q_3}{Q_2} \tag{2.1-9}$$

Solving Equation (2.1-9) for Q_3 and substituting this result into Equation (2.1-8) gives

$$\eta_{cc} = 1 - \left(\frac{Q_\ell + Q_2}{Q_1}\right) + \frac{Q_2}{Q_1}\eta_2 \tag{2.1-10}$$

As we shall soon see, a practical application for this combined cycle concept is the gas turbine cycle combined with a steam cycle. Reducing the heat loss Q_ℓ from the first or gas cycle will be tantamount to reducing the heat transfer to the environment, including stack gas losses. Changing the heat input Q_2 to the second cycle will be equivalent to changing the heat transfer in the boiler from the gas cycle to the steam cycle.

It can be easily shown that the above combined cycle concept is superior to an ordinary gas cycle with regeneration. Let us assume that again the gas cycle efficiency (or η_1 above) is 25 percent. In addition, we conservatively assume that as much as 50 percent of the rejected heat is used to help provide the heat input to the cycle by regeneration. This last assumption will put an upper bound on the gas cycle efficiency with regeneration, since it is unlikely that 50 percent of the heat source could be provided by this method. Let us arbitrarily normalize this brief calculation on 2 units of work. As shown in Figure 2.1-4, this implies 8 units of heat into the cycle with 3 coming from the

regenerated rejected heat and 5 coming from the high temperature reservoir. Only 3 units of heat are actually rejected to the low temperature reservoir. Again we see that the engine by itself is only 25 percent efficient, but the entire system taken together is 40 percent efficient. The combined cycle above was shown to have an efficiency as high as 44 percent under consistent assumptions. Clearly, the combined cycle concept has a higher potential to boost overall plant performance.

In summarizing, application of the combined cycle concept could result in a significant increase in thermodynamic efficiency. Better overall performance can be expected for the combined cycle than for the simple gas turbine cycle with regeneration. Two feasible gas-steam combined cycle concepts will now be discussed: the waste heat system and the supercharged boiler system.

A simple gas turbine cycle is shown schematically in Figure 2.1-5. Note that this is an open cycle, since the air and fuel, presumably in a different chemical form, are eventually expelled to the atmosphere. Air is compressed by a compressor to an elevated pressure, mixed with fuel, and burned in the combustor. The hot product gas then expands in the gas turbine where useful work is done by the fluid before being expelled to the atmosphere. This cycle is known as an open Brayton cycle. The purpose of the cycle, of course, is to produce net work. We shall see in Chapter 5 that this cycle by itself is not very efficient, but its use in combined cycles significantly enhances the overall cycle performance. Typical gas turbine exit temperatures are in excess

of 1000°F. There is enough sensible heat in this exhaust gas to generate a significant amount of superheated steam in a steam cycle.

A simple schematic of a closed steam cycle is shown in Figure 2.1-6. In fact, this particular cycle is known as a Rankine steam cycle. Steam which is generated in the boiler from an external heat source is expanded in a steam turbine to a very low pressure. The fluid is then condensed in a condenser before it is pumped back into the boiler to continue the cycle. As mentioned above, there is sufficient sensible heat in the gas turbine exhaust to supply the heat necessary in the boiler to raise about 1000°F superheated steam. The efficiency for this steam cycle can be quite good when improvements to the cycle are made, such as regenerative feedwater heating. Let us now expound on the concept of the waste heat system

It has already been agreed that it is feasible to use the gas turbine exhaust to provide the heat needed in the boiler. Because the waste heat from the gas cycle is being used in this boiler, it is referred to as a waste heat boiler. The resulting combined gas and steam cycle, or combined cycle for short, will be referred to as a waste heat boiler system or even a waste heat system. As discussed in more detail in the next chapter, the waste heat boiler is composed of three sections: the superheater (SH), the evaporator (EV), and the economizer (EC). Suffice it to say now that the exhaust gas passes through the gas-side of the waste heat boiler in the order of superheater, evaporator, and economizer and leaves the system through the stack. In Figure 2.1-7 the path of the gas from the combustor to the stack is summarized. Because of metallurgical considerations, the gas turbine inlet temperature for land-based

operation may not exceed 2000°F based on present technology. Because the adiabatic flame temperature of the gas is much higher than this, the gas will have to be burned with a great amount of excess air. The excess air serves as a diluent, of course, since it will enter the combustor at a temperature significantly below the adiabatic flame temperature.

A second feasible way in which the Brayton and Rankine cycles may be incorporated into a combined cycle will now be discussed. Instead of expanding the gas in the gas turbine before allowing it to enter the boiler, let us try to do the reverse; that is, let us try to burn the gas in the combustor, generate steam in the boiler, and then expand the gas in the gas turbine. First it should be noted that if the economizer is before the gas turbine, the gas turbine inlet temperature will be necessarily too low to produce a significant amount of work. As a minimum, the gas turbine will have to be located upstream of the economizer. Second it should be noted that the highest possible turbine inlet temperature, 2000°F, should be used to get the best cycle efficiency. In order to have 2000°F gas after the superheater and evaporator, a gas temperature much higher than this is needed at the inlet to the evaporator and superheater sections of the boiler; that is, the gas should be burned with a minimum of excess air in order to obtain a gas temperature near the adiabatic flame temperature. Finally, because of the extremely high combustor exhaust temperature, the evaporator section must be placed upstream of the superheater section with respect to the gas-side flow. The reason for this, of course, is that the boiling in the evaporator section results in much higher heat transfer coefficients than the

single-phase heat transfer which occurs in the superheater. The high heat transfer coefficients due to boiling in the evaporator can better accommodate the high heat flux associated with the very hot combustor exit gas. The path of gas from the combustor to the stack is summarized in Figure 2.1-8.

This arrangement of gas cycle and boiler components will be referred to as a supercharged boiler, and a combined cycle which uses this type of boiler will be referred to as a supercharged boiler system. Note that the distinguishing feature between the two combined cycle concepts that have been discussed is the path of the gas through the combined cycle along with the resulting implications. In the waste heat system, the gas proceeds from the combustor to the gas turbine followed by the waste heat boiler. In the supercharged boiler system, the gas proceeds from the combustor to part of the supercharged boiler before going to the gas turbine and finally the economizer. The implications are that the gas for the former must be burned with a large amount of excess air and that for the latter with a minimum of excess air.

As we shall see in the next chapter, this difference between the two combined cycle concepts results in two different modes of operation for the combustor model. For the waste heat system, we shall want to specify the turbine inlet temperature (which is the same as the combustor outlet temperature) with the amount of excess air to be calculated. For the supercharged boiler system, it will be convenient to be able to specify the amount of excess air to be supplied to the combustor with the combustor exit temperature

to be calculated. These modes are easily accommodated in our model as we shall see in Section 3.2.

Next, coal gasification is examined as a means of providing a clean gaseous fuel source for the two combined cycles that have just been discussed.

2.2 Coal Gasification

Let us define coal gasification as a process which converts coal into a gas which contains combustible chemical species. We shall see shortly some of the ways in which coal gasification may be accomplished. Also, we shall examine how the various processes affect the heating value of the gas which is produced, eventually limiting these alternatives to only two: adiabatic gasification of coal with air and steam and endothermic gasification with steam only. Let us initially limit the discussion to pure solid carbon (C) instead of the more problemsome coal to establish the distinguishing features of the various coal gasification processes. Of course, in the final analysis the carbon will be replaced by coal, which will significantly increase the complexity of the analysis.

Let us try to put coal gasification into perspective by considering first the basic combustion reaction of pure solid carbon (C) with stoichiometric air. For added simplicity, let us assume only nitrogen (N_2) and oxygen (O_2) are present in the air. The reaction equation is

$$C(s) + O_2 + 3.76N_2 \rightarrow CO_2 + 3.76N_2 \qquad (2.2\text{-}1)$$

where (s) denotes the solid phase and where it has been assumed that there are 3.76 moles of N_2 per mole of O_2 for the air for these simplified calculations only. Let us now consider a hypothetical experiment in which the

reactants enter a combustion chamber in a steady-flow process at ambient conditions and the products leave at the same conditions. Approximately 14,100 Btu of heat per pound of carbon will be given up to the environment during the process and the product gas will have no heating value; that is, the carbon dioxide (CO_2) is not capable of further combustion in air. In this somewhat simplified discussion the distinction between high and low heating values will not be made.

Next the carbon is reacted with only half of the stoichiometric air according to the following reaction

$$C(s) + 1/2\ O_2 + 1/2(3.76)N_2 \rightarrow CO + 1/2(3.76)N_2 \qquad (2.2\text{-}2)$$

Instead of forming CO_2, the reaction produces carbon monoxide (CO), which has a non-zero heating value since CO can be burned further in air to form CO_2. If the same type of experiment described above is performed, now only 3960 Btu of heat are given off per pound of carbon. However, the heating value of the CO makes up the difference. The reaction has produced a gas, composed of CO and the diluent N_2, which has an effective heating value of about 110 Btu per standard cubic foot (Btu/SCF) of product gas. It is important to remember that heat is released for this reaction. To put this in perspective, let us compare this heating value to that of natural gas which is approximately 1000 Btu/SCF. It is readily seen that the gas which was produced has about only 10 percent of the heating value of natural gas.

In order to eliminate the diluent N_2 from the product gas, the carbon may be reacted with half a mole of pure O_2 according to

$$C(s) + 1/2\ O_2 \rightarrow CO \qquad (2.2\text{-}3)$$

in which only CO is produced. Again this gives up about 3960 Btu of heat, but the heating value of the gas is now 310 Btu/SCF of product gas, or 30 percent of that of natural gas. However, the chief disadvantage of this process lies in the fact that pure O_2 is needed as a reactant. Let us now show how just about the same heating value may be obtained without the use of pure O_2.

Let us react the pure solid carbon with steam and, according to the following balanced chemical equation, produce CO and H_2 (hydrogen) gases.

$$C(s) + H_2O(g) \rightarrow CO + H_2 \qquad (2.2\text{-}4)$$

This reaction is endothermic, however, and *requires* about 9400 Btu of heat if the same kind of experiment is performed. However, a gas has been produced that has a heating value of about 290 Btu/SCF without the use of pure O_2. It is important to keep in mind that heat is required to effect this reaction.

Let us follow the usual convention used in the literature and refer to a gas with a heating value in the range of 0 to 200 Btu/SCF as a low-Btu fuel gas, one in the range of 200 to 400 Btu/SCF as an intermediate-Btu fuel gas, and one above 400 Btu/SCF as a high-Btu fuel gas. Natural gas and synthetic natural gas, of course, are included in the last category. Several coal gasification processes exist which produce a high-Btu gas. These processes are considerably more complex than those described above and require much additional equipment. Also, it makes no sense to produce

a high-Btu gas to be burned and used in an electrical power generation scheme. We shall see in Chapter 5 that very high flame temperatures are possible with a low- or intermediate-Btu gas. Let us restrict out attention, therefore, to only these two types of power gases.

It is instructive to summarize the above gasification reactions. By reacting carbon with half stoichiometric air, a low-Btu fuel gas was obtained, but heat was *produced*. By reacting carbon with pure O_2, an intermediate-Btu fuel gas resulted with heat again being produced. By reacting carbon with steam, an intermediate-Btu fuel gas was produced but heat was *required*. Let us now eliminate the process which requires pure O_2 from further consideration on the grounds that an expensive oxygen plant would be required and that an intermediate-Btu gas may be obtained by the endothermic reaction of carbon with steam anyway. It is rather easy to see that if the reaction in Equation (2.2-2) releases heat and the reaction in Equation (2.2-4) requires heat, then the two could be combined in such a way as to have no net heat transfer. We shall refer to this gasification process of carbon (and later coal) with steam and air with no net heat transfer as adiabatic gasification for short. In Chapter 5, it will be seen that this process produces a low-Btu fuel gas with a heating value of about 150 Btu/SCF, since the diluent N_2 is present in a significant amount from the air that is used. We shall refer to the gasification process of carbon with steam (and no air) and with heat transfer to the process as endothermic gasification for short. It will be seen that this process produces an intermediate-Btu fuel gas with a heating value of about 300 Btu/SCF.

It should be noted that later when the carbon is replaced by coal, compounds containing sulfur will be formed. Most of the sulfur fortunately

ends up as hydrogen sulfide (H_2S) and a much smaller amount as carbonyl sulfide (COS). In the next section the implications of this are discussed.

It is appropriate at this point to state some of the advantages of coal gasification to power an electrical power generation plant. The fact has been established that combined cycles have a high potential to increase overall power plant efficiency. It then followed that a gas and steam cycle could be combined in such a way to achieve this objective. Using natural gas or oil for this purpose may be ruled out because these sources are expected to be in short supply in the near future. Because of the high potential for blade erosion problems in gas turbines using the products of combustion from coal, a relatively clean fuel is needed in order that the working fluid in the gas cycle also be relatively clean. Coal gasification provides such a fuel because proven technology[1] is already available to clean the sulfur compounds (and particulates) out of the fuel if low temperature cleanup is accepted. In addition, it is more economical[1] to clean gas at elevated pressures (which we shall do) than at low pressures, and as we shall see in Chapter 5, there is a significant reduction in the amount of gas to be cleaned if it is cleaned before any combustion takes place. It is felt that these advantages provide enough incentive for looking for ways to utilize our most abundant, albeit dirty, domestic energy source. Coal gasification provides such a means.

It will be necessary, then, to operate the gasifier in two distinct modes: adiabatic gasification of coal with air and steam and endothermic gasification of coal with steam only. In the next section a possible source for the heat needed for the endothermic process will be identified. Also, it will be seen how these two gasification processes may be

integrated with the two combined cycle schemes to form four different electrical power generation plants.

2.3 Combined Cycle Power Plants Integrated with Coal Gasification Systems

In the last two sections, two practical combined cycles and two feasible coal gasification processes were discussed. This suggests four different possible cycle configurations: (1) an adiabatic gasifier integrated with a waste heat system, (2) an adiabatic gasifier integrated with a supercharged boiler system, (3) an endothermic gasifier integrated with a waste heat system, and (4) an endothermic gasifier integrated with a supercharged boiler system. Each of these basic configuration descriptions will now be used to put together the simplest possible cycle for each configuration. As will be seen shortly, each configuration will require the following components: a gasifier, air compressors, a steam generator, a gas throttle valve, a gas cooler, a combustor, a gas turbine, either a waste heat boiler or a supercharged boiler, steam throttle valves, steam turbines, pumps, and a condenser. In addition, a low temperature desulfurization process is needed in which unwanted species from the power gas are removed. Low temperature cleanup is used since proven technology already exists for it. It will be seen later that one such system could be the Benfield process. Let us now take each of these configurations in turn and lay out the simplest possible component arrangement.

2.3.1 Adiabatic Gasifier Integrated with Waste Heat System

It should first be noted that it is necessary to operate the gasifier under pressure, since the power gas is to fuel the Brayton cycle. An air

compressor is needed in order to supply the air for the gasification process. Since adiabatic gasification requires steam, a steam generator is required to generate the steam under pressure with the water being supplied by a pump. Since it will be possible to produce a very hot power gas, some of the sensible heat in this gas may be used to generate the required steam. This is not only feasible but also desirable, since the gas must be cooled anyway for the low-temperature cleanup process. Obviously, high temperature cleanup would be more efficient, but it is not yet technologically nor economically proven. A throttle valve will be placed in the gas flow path to make the operating pressures in the gasification and combustion systems compatible.

Because the steam generator will not necessarily be able to lower the gas temperature to within the operating range of the desulfurization process (between 200 and 260°F), a gas cooler will be needed to accomplish this. After the "dirty" power gas is cleaned via the desulfurization process to a specified purity, the "clean" gas is then burned in a combustor under pressure with the air supplied by a second air compressor. The hot combustor product gas is expanded in a gas turbine. The turbine exhaust gas then is used to supply the heat to the waste heat boiler, where superheated steam is generated for the Rankine cycle. The steam is expanded in a steam turbine with the turbine exhaust being condensed in a condenser. A feedwater pump is used to supply the feedwater to the steam-side of the waste heat boiler which operates under pressure, of course.

This relatively simple basic arrangement and all modified versions of it are hereinafter referred to as Configuration 1. A simplified schematic of this configuration is shown in Figure 2.3-1. The schematic representation

of each component will be formally introduced in the next chapter, where each component model is described. To avoid ambiguity on the schematic of Configuration 1 and on the other three schematics later, each component is labeled explicitly. Simplified schematics for the steam generator and waste heat boiler are used at this point.

2.3.2 Adiabatic Gasifier Integrated with Supercharged Boiler System

As the description of this configuration suggests, a system similar to that of Configuration 1 is sought, but the waste heat boiler is to be replaced by a supercharged boiler. The portion of the system from the gasifier to the combustor and its air compressor remain unchanged. However, the product gas from the combustor now enters the evaporator and superheater sections of the supercharged boiler before the gas turbine. The exhaust gas from the turbine then passes through the economizer section of the boiler. The steam cycle is identical to that of Configuration 1 and will not be discussed again here.

This arrangement, hereinafter referred to as Configuration 2, is shown schematically in Figure 2.3-2. Note that again a simplified representation is used.

2.3.3 Endothermic Gasifier Integrated with Waste Heat Boiler

Recall that, for endothermic gasification, coal is gasified with steam only. It follows that the air compressor serving the gasifier must be removed from the systems shown thus far. In addition, a provision for heat transfer to the gasifier must be included since endothermic gasification is desired. Because the gasifier could conceivably operate at high

temperatures (presumably well above 1000°F), a high temperature heat source must be used. Clearly, the combustor provides such a source, and by using some heat transfer medium, heat can be removed in the combustor and transferred to the gasifier. The technical feasibility of accomplishing this in practice will be discussed in Chapter 5. From the combustor to the stack, the gas cycle and the steam cycle remain the same as in Configuration 1. This basic arrangement shall hereinafter be referred to as Configuration 3, which is shown schematically in Figure 2.3-3.

2.3.4 Endothermic Gasifier Integrated with Supercharged Boiler

Clearly for this configuration the gasification system of Configuration 3 must be integrated with the combined cycle arrangement of Configuration 2. Indeed, nothing is new at this point. This cycle arrangement represents the final configuration and is shown schematically in Figure 2.3-4. This basic arrangement shall hereinafter be referred to as Configuration 4.

2.3.5 Remarks

Four basic cycle configurations have been developed which incorporate two gasification processes and two combined cycle systems. For each of these configurations, the open Brayton cycle and Rankine steam cycle are used. The components have been arranged in the simplest possible manner under the constraints of each respective configuration.

These four configurations represent the starting point from which the cycles may be optimized and improved. Recall that one of our goals is to improve the performance of each cycle by setting optimum operating conditions

and by adding components where necessary. This objective as well as the others stated in Chapter 1 can only be met through very tedious calculations, since the cost of an experimental undertaking would be extremely prohibitive. The need for a mathematical model of each configuration is obvious. This aspect of the problem is approached by modeling each component separately, which is done in Chapter 3. Also obvious is the need for computer capability, since it will be necessary to calculate the performance for many different operating conditions. The component models developed in Chapter 3 are used in the computer program, which is fully described in Chapter 4. Finally, in Chapter 5, an attempt will be made to improve the basic cycle configurations shown in Figures 2.3-1 to 2.3-4 by adding components and by specifying optimum operating conditions.

2.4 Background

Much work has been done on the design of various types of coal gasifiers and gas cleanup systems and surprisingly little on the integration of these systems to combined cycle power plants for the production of electrical energy. It is instructive to summarize some of these gasification and cleanup systems to demonstrate the large degree of flexibility in designing an integrated system. In fact, both the gasification and cleanup systems seem to be so flexibile that the results of this dissertation may be used as a basis for designing new systems. For example, one of the key results from Chapter 5 will be the optimum gasification temperature and pressure which fixes certain other parameters such as steam and, for the adiabatic case, air flow. This type of result may be helpful when one actually tries to design a coal gasifier capable of operation under conditions which are optimum with respect to overall performance.

It is a well-known fact today that some sort of coal gasification technology has been in existence for almost 150 years. In the early 1830's, Faur built a low-Btu gasifier for the production of a producer gas. In the 1920's, there were about 11,000 gasifiers of this type mostly used by the steel industry. Admittedly, these systems today are no longer feasible because of updated environmental constraints. In the mid 1870's, an intermediate-Btu fuel gas was made by the blue water gas process. More than fifty years later this was followed by the Lurgi process[2] which is now being used in at least fourteen industrial plants[3]. Clearly, processes for the production of low- and intermediate-Btu gas have been in existance for a long time.

The present state of affairs is summarized best by an ad hoc panel of the National Research Council which was established to assess the state of low- and intermediate-Btu coal gasification technology:

> ... there has been a long hiatus in the use of gas producers and in the development of new technology for making producer gas. Recent interest in the development of related technology stems from the hope that it will provide a means for producing a clean fuel from coal and, from the possibility of increasing the efficiency of coal conversion if the gas is generated under pressure and used in a combined cycle, helping to alleviate the shortage of scarce fuels.[1]

Many processes have since been devised, thus demonstrating the inherent flexibility in gasifying coal[1]. The coal and gas flows may be parallel-flow or counterflow. The gasifier may operate at atmospheric pressure or under pressurized conditions. Air or oxygen may be used in addition to steam. Heat may be added to the process, eliminating the need for pure oxygen[4]. Tar, soot, mercaptans, phenols, thiophenes, and so forth may be avoided by operating the gasifier at high temperatures. The ash may be removed in dry, slag, or agglomerated form. The gasifiers are typically

classified as fixed bed, fluidized bed, entrained flow, molten bath, and underground [1]. Obviously the last two types are not applicable to the problem of interest and will not be discussed further.

The fixed bed gasifier designs are well developed. Coal and gas flows are countercurrent. This type of gasifier typically has long residence times which allows for essentially complete carbon conversion. Operation at elevated pressures could be problemsome because of softening, sticking, and swelling of some bituminous coals [1]. Gas exit temperatures are usually less than 1200°F which means a large amount of tars, phenols, and so forth are formed. Among the dry-ash pressurized processes are Lurgi [2], Gegas [5], and MERC [6]. The present Lurgi process is capable of using air to produce a low-Btu gas or pure oxygen to produce an intermediate-Btu gas, which may then be used as a feed for the production of synthetic natural gas. The Gegas process has a much lower steam-to-air ratio than is typical of this type of gasifier. The MERC process produces about 3% tar, indicating a relatively low gasification temperature. The Wellman-Galusha [3] and Kellogg [7] systems use atmospheric dry-ash fixed-bed gasifiers. Among the slagging fixed-bed processes are the British Gas [8], ERDA/GFERC [6], and Thyssen-Galoczy [5], the last of which gasifies coal at almost 3000°F, but at atmospheric pressure.

Fluidized-bed gasifiers [9] are better suited for continuous gasification at high feed rates [1]. This gasifier type is capable of using a wide-range of coals. Again the ash can be removed in two different forms: dry or agglomerated. One dry ash process, Winkler [3], which has been commercial since 1926 [1], has a gasification temperature in the range of 1500°F to 1850°F and pressure at about atmospheric. Even at this relatively low

temperature no tar or hydrocarbons are formed. This system uses a heat recovery system before the gas purification stages. Sixteen industrial plants are presently in operation. Similar to this type of gasification system are the CO_2-Acceptor[3], Exxon[7], Synthane[3], and U-Gas[3] processes. These are basically used to provide an intermediate-Btu gas as a feed to the methanation step in the production of synthetic natural gas. The CO_2-Acceptor is somewhat unique in that heat is provided for the carbon and steam reaction by reacting the carbon dioxide with dolomite. This represents another way to get an intermediate-Btu gas without the use of pure oxygen. Operation is pressurized from 150 to 300 psia and gasification takes place at 1600°F. Dolomite serves a secondary purpose also; it is used to remove the H_2S (and CO_2) from the product gas. In the U-Gas process, gasification takes place at about 350 psia and 1900°F[3]. Again heat recovery takes place before the gas is cleaned. Among the agglomerating ash processes are those by Union Carbide[7] and by Westinghouse[3]. Although the Union Carbide system is designed for atmospheric pressure, plans for 100 psia operation are under way, for which higher feed rates are expected. A unique feature of this process is that heat for the carbon-steam reaction is provided by circulating hot ash. This process also has a heat recovery step before the purification system. Raw product gas leaves the gasifier at about 1800°F. The Westinghouse process incorporates high temperature (about 1400°F) desulfurization by using limestone or dolomite in the gasifier. Westinghouse plans to use this process in a combined cycle pilot plant.

Finally, there are gasifier designs which are of the entrained-flow type. Some of the advantages of this gasifier are little or no tar production, ease of adaptability to utilization of a wide range of coals, and

high reaction rates because of the high temperatures. Again, there are both dry-ash and slagging processes. Among the former are Bi-Gas[10], Combustion Engineering[7], and Foster-Wheeler[6]. The Bi-Gas process demonstrates that the gasification process itself is fairly insensitive to pressure since pressures from 500 to 1500 psia have been successfully tested. The Combustion Engineering process is presently designed for atmospheric operation, but operation at elevated pressures is contemplated, and apparently uses a heat exchanger before the gas cleanup stage. The slagging processes include Babcock and Wilcox[7], Koppers-Totzek[3], Ruhrgas[11], and Texaco[5]. Details of the Babcock and Wilcox process are largely unknown. Koppers-Totzek is presently designed for atmospheric pressure using pure O_2, but there are plans for pressurized operation. The gas exit temperature is extremely high (about 2750°F) and results in no tar, hydrocarbon, or phenol production. The Ruhrgas system apparently uses dirty power gas to raise steam for the gasification process. The Texaco gasifier is designed for operation at 2200 to 2500°F and 300 to 1200 psia[1]. The process uses a slurry of coal and water injected into the gasifier. Progress is reported on materials problems associated with coal slag[1].

The gas purification systems may be divided into two broad classifications: hot cleanup and cold cleanup. Hot cleanup takes place within the temperature range from 1000 to 2500°F and cold cleanup from 100 to 250°F. While it is reported that hot cleanup can increase the thermal efficiency of a combined cycle by about three percent, the technology is not well-proven and is expensive. For this reason low-temperature cleanup is accepted as being more viable, and hot cleanup is not discussed any further. The Ad Hoc Panel also points out that

> Most of the heat in the hot gases after gasification can be recovered by heat exchange so that the loss in thermal efficency is minimized.[1]

The Panel identifies at least six cold cleanup processes which are presently available or under development: (1) solid adsorbents, (2) membranes, (3) the Stretford process, (4) amine gas, (5) physical solvents, and (6) hot potassium carbonate. Reference 1 provides an excellent summary of these processes. Some of the characteristics of the hot potassium carbonate process, which is available commercially as the Benfield process, will be summarized since this type of cleanup system will be used in each configuration. Developed in the early 1950's, the Benfield process has been used for fourteen years. It is presently used on about 400 units for the removal of H_2S (and CO_2) from natural gas, ammonia synthesis gas, and hydrogen gas. The Panel points out further

> Where the purification of low- and intermediate-Btu gases from coal is concerned, the use of the Benfield process fits well into the usual process conditions. The gasification pressure usually ranges from 100 to 400 psig. The preferred method of dedusting and cleaning the gas is by water quench, resulting in a water-saturated gas that is at a temperature of 200 to 260°F.[1]

In addition, the Benfield process is compatible with a Claus plant, which may be used to convert the H_2S to elemental sulfur. At 90 to 95 percent H_2S removal, the cost of this process is estimated to be only $18/kw, but at 99 percent, the cost slightly more than doubles[1]. We shall see in Chapter 5 that 90 percent H_2S removal is more than sufficient to keep the SO_2 effluent in the stack well below the federal limit.

The concept of a combined cycle power plant is not new. Today it is receiving ever-increasing attention because of the growing awareness that conventional fuels are in finite and dwindling supply. Boosting cycle

efficiency helps to get more usable energy from the same amount of fuel. The most comprehensive study to date is the Energy Conversion Alternatives Study, known as ECAS. Actually, ECAS has examined about ten coal conversion power generation systems in Phase I of the study and seven in Phase II. One of these conversion concepts is the combined cycle integrated with a low-Btu gasifier. This study was essentially done in parallel by Westinghouse and General Electric and has culminated in several volumes of reports[12,13]. In this work, no attempt has been made to determine optimum conditions or plant configurations. They have both used advanced equipment, such as air- and water-cooled gas turbines. The NASA Lewis Research Center has evaluated these studies and has summarized its findings in a lengthy report[14].

It is difficult to compare the Westinghouse results with those of General Electric, since different operating conditions and plant layouts were used sometimes with different assumptions. However, the Westinghouse design appears to be 46.8 percent efficient compared to 39.6 percent for that of General Electric. Part of this difference is due to Westinghouse's using hot gas cleanup while General Electric elected to use cold. In any event, the thermodynamics of the integrated systems are obscured in many, many details. It is not clear how the systems evolved from a basic plant layout.

Ahner, et al.[15] have developed a design for an integrated gasification combined cycle plant without actually optimizing with respect to plant performance. However, the authors do provide a relatively simple equation which may be used to find the "first cost incentive" from some specified

base case. As mentioned in Chapter 1, however, an economic study is outside the scope of this dissertation.

Osterle[16] provided the basis for this dissertation by scoping the basic gasification reactions in a manner similar to that of Section 2.2. Intrigued by the many new degrees of freedom that a coal gasifier adds to the otherwise routine thermodynamic design process of a fossil-fueled power plant, Osterle incorporated his early work into a power cycle and performed many of the tedious hand calculations which were a necessary prelude to a computerized study. To help in this effort, Impink developed a large number of gas table property subprograms, processing codes, and the steam table processor subprogram (see subroutine FINDER in Section 4.5.2), many of which are used in this dissertation. Look developed the first computer model of an adiabatic model following Osterle's analytical model. Impink extended this model and developed the endothermic model, in which rather crude numerical methods were employed. Impink also developed many of the preliminary computerized component models, again following Osterle's analytical developemnt. Impink and Osterle then demonstrated the feasibility of modeling integrated coal gasification processes and combined cycle systems and introduced the initial elements of pollutant emission calculations. Finally, in addition to augmenting the gas table library, Candris developed a preliminary flue gas recirculation model following Osterle's derivation. Their work culminated in a report[17] to the Pennsylvania Science and Engineering Foundation, who supported some of their effort. Clearly, the present work is in a sense a culmination of several years of prior effort.

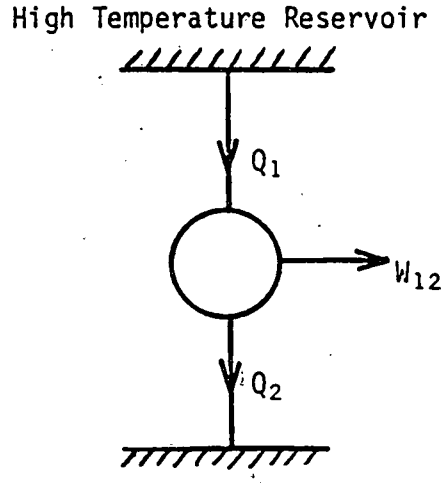

Figure 2.1-1 Schematic of Simple Heat Engine

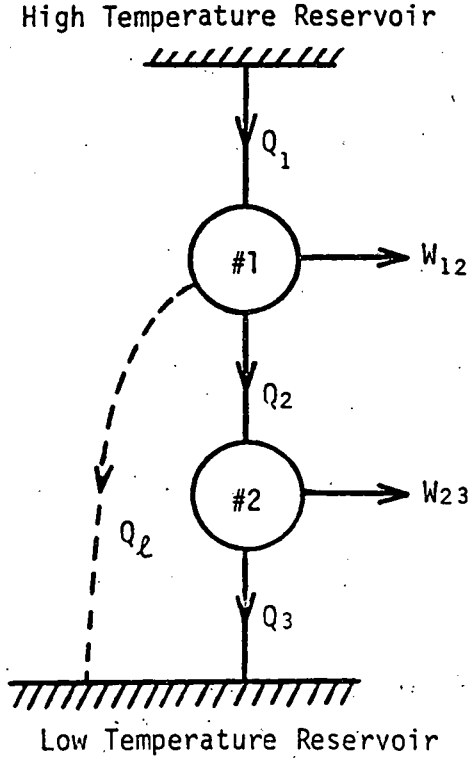

Figure 2.1-2 Schematic of Two Heat Engines Connected in Series with Loss

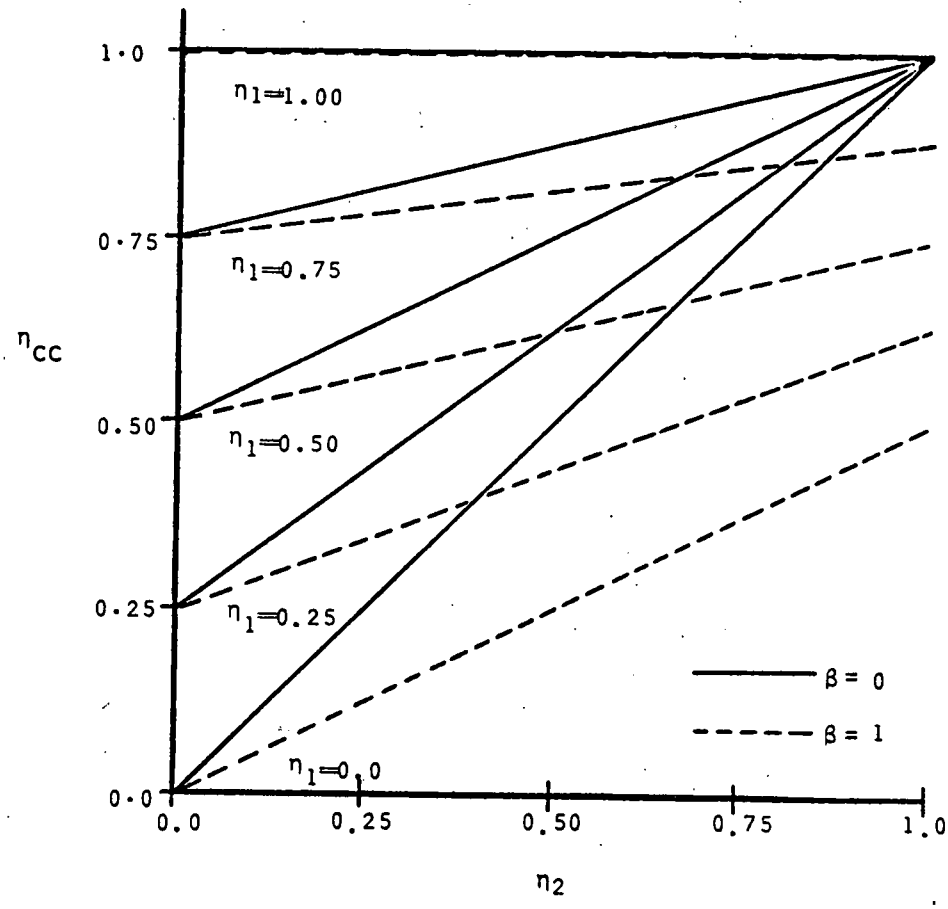

Figure 2.1-3 Combined Cycle Efficiency η_{cc} Versus Second Engine Efficiency η_2 with First Engine Efficiency η_1 as a Parameter for $\beta = 0$ and $\beta = 1$. (Refer to Eq. 2.1-7)

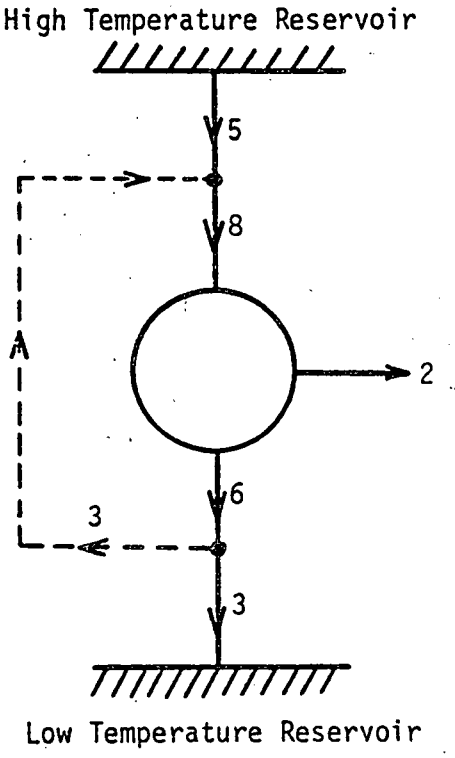

Figure 2.1-4 Schematic of Heat Engine with Efficiency of 25 Percent and with 50 Percent Regeneration Giving an Over-all Efficiency of 40 Percent

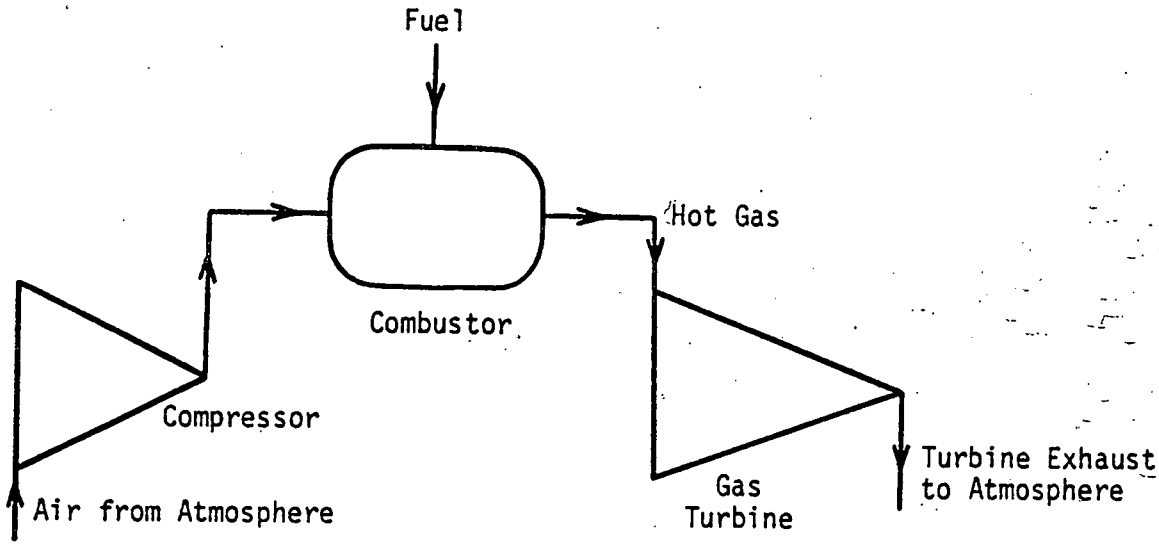

Figure 2.1-5 Simplified Schematic of Open Brayton Cycle

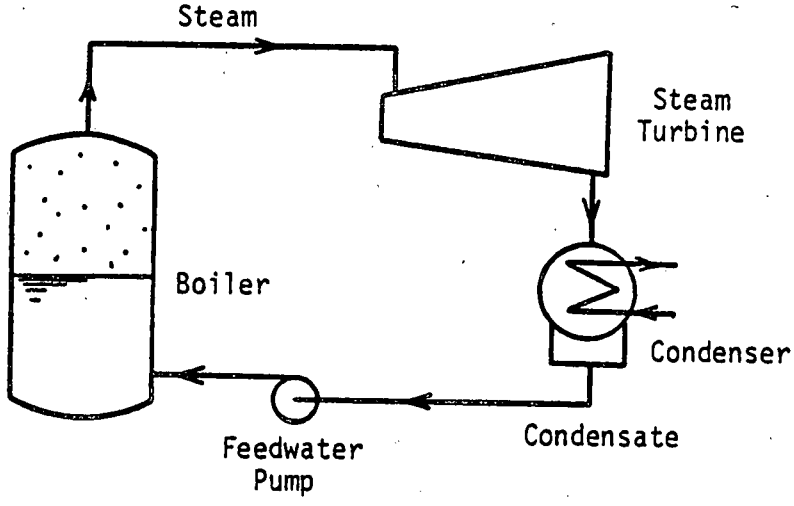

Figure 2.1-6 Simplified Schematic of Rankine Steam Cycle

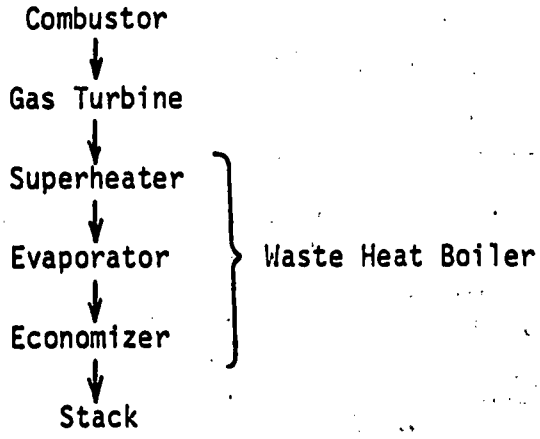

Figure 2.1-7 Path of Gas in Waste Heat System

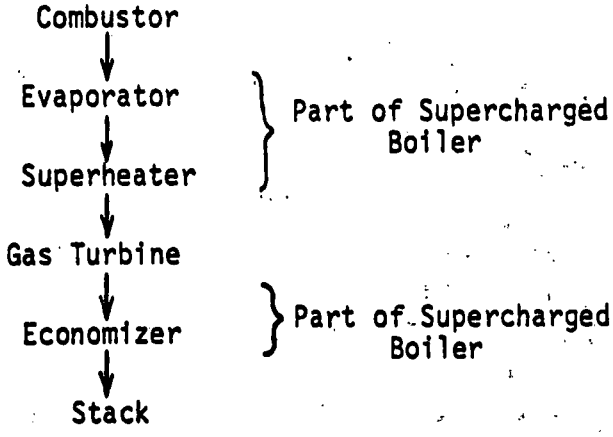

Figure 2.1-8 Path of Gas in Supercharged Boiler System

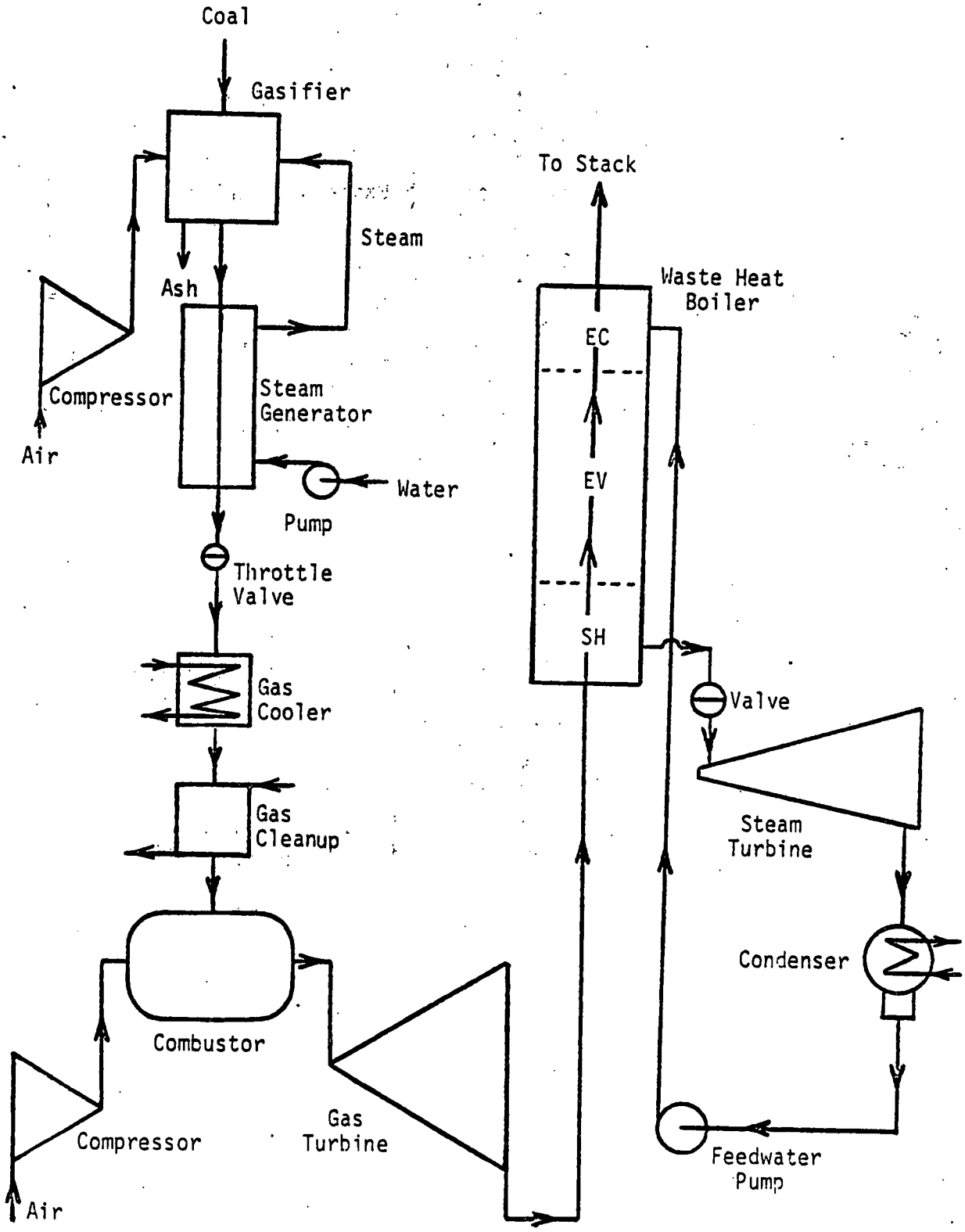

Figure 2.3-1 Simplified Schematic of Adiabatic Gasifier Integrated with Waste Heat Boiler Combined Cycle (Configuration 1)

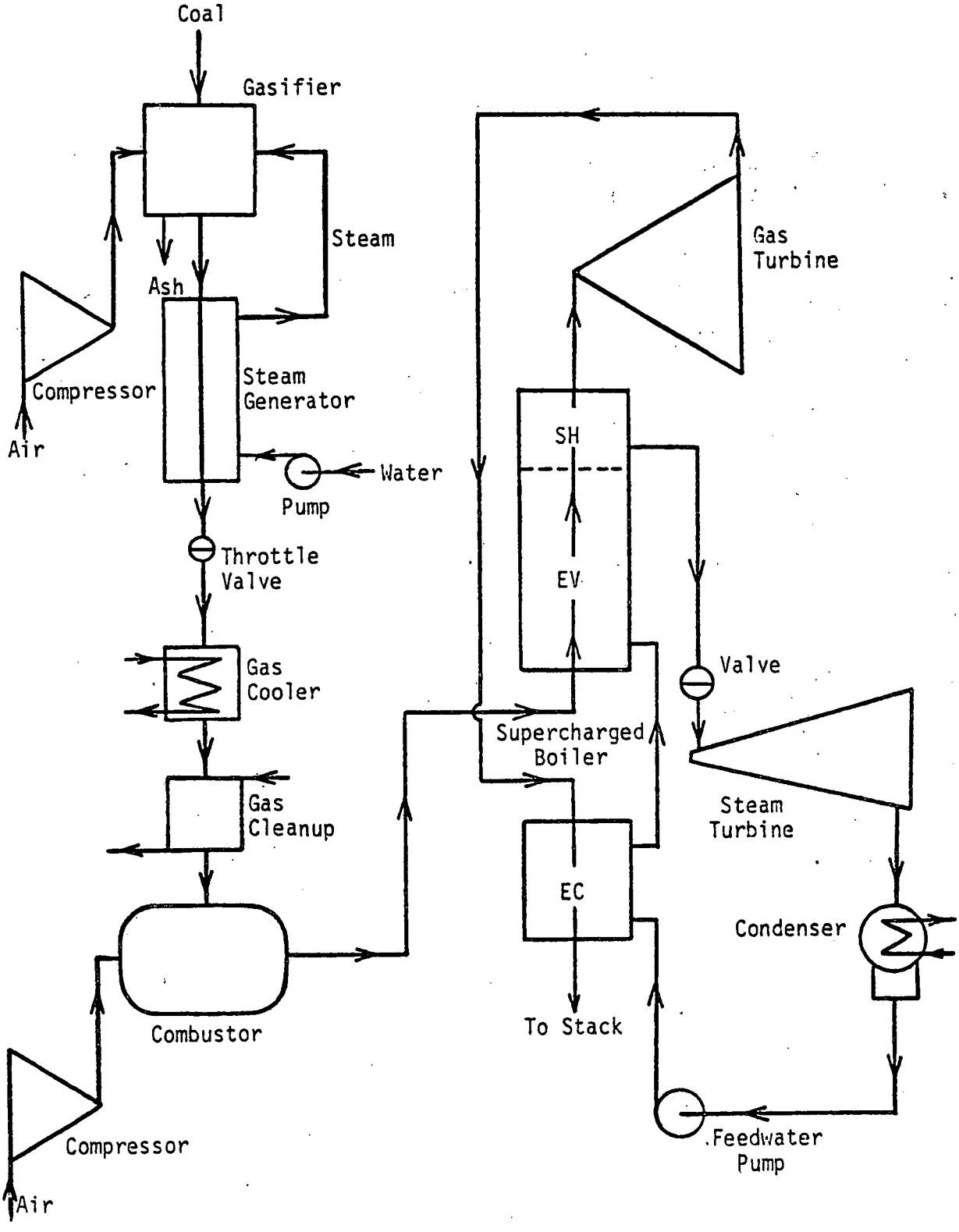

Figure 2.3-2 Simplified Schematic of Adiabatic Gasifier Integrated with Supercharged Boiler Combined Cycle (Configuration 2)

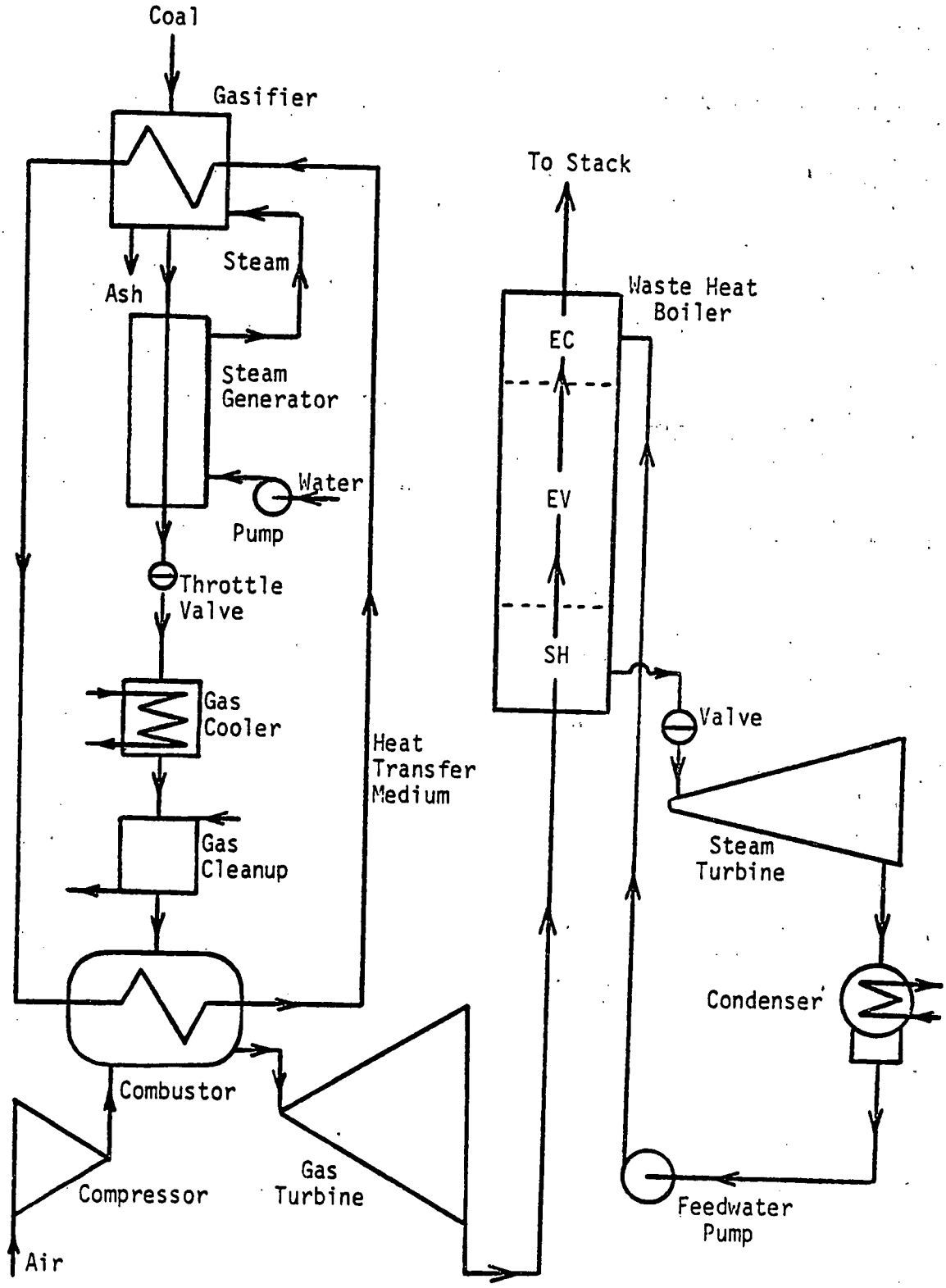

Figure 2.3-3 Simplified Schematic of Endothermic Gasifier Integrated with Waste Heat Boiler Combined Cycle (Configuration 3)

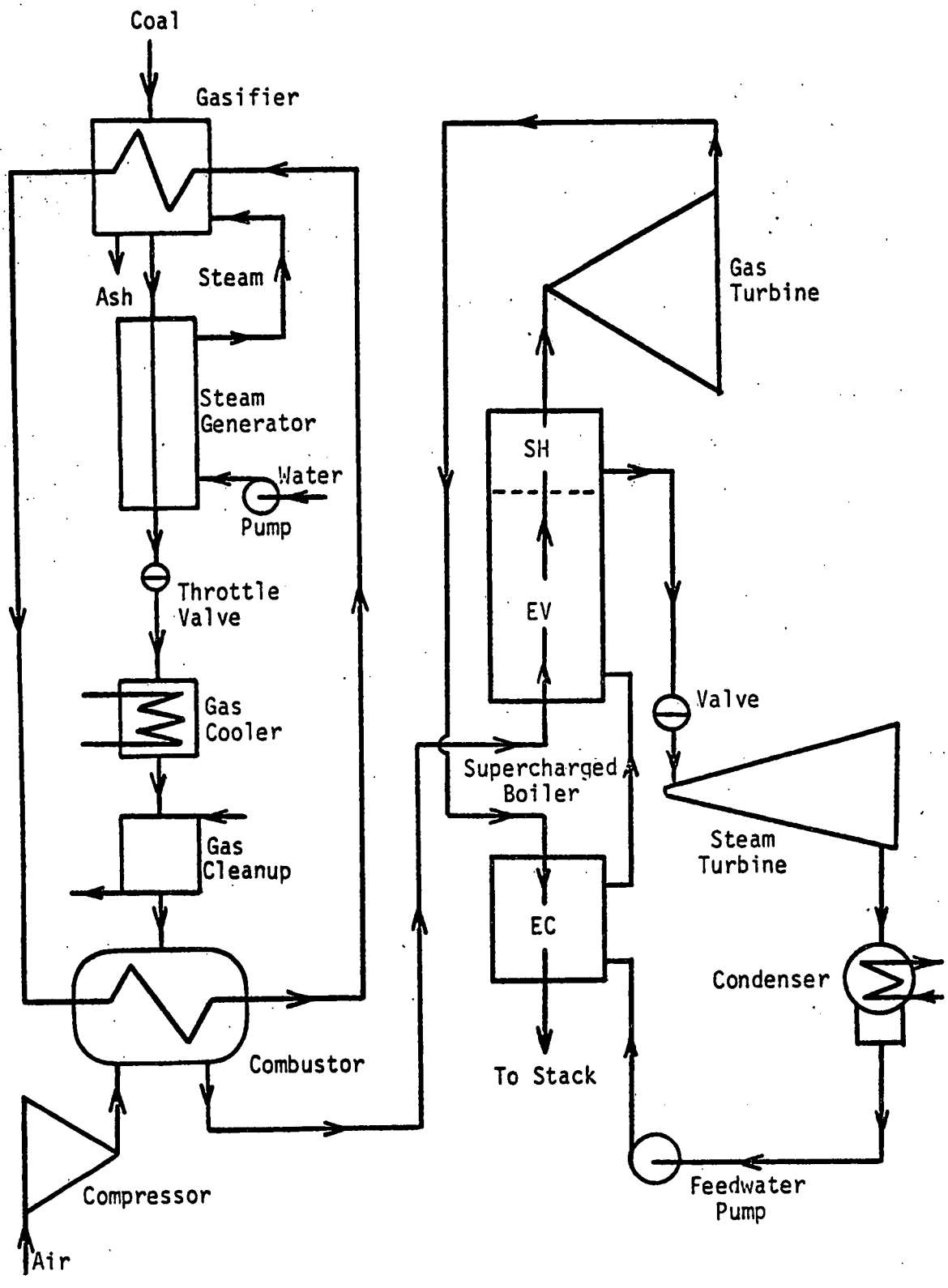

Figure 2.3-4 Simplified Schematic of Endothermic Gasifier Integrated with Supercharged Boiler Combined Cycle (Configuration 4)

CHAPTER 3

MATHEMATICAL MODELING OF COMPONENTS

3.1 Introduction

An obvious first step in the analysis of the systems described in Chapter 2 is the representation of each component in a particular cycle by a mathematical model. Because many components appear several times within a particular cycle and because a particular component is used in more than one cycle, it is advantageous to keep the models separate. We shall find it better to model each component, where possible, as a single entity. For example, the modeling of a two-stage intercooled compressor is accomplished by separately modeling a single stage compressor (which is then used twice) and an intercooler. This point will be more obvious in Chapter 4, where the models are cast into the form of subroutines.

It is important to remember that we are interested only in the steady-state thermodynamics of the four cycles. Consequently, the models will provide only a limited amount of information about a particular component. For example, the model for the adiabatic gasifier provides information like the air and steam flow rates and the outlet gas composition, but does not provide information like the size of the gasifier.

As expected, some of the models are more complex than others. The gasifier, combustor, waste heat boiler, and supercharged boiler models are among the most complicated. These particular ones will be described in considerable detail. Because the mathematical solution of the equations which represent the gasifier model is nearly identical to that of the combustor model, both of these are treated in Section 3.2, with the common method of solution also given. In Sections 3.3 and 3.4, the waste heat boiler and the supercharged boiler

models are developed, respectively. The more simple components are described and modeled in Sections 3.6 to 3.16.

3.2 Gasifier and Combustor

3.2.1 General Comments

These models are very similar in the sense that the same types of equations are provided by (1) mass balances on each of the elements, (2) the assumption of equilibrium of the various gaseous species, and (3) an energy balance. This approach results in 16 non-linear algebraic equations to describe the gasifier, and 21 similar equations for the combustor. Of course, there are 16 and 21 unknowns for the gasifier and combustor, respectively.

As discussed in Section 2.2, provisions must be made to operate the gasifier in two specific modes: adiabatic gasification of coal with steam and air and endothermic gasification of coal with steam. And, as discussed in Section 2.1, provisions must also be made to operate the combustor in two different modes: one in which the combustor outlet temperature is specified (the excess air is then calculated), and the other in which the excess air is specified (the outlet temperature is then calculated). These last two modes correspond to uses in the waste heat system and supercharged boiler system, respectively. As discussed in the next few sections, these provisions on the gasifier and combustor models are easily implemented.

3.2.1.1 Gasifier Model

The endothermic mode for the gasifier will be shown later to be a special case of the adiabatic mode. Therefore, the most general gasifier

model can be obtained by assuming that coal is to be reacted with air and steam, subject to the adiabatic constraint.

The question arises, however, of how one should obtain the enthalpy of the coal, which is needed for the energy balance. This problem is resolved by using the Dulong approximation for enthalpy determination purposes which is accurate to about 3 percent[18]. The Dulong approximation may be summarized as follows. The carbon given by the ultimate analysis is assumed to be fixed carbon. All the oxygen is assumed to combine with the necessary amount of hydrogen to form water vapor with the remaining hydrogen forming only diatomic hydrogen gas. The nitrogen and sulfur are assumed to be in the form of their respective elemental gaseous compounds and the moisture is taken as liquid water. (The sensible heat associated with the ash will be accounted for by using a suitable specific heat.)

The basic reaction for the adiabatic mode is

Coal + Air + Steam → Gas + Ash

Let us normalize the calculation by assuming a unit mass of coal, whose ultimate analysis is given. That is, the weight fraction is given for the following: carbon (C), hydrogen (H), oxygen (O), nitrogen (N), sulfur (S), liquid water (H_2O), and ash. Also let us assume that the composition of the air by weight fraction is also specified, with provisions for nitrogen (N_2), oxygen (O_2), argon (Ar), and water vapor (H_2O). The steam which is required by the gasifier is assumed to be pure superheated water vapor (H_2O). The power gas which is produced is assumed to have the following chemical species present: hydrogen (H_2), carbon monoxide (CO), methane (CH_4), water vapor (H_2O), carbon dioxide (CO_2),

nitrogen (N_2), argon (Ar), hydrogen sulfide (H_2S), carbonyl sulfide (COS), and ammonia (NH_3). Finally, the ash in the coal is assumed to exit from the gasifier at some specified temperature presumably no higher than the gas exit temperature.

We are now in a position to write the mass balance equations. Since we have present C, H, O, N, S, and Ar, we expect to have six such equations. Let ω_{ci} be the weight fraction of component i in the coal, where i takes on values from 1 to 7 as summarized in Table 3.2-1. Let ν_{ci} be the molecular

Table 3.2-1
Meaning of Subscripts Applied to Coal

Subscript (ci)	Component in Coal
c1	C
c2	H
c3	O
c4	N
c5	S
c6	$H_2O(\ell)$
c7	Ash

weight of component i in the coal, where again i is defined according to Table 3.2-1. Similarly, we define ω_{ai} and ν_{ai} to be the weight fraction and the molecular weight of species i, respectively, for the air. As shown in Table 3.2-2, i now takes on values of 1 to 4. Furthermore, let

Table 3.2-2
Meaning of Subscripts Applied to Air

Subscript (ai)	Species in Air
a1	N_2
a2	O_2
a3	Ar
a4	$H_2O(g)$

w_a be the mass of air required, and let w_s be the mass of steam required each per unit mass of coal. The molecular weight of steam (or water) will be denoted as ν_s. Having defined the necessary parameters associated with the reactants, we now turn to the products.

Let n_{gi} be the number of moles of species i formed per unit mass of coal, where i now takes on values of 1 to 10, as defined in Table 3.2-3.

Table 3.2-3
Meaning of Subscripts Applied to Power Gas

Subscript (gi)	Species in Gas
g1	H_2
g2	CO
g3	CH_4
g4	$H_2O(g)$
g5	CO_2
g6	N_2
g7	Ar
g8	H_2S
g9	COS
g10	NH_3

Let N_g be the sum of the n_{gi} from i = 1 to 10; that is,

$$N_g = \sum_{i=1}^{10} n_{gi}$$

Note then that N_g is the total number of moles of power gas produced per unit mass of coal. The composition of the power gas by mole fraction (y_{gi}) is then given by

$$y_{gi} = n_{gi}/N_g.$$

Now based on a unit mass of coal, the number of moles of C in the reactants is simply ω_{C_1}/ν_{C_1} and the number of moles of C in the products

is given by $n_{g2} + n_{g3} + n_{g5} + n_{g9}$. These two expressions must be equal in order to satisfy the mass balance requirement on carbon and the mass balance equation for C becomes

$$\frac{\omega_{C1}}{\nu_{C1}} = n_{g2} + n_{g3} + n_{g5} + n_{g9} \tag{3.2-1}$$

The mass balance on H is slightly more complicated because hydrogen appears in all three reactants. The number of moles of H in the coal is $\omega_{C2}/\nu_{C2} + 2\omega_{C6}/\nu_{C6}$, while the air, $2w_a\ \omega_{a4}/\nu_{a4}$, and due to the reactant steam, $2w_s/\nu_s$. The number of moles of H in the products is given by $2n_{g1} + 4n_{g3} + 2n_{g4} + 2n_{g8} + 3n_{g10}$. Again the sum of moles of H in the reactants must equal the sum of the moles of H in the products so the mass balance equation for H is

$$\frac{\omega_{C2}}{\nu_{C2}} + \frac{2\omega_{C6}}{\nu_{C6}} + 2w_a \frac{\omega_{a4}}{\nu_{a4}} + 2w_s \frac{1}{\nu_s} = 2n_{g1} + 4n_{g3} + 2n_{g4} + 2n_{g8} + 3n_{g10} \tag{3.2-2}$$

Similarly for O, N, S, and Ar we get, respectively,

$$\frac{\omega_{C3}}{\nu_{C3}} + \frac{\omega_{C6}}{\nu_{C6}} + w_a \left(2\frac{\omega_{a2}}{\nu_{a2}} + \frac{\omega_{a4}}{\nu_{a4}} \right) + \frac{w_s}{\nu_s} = n_{g2} + n_{g4} + 2n_{g5} + n_{g9}, \tag{3.2-3}$$

$$\frac{\omega_{C4}}{\nu_{C4}} + 2w_a \frac{\omega_{a1}}{\nu_{a1}} = 2n_{g6} + n_{g10}, \tag{3.2-4}$$

$$\frac{\omega_{C5}}{\nu_{C5}} = n_{g8} + n_{g9}, \tag{3.2-5}$$

and

$$w_a \frac{\omega_{a3}}{\nu_{a3}} = n_{g7}. \qquad (3.2\text{-}6)$$

Because mole fractions will appear in the equilibrium equations, it is advantageous to work with mole fractions rather than mole numbers. Therefore, we divide Equations (3.2-1) to (3.2-6) by N_g. However, we then solve equation 3.2-1 for N_g, which can be used in the remaining five equations. Accordingly,

$$N_g = \frac{\omega_{c1}/\nu_{c1}}{y_{g2} + y_{g3} + y_{g5} + y_{g9}}. \qquad (3.2\text{-}7)$$

The five remaining equations, Equations (3.2-2) to (3.2-6), are changed only in that the left-hand side of each is multiplied by the reciprocal of N_g, with N_g given by Equation (3.2-7), and each n_{gi} is replaced by y_{gi}. The final form of the mass balance equations is as follows:

$$\left\{\frac{\omega_{c2}}{\nu_{c2}} + 2\frac{\omega_{c6}}{\nu_{c6}} + 2w_a \frac{\omega_{a4}}{\nu_{a4}} + \frac{2w_s}{\nu_s}\right\}\left\{\frac{\omega_{c1}}{\nu_{c1}}(y_{g2} + y_{g3} + y_{g5} + y_{g9})\right\} = 2y_{g1} + 4y_{g3} + 2y_{g4} + 2y_{g8} + 3y_{g10} \qquad (3.2\text{-}8)$$

$$\left\{\frac{\omega_{c3}}{\nu_{c3}} + \frac{\omega_{c6}}{\nu_{c6}} + w_a\left(2\frac{\omega_{a2}}{\nu_{a2}} + \frac{\omega_{a4}}{\nu_{a4}}\right) + \frac{w_s}{\nu_s}\right\}\left\{\frac{\omega_{c1}}{\nu_{c1}}(y_{g2} + y_{g3} + y_{g5} + y_{g9})\right\} = y_{g2} + y_{g4} + 2y_{g5} + y_{g9} \qquad (3.2\text{-}9)$$

$$\left\{\frac{\omega_{C4}}{\nu_{C4}} + 2w_a \frac{\omega_{a1}}{\nu_{a1}}\right\} \left\{\frac{\omega_{C1}}{\nu_{C1}} (y_{g2} + y_{g3} + y_{g5} + y_{g9})\right\} = 2y_{g6} + y_{g10} \tag{3.2-10}$$

$$\left\{\frac{\omega_{C5}}{\nu_{C5}}\right\} \left\{\frac{\omega_{C1}}{\nu_{C1}} (y_{g2} + y_{g3} + y_{g5} + y_{g9})\right\} = y_{g8} + y_{g9} \tag{3.2-11}$$

$$\left\{w_a \frac{\omega_{a3}}{\nu_{a3}}\right\} \left\{\frac{\omega_{C1}}{\nu_{C_1}} (y_{g2} + y_{g3} + y_{g5} + y_{g9})\right\} = y_{g7} \tag{3.2-12}$$

The sixth equation, of course, is provided by the fact that the sum of mole fractions must equal unity, or

$$\sum_{i=1}^{10} y_{gi} = 1 \tag{3.2-13}$$

This completes the six equations provided by the mass balances.

At this point, we see that there are twelve unknowns: the ten mole fractions, the steam flow, and the air flow. Additional equations are provided by invoking the assumption of thermodynamic equilibrium. The validity of this assumption is established in Section 5.8.

The species assumed to be present in the power gas imply that five independent reactions are taking place. Using (s) to denote the solid phase and no phase designation to imply the gas phase, we may assume the following arbitrary (but independent) reactions:

$$C(s) + 2H_2 \rightleftarrows CH_4 \qquad (3.2\text{-}13a)$$

$$C(s) + H_2O \rightleftarrows CO + H_2 \qquad (3.2\text{-}13b)$$

$$C(s) + CO_2 \rightleftarrows 2CO \qquad (3.2\text{-}13c)$$

$$N_2 + 3H_2 \rightleftarrows 2NH_3 \qquad (3.2\text{-}13d)$$

$$H_2S + CO \rightleftarrows COS + H_2 \qquad (3.2\text{-}13e)$$

Then the equilibrium condition for each reaction can be written. For example, for the reaction in Equation (3.2-13a), we could write

$$K_p = \frac{\left(y_{CH_4} P\right)}{\left(y_{H_2} P\right)^2} \qquad (3.2\text{-}14)$$

where again y_i denotes the mole fraction of species i and P is the total pressure in atmospheres since the equilibrium constant, K_p, is assumed to be based on atmospheres. For a given reaction, the equilibrium constant, which is a function of temperature only, can be obtained from an appropriate handbook. In Equation (3.2-14), it is assumed that the mixture behaves like an ideal gas; otherwise, the mole fraction and pressure products would be replaced by the fugacities. Because the carbon is in the solid phase, there is no "RT ℓn" correction on the Gibbs free energy for solid carbon and, therefore, Equation (3.2-14) is valid as written. Similar equations could be written for the remaining reactions.

Although the equilibrium equations in the form of Equation (3.2-14) could be used directly in the solution to our problem, it is better to modify them to effect a more general solution strategy. One such modification would be to use the logarithmic form of the equilibrium equations For example Equation (3.2-14) would become

$$\ell n K_p = \ell n(y_{CH_4} P) - 2\ell n(y_{H_2} P). \qquad (3.2\text{-}14a$$

However, we would then need to have K_p for each reaction. While this is a trivial point for Equation (3.2-14a) since we conveniently have a formation reaction, this is an important consideration for reactions like that in Equation (3.2-13e). If the equilibrium constant for this kind of reaction is not found in any handbook, then we would have to reconstruct it from the formation reactions. In addition, taking equilibrium constants from many sources is undesirable, since there is no guarantee that the data would be consistent among the various sources. We shall use an alternate approach which does not have either of the above mentioned deficiencies and *which does not depend on the reactions chosen.* For this alternate method we shall see that we need to specify only the participating chemical species and not the reactions.

Smith and Van Ness[19] describe a method for obtaining the equilibrium composition of a mixture of gases where several reactions are actually proceeding. This method is really based on the fact that at equilibrium the Gibbs free energy for the system is a minimum. This condition, however, is subject to the constraints provided by the mass balances.

Since we have a minimization problem subject to constraints, the method of Lagrange multipliers is directly applicable.

Let us briefly outline the derivation of this equilibrium condition. Let $G(n_1, n_2, \ldots, n_n)$ represent the total Gibbs free energy for the system with the mole numbers of the various species i represented by the n_i. Let the m mass balance equations be

$$f_1(n_1, n_2, \ldots, n_n) = 0$$

$$f_2(n_1, n_2, \ldots, n_n) = 0$$

$$\vdots$$

$$f_m(n_1, n_2, \ldots, n_n) = 0$$

and since we have m constraints, then we introduce m Lagrange multipliers, $\lambda_1, \lambda_2, \ldots, \lambda_m$. If we want to minimize G, then we may minimize $G + \sum_{k=1}^{m} \lambda_k f_k$ since the f_k are zero and we have not changed the function to be minimized. Differentiating this new function with respect to each of the n_i in turn gives n equations which must hold at the minimum (or maximum). These equations are

$$\frac{\partial G}{\partial n_i} + \sum_{k=1}^{m} \lambda_k \frac{\partial f_k}{\partial n_i} = 0 \qquad (i = 1, 2, \ldots, n)$$

Then n "equilibrium" equations and the m contraint equations ($f_\ell = 0$ for $\ell = 1, 2, \ldots, m$) are used to solve for the n_i which minimize $G(n_1, n_2, \ldots, n_n)$. When this method is applied to our equilibrium

problem, the equilibrium condition becomes for gas phase reactions

$$\Delta G^{\circ}_{f_{gi}}(T_e) + RT_e \ell n(y_{gi}\hat{\phi}_{gi}P) + \sum_k \lambda_k a_{ik} = 0 \quad \text{for } i = 1, 2, \ldots, N \tag{3.2-15}$$

where the meaning of the nomenclature is as follows. We first note that the fugacity coefficients for a solution, ϕ_{gi}, have been introduced. Since we assume our gaseous mixture to behave like an ideal gas, all the $\hat{\phi}_{gi}$ are unity. The meaning of the subscript is unchanged from its previous definition in Table 3.2-3, except that we do not write an equilibrium equation for Ar(i=7), since argon is inert. The standard Gibbs free energy of formation at temperature T_e for species i is denoted by $\Delta G^{\circ}_{f_{gi}}(T_e)$. Like the equilibrium constant, K_p, this parameter is a function of temperature only. The Gibbs free energy of formation is assumed to be zero for the elemental compounds; for example, $\Delta G^{\circ}_f = 0$ for H_2, N_2, and so forth. R is the universal gas constant, and T_e is the absolute temperature at which the reactions are proceeding. Of course, the product RT_e must be in consistent units with the values for the Gibbs free energy. The argument of the natural logarithm is essentially the fugacity, $\hat{f}_{gi}$, of the species i, which, because of the ideal gas assumption, reduces to the product of the mole fraction and system pressure in atmospheres, or the partial pressure in atmospheres. The λ_k's are the Lagrange multipliers. One Lagrange multiplier should be introduced for each constraint provided by the mass balances. So one might expect to have six Lagrange multipliers for the adiabatic gasifier; that is λ_C, λ_H, λ_O, λ_N, λ_S, and λ_{Ar}.

However, as already mentioned, argon is inert and so λ_{Ar} is meaningless. We shall show later that taking λ_C to be zero is consistent with Equation (3.2-14). From the definition of the λ_k we see that the subscript k is associated with a particular elemental atom present in the system. The a_{ik} represent the number of atoms of element k per molecule of species i. Table 3.2-4 gives this matrix for the gasifier model.

Table 3.2-4
Assignment of Values to the a_{ik}
for the Gasifier Model

Species	i	Element (k)				
		C(1)	H(2)	O(3)	N(4)	S(5)
H_2	1	0	2	0	0	0
CO	2	1	0	1	0	0
CH_4	3	1	4	0	0	0
H_2O	4	0	2	1	0	0
CO_2	5	1	0	2	0	0
N_2	6	0	0	0	2	0
Ar	7	0	0	0	0	0
H_2S	8	0	2	0	0	1
COS	9	1	0	1	0	1
NH_3	10	0	3	0	1	0

Now Equation 3.2-15 can be readily applied to each of the reacting species assumed to be present in the gasifier. For generality, the fugacity coefficients, $\hat{\phi}_{gi}$, will be kept in the equations with the understanding that each will be taken to have a value of unity. Also, it is advantageous to divide the equilibrium equations by RT_e. The reason for doing this will be explained in Subsection 3.2.2. The equilibrium equations become

$$\Delta G^{\circ}_{f_{H_2}}(T_e)/RT_e + \ell n(y_{g_1}\hat{\phi}_{g_1}P_g) + 2\lambda_H/RT_e = 0 \qquad (3.2\text{-}16)$$

0

$$\Delta G^\circ_{f_{CO}}(T_e)/RT_e + \ell n(y_{g_2}\hat{\phi}_{g_2}P_g) + \lambda_O/RT_e = 0 \qquad (3.2\text{-}17)$$

$$\Delta G^\circ_{f_{CH_4}}(T_e)/RT_e + \ell n(y_{g_3}\hat{\phi}_{g_3}P_g) + 4\lambda_H/RT_e = 0 \qquad (3.2\text{-}18)$$

$$\Delta G^\circ_{f_{H_2O}}(T_e)/RT_e + \ell n(y_{g_4}\hat{\phi}_{g_4}P_g) + 2\lambda_H/RT_e + \lambda_O/RT_e = 0 \qquad (3.2\text{-}19)$$

$$\Delta G^\circ_{f_{CO_2}}(T_e)/RT_e + \ell n(y_{g_5}\hat{\phi}_{g_5}P_g) + 2\lambda_O/RT_e = 0 \qquad (3.2\text{-}20)$$

$$\Delta G^\circ_{f_{N_2}}(T_e)/RT_e + \ell n(y_{g_6}\hat{\phi}_{g_6}P_g) + 2\lambda_N/RT_e = 0 \qquad (3.2\text{-}21)$$

$$\Delta G^\circ_{f_{H_2S}}(T_e)/RT_e + \ell n(y_{g_8}\hat{\phi}_{g_8}P_g) + 2\lambda_H/RT_e + \lambda_S/RT_e = 0 \qquad (3.2\text{-}22)$$

$$\Delta G^\circ_{f_{COS}}(T_e)/RT_e + \ell n(y_{g_9}\hat{\phi}_{g_9}P_g) + \lambda_O/RT_e + \lambda_S/RT_e = 0 \qquad (3.2\text{-}23)$$

$$\Delta G^\circ_{f_{NH_3}}(T_e)/RT_e + \ell n(y_{g_{10}}\hat{\phi}_{g_{10}}P_g) + 3\lambda_H/RT_e + \lambda_N/RT_e = 0 \qquad (3.2\text{-}24)$$

The total number of equations for the adiabatic gasifier model is now fifteen, but we have introduced four more unknowns, namely λ_H, λ_O, λ_N, and λ_S, making the total number of unknowns sixteen. The energy equation provides us with the sixteenth equation.

Before we consider the energy equation, let us first show that our taking λ_C to be zero is consistent with the quilibrium condition expressed by Equation (3.2-14). Multiplying Equation (3.2-16) by 2 and subtracting the resulting equation from Equation (3.2-18) gives (taking $\hat{\phi}_{gi}$=1):

$$\Delta G^\circ_{f_{CH_4}}/RT_e + \ell n(y_{CH_4}P) - 2\Delta G^\circ_{f_{H_2}}/RT_e - 2\ell n(y_{H_2}P) = 0$$

Rewriting in a more suitable form gives

$$\Delta G^\circ_{f_{CH_4}} - 2\Delta G^\circ_{f_{H_2}} = -RT_e \ell n[(y_{CH_4}P)/(y_{H_2}P)^2]$$

But the change in Gibbs free energy for the reaction is given by

$$\Delta G = \Delta G^\circ_{f_{CH_4}} - 2\Delta G^\circ_{f_{H_2}}$$

and the definition of K_p is given by

$$\ell n K_p = -\Delta G/RT_e$$

and so we get

$$K_p = \frac{(y_{CH_4}P)}{(y_{H_2}P)^2}$$

which is precisely the expression for K_p given by Equation (3.2-14). If all the λ's were eliminated in Equations (3.2-16) to 3.2-24) and the definition of K_p were used, we would get the conventional equilibrium equations of the form of Equations (3.2-14). Clearly the two methods are completely equivalent.

As we have discussed earlier, the effective enthalpy of the coal is obtained by using the Dulong approximation to give the coal composition in terms of fixed carbon (C), hydrogen (H_2), water vapor (H_2O), nitrogen (N_2), and sulfur (S_2). The weight fraction of liquid water and ash in the coal remains unchanged. Let ω_{di} be the weight fraction of species i

in the coal after application of the Dulong approximation, where i takes on values 1 to 7 as shown in Table 3.2-5. Similarly, let ν_{di} be the molecular weight of species i, where i again is defined by Table 3.2-5.

Table 3.2-5
Meaning of the Subscripts Applied to Coal after Application of Dulong Approximation

Subscript (di)	Species
d1	C
d2	H_2
d3	$H_2O(g)$
d4	N_2
d5	S_2
d6	$H_2O(\ell)$
d7	Ash

The first law of thermodynamics may now be written for the gasifier:

$$h_{afc}(T_c,P_c) + c_{p_{ash}}\omega_{d7}(T_c - T_{ref}) + w_a\bar{h}_a(T_a,P_a)/\nu_a + Q_{gas} + w_s h_s = N_g\bar{h}_g(T_g,P_g) + c_{p_{ash}}\omega_{d7}(T_{ash}-T_{ref}) \qquad (3.2\text{-}25)$$

where the subscripts are defined as follows: 'afc' denotes ash-free coal, 'a' air, 'c' coal with ash, and 'g' gasifier outlet gas. The enthalpy of the ash-free coal (based on a unit mass of coal with ash) at temperature T_c and pressure P_c is denoted by $h_{afc}(T_c,P_c)$, and the heat added to the gasification process per unit mass of coal is Q_{gas}, while $\bar{h}_a(T_a,P_a)$ and $\bar{h}_g(T_g,P_g)$ are the enthalpy per mole (or molar enthalpy) of air and product gas, respectively, at the indicated temperatures (T) and pressures (P). Finally $c_{p_{ash}}$ is the specific heat of the ash (assumed to be constant), T_{ash} is the ash discharge

temperature, and T_{ref} is an arbitrary reference temperature which cancels out of the final form of the energy equation.

The enthalpy of the ash free coal, h_{afc}, per unit mass of coal is given by

$$h_{afc}(T_c,P_c) = \sum_{i=1}^{6} (\omega_{di}/\nu_{di})\bar{h}_{di}(T_c,\mu_{di}P_c)$$

where $\bar{h}_{di}$ is the molar enthalpy of species i at a specified temperature T_c and pressure P_c and μ_{di} is the mole fraction of species i based on the Dulong approximation. It is tacitly implied by the nomenclature $\bar{h}_g(T_g,P_g)$ and $\bar{h}_a(T_a,P_a)$ that the composition of the gas indicated by the subscript is an argument of the enthalpy function. For conciseness, we do not write this explicitly. The enthalpy of the air, h_a, per unit mass of air is given by

$$h_a(T_a,P_a) = \sum_{i=1}^{4} (\omega_{ai}/\nu_{ai})\bar{h}_{ai}(T_a,\mu_{ai}P_a)$$

where μ_{ai} is the mole fraction of species i for the air. On a basis of a unit mass of coal, the enthalpy of the air is $w_a h_a$, since there are w_a unit masses of air per unit mass of coal. Similarly, the enthalpy of the steam used in the gasification process is simply $w_s h_s(P_s,T_s)$ where h_s is specific enthalpy of steam and w_s is the mass of steam required per unit mass of coal. Clearly, the subscript 's' denotes that the fluid is steam or water. Finally, the enthalpy of the gaseous products per unit mass of coal is given by

$$N_g\bar{h}_g(T_g,P_g) = \sum_{i=1}^{10} n_{gi}\bar{h}_{gi}(T_g,\mu_{gi}P_g)$$

where μ_{gi} is the mole fraction of species i for the power gas. Again note that the enthalpy has an implied mole fraction dependency. It should be noted that when a summation occurs, one should use the appropriate table to get the correspondence between subscripts ci, ai, gi, and di and the corresponding species. Before substituting all these expressions into Equation 3.2-25, let us divide it first by N_g since again we prefer to work with mole fractions instead of mole numbers. The final form of the energy equation for the gasifier then becomes:

$$\left\{ \sum_{i=1}^{6} (\omega_{di}/\nu_{di})\bar{h}_{di}(T_c,\mu_{di}P_c) + c_{p_{ash}}\omega_{d7}(T_c - T_{ash}) + w_s h_s(T_s,P_s) + w_a \sum_{i=1}^{4} (\omega_{ai}/\nu_{ai})\bar{h}_{ai}(T_a,\mu_{ai}P_a) + Q_{gas} \right\} \left[(\omega_{c_1}/\nu_{c_1})(y_{g_2} + y_{g_3} + y_{g_5} + y_{g_9})\right] = \sum_{i=1}^{10} y_{gi}\bar{h}_{gi}(T_g,y_{gi}P_g) \qquad (3.2\text{-}26)$$

In this equation, the y_{gi} are unknown along with w_a and w_s. All other parameters are either specified in the input to this model or are calculated directly from the input.

We have thus identified sixteen equations which we may use to solve for the sixteen unknowns. We complete the model by noting that the mass flow of the product gas w_g per unit mass flow of coal is given by

$$w_g = 1 + w_a + w_s - \omega_{c_7}$$

and it is a trivial matter to get the corresponding mole flows. Finally, the higher and lower heating values of the power gas can be computed since

we know the gas composition, after we solve for the y_{gi}'s. We get conservatively low estimates for the heating values by assuming only H_2, CO, and CH_4 contribute to the heating values of the power gas.

In summarizing, we have identified sixteen unknown parameters: the ten mole fractions, the four Lagrange multipliers (which have no obvious physical significance), the steam flow, and the air flow. Fortunately sixteen equations in these same variables have also been identified: six mass balances, nine equilibrium equations, and the energy equation. The method of solution is presented in Section 3.2.2

Now we can readily see why the endothermic gasifier model is a special case of the one above. We have already agreed that for endothermic gasification, we want to gasify the coal with steam only; that is, the air flow, w_a, is zero. Setting w_a equal to zero in the six mass balance equations and nine equilibrium equations and solving the resulting system of fifteen equations gives values to the fifteen unknowns. The energy equation is then solved for the amount of heat, Q_{gas}, needed to allow gasification of coal without any air. Again the method of solution given in Section 3.2.2 easily accommodates this mode of gasifier operation.

Before leaving this model, a subtle point should be made with regard to the temperature T_e used in the nine equilibrium equations and the temperature T_g used in the energy equation. While these should be equal to be consistent with our assumption of thermodynamic equilibrium, the provision has been made to allow for them to be different. This was done to allow for the possibility of "freezing" the reactions at a certain temperature which is sometimes done or implied in the literature.

3.2.2 Combustor Model

Like the case in the gasifier model, we must have provisions for two different modes of operation. One mode allows the combustor outlet temperature to be specified and the other allows the excess air to be specified. These parameters will become apparent in the development of the combustor model. The method of solution for each of these modes is presented in Section 3.2.2. The basic reaction for the combustor is

Fuel + Air → Products.

We normalize the calculation by assuming a mole of gaseous fuel, not a unit mass of fuel as was the case in the gasifier model.

Let us assume that the composition of the gaseous fuel by mole fraction μ_{fi} is specified along with its pressure P_f and temperature T_f. Again Table 3.2-3 must be used to correlate the subscript i with a particular chemical species. Let us further assume that the air composition by weight fraction ω_{ai} is specified, where Table 3.2-2 provides the meaning of the subscript ai. This composition by weight fraction can easily be converted to one by mole fraction μ_{ai} where again Table 3.2-2 is applicable. Let us also assume the pressure P_a and temperature T_a of the air entering the combustor are specified. Denoting the number of moles of stoichiometric air per mole of fuel as β and the excess air fraction as ξ, the number of moles of air per mole of fuel becomes $\beta(1+\xi)$. Finally, let n_{pi} be the number of moles of species i in the product gas per mole of fuel, where species i is identified in Table 3.2-6. From this table, we see that the following species are assumed to be present in the product gas: carbon dioxide (CO_2), water vapor (H_2O), nitrogen (N_2), oxygen (O_2), argon (Ar),

nitric oxide (NO), carbon monoxide (CO), monatomic hydrogen (H), monatomic oxygen (O), hydroxyl (OH), hydrogen (H_2), nitrogen dioxide (NO_2), sulfur monoxide (SO), sulfur dioxide (SO_2), and sulfur trioxide (SO_3).

Table 3.2-6
Meaning of Subscripts Applied to Products of Combustion

Subscript (pi)	Species in Gas
p1	CO_2
p2	$H_2O(g)$
p3	N_2
p4	O_2
p5	Ar
p6	NO
p7	CO
p8	H
p9	O
p10	OH
p11	H_2
p12	NO_2
p13	SO
p14	SO_2
p15	SO_3

Let the pressure of the product gas be P_p, which is presumably specified, and the temperature be T_p, which may be either an unknown or is assumed to be specified. We will eventually get an expression for β which will depend on known parameters, and ξ is either an unknown (T_p must be specified) or is specified (T_p is then one of the unknowns).

Because it is shown in Section 5.5, that a nitric oxide (NO) emission problem exists for the waste heat combined cycle configurations, flue gas recirculation is used as a means to reduce the amount of NO which goes up the stack and into the atmosphere. In other words, a

certain fraction, ρ, of the flue gas at near atmospheric pressure is compressed, cooled to a specific temperature, T_r, and fed into the combustor at pressure P_r. The combustor model then must include a provision for flue gas recirculation. With this modification, the basic reaction in the combustor becomes

$$\text{Fuel} + \rho(\text{Products}) + \text{Air} \rightarrow \text{Products}$$

and we are now in a position to develop the mass balance equations.

First, we do a mass balance on carbon (C). By referring to Table 3.2-2 for the species in the air, Table 3.2-3 for the species in the fuel, and Table 3.2-6 for the species in the product gas, the first mass balance on carbon becomes

$$\mu_{f_2} + \mu_{f_3} + \mu_{f_5} + \mu_{f_9} + \rho n_{p_1} + \rho n_{p_7} = n_{p_1} + n_{p_7}$$

or

$$\mu_{f_2} + \mu_{f_3} + \mu_{f_5} + \mu_{f_9} = (1-\rho)(n_{p_1} + n_{p_7}) \tag{3.2-27}$$

Similarly, a mass balance on H, O, N, S, and Ar gives the following five relationships

$$\begin{aligned} &2\mu_{f_1} + 4\mu_{f_3} + 2\mu_{f_4} + 2\mu_{f_8} + 3\mu_{f_{10}} + 2\beta(1+\xi)\mu_{a_4} \\ &\quad = (1-\rho)(2n_{p_2} + n_{p_8} + n_{p_{10}} + 2n_{p_{11}}), \end{aligned} \tag{3.2.28}$$

$$\begin{aligned} &\mu_{f_2} + \mu_{f_4} + 2\mu_{f_5} + \mu_{f_9} + (2\mu_{a_2} + \mu_{a_4})(1+\xi)\beta = \\ &\quad = (1-\rho)(2n_{p_1} + n_{p_2} + 2n_{p_4} + n_{p_6} + n_{p_7} + n_{p_9} \\ &\qquad + n_{p_{10}} + 2n_{p_{12}} + n_{p_{13}} + 2n_{p_{14}} + 3n_{p_{15}}), \end{aligned} \tag{3.2-29}$$

$$2\mu_{f_6} + \mu_{f_{10}} + 2\beta(1+\xi)\mu_{a_1} = (1-\rho)(2n_{p_3} + n_{p_6} + n_{p_{12}}), \tag{3.2-30}$$

$$\mu_{f_8} + \mu_{f_9} = (1-\rho)(n_{p_{13}} + n_{p_{14}} + n_{p_{15}}), \tag{3.2-31}$$

and

$$\mu_{f_7} + \beta(1+\xi)\mu_{a_3} = (1-\rho)(n_{p_5}), \tag{3.2-32}$$

respectively.

Again we prefer to work with mole fractions, y_{pi}, instead of mole numbers, n_{pi}. Dividing Equation (3.2-27) by N_c, where

$$N_c = \sum_{i=1}^{15} n_{pi},$$

and solving the resulting equation for N_c gives

$$N_c = \frac{\mu_{f_2} + \mu_{f_3} + \mu_{f_5} + \mu_{f_9}}{(1-\rho)(y_{p_1} + y_{p_7})} \tag{3.2-33}$$

where $y_{pi} = n_{pi}/N_c$ has been used. Now dividing each of the remaining mass balance equations (3.2-28 to 3.2-32) by N_c and using $y_{pi} = n_{pi}/N_c$ gives the following relations where the factor $(1-\rho)$ has been divided from both sides and, therefore, no longer appears in the mass balances

$$\left[2\mu_{f_1} + 4\mu_{f_3} + 2\mu_{f_4} + 2\mu_{f_8} + 3\mu_{f_{10}} + 2\beta(1+\xi)\mu_{a_4}\right]\left\{\frac{y_{p_1} + y_{p_7}}{\mu_{f_2} + \mu_{f_3} + \mu_{f_5} + \mu_{f_9}}\right\}$$
$$= 2y_{p_2} + y_{p_8} + y_{p_{10}} + 2y_{p_{11}} \tag{3.2-34}$$

$$\left[\mu_{f_2} + \mu_{f_4} + 2\mu_{f_5} + \mu_{f_9} + (2\mu_{a_2} + \mu_{a_4})(1+\xi)\beta\right]\left\{\frac{y_{p_1} + y_{p_7}}{\mu_{f_2} + \mu_{f_3} + \mu_{f_5} + \mu_{f_9}}\right\}$$
$$= 2y_{p_1} + y_{p_2} + 2y_{p_4} + y_{p_6} + y_{p_7} + y_{p_9}$$
$$+ y_{p_{10}} + 2y_{p_{12}} + y_{p_{13}} + 2y_{p_{14}} + 3y_{p_{15}} \tag{3.2-35}$$

$$\left[2\mu_{f_6} + \mu_{f_{10}} + 2\beta(1+\xi)\mu_{a_1}\right]\left\{\frac{y_{p_1} + y_{p_7}}{\mu_{f_2} + \mu_{f_3} + \mu_{f_5} + \mu_{f_9}}\right\} = 2y_{p_3} + y_{p_6} + y_{p_{12}} \quad (3.2\text{-}36)$$

$$\left[\mu_{f_8} + \mu_{f_9}\right]\left\{\frac{y_{p_1} + y_{p_7}}{\mu_{f_2} + \mu_{f_3} + \mu_{f_5} + \mu_{f_9}}\right\} = y_{p_{13}} + y_{p_{14}} + y_{p_{15}} \quad (3.2\text{-}37)$$

$$\left[\mu_{f_7} + \beta\,(1+\xi)\mu_{a_3}\right]\left\{\frac{y_{p_1} + y_{p_7}}{\mu_{f_2} + \mu_{f_3} + \mu_{f_5} + \mu_{f_9}}\right\} = y_{p_5} \quad (3.2\text{-}38)$$

Like the gasifier model, the sixth equation is provided by the fact that the sum of the mole fractions must be unity:

$$\sum_{i=1}^{15} y_{pi} = 1 \quad (3.2\text{-}39)$$

It is important to remember that it is the y_{pi} and possibly ξ that are the unknowns in the last six equations. An expression for β, the number of moles of stoichiometric air per mole of fuel, may now be developed.

The following species, present in the gaseous fuel, are capable of combustion with the oxygen in the air: hydrogen (H_2), carbon monoxide (CO), methane (CH_4), hydrogen sulfide (H_2S), carbonyl sulfide (COS), and ammonia (NH_3). The number of moles of oxygen (O_2) required for complete combustion of each of the above constituents is easily determined from the following balanced chemical equations:

$$H_2 + 1/2\ O_2 \rightarrow H_2O$$

$$CO + 1/2\ O_2 \rightarrow CO_2$$

$$CH_4 + 2\ O_2 \rightarrow CO_2 + 2H_2O$$

$$H_2S + 3/2\ O_2 \rightarrow H_2O + SO_2$$

$$COS + 3/2\ O_2 \rightarrow CO_2 + SO_2$$

$$NH_3 + 3/4\ O_2 \rightarrow 3/2\ H_2O + 1/2\ N_2$$

From the first reaction, we see that 1/2 mole of O_2 is required for each mole of H_2, but there are μ_{f_1} moles of H_2 per mole of fuel, so there are $1/2\ \mu_{f_1}$ moles of O_2 required per mole of fuel due to the H_2 only. A similar line of reasoning results in the following O_2 requirements in moles of O_2 per mole of fuel: $1/2\mu_{f_2}$ due to the CO, $2\mu_{f_3}$ due to the CH_4, $3/2\mu_{f_8}$ due to the H_2S, $3/2\mu_{f_9}$ due to the COS, and $3/4\mu_{f_{10}}$ due to the NH_3. The total oxygen requirement is clearly the sum of these. But there are μ_{a_2} moles of O_2 per mole of air, so

$$\beta = \frac{1/2\mu_{f_1} + 1/2\mu_{f_2} + 2\mu_{f_3} + 3/2\mu_{f_8} + 3/2\mu_{f_9} + 3/4\mu_{f_{10}}}{\mu_{a_2}} \qquad (3.2\text{-}40)$$

which is the theoretical air requirement in moles of air per mole of fuel. Clearly, the number of moles of air per mole of fuel actually used depends on the excess air fraction ξ and is equal to $\beta(1+\xi)$. This fact has been used in the derivation of the mass balance equations. Note that in Equation (3.2-40) since all the parameters on the right-hand side are known, β can be readily calculated.

Before writing the equilibrium equations, nine independent reactions among the gaseous species may be identified. One should clearly understand, however, that identification of these reactions is *not* necessary to the Lagrange multiplier approach. One possible set of reactions is as follows:

$$CO + 1/2\ O_2 \rightleftarrows CO_2$$

$$H_2 + 1/2\ O_2 \rightleftarrows H_2O$$

$$N_2 + O_2 \rightleftarrows 2\,NO$$

$$H_2 \rightleftarrows 2\,H$$

$$O_2 \rightleftarrows 2\,O$$

$$H_2O + 1/2\,O_2 \rightleftarrows 2\,OH$$

$$N_2 + 2\,O_2 \rightleftarrows 2\,NO_2$$

$$SO + 1/2\,O_2 \rightleftarrows SO_2$$

$$SO + O_2 \rightleftarrows SO_3$$

Now the equilibrium equations may be written using Equation (3.2-15) applied to the combustor product gas (after changing T_e to T_p and dividing by RT_p). The a_{ik} matrix is given in Table 3.2-7. The subscript i on the

Table 3.2-7
Assignment of Values to the a_{ik}
for the Combustor Model

Species	i	Element (k)				
		C(1)	H(2)	O(3)	N(4)	S(5)
CO_2	1	1	0	2	0	0
H_2O	2	0	2	1	0	0
N_2	3	0	0	0	2	0
O_2	4	0	0	2	0	0
Ar	5	0	0	0	0	0
NO	6	0	0	1	1	0
CO	7	1	0	1	0	0
H	8	0	1	0	0	0
O	9	0	0	1	0	0
OH	10	0	1	1	0	0
H_2	11	0	2	0	0	0
NO_2	12	0	0	2	1	0
SO	13	0	0	1	0	1
SO_2	14	0	0	2	0	1
SO_3	15	0	0	3	0	1

y_{pi} now correspond, of course, to those in Tables 3.2-6 or 3.2-7. The following equilibrium equations are to be satisfied:

$$\Delta G^\circ_{f_{CO_2}}(T_p)/RT_p + \ell n(y_{p_1}\hat{\phi}_{p_1}P_p) + \lambda_C/RT_p + 2\lambda_O/RT_p = 0 \qquad (3.2\text{-}41)$$

$$\Delta G^\circ_{f_{H_2O}}(T_p)/RT_p + \ell n(y_{p_2}\hat{\phi}_{p_2}P_p) + 2\lambda_H/RT_p + \lambda_O/RT_p = 0 \qquad (3.2\text{-}42)$$

$$\Delta G^\circ_{f_{N_2}}(T_p)/RT_p + \ell n(y_{p_3}\hat{\phi}_{p_3}P_p) + 2\lambda_N/RT_p = 0 \qquad (3.2\text{-}43)$$

$$\Delta G^\circ_{f_{O_2}}(T_p)/RT_p + \ell n(y_{p_4}\hat{\phi}_{p_4}P_p) + 2\lambda_O/RT_p = 0 \qquad (3.2\text{-}44)$$

$$\Delta G^\circ_{f_{NO}}(T_p)/RT_p + \ell n(y_{p_6}\hat{\phi}_{p_6}P_p) + \lambda_O/RT_p + \lambda_N/RT_p = 0 \qquad (3.2\text{-}45)$$

$$\Delta G^\circ_{f_{CO}}(T_p)/RT_p + \ell n(y_{p_7}\hat{\phi}_{p_7}P_p) + \lambda_C/RT_p + \lambda_O/RT_p = 0 \qquad (3.2\text{-}46)$$

$$\Delta G^\circ_{f_{H}}(T_p)/RT_p + \ell n(y_{p_8}\hat{\phi}_{p_8}P_p) + \lambda_H/RT_p = 0 \qquad (3.2\text{-}47)$$

$$\Delta G^\circ_{f_{O}}(T_p)/RT_p + \ell n(y_{p_9}\hat{\phi}_{p_9}P_p) + \lambda_O/RT_p = 0 \qquad (3.2\text{-}48)$$

$$\Delta G^\circ_{f_{OH}}(T_p)/RT_p + \ell n(y_{p_{10}}\hat{\phi}_{p_{10}}P_p) + \lambda_H/RT_p + \lambda_O/RT_p = 0 \qquad (3.2\text{-}49)$$

$$\Delta G^\circ_{f_{H_2}}(T_p)/RT_p + \ell n(y_{p_{11}}\hat{\phi}_{p_{11}}P_p) + 2\lambda_H/RT_p = 0 \qquad (3.2\text{-}50)$$

$$\Delta G^\circ_{f_{NO_2}}(T_p)/RT_p + \ell n(y_{p_{12}}\hat{\phi}_{p_{12}}P_p) + 2\lambda_O/RT_p + \lambda_N/RT_p = 0 \qquad (3.2\text{-}51)$$

$$\Delta G^\circ_{f_{SO}}(T_p)/RT_p + \ell n(y_{p_{13}}\hat{\phi}_{p_{13}}P_p) + \lambda_O/RT_p + \lambda_S/RT_p = 0 \qquad (3.2\text{-}52)$$

$$\Delta G^\circ_{f_{SO_2}}(T_p)/RT_p + \ell n(y_{p_{14}}\hat{\phi}_{p_{14}}P_p) + 2\lambda_O/RT_p + \lambda_S/RT_p = 0 \qquad (3.2\text{-}53)$$

$$\Delta G^{\circ}_{f_{SO_3}}(T_p)/RT_p + \ell n(y_{p_{15}}\hat{\phi}_{p_{15}}P_p) + 3\lambda_O/RT_p + \lambda_S/RT_p = 0 \qquad (3.2\text{-}54)$$

Note that for the combustor model, λ_C is not necessarily zero and that, as was the case with the gasifier model, no equilibrium equation is written for argon, since it is inert.

The total number of equations for the combustor model is now twenty: six mass balances and fourteen equilibrium equations. But there are now twenty-one unknowns: the fifteen mole fractions, the five Lagrange multipliers, and either the excess air fraction ξ or the combustor outlet temperature T_p. Again, the energy equation provides the final necessary relationship to completely define the model.

The first law of thermodynamics for the combustor may be written as

$$\bar{h}_f(T_f,P_f) + \beta(1+\xi)\bar{h}_a(T_a,P_a) + \rho N_c\bar{h}_p(T_r,P_r) + Q_{cmb} = N_c\bar{h}_p(T_p,P_p) \qquad (3.2\text{-}55)$$

where the subscript "f" corresponds to the fuel, "a" to the air, "r" to the flue gas recirculation inlet flow, and "p" to the products of combustion. The variable $\bar{h}(T,P)$ has the same meaning as in Section 3.2.1.1, and Q_{cmb} is heat added to the combustion process per mole of fuel (if heat is removed, Q_{cmb} is negative). All other variables have previously been defined. Again it is tacitly implied by the nomenclature, $\bar{h}(T,P)$, that the composition of the gas is also part of the argument since the partial pressure is really the pressure for which $\bar{h}$ is to be evaluated and the partial pressure of species i in a gaseous mixture is given by $\mu_i P$.

Since the composition of the fuel is specified by the mole fractions, μ_{fi}, the enthalpy of the fuel per mole of fuel is simply

$$\bar{h}_f(T_f,P_f) = \sum_{i=1}^{10} \mu_{fi}\bar{h}_{fi}(T_f,\mu_{fi}P_f) \tag{3.2-56}$$

where i denotes the particular species shown in Table 3.2-3 with fi replacing gi. The enthalpy of the incoming air is similarly written

$$\beta(1+\xi)\bar{h}_a(T_a,P_a) = \beta(1+\xi) \sum_{i=1}^{4} \mu_{ai}\bar{h}_{ai}(T_a,\mu_{ai}P_a). \tag{3.2-57}$$

For the product gas at T_r and P_r,

$$\bar{h}_p(T_r,P_r) = \sum_{i=1}^{15} y_{pi}\bar{h}_{pi}(T_r,y_{pi}P_r) \tag{3.2-58}$$

and at T_p and P_p,

$$\bar{h}_p(T_p,P_p) = \sum_{i=1}^{15} y_{pi}\bar{h}_{pi}(T_p,y_{pi},P_p). \tag{3.2-59}$$

It is to be understood that the partial pressure arguments above are to be deleted for those species which are assumed to be ideal gases (all but H_2O, CH_4, and CO_2). Using the expression for N_c from Equation (3.2-33), and Equations (3.2-56) to (3.2-59), Equation (3.2-55) becomes

$$\left\{\frac{(1-\rho)(y_{p_1} + y_{p_7})}{(\mu_{f_2} + \mu_{f_3} + \mu_{f_5} + \mu_{f_9})}\right\}\left\{\sum_{i=1}^{10} \mu_{fi}\bar{h}_{fi}(T_f,\mu_{fi}P_f) + \beta(1+\xi)\sum_{i=1}^{4} \mu_{ai}\bar{h}_{ai}(T_a,\mu_{ai}P_a) + Q_{cmb}\right\} = \sum_{i=1}^{15} y_{pi}\bar{h}_{pi}(T_p,y_{pi}P_p) - \rho\sum_{i=1}^{15} y_{pi}\bar{h}_{pi}(T_r,y_{pi}P_r) \tag{3.2-60}$$

This is the final form of the energy equation for the combustor. In this model, unlike the gasifier model, the temperature used in the equilibrium equations is the same as that of the product gas leaving the combustor. "Freezing" of the NO producing reaction is handled in a simpler way and is explained in Section 4.6. Equation (3.2-60) provides the twenty-first equation thus enabling a unique solution for the twenty-one unknowns.

Three important points should be made with respect to the flue gas recirculation. The first is that the flue gas recirculation parameter ρ appears only in the energy equation, since we elected to work in terms of mole fractions instead of mole numbers. Secondly, when no recirculation is assumed, Equation (3.2-60) reduces to the correct form of the first law of thermodynamics for a combustor without recirculation; that is, the enthalpy of the fuel, plus that of the air, plus the heat added must equal the enthalpy of the product gas. Finally, if the temperature of the recirculation gas T_r equals the combustor exit temperature T_p (and $P_r=P_p$), then a factor of $(1-\rho)$ may be divided from both sides of Equation (3.2-60) and the benefit associated with flue gas recirculation in reducing NO effluents is lost. We shall see in Chapter 5 how this affects the power plant efficiency.

We have identified twenty-one equations which we may use to solve for the twenty-one unknowns. We complete the model by noting that the mass flow of air w_a into the combustor (per unit mass of coal into the gasifier) is given by

$$w_a = \beta(1+\xi)\nu_a w_f/\nu_f$$

where ν_a and ν_f are the molecular weights of the air and fuel respectively and w_f is mass flow of fuel (per unit mass of coal). A mass balance on the entire combustor gives

$$w_f + w_a + \rho w_p = w_p$$

where w_p is the mass flow of product gas from the combustor (per unit mass of coal). The last equation may be solved for w_p as

$$w_p = \frac{w_f + w_a}{1-\rho} .$$

This completes the combustor model. In the next section, we shall see how a solution to these systems of non-linear equations for the gasifier and combustor model can be obtained.

3.2.2 Method of Solution

As we have seen, a system of non-linear algebraic equations results when the steady-state thermodynamic models for the gasifier and combustor are developed. One method of solution is brute force. Osterle, Impink, and Lipner[17] have succeeded in reducing the gasifier equations to two equations in two unknowns (with no COS or NH_3 assumed to be present in the power gas). The resulting equations, although complicated, are solved using a search routine. The chief disadvantage of this approach arises when one wants to add more species to the model or otherwise change the model, since the algebraic exercise must be repeated. An approach which can easily accommodate changes in the model was sought.

A multi-dimensional Newton-Raphson iterative method of solution provides such a solution. The system of equations can be "stored" in a computer subroutine practically in the form in which we wrote them. Changing the model means changing the affected equations and not redoing the algebra. Also, as we shall see, it is a trivial matter to accommodate the two gasifier modes and the two combustor modes. The general method will be developed with its application to the two mathematical models then indicated.

Consider a system of n general non-linear algebraic equations of the form

$$f_1(x_1, x_2, \ldots, x_n) = 0$$
$$f_2(x_1, x_2, \ldots, x_n) = 0$$

$$f_n(x_1, x_2, \ldots, x_n) = 0$$

where the x_j are the unknowns and the usual functional notation is employed. This may be represented more concisely as

$$\vec{f}(\vec{x}) = \vec{0} \qquad (3.2\text{-}61)$$

where vector notation is now indicated by the overscript ($\rightarrow$). A more general form of Taylor's Theorem may be applied to the left-hand side of Equation (3.2-61) to give

$$\vec{f}(\vec{x} + \Delta\vec{x}) = \vec{f}(\vec{x}) + [\nabla\vec{f}(\vec{x})]\Delta\vec{x} \qquad (3.2\text{-}62)$$

where the gradient of the vector $\vec{f}(\vec{x})$ is indicated by $\nabla\vec{f}(\vec{x})$ and $\Delta\vec{x}$ is an incremental change in the vector $\vec{x}$. Now let us associate the k-th set

of values for the vector $\vec{x}$ by $\vec{x}_k$; that is, the k-th iteration. For this particular interation, $\Delta\vec{x}_k = \vec{x}_{k+1} - \vec{x}_k$ and Equation (3.2-62) becomes

$$\vec{f}(\vec{x}_{k+1}) = \vec{f}(\vec{x}_k) + [\nabla\vec{f}(\vec{x}_k)](\vec{x}_{k+1} - \vec{x}_k). \tag{3.2-63}$$

But we would like the k+1-th set of values for $\vec{x}$ to be close to the solution if convergence is to take place or $\vec{f}(\vec{x}_{k+1}) \approx \vec{0}$. Indeed let us force $\vec{f}(\vec{x}_{k+1})$ to be zero and see if the resulting condition is capable of converging to the solution. So, solving Equation (3.2-63) for $\vec{x}_{k+1}$ after setting $\vec{f}(\vec{x}_{k+1})$ equal to zero gives

$$\vec{x}_{k+1} = \vec{x}_k - [\nabla\vec{f}(\vec{x}_k)]^{-1}\vec{f}(\vec{x}_k) \tag{3.2-64}$$

where the inverse of the gradient matrix is indicated. Note that if $\vec{f}(\vec{x}_k) = \vec{0}$ (that is, the $\vec{x}_k$ are a solution), then $\vec{x}_{k+1} = \vec{x}_k$ as it should. We see that the correction vector $\Delta\vec{x}_k$ to the previous iteration ($\vec{x}_k$) is

$$\Delta\vec{x}_k = -[\nabla\vec{f}(\vec{x}_k)]^{-1}\vec{f}(\vec{x}_k). \tag{3.2-65}$$

The meaning of $\nabla\vec{f}(\vec{x}_k)$ is evident from the following matrix representation

$$\nabla\vec{f}(\vec{x}_k) = \begin{bmatrix} \frac{\partial f_1}{\partial x_1} & \frac{\partial f_1}{\partial x_2} & \cdots & \frac{\partial f_1}{\partial x_n} \\ \frac{\partial f_2}{\partial x_1} & & & \frac{\partial f_2}{\partial x_n} \\ \vdots & & & \\ \frac{\partial f_n}{\partial x_1} & \frac{\partial f_n}{\partial x_2} & & \frac{\partial f_n}{\partial x_n} \end{bmatrix}$$

where each entry is to be evaluated for values of $\vec{x}$ at the k-th iteration. However, since the computer will be used to get a solution, this gradient

matrix may be approximated to a high degree of accuracy by using a central difference approximation to each partial derivative indicated. This eliminates the need to provide the computer with these partial derivatives. In fact, it is impossible to generate explicit formulas for some of the derivatives anyway; for example, the mole fraction of water vapor appears as an argument in the enthalpy function.

One more point should be made regarding Equations (3.2-64) and (3.2-65) before we apply this method to our two mathematical models. During the implementation of this scheme, it often happened that the next value for a particular unknown would become negative. This is disastrous if the unknown happens to be a mole fraction, since we must take the natural logarithm in the equilibrium equation for that species. This problem must be avoided if we are to use this method. The following slight modification happens to solve the problem. Let us concentrate on only one of the unknowns x (x could be x_1, x_2, or x_n and may represent a mole fraction). Let the correction to x be given by δ [provided by Equation (3.2-65)], and let x^1 be the value of x at the next iteration. Then

$$x^1 = x + \delta$$

and dividing by x gives

$$\frac{x^1}{x} = 1 + \frac{\delta}{x}$$

Now assuming that $|\delta/x| << 1$, and using the fact that $\ell n(1 + \delta/x) \approx \delta/x$, we can take the natural logarithm of both sides of the last equation to give

$$\ell n(x^1/x) \approx \delta/x$$

or

$$x^1 = xe^{\delta/x} \qquad (3.2\text{-}66)$$

Note if we are at the solution (δ=0), then x^1=x as it should. Whenever a particular variable (unknown) must remain positive, Equation (3.2-66) is used in the iteration to get the next value for the unknown. Otherwise, Equation (3.2-64) is used directly.

Now we apply this solution method to the mathematical models of the gasifier and combustor. The adiabatic gasifier will be discussed first. The first ten unknowns are taken to be the mole fractions of the ten species indicated in Table 3.2-3, where the reason for numbering the species is now apparent. The next four unknowns are λ_H/RT_e, λ_O/RT_e, λ_N/RT_e, and λ_S/RT_e respectively. The fifteenth unknown is the steam flow and the sixteenth one is the air flow. By including RT_e in the terms containing the Lagrange multipliers, we get a much better conditioned gradient matrix which ensures a well-behaved matrix inversion. This scaling was crucial to the success of this method of solution. Without this simple modification, the iteration would not converge properly. A typical case takes seven iterations to get five significant figures on each mole fraction.

As mentioned during the development of the gasifier model, the endothermic gasifier is a special case of the adiabatic gasifier. By setting the sixteenth unknown, w_a, equal to zero (zero air flow) and solving the first fifteen equations, a unique solution is obtained.

Then the energy equation is used to calculate the amount of heat, Q_{gas}, which is required. Note that f_1 to f_6 are the mass balance equations, f_7 to f_{15} are the equilibrium equations, and f_{16} is the energy equation. Thus, the two gasifier modes are easily accommodated.

A very similar approach is taken to obtain a solution to the combustor equations. Now the first fifteen unknowns are taken to be the mole fractions of the fifteen species indicated in Table 3.2-6. The next five unknowns are λ_C/RT_p, λ_H/RT_p, λ_O/RT_p, λ_N/RT_p, and λ_S/RT_p. The twenty-first and final unknown is either the excess air fraction ξ (with T_p specified) or the product gas exit temperature T_p (with ξ specified). When the endothermic gasifier mode is needed in a cycle, the heat which must be supplied to the gasifier comes from the combustor so $Q_{cmb} = -Q_{gas}/N_{cl}$ where N_{cl} represents the number of moles of clean power gas produced per pound of coal (after the desulfurization process). Note now that f_1 to f_6 are the mass balance equations, f_7 to f_{20} are the equilibrium equations, and f_{21} is the energy equation. Convergence to five significant figures on the mole fractions usually occurs within eight iterations.

3.3 Waste Heat Boiler

The waste heat boiler is composed of three sections: an economizer (EC), an evaporator (EV), and a superheater (SH). The economizer section acts essentially as an additional stage of feedwater heating where the relatively hot combustion gases provide the necessary heat instead of steam extraction from the steam turbine. Without the

economizer, more energy would be lost through the stack as sensible heat. The evaporator section is self-descriptive. The slightly subcooled water which enters the boiler is evaporated to dry saturated steam by the heat provided by the hot combustion gases. Finally, the superheater section superheats the steam. A schematic representation of the waste heat boiler is shown in Figure 3.3-1.

It is instructive to construct a T-Q or temperature-heat flow diagram. This is shown in Figure 3.3-2 not necessarily to any scale. The upper unbroken line represents the flow of the hot product gases from the entrance to gas-side of the boiler, through the superheater, evaporator, and economizer sections respectively, and finally to the stack. The lower broken line represents the flow on the water side of the boiler. Feedwater enters the water-side of the economizer section in a counterflow arrangement, boils in the evaporator section, and finally is superheated in the superheater section again in a counterflow arrangement.

The temperature nomenclature at key points in the boiler for both the steam- and gas-sides is indicated on Figure 3.3-2. The same subscripts will be used for the other properties (enthalpy and pressure) for these points. The pressure is denoted by the symbol P, while the molar enthalpy is represented by $\bar{h}$ and specific enthalpy by h. Furthermore, let m_G represent the number of moles of product gas and w_S the mass flow of steam generated in the waste heat boiler. Let us further define the pinch point temperature difference ΔT_{pp} to be the minimum temperature difference between the gas-side and water-side of the

boiler. We do not know a priori if this is $T_{G1} - T_{S4}$, $T_{G3} - T_{S3g}$, or $T_{G4} - T_{S1}$. The determination of where the actual pinch point occurs makes this model somewhat interesting.

Before explaining how the pinch point is found, it is appropriate now to mention the variables which we assume to have known values. As in all the models, the pressures at each point are specified: P_{G1}, P_{G2}, P_{G3}, P_{G4}, P_{S1}, P_{S2}, P_{S3f}, and P_{S4}. Both the number of moles of gas, m_G, and the composition of this gas are presumably known (from prior component calculations). While the composition dependency on enthalpy for the gas is not explicity written, it is implied; for example, h_{G3} is written with the understanding that the pressure P_{G3}, the temperature T_{G3}, amd the mole fractions are all implied arguments. The temperatures T_{G1} and T_{S4} are assumed to be known. However, we shall see very shortly that it may become necessary to lower T_{S4}. Finally, the pinch point temperature difference ΔT_{pp} and the degrees of subcooling of the inlet fluid to the evaporator section ΔT_{sc} are also presumably specified. All other temperatures, enthalpies, mass flows, and heat flows are calculated. One more restriction, however, must be imposed: the stack gas temperature T_{G4} must be above the dew point temperature. This ensures that the water vapor in the gas does not condense, thus avoiding possible corrosion problems in a real plant.

Now the solution strategy can be discussed. First, the possible pinch point between T_{G1} and T_{S4} must be checked to ensure that the difference $T_{G1} - T_{S4}$ is greater than or equal to ΔT_{pp}. If it is not, the input value of T_{S4} is modified according to

$$T_{S4} = T_{G1} - \Delta T_{pp}. \qquad (3.3\text{-}1)$$

Otherwise, T_{S4} is unchanged. In any event, the next step is to assume a location for the actual pinch point. From Figure 3.3-2, this can be either between T_{G3} and T_{S3g} or between T_{G4} and T_{S1}. The latter is assumed first and all calculations proceed on this basis. This assumption is checked by calculating $T_{G3} - T_{S3g}$ and verifying that this difference is larger than ΔT_{pp}. If it is not, then the pinch point is assumed to be between T_{G3} and T_{S3g} with the calculations proceeding on this basis. (A redundant check is provided by checking to see if $T_{G4} - T_{S1}$ is greater than ΔT_{pp}; at this point, it must be or there is no solution.) After the pinch point has been located, the remaining unknown parameters can be calculated.

No matter where the pinch point occurs, T_{S3f} is immediately known since P_{S3f} is specified and the water is in the saturation state. Also, $T_{S3g} = T_{S3f}$, since we further assume no pressure drop in the saturation portion of the evaporator section; that is, $P_{S3g} = P_{S3f}$. Then T_{S2} is also easily calculated from

$$T_{S2} = T_{S3f} - \Delta T_{sc} \qquad (3.3\text{-}2)$$

As mentioned above, T_{S4} either is a specified input or is modified according to Equation (3.3-1).

3.3.1 Pinch Point between T_{G4} and T_{S1}

By assumption

$$T_{G4} = T_{S1} + \Delta T_{pp}$$

and since P_{G1}, T_{G1} and P_{G4}, T_{G4} (and the gas composition) all have known values, $\bar{h}_{G1}$ and $\bar{h}_{G4}$, respectively, are obtained via the property relations. Similarly, h_{S1} and h_{S4} are also easily determined from the steam tables since P_{S1}, T_{S1} and P_{S4}, T_{S4}, respectively, are known. An energy balance on the entire waste heat boiler gives

$$w_S(h_{S4} - h_{S1}) = m_G(\bar{h}_{G1} - \bar{h}_{G4})$$

which may be solved for the steam flow,

$$w_S = m_G\left(\frac{\bar{h}_{G1} - \bar{h}_{G4}}{h_{S4} - h_{S1}}\right) \qquad (3.3\text{-}3)$$

Because T_{S2}, P_{S2} are known, h_{S2} is known and an energy balance on the superheater and evaporator sections taken together gives

$$w_S(h_{S4} - h_{S2}) = m_G(\bar{h}_{G1} - \bar{h}_{G3})$$

which may be solved for $\bar{h}_{G3}$ as

$$\bar{h}_{G3} = \bar{h}_{G1} - \frac{w_S}{m_G}(h_{S4} - h_{S2}) \qquad (3.3\text{-}4)$$

Now since P_{G3} and $\bar{h}_{G3}$ (and the gas composition) are known, T_{G3} is found from the property relations. If $T_{G3} - T_{S3g}$ is greater than or equal

to ΔT_{pp}, then the correct pinch point has been assumed. Otherwise, the pinch point must be between T_{G3} and T_{S3g}.

3.3.2 Pinch Point between T_{G3} and T_{S3g}

By assumption, P_{G3} is known and

$$T_{G3} = T_{S3g} + \Delta T_{pp}$$

from which $\bar{h}_{G3}$ may be found from the property relations. Now an energy balance on the superheater and evaporator sections taken together gives

$$w_S(h_{S4} - h_{S2}) = m_G(\bar{h}_{G1} - \bar{h}_{G3})$$

which may be solved for the corrected steam flow, or

$$w_S = m_G\left(\frac{\bar{h}_{G1} - \bar{h}_{G3}}{h_{S4} - h_{S2}}\right) \qquad (3.3\text{-}5)$$

Now an energy balance on the entire boiler gives

$$w_S(h_{S4} - h_{S1}) = m_G(\bar{h}_{G1} - \bar{h}_{G4})$$

from which $\bar{h}_{G4}$ may be obtained,

$$\bar{h}_{G4} = \bar{h}_{G1} - \frac{w_S}{m_G}(h_{S4} - h_{S1}) \qquad (3.3\text{-}6)$$

where w_S is provided by Equation (3.3-5). Since $\bar{h}_{G4}$ and P_{G4} are known, T_{G4} is obtained via the property relations and $T_{G4} - T_{S1}$ must be greater than ΔT_{pp} or else no solution is possible. This fact is used to provide a check, since physically a solution must exist.

3.3.3 Check of Dew Point Temperature

Let the mole fraction of water vapor in the gas be denoted by μ_{H_2O}. Then the partial pressure of the water vapor p_{H_2O} in the stack is given by

$$p_{H_2O} = \mu_{H_2O} P_{G4}$$

From the steam tables, we can obtain the saturation temperature corresponding to p_{H_2O} which is, by definition, the dew point temperature, T_{DP}. If T_{G4} is not greater than T_{DP}, the analyst is alerted (by an appropriate message in the corresponding computer subroutine). However, the calculations described in Section 3.3.4 still proceed.

3.3.4 Calculation of Remaining Unknown Parameters

Since P_{S3g} and T_{S3g} are known, h_{S3g} is readily determined from the gas tables, and an energy balance on the superheater gives

$$w_S(h_{S4} - h_{S3g}) = m_G(\bar{h}_{G1} - \bar{h}_{G2})$$

which may be solved for $\bar{h}_{G2}$ as

$$\bar{h}_{G2} = \bar{h}_{G1} - \frac{w_S}{m_G}(h_{S4} - h_{S3g}). \qquad (3.3\text{-}7)$$

Since P_{G2} is also known, T_{G2} may be obtained from the property relations. It should be noted that the proper relation for w_S must be used in Equation (3.3-7) depending on the location of the pinch point. Let the amount of heat transferred in the economizer, evaporator, and

superheater sections be Q_{EC}, Q_{EV}, and Q_{SH}, respectively. It immediately follows that

$$Q_{EC} = w_S(h_{S2} - h_{S1}),$$

$$Q_{EV} = w_S(h_{S3g} - h_{S2}),$$

and

$$Q_{SH} = w_S(h_{S4} - h_{S3g}).$$

For completeness, h_{S3f} is easily obtained from the steam tables since T_{S3f} is known.

This completes the derivation of the mathematical model for the waste heat boiler.

3.4 Supercharged Boiler

Like the waste heat boiler, the supercharged boiler is composed of three sections: an economizer (EC), and evaporator (EV), and a superheater (SH). These serve the same purpose as in the waste heat boiler and the discussion at the beginning of Section 3.3 will not be repeated here. A schematic representation of the supercharged boiler is shown in Figure 3.4-1. Note that we shall include the gas turbine as part of the model. The reason for doing this will become apparent when we develop the governing equations.

As mentioned in Section 2.1, the path of the gases in the supercharged boiler is different than that in the waste heat boiler. In the latter, the gas which is exhausted from the gas turbine enters the

superheater, evaporator, and economizer sections in that order before exiting the system through the stack. In the former, the hot gas directly from the combustor first enters the evaporator and then the superheater. The exhaust gas from the superheater enters the gas turbine where useful work is obtained from the fluid. The exhaust gas from the turbine then enters the economizer before exiting the system through the stack.

Once again it is useful to construct a T-Q or temperature-heat flow diagram, which is shown in Figure 3.4-2, again not necessarily to any scale. The upper line represents the flow of the hot gas as it is cooled in the boiler. The drop in temperature of the gas between the superheater and economizer sections is due to the presence of the gas turbine at this point. The lower broken, dashed line represents the flow on the water side of the boiler. Feedwater enters the water-side of the economizer in a counterflow arrangement, boils in the evaporator section, and finally is superheated in the superheater section again in a counterflow arrangement.

The temperature nomenclature at key points in the boiler for both the steam- and gas-sides is indicated in Figure 3.4-2. Again, these same subscripts will be used for the other properties (pressure and enthalpy) for these points. The pressure is once again denoted by P, the molar enthalpy by $\bar{h}$, and the specific enthalpy by h. Once more, let m_G represent the number of moles of product gas and w_S the mass flow of steam generated in the supercharged boiler. Again we define the pinch point temperature difference ΔT_{pp} as in Section 3.3, but now we do know where this will occur in the boiler. Because of the magnitudes of the temperatures at each of these points (see Chapter 5),

the pinch point will invariably occur at the exit of the stack. However, for this model, we shall see that T_{S2} is not simply calculated as it was for the waste heat boiler but rather has a value which depends on the energy balances as shown below.

The following variables are assumed to have known values. As in all the models, the pressures at each point are specified: P_{G1}, P_{G2}, P_{G3}, P_{G4}, P_{G5}, P_{S1}, P_{S2}, P_{S3f}, and P_{S4}. Again both m_G and the gas composition are presumably known, as well as the temperatures T_{G1}, T_{G3}, T_{S1}, and T_{S4}. The minimum pinch point temperature difference ΔT_{pp} and the minimum number of degrees of subcooling of the inlet fluid to the evaporator section ΔT_{min} are also assumed to be specified. Because the gas turbine is included in the model, we assume also that the gas turbine efficiency is specified. (See Section 3.10). If the dewpoint temperature T_{DP} of the stack gas is reached, then the stack gas temperature is raised appropriately, increasing the effective pinch point temperature difference. We shall see shortly that the effective ΔT_{pp} at the stack may be increased for another reason.

Now we are in a position to discuss the solution strategy. First, the dew point temperature T_{DP} must be found to ensure that T_{G5} is greater than T_{DP}. Let μ_{H_2O} be the mole fraction of water vapor in the stack gas. The partial pressure of the water vapor p_{H_2O} in the stack gas is then given by

$$p_{H_2O} = \mu_{H_2O} P_{G5} \qquad (3.4\text{-}1)$$

Now from the steam tables, we can obtain the saturation temperature corresponding to p_{H_2O} which is, by definition, the dew point temperature

T_{DP}. If $T_{DP} - T_{S1}$ is greater than ΔT_{pp}, then T_{G5} is taken to be equal to T_{DP}. Otherwise, T_{G5} is taken to be equal to $T_{S1} + \Delta T_{pp}$. Next, since the gas turbine efficiency is specified, along with P_{G3}, T_{G3}, P_{G4}, and the gas composition, the gas turbine model described in Section 3.10 gives values for T_{G4}, $\bar{h}_{G3}$, and $\bar{h}_{G4}$ (as well as the work done per unit mass of fluid). Because P_{S4}, T_{S4} and P_{S1}, T_{S1} are known, h_{S4} and h_{S1} are determined from the steam tables. Similarly, P_{G1} and T_{G1} (and the gas composition) uniquely determines $\bar{h}_{G1}$ from the gas table property relations. It is assumed that $P_{S3g} = P_{S3f}$ and so it follows that $T_{S3g} = T_{S3f}$ where T_{S3f} is the saturation temperature corresponding to P_{S3f} from the steam tables. Similarly we get h_{S3f} and h_{S3g}.

Using the value for T_{G5} as described above with that for P_{G5}, we can get h_{G5} from the gas tables. By defining ψ to be the following ratio

$$\psi = \frac{\bar{h}_{G4} - \bar{h}_{G5}}{\bar{h}_{G1} - \bar{h}_{G3}} \tag{3.4-2}$$

where all the $\bar{h}$'s now have known values, we can show that $\bar{h}_{S2}$ is then given by

$$h_{S2} = \frac{h_{S1} + \psi h_{S4}}{1 + \psi} \tag{3.4-3}$$

Note that all the parameters on the right-hand side are known. Then P_{S2} and h_{S2} may be used to get T_{S2} from the steam tables. If the difderence between T_{S3f} and T_{S2} is not greater that ΔT_{min}, then T_{G5} is increased by 10 degree Fahrenheit increments and the calculation beginning with Equation (3.4-2) is repeated until $T_{S3f} - T_{S2}$ is greater than

ΔT_{min}. In any event, once h_{S2} is known, the steam flow w_S may be found by the following energy balance on the economizer

$$w_S(h_{S2} - h_{S1}) = m_G(\bar{h}_{G4} - \bar{h}_{G5}) \tag{3.4-4}$$

which may be solved for w_S as

$$w_S = m_G\left(\frac{\bar{h}_{G4} - \bar{h}_{G5}}{h_{S2} - h_{S1}}\right) \tag{3.4-5}$$

An energy balance on the superheater gives

$$w_S(h_{S4} - h_{S3g}) = m_G(\bar{h}_{G2} - \bar{h}_{G3})$$

which may be solved for $\bar{h}_{G2}$ as

$$\bar{h}_{G2} = \bar{h}_{G3} + \frac{w_S}{m_G}(h_{S4} - h_{S3g}). \tag{3.4-6}$$

This result and the known value for P_{G2} determines T_{G2}. Finally, the amount of heat transferred in the economizer, evaporator, and superheater sections are

$$Q_{EC} = w_S(h_{S2} - h_{S1}) \tag{3.4-7}$$

$$Q_{EV} = w_S(h_{S3g} - h_{S2}), \tag{3.4-8}$$

and

$$Q_{SH} = w_S(h_{S4} - h_{S3g}),$$

respectively.

Equation (3.4-3) will now be justified. An energy balance on the evaporator and superheater taken together gives

$$w_S(h_{S4} - h_{S2}) = m_G(\bar{h}_{G1} - \bar{h}_{G3})$$

which when considered with Equation (3.4-4), may be solved for h_{S2} as

$$h_{S2} = \frac{h_{S1} + \left(\frac{\bar{h}_{G4} - \bar{h}_{G5}}{\bar{h}_{G1} - \bar{h}_{G3}}\right) h_{S4}}{1 + \left(\frac{\bar{h}_{G4} - \bar{h}_{G5}}{\bar{h}_{G1} - \bar{h}_{G3}}\right)} \qquad (3.4\text{-}3a)$$

which is Equation (3.4-3) with the term in the parentheses being ψ defined by Equation (3.4-2). In retrospect, it probably would have been better to specify T_{S2} (or ΔT_{sc} instead of ΔT_{min} with $T_{S2} = T_{S3f} - \Delta T_{sc}$) which along with P_{S2} would establish h_{S2}. Then Equation (3.4-3a) could have been solved for $\bar{h}_{G5}$ which with P_{G5} would establish T_{G5}. The pinch point temperature difference ΔT_{pp} would then only be used as a check to ensure that this minimum difference is not violated. This alternate approach would yield a value for T_{G5} within 10 degrees Fahrenheit of that from the original formulation. This difference is not significant and, furthermore, the amount of subcooling is somewhat arbitrary anyway.

This completes the derivation of the mathematical model for the supercharged boiler.

3.5 Air and Gas Compressor

Consider the adiabatic compression of a mole of a gaseous fluid (air or another gaseous mixture) from pressure P_1 to pressure P_2 in a steady-flow process for which the kinetic and potential energy changes are negligible. A schematic representation of such a device

is shown in Figure 3.5-1. Because there are irreversibilities associated with the compression process, the molar entropy $\bar{s}$ must increase since we already assumed the process to be adiabatic. The irreversible process is shown in Figure 3.5-2 in temperature-entropy coordinates as a dashed line since the path is not really known. The isentropic compression from P_1 to P_2 is shown as a solid line on the same figure.

For this type of process, we use the usual definition for the efficiency η_c which is defined to be the ratio of the isentropic work required $\bar{W}_{isen}$ to the actual work required $\bar{W}_{act}$ both defined here on a mole basis,

$$\eta_c = \frac{\bar{W}_{isen}}{\bar{W}_{act}} \tag{3.5-1}$$

Denoting the properties at the end of the isentropic process by the prime ($'$) and those at the end of the actual process without the prime, we may write from the first law.

$$\bar{W}_{isen} = \bar{h}_2' - \bar{h}_1$$

and

$$\bar{W}_{act} = \bar{h}_2 - \bar{h}_1 \tag{3.5-2}$$

where the h_1, h_2, and h_2' are molar enthalpies. Therefore, the definition of compressor efficiency then becomes

$$\eta_c = \frac{\bar{h}_2' - \bar{h}_1}{\bar{h}_2 - \bar{h}_1} \tag{3.5-3}$$

The following parameters are assumed to be known: the gas or air composition, the pressure P_1 and P_2, the temperature T_1, and the efficiency

η_c. The state at the end of the actual process is to be determined as well as the amount of work required during the process.

Since P_1, T_1, and the gas or air composition are known, the state at the beginning of the process is completely specified. From the gas tables we may get both $\bar{h}_1$ and $\bar{s}_1$ where $\bar{s}$ denotes the molar entropy. But by definition $\bar{s}_2' = \bar{s}_1$ which considered with P_2 completely specifies the state at the end of the isentropic process. Therefore, $\bar{h}_2'$ is determined. Now Equation (3.5-3) may be solved for $\bar{h}_2$ as

$$\bar{h}_2 = \bar{h}_1 + \frac{\bar{h}_2' - \bar{h}_1}{\eta_c} \qquad (3.5\text{-}4)$$

The actual work required W_{act} per unit mass is then given by

$$W_{act} = (\bar{h}_2 - \bar{h}_1)/\nu$$

where ν is the molecular weight of either the air or gas under consideration. We have, therefore, determined the work done during the process and the state of the fluid at the end of the irreversible process.

3.6 Condenser

Let us consider the condensation of wet steam to a saturated liquid condition on the shell-side of a condenser by the transfer of the latent heat to a secondary water stream on the tube-side. To be more general we allow for a second inlet stream on the steam-side to the hotwell, since we anticipate that the condensate from the feedwater heater closest to the condenser will be flashed through a throttle valve and finally through a return line into the hotwell. A schematic representation of the condenser is shown in Figure 3.6-1.

It is convenient to assume that the following parameters are specified: the temperature T_{W1} and pressure P_{W1} of the cooling water inlet; the pressure P_{W2} of the cooling water outlet; the temperature rise of the cooling water ΔT_W; the pressure P_{S1}, the quality x_{S1}, and the mass flow of steam-water mixture w_{S1} into the condenser (from the steam turbine); the pressure P_{S2} of the saturated liquid condensate; and, finally, the pressure P_R, the quality x_R, and the mass flow w_R for the return line.

In practice, P_R is generally equal to P_{S1} since a throttle valve is used in the return line to make these pressures compatible. Also, since no pressure drop is assumed on the shell-side, then P_{S2} is equal to P_{S1}. Furthermore, the fluid at the shell-side outlet is assumed to be saturated liquid water. The temperature-heat flow diagram is shown in Figure 3.6-2. The condensing steam line in this figure is horizontal since the saturation temperature is constant for a constant pressure.

The same subscript designation will also be applied to the specific enthalpies, thus defining h_{S1}, h_{S2}, h_R, h_{W1}, and h_{W2}. From the steam tables we immediately can determine values for h_{S1}, h_R, and h_{W1} since the corresponding states are completely specified. Clearly,

$$T_{W2} = T_{W1} + \Delta T_W \tag{3.6-1}$$

by definition, which with P_{W2}, completely specifies the state of the cooling water at the exit; therefore, h_{W2} is determined from the steam tables. Because the condensate leaving the hotwell is assumed to be in a saturated liquid condition and the pressure at this state is known, we determine T_{S2} from the steam tables as the saturation temperature

corresponding to P_{S2}, and h_{S2} is also easily determined. From continuity of mass, we must have

$$w_{S2} = w_{S1} + w_R \tag{3.6-2}$$

for the shell-side of the condenser. Now an energy balance on the entire condenser gives

$$w_W(h_{W2} - h_{W1}) = w_{S1}h_{S1} + w_R h_R - w_{S2}h_{S2}$$

which we may solve for the cooling water flow w_W as

$$w_W = \frac{w_{S1}h_{S1} + w_R h_R - w_{S2}h_{S2}}{h_{W2} - h_{W1}} \tag{3.6-3}$$

The amount of heat rejected Q_W is then obviously

$$Q_W = w_W(h_{W2} - h_{W1}). \tag{3.6-4}$$

For completeness, T_R is also determined since P_R is known and the fluid is a saturated steam-water mixture.

3.7 Deaerator

Many times a deaerator is referred to as an open feedwater heater. These two terms can be used interchangeably. In order to avoid corrosion problems in the heat transfer devices, it is necessary to remove the entrapped air in the feedwater. This is most commonly done by using an open feedwater heater. For our purposes, we do not have to actually model the air ejection, since this is not relevant to our problem. Therefore, we shall treat the deaerator as a simple open feedwater heater.

A schematic representation is shown in Figure 3.7-1. Again we include the possibility of a return line for a reason similar to that cited in the development of the condenser model in Section 3.6.

We assume the following parameters are specified: the pressure P_{L1} and temperature T_{L1} of the feedwater into the deaerator; the outlet pressure P_{L2} and the outlet flow w_{L2}; the pressure P_R, the quality x_R, and the mass flow w_R of the saturated steam-water mixture in the return line; the pressure P_S and either the quality x_S (if saturated) or the temperature T_S (if superheated) of the extraction fluid. By definition of an open feedwater heater, the mass flows into the heater intimately mix, producing one outlet flow stream in a saturated liquid condition.

As is the usual case, the same subscript designations will be applied to the specific enthalpies, thus defining h_S, h_R, h_{L1}, and h_{L2}. From the steam tables, we can immediately determine values for h_S, h_R, and h_{L1} since the corresponding states are completely defined. If the extraction fluid is saturated, then specifying P_S fixes T_S as the saturation temperature corresponding to P_S; if superheated, x_S is no longer meaningful. The temperature T_{L2} at the feedwater outlet is also easily obtained from the steam tables as the saturation temperature corresponding to pressure P_{L2}, and h_{L2} is simply the saturated liquid enthalpy of the outlet fluid. Because the return flow fluid is saturated, T_R is the saturation temperature corresponding to P_R.

Now with all the appropriate enthalpies at each state point specified, an energy balance on the deaerator will give an expression for the extraction flow w_S as follows. The energy balance yields

$$w_{L1}h_{L1} + w_S h_S + w_R h_R = w_{L2}h_{L2} \tag{3.7-1}$$

which when the mass balance equation

$$w_{L2} = w_{L1} + w_S + w_R \tag{3.7-2}$$

is considered to eliminate the unknown mass flow w_{L1} between Equations (3.7-1) and (3.7-2) we may solve for w_S as

$$w_S = \frac{w_{L2}(h_{L2} - h_{L1}) + w_R(h_{L1} - h_R)}{h_S - h_{L1}} \tag{3.7-3}$$

Now with w_S known, Equation (3.7-2) may be solved for the unknown feedwater inlet flow as

$$w_{L1} = w_{L2} - w_S - w_R. \tag{3.7-4}$$

Thus, the states and mass flows of the four flow streams are completely specified.

One may ask why w_{L2} is considered to be a known while w_{L1} is unkonwn. This is most simply answered by referring to Figures 2.3-1, 2.3-2, 2.3-3, or 2.3-4. When we add feedwater heaters later the last component in the feedwater train will be a deaerator. Since the steam flow to the steam turbine is presumed to be known at this point in the cycle calculation, it is easily seen in these figures that w_{L2} is precisely equal to steam turbine inlet flow which is known from a prior component calculation, namely the waste heat or supercharged boiler calculations discussed in Sections 3.3 and 3.4, respectively. This kind of reasoning is used throughout the model development and has resulted in simplifying the

complexity of the model input and output considerably. In rare cases where an assumed input parameter is not really known, an iterative procedure using the model as developed could be easily implemented.

3.8 Closed Feedwater Heater

A closed feedwater heater is a heat exchanger in which steam extracted from a steam turbine provides the heat necessary to raise the temperature of the feedwater. A schematic representation is shown in Figure 3.8-1. As we have done in the condenser and deaerator models, we shall allow for more flexibility by including a return line from a downstream feedwater heater to the shell side of the feedwater heater under consideration.

Now it is convenient to assume the following parameters are specified from the outset: the pressure P_{L1}, the temperature T_{L1}, and the mass flow w_{L1} of the feedwater into the heater; the pressure P_{S1} and either the quality x_{S1} or temperature T_{S1} of the steam extraction fluid; the pressure P_R, the quality x_R, and the mass flow w_R of the fluid entering the shell-side through the return line; the pressure P_{L2} of the feedwater outlet flow; and, finally, the terminal temperature difference ΔT_{TTD} between the shell-side temperature T_{S1} (or T_{S2} or T_R) and the temperature T_{L2} of the feedwater outlet.

As in the condenser model, the return line pressure P_R is in general equal to P_{S1}. Also, since no pressure drop is assumed on the shell-side, then P_{S2} is equal to P_{S1}. Furthermore, the fluid at the shell-side outlet is assumed to be saturated liquid water. The temperature-heat flow diagram is shown in Figure 3.8-2, where the terminal temperature difference ΔT_{TTD} is indicated. The condensing steam line in this figure is

horizontal since the saturation temperature is constant for a constant pressure.

We note that the model allows for specification of the state of the steam extraction fluid by either P_{S1}, x_{S1} if saturated or P_{S1}, T_{S1} if superheated. It is a simple matter to then determine T_{S1} in the former as the saturation temperature corresponding to P_{S1}. If the fluid is superheated steam, then x_{S1} is not meaningful. In any event, the specific enthalpy h_{S1} is also easily obtained from the steam tables. Figure 3.8-2 is valid only if the steam extraction fluid is in a saturated state, which is the usual case in practice.

The steam tables once again provide us with the enthalpies of the states which are completely specified by the variables assumed to be known. First, P_{L1}, T_{L1} determine h_{L1}. Since we assume the shell-side outlet fluid to be saturated water, then T_{S2} is the saturation temperature corresponding to the pressure P_{S2} which is taken to be equal to P_{S1}. Clearly, this is also fixes h_{S2}. Then from the definition of the terminal temperature difference,

$$T_{L2} = T_{S2} - \Delta T_{TTD}. \tag{3.8-1}$$

This with P_{L2} fixes h_{L2}, since we have a subcooled liquid state. Finally, P_R and x_R completely fix h_R. Now with all the enthalpies known, the energy balance equation for the entire heater is

$$w_{L2}h_{L2} - w_{L1}h_{L1} = w_{S1}h_{S1} + w_R h_R - w_{S2}h_{S2} \tag{3.8-2}$$

But by continuity of mass on the tube-side, we have

$$w_{L2} = w_{L1}, \tag{3.8-3}$$

and on the shell side,

$$w_{S2} = w_{S1} + w_R. \tag{3.8-4}$$

Using Equations (3.8-4) and (3.8-3) in Equation (3.8-2) and solving for w_{S1}, we get

$$w_{S1} = \frac{w_{L1}(h_{L2} - h_{L1}) - w_R(h_R - h_{S2})}{h_{S1} - h_{S2}} \tag{3.8-5}$$

With the steam extraction flow w_{S1}, fixed by Equation (3.8-5), the shell-side outlet flow is given by Equation (3.8-4). We have thus determined all the remaining unknown parameters.

3.9 Gas Cooler

This model is especially simple since the main purpose is to calculate the amount of heat which is discarded. Because the rejected heat is not used, this represents a heat loss from the cycle in which such a component is used but does not necessarily lower cycle performance. This particular component may be part of an intercooled compressor as mentioned in Section 3.1 or, as we shall see later, it may be used to cool the gas before the sulfur removal process.

It is convenient to assume the following parameters are known in the model: the gas composition, the pressure P_1 and temperature T_1 at the

inlet, the pressure P_2 and temperature T_2 at the outlet, and the number of moles, m, of gas passing through the intercooler. Figure 3.9-1 shows the schematic representation of a gas cooler, which may at times be referred to as an intercooler. The heat removed Q from the gas is then simply

$$Q = m(\bar{h}_1 - \bar{h}_2)$$

where T_1 is assumed to be greater than T_2, and $\bar{h}_1$ and $\bar{h}_2$ are the molar enthalpies of the inlet and outlet fluids respectively.

3.10 Gas Turbine

Now we consider the reverse of the process described in the air and gas compressor models. We want to model the adiabatic expansion of a mole of a mixture of gases from a pressure P_1 to a pressure P_2 in a steady-flow process. Again we neglect the changes the kinetic and potential energy and heat losses. A schematic representation of the gas turbine is shown in Figure 3.10-1. Like the compression process we have irreversibilities associated with the expansion process. Thus the molar entropy $\bar{s}$ must increase during the process. We show the irreversible process in Figure 3.10-2 on temperature-entropy coordinates as a dashed line since the path is not really known. The isentropic expansion from P_1 to P_2 is shown as a solid line on the same figure.

Now we define the efficiency of the gas turbine η_T to be the ratio of the actual work produced W_{act} to the isentropic work produced W_{isen}, both defined here on a mole basis, or

$$\eta_T = \frac{\overline{W}_{act}}{\overline{W}_{isen}} \tag{3.10-1}$$

Following our convention of denoting the state at the end of an isentropic process by a prime ($'$), we can write from the first law that

$$\overline{W}_{isen} = \overline{h}_1 - \overline{h}_2' \tag{3.10-2}$$

and

$$\overline{W}_{act} = \overline{h}_1 - \overline{h}_2 \tag{3.10-3}$$

where the $\overline{h}$'s are all molar enthalpies at the states indicated by the subscripts. So the efficiency becomes

$$\eta_T = \frac{\overline{h}_1 - \overline{h}_2}{\overline{h}_1 - \overline{h}_2'} \tag{3.10-4}$$

For convenience, we assume the following parameters are known: the gas composition, the pressures P_1 and P_2, and temperature T_1 , and the efficiency η_T. We want to determine the state of the gas mixture at the end of the expansion and the actual amount of work produced on a mass basis, W_{act}.

Since the gas composition, P_1, and T_1 are known, the state at the beginning of the process is completely determined. We get both $\overline{h}_1$ and $\overline{s}_1$

from the gas table properties. Then by definition, $\bar{s}_2' = \bar{s}_1$, and with P_2 fixed, we have established $\bar{h}_2'$. Solving Equation (3.10-4) for $\bar{h}_2$ gives

$$\bar{h}_2 = \bar{h}_1 - \eta_T(\bar{h}_1 - \bar{h}_2'). \tag{3.10-5}$$

If we denote the molecular weight of the gaseous mixture as ν, then the actual work produced on a pound basis is given by

$$W_{act} = (\bar{h}_1 - \bar{h}_2)/\nu \tag{3.10-6}$$

With $\bar{h}_2$ and P_2 fixed, we can easily get the temperature T_2 of the fluid at the end of the actual expansion, as well as any other property.

3.11 Gas-to-Gas Counterflow Heat Exchanger

The concept of heat exchanger effectiveness may be used to advantage in a thermodynamic analysis of any power cycle in which heat exchangers may be required. Earlier we have recognized the fact that we are limiting this modeling effort to the thermodynamics of the processes only. We agreed that for our purposes it is not necessary to know how large a particular component would have to be. But the very concept of a heat exchanger entails considering such factors as heat transfer coefficients, heat transfer areas, and so forth, which all depend on the geometry of the device. We shall see below how our using the effectiveness ε, defined to be the ratio of the actual heat transfer to the maximum possible, sufficiently characterizes the heat exchanger to enable us to retain our thermodynamic approach. We further limit this model to gas-to-gas heat

exchange in a counterflow arrangement because in Chapter 5 we shall see that this particular component will improve the cycle performance significantly.

A schematic representation of the gas-to-gas counterflow heat exchanger is shown in Figure 3.11-1. Because we shall use this device to regenerate heat from one fluid to another, we may also refer to this component as a regenerator. Let us assume the following parameters are specified from the outset: the effectiveness ε; the molar flows of the hot and cold fluids, m_h and m_c, respectively; the pressures at inlet to and outlet from the hot side or P_{h1} and P_{h2}, respectively, and at the inlet to and outlet from the cold side or P_{c1} and P_{c2} respectively; the temperatures at the inlet to both the hot and cold sides or T_{h1} and T_{c1}, respectively; and finally, the composition of the gases on both sides.

Depending on the relative heat capacities which is the product of the molar flows and molar specific heats, we may get two different temperature-heat flow diagrams as shown in Figure 3.11-2. In Figure 3.11-2(a), the hotter fluid is assumed to have the smaller heat capacity or $m_h\bar{c}_{Ph}$ is less than $m_c\bar{c}_{Pc}$ where $\bar{c}_{Ph}$ and $\bar{c}_{Pc}$ are the molar specific heats of the hot and cold fluids, respectively. In Figure 3.11-2(b), we assume $m_c\bar{c}_{Pc}$ is less than $m_h\bar{c}_{Ph}$. These devices are usually well insulated and so it is reasonable to assume no heat loss. An energy balance on entire regenerator then gives

$$m_c\bar{c}_{Pc}(T_{c2} - T_{c1}) = m_h\bar{c}_{Ph}(T_{h1} - T_{h2}) \qquad (3.11\text{-}1)$$

From this equation, we see that the difference between T_{h1} and T_{h2} must be larger than that between T_{c2} and T_{c1} when $m_h\bar{c}_{Ph}$ is less than $m_c\bar{c}_{Pc}$,

and vice versa. Based on our definition of effectiveness, we can get two different expressions depending on which fluid has the minimum heat capacity. If the hot fluid is assumed, then

$$\varepsilon = \frac{T_{h1} - T_{h2}}{T_{h1} - T_{c1}} \qquad (3.11\text{-}2a)$$

but if the cold fluid is assumed, then

$$\varepsilon = \frac{T_{c2} - T_{c1}}{T_{h1} - T_{c1}} \; . \qquad (3.11\text{-}2b)$$

We must be careful, therefore, in choosing the correct defining equation for the effectiveness.

Because we prefer to work with enthalpies rather than specific heats, an alternate equivalent approach will be taken. We shall first assume the hot fluid has the minimum heat capacity and use Equation (3.11-2a) to solve for T_{h2}. Then an energy balance will give T_{c2}. The amount of heat transfer is then readily calculated. Then, we shall assume the cold fluid has the minimum heat capacity and use Equation (3.11-2b) to solve for T_{c2}. Now the energy balance will give T_{h2} and again the amount of heat transfer may be calculated. The minimum fluid must be the one which, when assumed as above, results in the smaller amount of heat transfer, since the heat transfer Q is given by[20]

$$Q = \varepsilon(m\bar{c}_p)_{min}(T_{h1} - T_{c1})$$

where $(m\bar{c}_p)_{min}$ is the smaller of $m_c\bar{c}_{Pc}$ and $m_h\bar{c}_{Ph}$.

First, we assume that the hot fluid is the minimum one. Then Equation (3.11-2a) is solved for T_{h2} as

$$T_{h2} = T_{h1} - \varepsilon(T_{h1} - T_{c1}) \tag{3.11-3}$$

With T_{h2} fixed by Equation (3.11-3) and with P_{h2} known (the gas composition is also known), we can get h_{h2} from the property tables. Similarly P_{c1}, T_{c1} and P_{h1}, T_{h1} fix $\bar{h}_{c1}$ and $\bar{h}_{h1}$. The energy balance in terms of the entahlpies becomes

$$m_h(\bar{h}_{h1} - \bar{h}_{h2}) = m_c(\bar{h}_{c2} - \bar{h}_{c1}) \tag{3.11-4}$$

which may be solved for $\bar{h}_{c2}$ as

$$\bar{h}_{c2} = \bar{h}_{c1} + \frac{m_h}{m_c}(\bar{h}_{h1} - \bar{h}_{h2}). \tag{3.11-5}$$

Since P_{c2} (along with the gas composition) is known and $\bar{h}_{c2}$ is fixed by Equation (3.11-5), we can obtain T_{c2} from the property tables. The heat transfer Q_H, if the hot fluid is the minimum one, may then be given as

$$Q_H = m_h(\bar{h}_{h1} - \bar{h}_{h2}) \tag{3.11-6}$$

Next, we follow a similar procedure by now assuming the cold fluid is the minimum one. Now Equation (3.11-2b) is solved for T_{c2} as

$$T_{c2} = T_{c1} + \varepsilon(T_{h1} - T_{c1}). \tag{3.11-7}$$

We then get $\bar{h}_{c2}$ from the gas tables, which we use in Equation (3.11-4) which we solve for $\bar{h}_{h2}$ to get

$$\bar{h}_{h2} = \bar{h}_{h1} - \frac{m_c}{m_h}(\bar{h}_{c2} - \bar{h}_{c1}) \qquad (3.11\text{-}8)$$

This fixes T_{h2}. Now the heat transfer Q_C may be taken as

$$Q_C = m_h(\bar{h}_{h1} - \bar{h}_{h2}). \qquad (3.11\text{-}9)$$

If Q_H is greater than Q_C, then the cold fluid has the minimum heat capacity and we use Equations (3.11-7)to (3.11-9) to describe the heat exchanger. If Q_C is greater than Q_H, then Equations (3.11-3) to (3.11-6) are used.

3.12 Steam Generator

The steam generator provides the steam needed by the coal gasifier by utilizing the sensible heat in the gasifier power gas. A schematic representation is shown in Figure 3.12-1. The model for the steam generator appears on the surface to be identical to that of the waste heat boiler. However, they are quite different since the parameters which are known are different. For example, in the waste heat boiler model we had to determine the steam flow using the fact that the minimum pinch point temperature difference was to be respected. Here, the steam flow is known (fixed by the gasifier model) with the pinch point temperature difference being used only to determine if, in fact, it is even possible to raise the required amount of steam. Fortunately, in every case of practical interest, we are able to do this.

It is convenient to assume the following parameters are initially known: the pressure P_L and temperature T_L of the water flowing into the steam generator; the pressure P_S and temperature T_S of the superheated steam; the mass flow of steam w_S; the pressure P_{G1} and temperature T_{G1}

of the power gas flowing into the gas-side; the molar flow of power gas m_G and the gas composition (which, as usual, is needed to determine the enthalpies); the pressure P_{G3} of the gas flowing out of the gas-side; the pressure P_{G2} of the gas at the internal pinch point shown in Figure 3.12-2; and, finally, the minimum pinch point temperature difference ΔT_{pp}.

The temperature-heat flow diagram is shown in Figure 3.12-2 for the steam generator. From the steam tables we may immediately obtain the specific enthalpies h_S and h_L. The required amount of heat is then given by

$$Q_{SG} = w_S(h_S - h_L). \tag{3.12-1}$$

Since we assume no heat losses, this also must be equal to

$$Q_{SG} = m_G(\bar{h}_{G1} - \bar{h}_{G3}) \tag{3.12-2}$$

where $\bar{h}_{G1}$ is the molar enthalpy from the gas tables since the corresponding state is specified. Equating the right-hand sides of Equations (3.12-1) and (3.12-2), we may then solve for $\bar{h}_{G3}$ as

$$\bar{h}_{G3} = \bar{h}_{G1} - \frac{w_S}{m_G}(h_S - h_L) \tag{3.12-3}$$

which, with P_{G3}, fixes T_{G3}. An energy balance on the section in the steam generator between T_{G2} and T_{G3} gives an expression which may be solved for $\bar{h}_{G2}$ as

$$\bar{h}_{G2} = \bar{h}_{G3} + \frac{w_S}{m_G}(h_{LS} - h_L) \tag{3.12-4}$$

where h_{LS} is the saturated liquid enthalpy for water at pressure P_{LS} which is taken to be equal to P_L. From the steam tables we also get T_{LS} which is the saturation temperature corresponding to P_{LS}. With $\bar{h}_{G2}$ fixed by Equation (3.12-4) and P_{G2} known, we get T_{G2} from the gas table properties.

We complete the model by checking to make sure that $T_{G1} - T_S$, $T_{G2} - T_{LS}$, and $T_{G3} - T_L$ are all greater than ΔT_{pp}. If this were not the case, then it would be impossible to raise the required amount of steam by this method and an alternative method would have to be found. Fortunately, this is not the case as we shall see in Chapter 5.

3.13 Steam Turbine

The steam turbine model is very similar to the gas turbine model. There are two key differences, however. The first is the fact that the inlet fluid to the turbine may be superheated steam or a saturated steam-water mixture, making the model more complicated. The second, which simplifies the model, is that we have only one species to consider, namely H_2O.

We find it convenient to assume the following parameters are initially known: the pressures P_1 and P_2 at the inlet and outlet of the steam turbine; the efficiency η_T defined similarly to that in Section 3.10 for the gas turbine; and finally either the temperature T_1 or quality x_1 of the inlet fluid. A schematic representation of the steam turbine is shown in Figure 3.13-1.

To get a multi-stage steam turbine with steam extraction for feedwater heating we simply connect as many of these single-stage models in series as are required. This approach allows much flexibility in the use of this single model. If we were to try to actually model a multi-stage steam turbine with extraction, we would see that the feedwater heater models are coupled to the steam turbine model through the extraction flows. We avoid this complication by obeying our general rule to model each process via a single component model where possible.

The solution procedure is similar to that of the gas turbine model. First, we construct the temperature-entropy diagrams shown in Figure 3.13-2. In Figure 3.13-2(a), the fluid is assumed to be initially in a superheated state and in Figure 3.13-2(b) a steam-water saturated state. The final state is shown in the saturation region but we shall allow in our model for the final state to be either superheated steam or wet steam. For the case shown in Figure 3.13-2(a), we define the initial state by P_1 and T_1 since these properties are independent. For that shown in Figure 3.13-2(b), the initial state is defined by P_1 and x_1, where x is used to denote steam quality. In any event, we can easily obtain the specific enthalpy h_1 and specific entropy s_1 from the steam tables. Again we denote the states at the end of the isentropic process by the prime ($'$), so by definition $s_2' = s_1$. But P_2 is known so, h_2' may be found from the steam tables. But η_T is defined by

$$\eta_T = \frac{h_1 - h_2}{h_1 - h_2'} \qquad (3.13\text{-}1)$$

which we may solve for h_2 as

$$h_2 = h_1 - \eta_T(h_1 - h_2'). \tag{3.13-2}$$

The work done by the fluid on a unit mass basis W_{act} is then

$$W_{act} = h_1 - h_2 \tag{3.13-3}$$

If the state at the end of the expansion process turns out to be in saturated region, the quality x_2 can be easily calculated. The temperature T_2 is also now fixed since P_2, h_2 specify the state at the end of the actual expansion process.

3.14 Gas Cleanup System

The purpose of the gas cleanup system is to remove a significant amount of the undesirable species in the power gas produced in the coal gasifier. For example, as we shall see in Chapter 5, most of the sulfur in the coal combines with some of hydrogen present to form hydrogen sulfide, H_2S, with a smaller amount combining with carbon and oxygen to form carbonyl sulfide, COS. Fortunately, as we saw in Chapter 2, there are many well-known processes which are designed to remove H_2S from a gas to just about any desired purity. In fact, as we have discussed in Section 2.2, this is one of the motivating reasons for gasifying the coal in the first place. A schematic representation is shown in Figure 3.14-1.

It is convenient to assume that the following parameters are known: the composition of the power gas into the gas cleanup system

on a mole fraction basis $\mu_{i,1}$; the pressure P_{G1} and temperature T_{G1} of the dirty power gas; the pressure P_{G2} of the clean power gas; the mass flow w_{G1} of the dirty power gas; and finally the removal efficiencies of the hydrogen sulfide, carbonyl sulfide, carbon dioxide, and ammonia vapor or η_{H_2S}, η_{COS}, η_{CO_2}, and η_{NH_3}, respectively.

Given the gas composition into the system on a mole fraction basis $\mu_{i,1}$ it is simple to convert it to a composition on a weight fraction basis $\omega_{i,1}$. Having done this, we can get the mass flow of the waste product stream w_{WPS} from

$$w_{WPS} = w_{G1}[\eta_{H_2S}\omega_{H_2S,1} + \eta_{COS}\omega_{COS,1} + \eta_{CO_2}\omega_{CO_2,1} + \eta_{NH_3}\omega_{NH_3,1}] \quad (3.14\text{-}1)$$

where, as above, the removal efficiencies η_i are defined to be the ratio of the mass of species i removed per unit mass present. The weight fractions $\omega_{i,2}$ of the gas leaving the system may now be adjusted by defining Ω as

$$\Omega = \sum_{i=1}^{10} (1-\eta_i)\omega_{i,1} \quad (3.14\text{-}2)$$

where the η_i are zero for those species which are not H_2S, COS, CO_2, or NH_3. Table 3.2-3 defines the species associated with each subscript i. Now we get the composition of the gas $\omega_{i,2}$ on a weight fraction basis leaving the cleanup system as

$$\omega_{i,2} = \omega_{i,1}/\Omega \quad (3.14\text{-}3a)$$

for all species but H_2S, COS, CO_2, and NH_3 and as

$$\omega_{i,2} = (1-\eta_i)\omega_{i,1}/\Omega \qquad (3.14\text{-}3b)$$

for these species. The molecular weight of the gas ν_{G2} out of the system is given by

$$\nu_{G2} = \sum_{i=1}^{10} \frac{\omega_{i,2}}{\nu_i} \qquad (3.14\text{-}4)$$

where the ν_i are the molecular weights of the individual species. The outlet gas composition $\mu_{i,2}$ on a mole fraction basis becomes

$$\mu_{i,2} = \nu_{G2}\frac{\omega_{i,2}}{\nu_i} \qquad (3.14\text{-}5)$$

for each of the ten species in Table 3.2-3. The mole flow of gas m_{G2} out of the system becomes

$$m_{G2} = (w_{G1} - w_{WPS})/\nu_{G2} \qquad (3.14\text{-}6)$$

At this point, we restrict our model to those sulfur removal processes which use water as the solvent. The gas leaving the cleanup system is then assumed to be saturated with water vapor. We further assume that T_{G2} is equal to T_{G1}. So the mole fraction of water vapor in the clean gas μ_{REQ} is given by

$$\mu_{REQ} = \frac{P_{sat}}{P_{G2}} \qquad (3.14\text{-}7)$$

where P_{sat} is the saturation pressure corresponding to temperature T_{G2}. The number of moles of H_2O, m_{H_2O}, required to saturate the gas can be shown to be given by

$$m_{H_2O} = \frac{m_{G2}(\mu_{REQ} - \mu_{H_2O,2})}{1 - \mu_{REQ}} \tag{3.14-8}$$

and so the mass of water w_{H_2O} which is required is

$$w_{H_2O} = m_{H_2O}\nu_{H_2O} \tag{3.14-9}$$

The actual mass flow of clean saturated gas $w_{G2_{sat}}$ out of the system is

$$w_{G2_{sat}} = w_{G1} - w_{WPS} + w_{H_2O} \tag{3.14-10}$$

The mole fractions of the saturated gas $\mu_{i,2_{sat}}$ must be adjusted by

$$\mu_{i,2_{sat}} = \frac{m_{G2}\mu_{i,2}}{m_{G2} + m_{H_2O}} \tag{3.14-11}$$

Finally, the mole flow of clean saturated gas $m_{G2_{sat}}$ is given by

$$m_{G2_{sat}} = \frac{w_{G2_{sat}}}{\nu_{G2}} \tag{3.14-12}$$

It is then a simple matter to get the corresponding composition of the clean saturated gas on a mass fraction basis.

3.15 Throttle Valve

The throttle valve is a very simple component which is used to reduce the pressure of the incoming fluid. A schematic representation is shown in Figure 3.15-1. By neglecting changes in kinetic and potential energy and heat losses, we see that the first law of thermodynamics for this steady-flow process reduces to

$$h_1 = h_2 \tag{3.15-1}$$

where the specific enthalpies are denoted by h and the subscripts, 1 and 2, correspond to the incoming fluid at pressure P_1 and pressure P_2, respectively.

Rather than combining the two possible fluids that we need to consider into one model, we shall develop one model for gas and one for steam. As one might expect, however, the calculations involved are very simple.

3.15.1 Throttle Valve for Mixture of Gases

In this model, we assume that the pressure P_1 and temperature T_1 of the incoming fluid are known, as well as the downstream pressure P_2 and the gas composition. From this information, the molar enthalpy $\bar{h}_1$ for the incoming gas is easily obtained from the gas tables. Equation (3.15-1) may be written in terms of molar enthalpies $\bar{h}$ as

$$\bar{h}_1 = \bar{h}_2 \tag{3.15-2}$$

So the final state is completely specified by P_2, $\bar{h}_2$, and the gas composition. The temperature T_2 of the gas at the end of the throttling

process may then be obtained from the gas tables. It is this temperature T_2 that we need to know, since it inevitably will provide an input to another component model in our cycle.

3.15.2 Throttle Valve for Steam

We now assume that the pressure P_1 and the temperature T_1 (if superheated or subcooled) or steam quality x_1 (if saturated) for the incoming fluid are known, as well as the downstream fluid pressure P_2. If the state of the incoming fluid is superheated or subcooled, we use P_1 and T_1 to determine h_1. However, if the incoming fluid is saturated, we use P_1 and x_1 to determine h_1. In any event, by Equation (3.15-1), we take h_2 to be equal to h_1. Then with P_2 and h_2 fixed, we can with the help of the steam tables determine T_2. Again, it is important to know the value of T_2, since this temperature is inevitably an input (along with P_2) to another component model in the cycle.

3.16 Water Pump

The primary purpose of a water pump is to raise the pressure of the subcooled water by doing work on the fluid. If we assume the changes in kinetic and potential energy during the process and the heat loss from the fluid are negligible, then the first law for this steady-flow process reduces to

$$W_{act} = h_2 - h_1 \qquad (3.16\text{-}1)$$

where h_1 and h_2 are the specific enthalpy of the fluid into and out of the pump, respectively, and W_{act} is the work required per unit mass of water. A schematic representation is shown in Figure 3.16-1

Again we denote the end of the isentropic process shown in Figure 3.16-2 by the prime (′) and using a definition of efficiency η_p similar to that of the air or gas compressor, we write

$$\eta_p = \frac{h_2' - h_1}{h_2 - h_1} \tag{3.16-2}$$

We find it convenient now to assume the following parameters are known: the pressure P_1 and temperature T_1 of the subcooled inlet to the pump, the outlet pressure P_2, and the pump efficiency η_p.

Since we have a single species fluid, we may write

$$dh = v\, dP + T\, ds \tag{3.16-3}$$

from elementary thermodynamics, where v is the specific volume and T is the temperature of the fluid and dh, dP, and ds are infinitesimal changes in specific enthalpy, pressure, and specific entropy, respectively. But for an isentropic process,

$$ds \equiv 0$$

and so

$$dh' = v\, dP \tag{3.16-4}$$

which may be integrated between the two states to give

$$h_2' - h_1 = \int_{P_1}^{P_2} v \, dP. \qquad (3.16\text{-}5)$$

So Equation (3.16-1) becomes with the help of Equation (3.16-2) and the last equation

$$W_{act} = \frac{1}{n_p} \int_{P_1}^{P_2} v \, dP \qquad (3.16\text{-}6)$$

Furthermore, since subcooled water is practically incompressible, we may approximate Equation (3.16-6) by taking the specific volume v in the integrand to be v_1, a constant, and get

$$W_{act} = \frac{v_1}{n_p}(P_2 - P_1) \qquad (3.16\text{-}7)$$

We then get h_2 from Equation (3.16-1) or

$$h_2 = h_1 + W_{act}. \qquad (3.16\text{-}8)$$

The solution procedure is obvious by now. We get v_1 and h_1 from the steam tables using P_1 and T_1 to define the state. We compute W_{act} according to Equation (3.16-7) and then h_2 from Equation (3.16-8). Then T_2 may be determined from the steam tables since P_2 and h_2 define this state. The appropriate conversion factors, of course, must be used to make the units consistent.

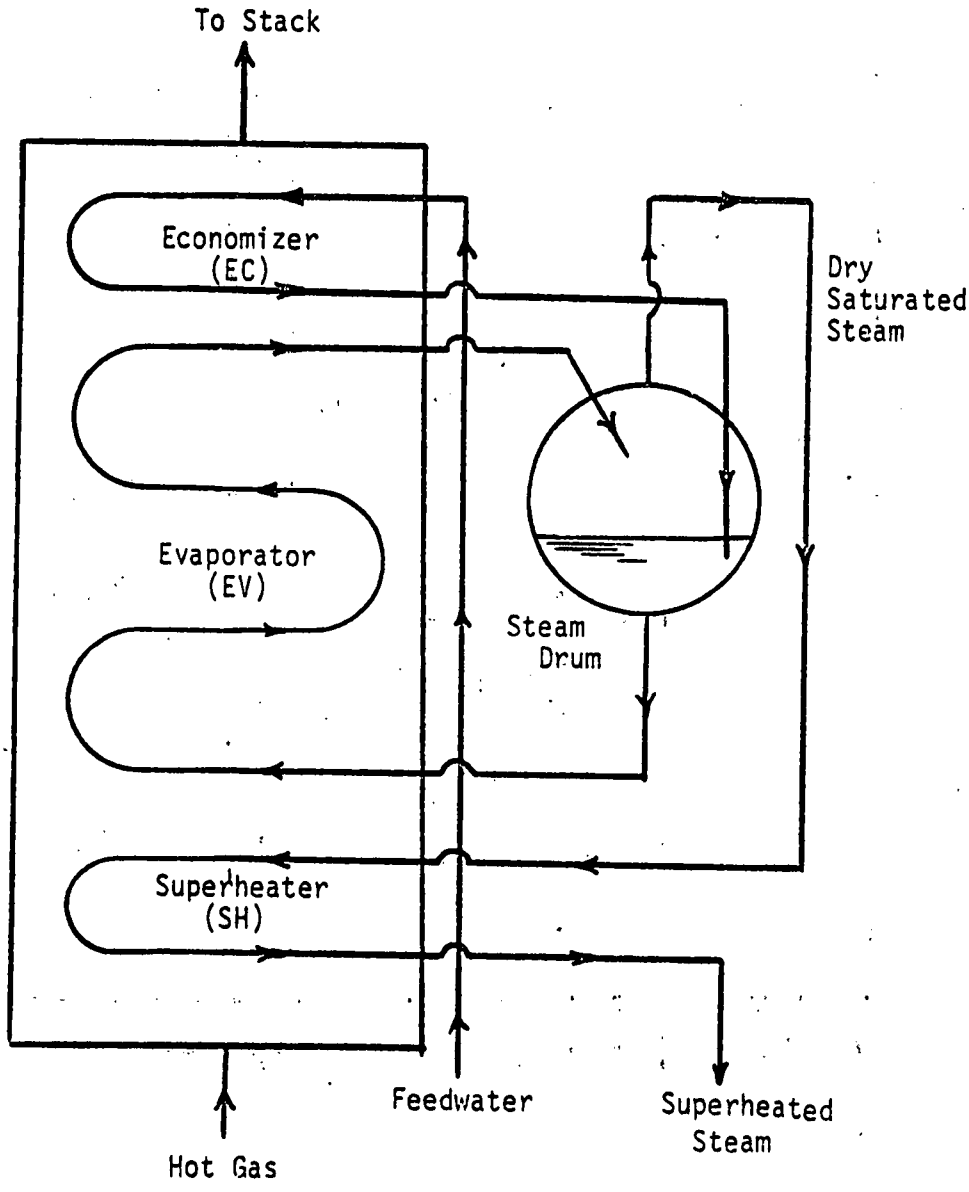

Figure 3.3-1 Schematic of Waste Heat Boiler

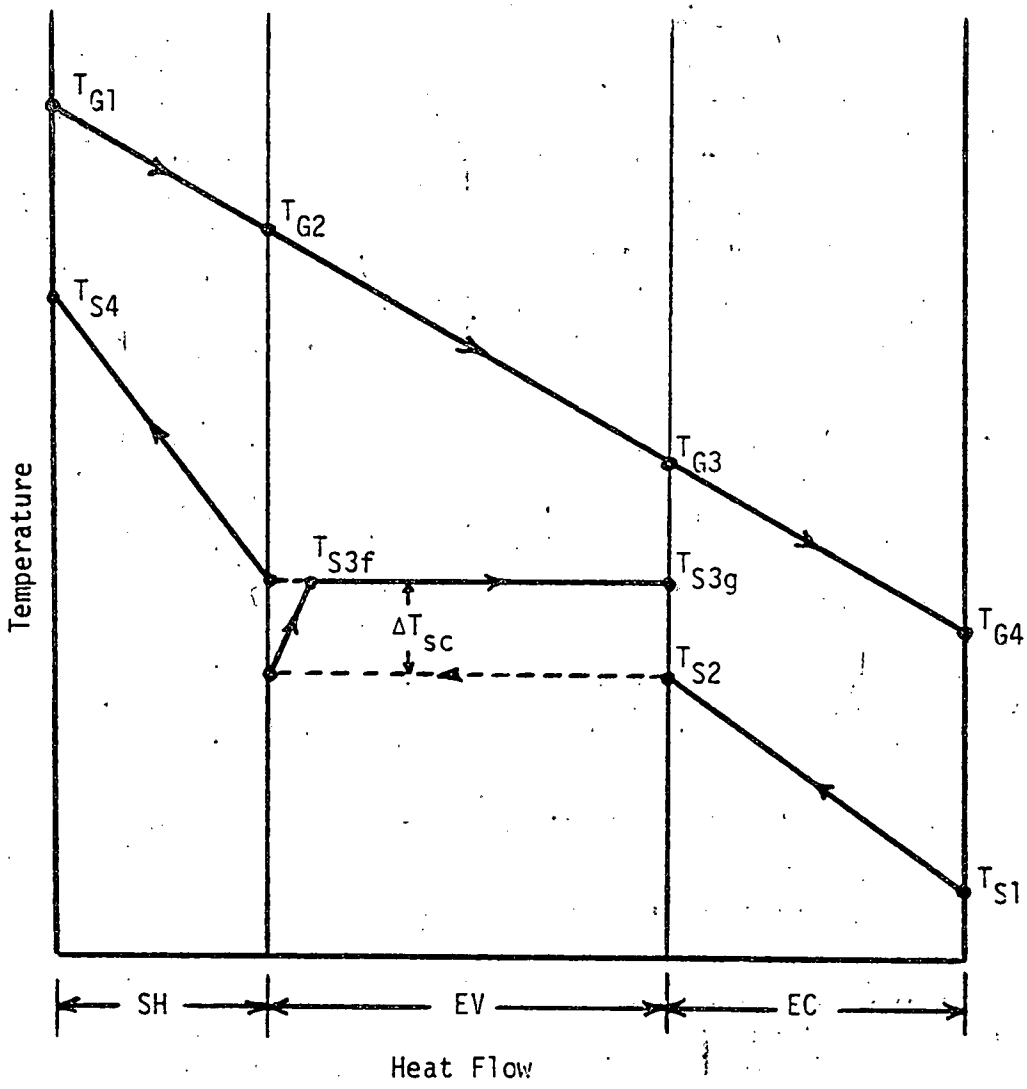

Figure 3.3-2 Temperature-Heat Flow Diagram for Waste Heat Boiler

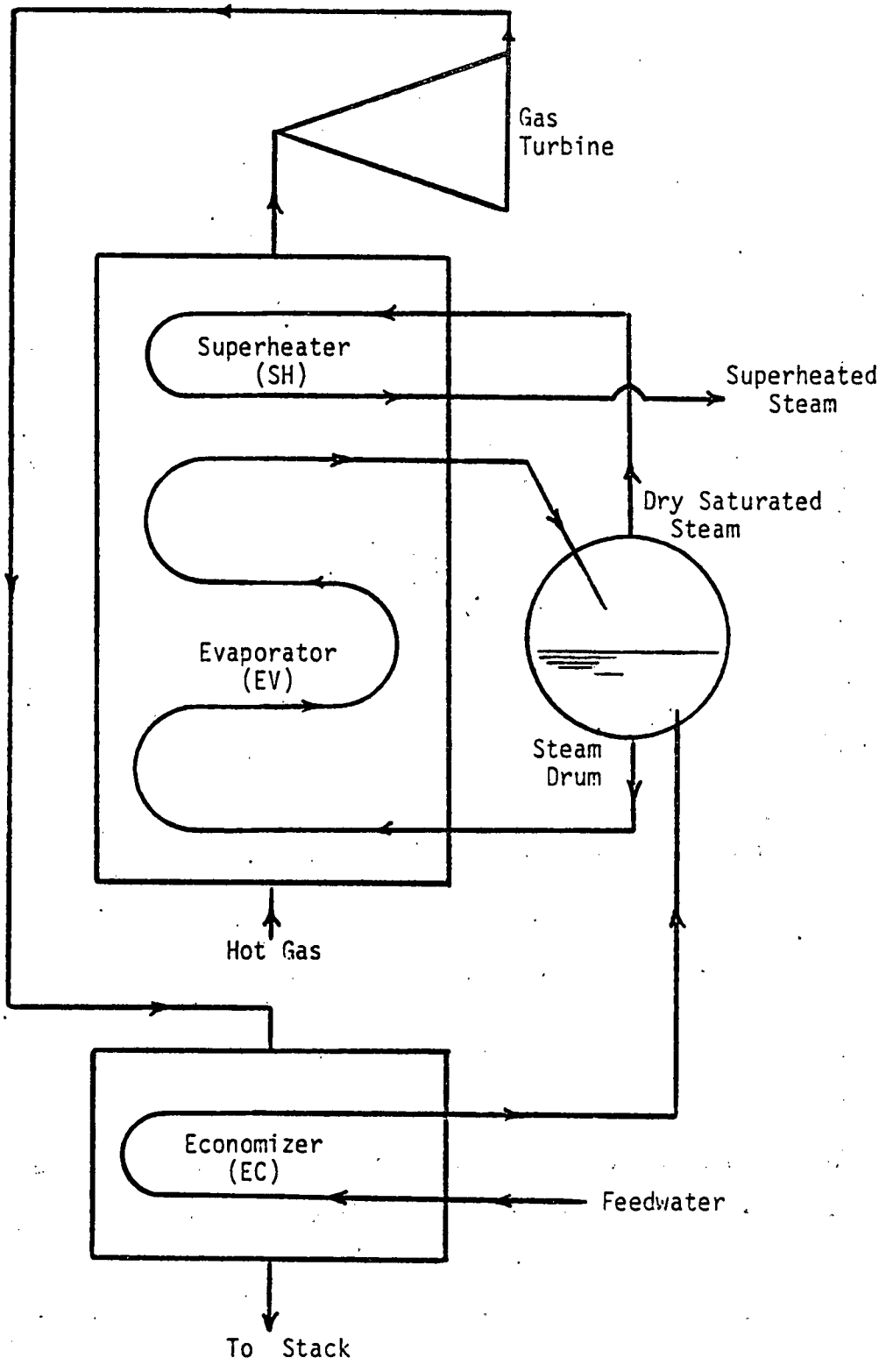

Figure 3.4-1 Schematic of Supercharged Boiler with Gas Turbine

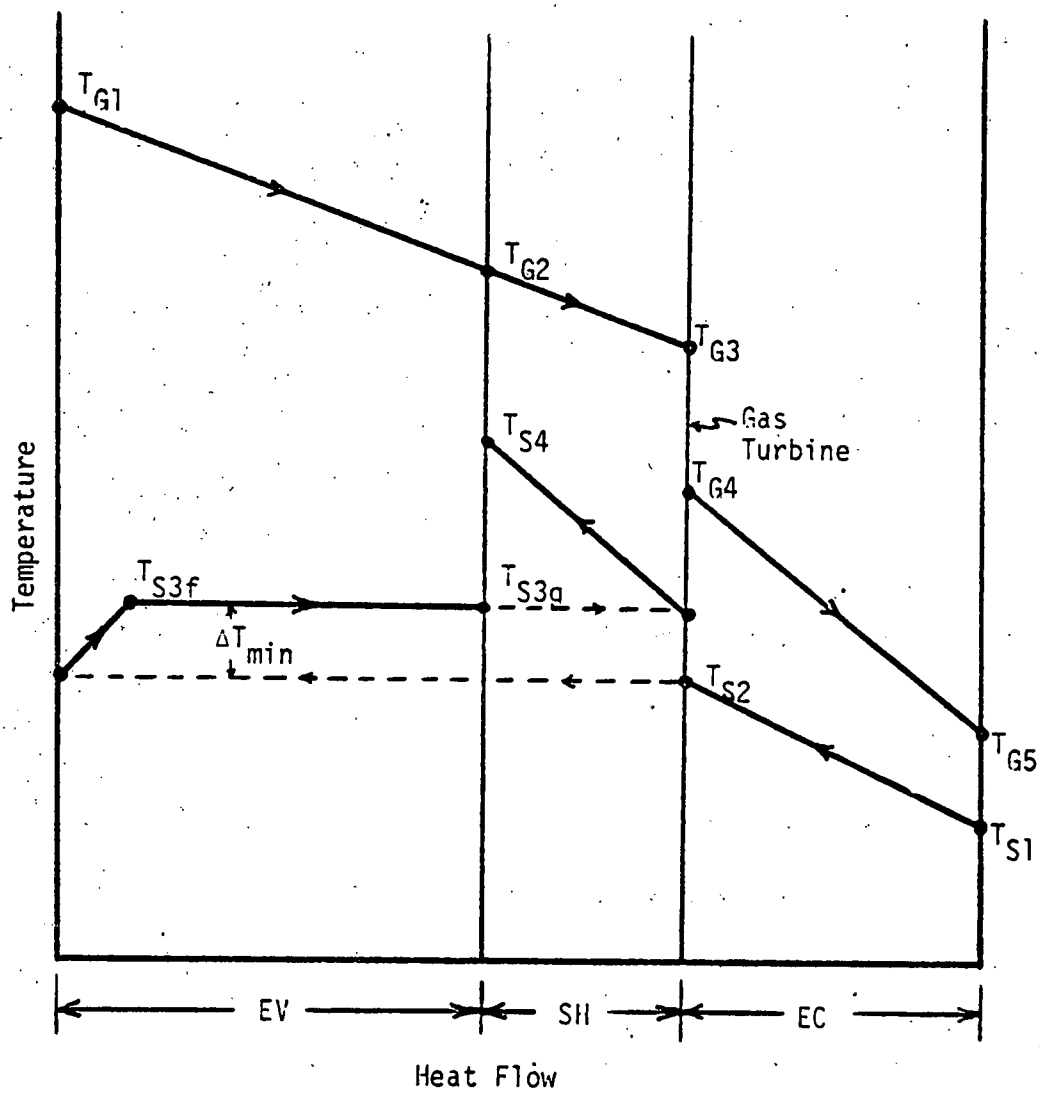

Figure 3.4-2 Temperature-Heat Flow Diagram for Supercharged Boiler

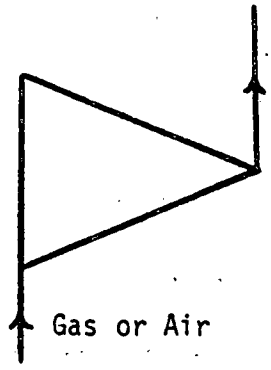

Figure 3.5-1 Schematic of Air and Gas Compressor

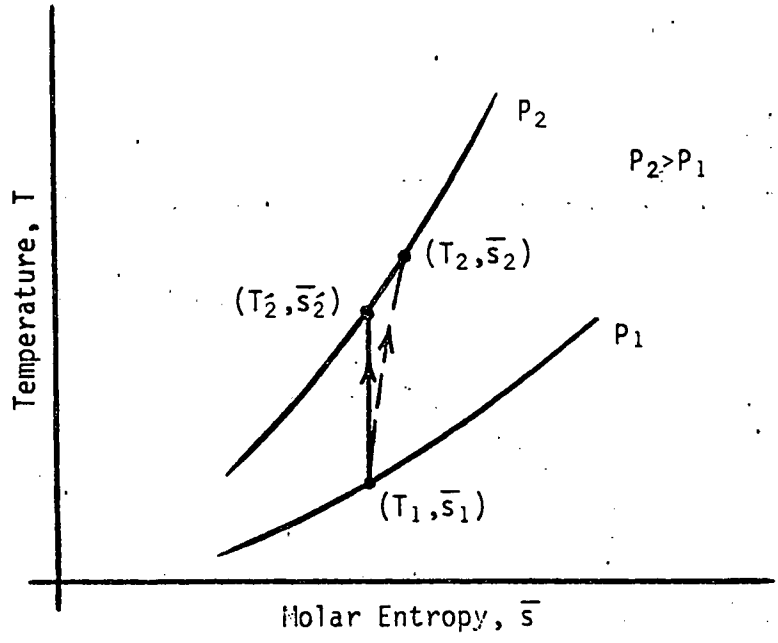

Figure 3.5-2 Temperature-Entropy Diagram for Compression of a Gaseous Fluid

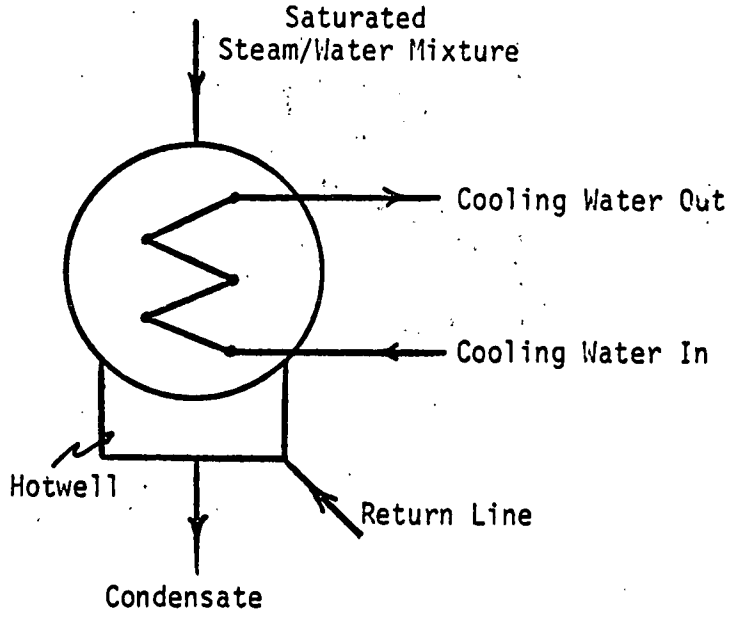

Figure 3.6-1 Schematic of Condenser

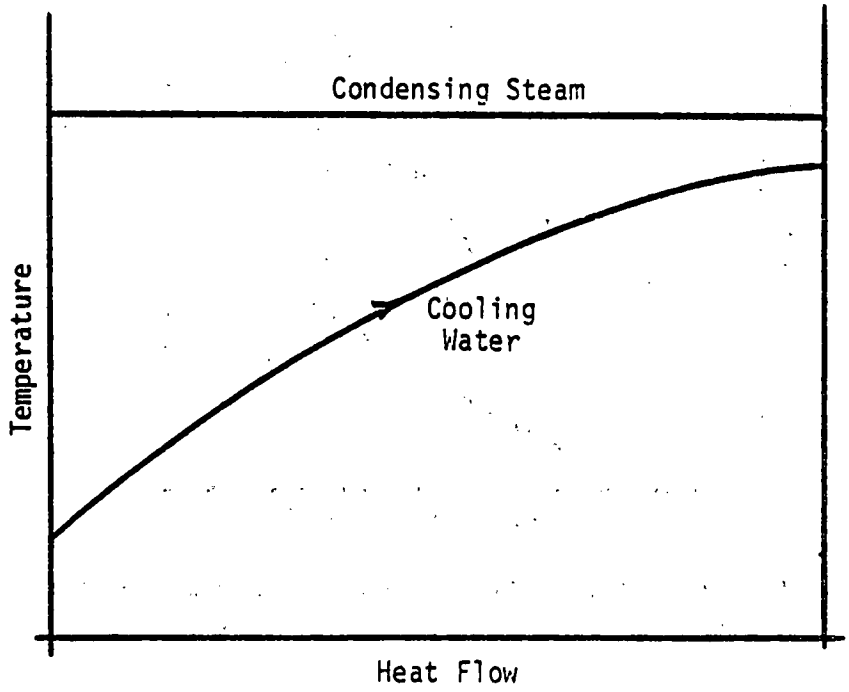

Figure 3.6-2 Temperature-Heat Flow Diagram for Condenser

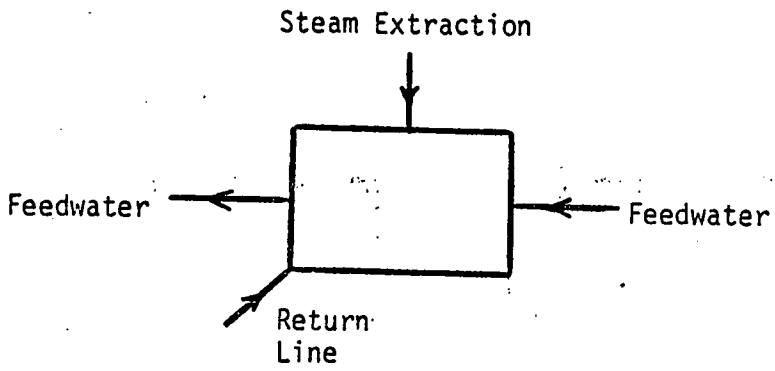

Figure 3.7-1 Schematic of Deaerator

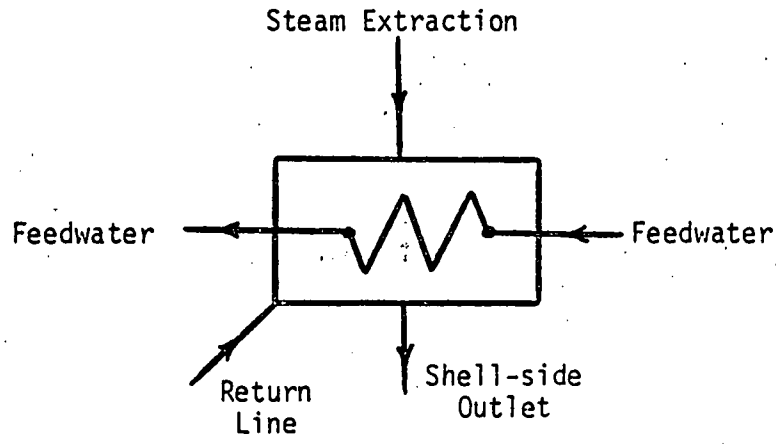

Figure 3.8-1 Schematic of Closed Feedwater Heater

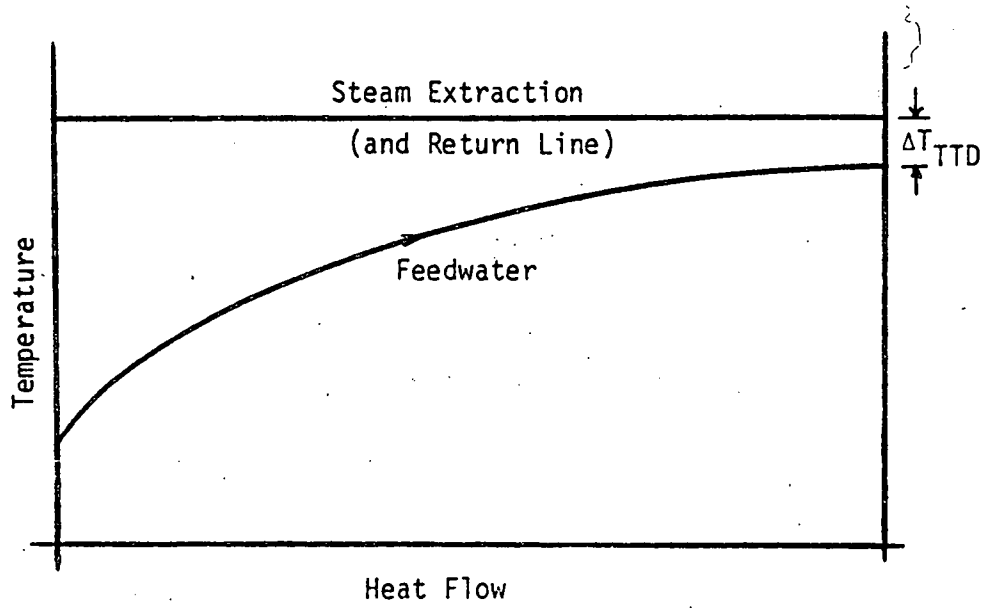

Figure 3.8-2 Temperature-Heat Flow Diagram for Closed Feedwater Heater

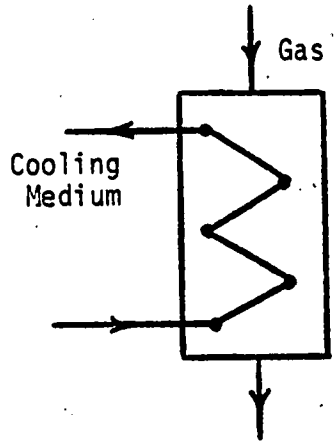

Figure 3.9-1 Schematic of Gas Cooler

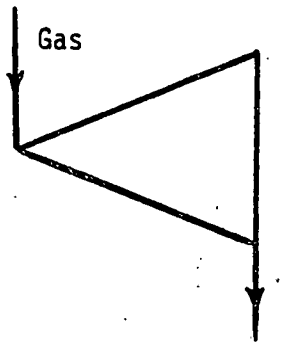

Figure 3.10-1 Schematic of Gas Turbine

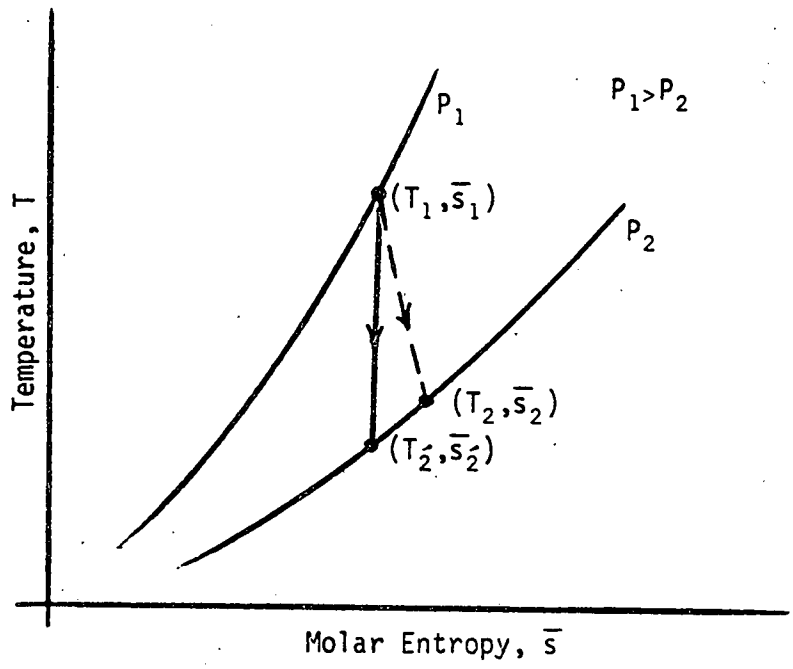

Figure 3.10-2 Temperature-Entropy Diagram for Expansion of a Gaseous Fluid

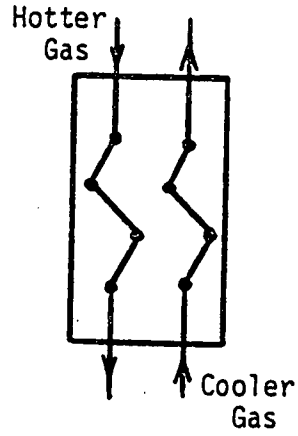

Figure 3.11-1 Schematic of Gas-to-Gas Counterflow Heat Exchanger

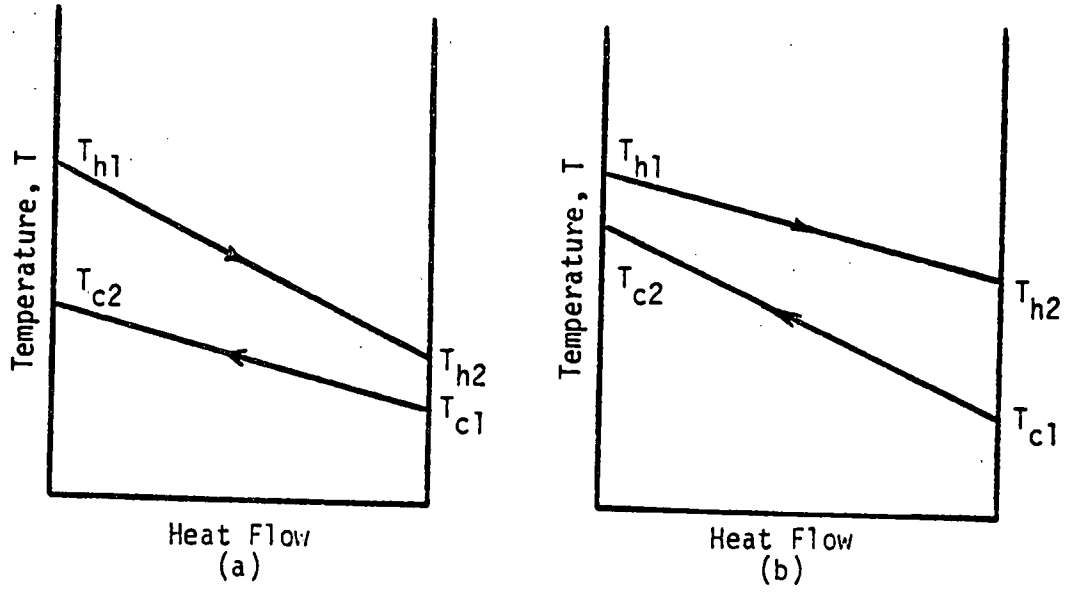

Figure 3.11-2 Temperature-Heat Flow Diagram Assuming Minimum Heat Capacity Associated with (a) Hotter and (b) Cooler Fluid

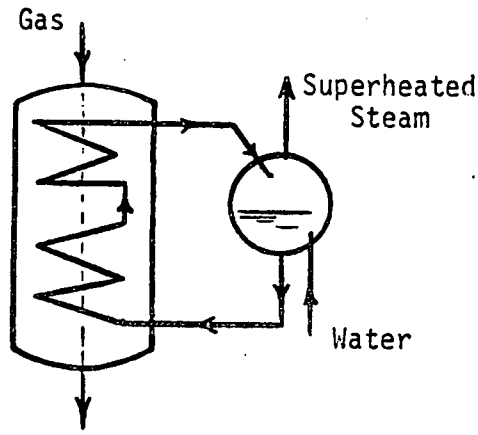

Figure 3.12-1 Schematic of Steam Generator

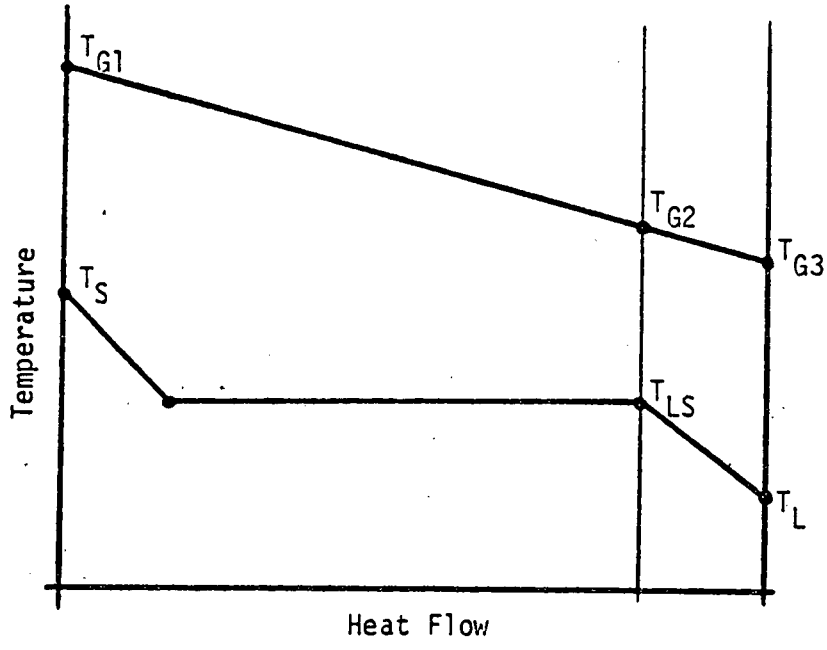

Figure 3.12-2 Temperature-Heat Flow Diagram for Steam Generator

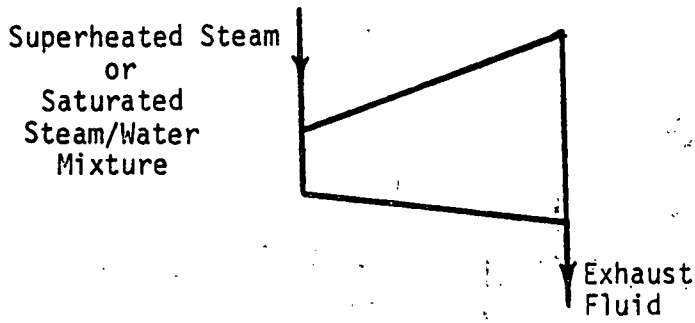

Figure 3.13-1 Schematic of Steam Turbine

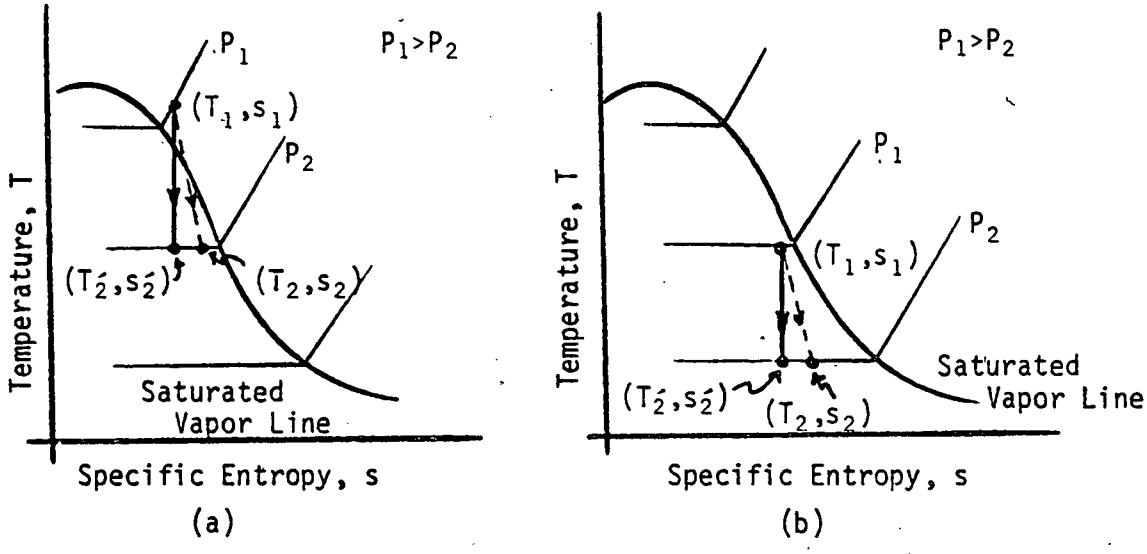

Figure 3.13-2 Temperature-Entropy Diagram for Expansion of (a) Superheated Steam or (b) Saturated Steam-Water Mixture into Saturated Region

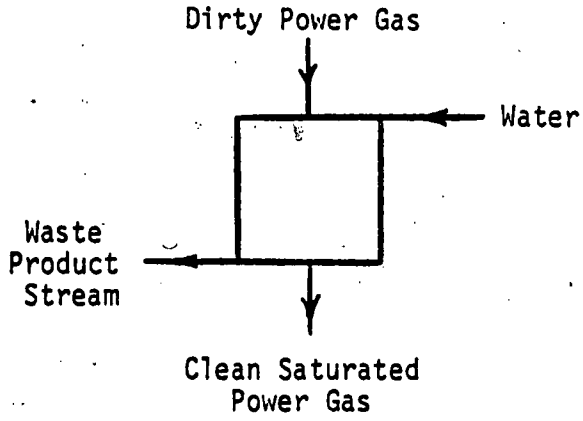

Figure 3.14-1 Schematic of Gas Clean-up System

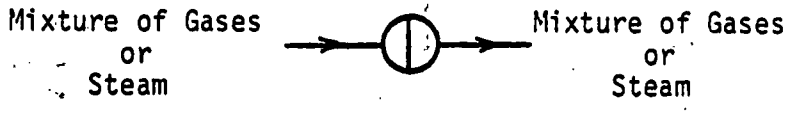

Figure 3.15-1 Schematic of Throttle Valve

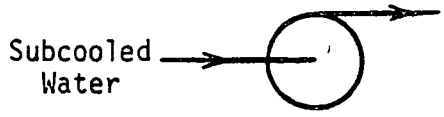

Figure 3.16-1 Schematic of Water Pump

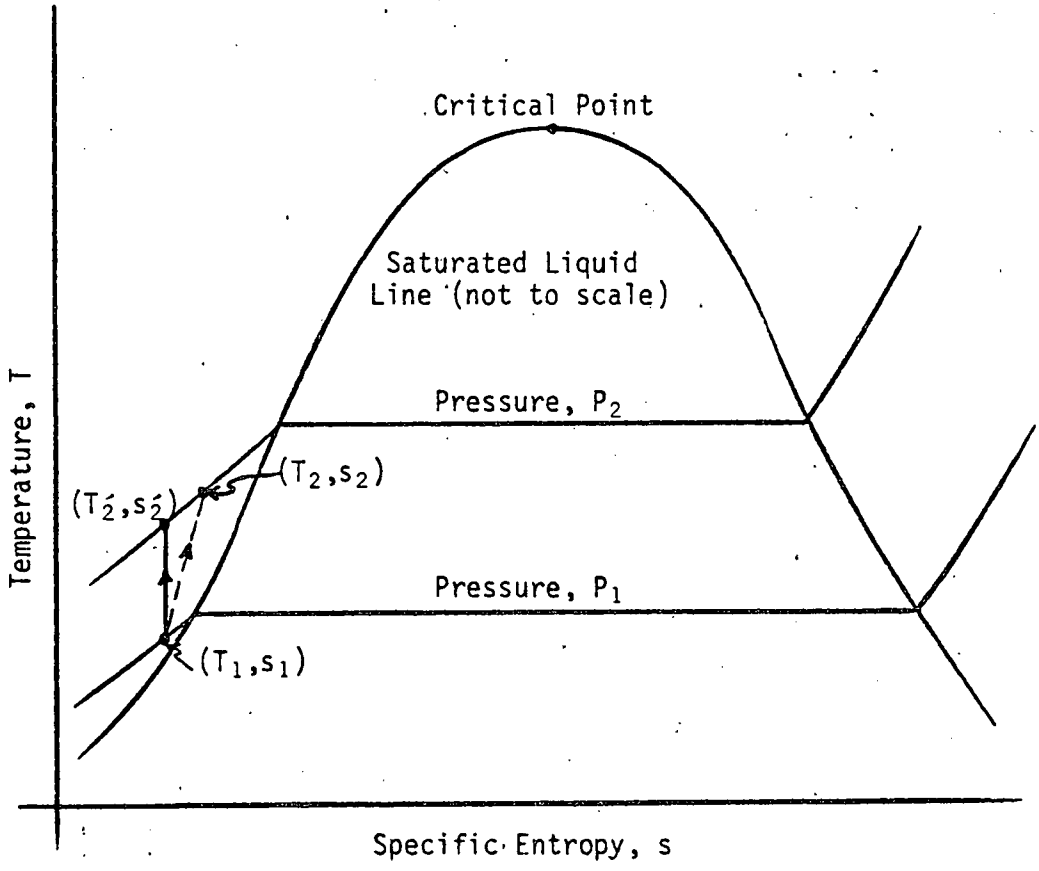

Figure 3.16-2 Temperature-Entropy Diagram for Pumping Process
(Not to any scale)

CHAPTER 4

THE COMPUTER PROGRAM AND SUPPORTIVE CALCULATIONS

4.1 Introduction

In this chapter, we shall indicate how the four cycle configurations which we discussed in Chapter 2 are actually assembled in a FORTRAN computer program. The program structure has been designed to be modular. The main program CGACC, which stands for Coal Gasification and Combined Cycles, calls only the four configuration subprograms CNFG1, CNFG2, CNFG3, and CNFG4, depending on the configuration that the analyst wishes to study. In these subprograms, all the component subroutines, whose mathematical models were developed in Chapter 3, are connected together in a way which models the configuration of interest. Also special duty subroutines, which contain the default values (Subroutine DINTi), initialize the cycle point pressures (Subroutine PRIi) and print the results (Subroutine PRINi) and which are unique to CNFGi, are used. As we saw in Chapter 3, the steam table and gas table properties were used extensively in all the component models. The need for casting these properties into subroutines or functions for use on the computer is obvious. Finally, for completeness we shall also list all auxiliary subroutines and functions which facilitated the programing effort.

The input and output to CGACC are described in Appendices B and C respectively. However, several comments should be made at this point. The basic data packet (only batch input is available) consists of three items. The first is a title card, which if blank terminates execution of the program. It is convenient to describe the case under consideration on this card. The second item is the namelist $MASTER, which is

always read no matter what configuration is being analyzed. It is through $MASTER that the user tells the computer which configuration he wishes to study via the variable CONFIG. Based on this value (CONFIG=i, where i may be 1, 2, 3, or 4), the third item in the data packet, namelist $CONFi, is read. The namelist is unique to Configuration i. Each variable in all of these namelists has a built-in default value which the computer uses if the user does not redefine its value. Appendix B defines all the input parameters as well as the default values and units for each of the five namelists.

It should be noted that "canned" programs are available to do much of the same type of calculations that we require here. In one such program, it is claimed that any cycle can be modeled by appropriate input of FORMAT data cards. While this is an excellent approach on the part of the programmer, it is a "black box" approach on the part of a user who has not written the program. The user cannot easily modify the program and must accept results on blind faith. Also, the advantages of the quick, easy input are lost since bulky input decks using FORMAT must be prepared. Aside from the cost consideration, the disadvantages of using these programs are significant enough to warrant development of a personalized computer program.

The program hierarchy is summarized in Figure 4.1-1. The main program will be discussed further in Section 4.2, the configuration subroutines in Section 4.3, the component subroutines in Section 4.4, the property subprograms in Section 4.5, and finally the auxiliary subprograms in Section 4.6.

4.2 Main Program

The primary purpose of the main program CGACC is to allow access to the appropriate configuration which we wish to analyze. A flow chart of the main program is shown in Figure 4.2-1. From this flow chart, we see that the first task to be done by CGACC is to read a title card, which we may use to document the case since this is printed near the top of every output page (see Appendix C). If this card is blank, execution is terminated. Otherwise, the computer will then read the namelist $MASTER, which among other parameters contains the variable CONFIG. The user is able to analyze configuration i by specifying CONFIG=i in this namelist. Another variable in $MASTER, called LISTIN, enables the user to list the current values of all the variables in $MASTER by setting LISTIN to an integer different than zero. In other words, if LISTIN equals zero, then the current values of variables in $MASTER are not printed in the output. Finally, based on the value of the variable CONFIG, the appropriate configuration subroutine is called. When the calculations in CNFGi are finished, control is transferred back to the main program and a new title card, indicating a new case, is read. If the title card is blank, execution is terminated; otherwise, the above is repeated.

Appendix B.2 should be consulted for a complete list of variables in namelist $MASTER and their associated definitions and default values.

4.3 Configuration Subroutines

As we have mentioned before, the configuration subroutines are actually the subprograms in which we assemble the component models to

model the cycle configuration of interest. Let us remain general in our discussion by discussing configuration subroutine CNFGi. A simplified flow chart is shown in Figure 4.3-1. It is simplified in the sense that all the CALL statements for the component subroutines are lumped together in the area within the dashed box in the figure.

Subroutine CNFGi first initializes all the input parameters in namelist $CONFi if the variable DINT read in namelist $MASTER is not equal to zero, or if this case is the first one of Configuration i to be analyzed in the data deck. This data initialization is accomplished by calling subroutine DINTi. The default values of the input parameters are given in Appendix B.3 along with their meanings and units. Next, the second and final namelist $CONFi for this case is read which enables the user to change the built-in values for the various parameters for Configuration i. If the variable LISTIN is different than zero (defined in namelist $MASTER), then each variable in $CONFi is printed in the output with its current value for the case under consideration. Then, all cycle point pressures are calculated in subroutine PRIi using the pressure drop data which are input (or the default values used). All the component subroutines are then called with the output from one providing the input to the next. By referring to the listing of the configuration subroutines in Appendix A, we may see that very little additional programming is done. Finally, all the various efficiencies are calculated in subroutine EFFICY, the gaseous air pollution effluents in subroutine POLUTE, and the results printed by subroutine PRINi. Refer to Appendix C for a brief description of the output. The various

efficiencies which are calculated in EFFICY are defined in Section 4.6, which also describes how the pollution information is generated, since these are considered to be auxiliary calculations.

By way of summary, we list in Table 4.3-1 the cycle configuration description associated with each of the four configuration subroutines. In Chapter 5, we shall see how the configurations presented in Chapter 2 may be improved by the addition of certain components. At that time, we shall expound on the details of each configuration after it has been modified to improve cycle performance and to meet the air pollution criteria set by the federal government. The basic computer program structure, however, remains unchanged from the description given in the present chapter.

Table 4.3-1
Summary of Configuration Subroutines

Configuration Number	Subroutine	Description of Cycle	Subroutines which are Uniquely Called
1	CNFG1	Adiabatic gasifier integrated with waste heat boiler combined cycle.	DINT1 PRI1 PRIN1
2	CNFG2	Adiabatic gasifier integrated with super-charged boiler combined cycle.	DINT2 PRI2 PRIN2
3	CNFG3	Endothermic gasifier integrated with waste heat boiler combined cycle.	DINT3 PRI3 PRIN3
4	CNFG4	Endothermic gasifier integrated with super-charged boiler combined cycle.	DINT4 PRI4 PRIN4

4.4 Component Subroutines

Each of the component models described in Chapter 3 has been cast into the form of easy-to-use subroutines. We can distinguish at a glance which variables are input, which are output, and which may be input or output. This is done by interpreting the parameter list after the subroutine name as described below.

To be specific, let us consider the subroutine FWHTR, which models the closed feedwater heater according to Section 3.8. By referring to the listing of subroutine FWHTR in Appendix A, we see that the subroutine declaration statement is

```
      SUBROUTINE FWHTR(PLIN,TLIN,WLIN,PSIN,PLOUT,TTD,PRIN,
     X     QRIN,WRIN,
     Y     QSIN,TSIN,
     Z     HLIN,WSIN,HSIN,WLOUT,HLOUT,TLOUT,TRIN,HRIN,TSOUT,
     Z     HSOUT,WSOUT,QSOUT)
```

where the following input/output convention is adopted. The parameters which are always input to the subroutine are those on the first line or those on a line on which an "X" appears in the card continuation column (column 6). The parameters which are sometimes input and/or sometimes output are those which appear on cards with a "Y" in the card continuation column. Finally, the parameters which are always output are located on cards with a "Z" in the continuation column. This convention greatly facilitates the use of these subroutines.

The gasifier and combustor component subroutines have been subdivided to make them more manageable since the models were quite lengthy. In particular, the system of equations for each model are contained in the

auxiliary subroutine called SYSTEM with the equations practically in the same form in which we wrote them in Section 3.2 The multi-dimensional Newton-Raphson iteration procedure described in Section 3.2.2 to obtain a solution to these non-linear algebraic governing equations is programmed in auxiliary subroutine NEWTON. These two subroutines along with all the other auxiliary subroutines are discussed in Section 4.6.

The component subroutines are summarized in Table 4.4-1. The component subroutine listings in Appendix A should be consulted to determine the input and output parameters. Also for convenience, comment cards after the subroutine statement in the listing indicate what the subroutine calculates. The correlation between the Fortran variables and those in the model developments in Chapter 3 should be made rather easily.

Table 4.4-1
Summary of Component Subroutines

Component Model	Subroutine Name	For Model Description Refer to Section
Gasifier	GSFR	3.2.1.1
Combustor	CMBSTR	3.2.1.2
Waste Heat Boiler	WHBOIL	3.3
Supercharged Boiler	SCBOIL	3.4
Air Compressor	AIRCOM	3.5
Gas Compressor	GASCOM	3.5
Condenser	CNDSR	3.6
Deaerator	DATOR	3.7
Closed Feedwater Heater	FWHTR	3.8
Gas Cooler	GASCLR	3.9
Gas Turbine	GASTUR	3.10
Gas-to-Gas Counterflow Heat Exchanger	HXCGG	3.11
Steam Generator	STMGEN	3.12
Steam Turbine	STURB	3.13
Gas Cleanup	SULREM	3.14
Gas Throttle Valve	THRGAS	3.15.1
Steam Throttle Valve	THRSTM	3.15.2
Water Pump	PUMPW	3.16

4.5 Property Subprograms

The property subprograms take the form of Fortran functions. Furthermore, we may divide the property routines into two broad classes: those associated with the gas tables and those with the steam tables. Most of the gas table property subprograms were developed by Osterle and Impink[17] for use in their work for the Pennsylvania Science and Engineering Foundation (see Section 2.4). They elected to curve fit the properties using a least squares method. When the need arose in the present work for additional properties (like the Gibbs free energy of formation) or the same properties for new species (like the enthalpy and entropy for COS, NH_3, and so forth), it was decided to use a table form for the property routines with linear interpolation. This approach saved a significant amount of time in programming the new properties. Arbitrary accuracy may be achieved by including more data in the tables.

In this section, we shall include only those routines which are the basic property subprograms. For example, it was convenient to write some auxiliary subroutines like TGASS which calculates the temperature of the gas using the gas composition, pressure, and molar entropy to define the state. Somewhat arbitrarily, we shall refer to this type of subroutine as an auxiliary subprogram, to be discussed in Section 4.6.

4.5.1 Gas Table Property Subprograms

By referring to Tables 3.2-2, 3.2-3, 3.2-5, and 3.2-6, we see that we need to consider the thermodynamic properties of twenty gaseous species and, although not a gas, the enthalpy of solid carbon. We need the standard Gibbs free energy change of formation, the molar enthalpy, and

the molar entropy for each of these gaseous species. Some of the properties like the Gibbs free energy of formations may, in fact, be zero. In addition, we shall need the equilibrium constant K_p for the reaction $1/2\ N_2 + 1/2\ O_2 \rightleftarrows NO$ for reasons which will become apparent in Section 4.6.

All of the enthalpies are assumed to be functions of the gas temperature only, consistent with the ideal gas assumption, except for carbon dioxide (CO_2), methane (CH_4), and water vapor (H_2O) for which the pressure effect is included. The entropy, of course, is a function of both the temperature and pressure, even for an ideal gas. The enthalpy of a species in reaction may be considered to be composed of three terms: the enthalpy of formation at some reference temperature minus the sensible enthalpy at the same reference temperature plus the sensible enthalpy at the temperature of interest. The reference temperature is taken to be absolute zero. Each of the above terms may be taken directly from the JANAF[21] tables, which uses the usual convention for enthalpy of formation; namely, the enthalpy of formation for an elemental gaseous compound (H_2, O_2, and so forth) is zero. The entropy and standard Gibbs free energies of formation are also taken directly from the JANAF tables. The pressure correction on entropy amounts to subtracting the product of the universal gas constant and the natural logarithm of the partial pressure (psia) of the species under consideration, which implies an arbitrary reference pressure of 1 psia. The gas table property subprograms are also listed in Appendix A.

The JANAF[21] tables have been used for all the properties except for the enthalpy of the CO_2, CH_4, and H_2O vapor, mentioned above. For these species, the steam tables and various thermodynamic charts have been used

in order to include the pressure effect. Before listing the purpose, the calling sequence, and the limitations for each routine, let us establish the following notation:

Symbol	FORTRAN Symbol	Meaning (Units)
ΔG_f°	DG	Standard Gibbs free energy of formation (Btu/lbmole)
$\bar{h}$	H	Molar enthalpy (Btu/lbmole)
$\bar{s}$	S	Molar entropy (Btu/lbmole-°R)
P	P	Pressure (psia)
p_i	Pi	Partial pressure (psia) of species i
T	T	Temperature (°F)
$K_{p_{NO}}$	KPNO	Equilibrium constant of NO formation reaction

4.5.1.1 Hydrogen (H_2)

Function HH2

Purpose: Computes the enthalpy of hydrogen as a function of temperature; $\bar{h} = f(T)$

Form: H = HH2(T)

Restrictions: Ideal gas

Function SH2

Purpose: Computes the entropy of hydrogen as a function of temperature and pressure; $\bar{s} = f(T, p_{H_2})$

Form: S = SH2(T, PH2)

Restrictions: Ideal gas
$p_{H_2} > 0$

4.5.1.2 Methane (CH_4)

Function HCH4

Purpose: Computes the enthalpy of methane as a function of temperature and pressure; $\bar{h} = f(T, p_{CH_4})$

Form: H = HCH4(T,PCH4)

Restrictions: Limited to vapor region

Function SCH4

Purpose: Computes the entropy of methane as a function of temperature and pressure; $\bar{s} = f(T, p_{CH_4})$

Form: S = SCH4(T,PCH4)

Restrictions: Limited to vapor region
$p_{CH_4} > 0$

Function DGCH4

Purpose: Computes the standard Gibbs free energy change of formation for methane as a function of temperature; $\Delta G_f^\circ = f(T)$

Form: DG = DGCH4(T)

Restrictions: Ideal gas
$80 < T < 5300$

4.5.1.3 Water Vapor (H_2O)

Function HH2O

Purpose: Computes the enthalpy of water vapor as a function of temperature and pressure; $\bar{h} = f(T, p_{H_2O})$

Form: H = HH2O(T,PH2O)

Restrictions: Limited to vapor region

Function SH2O

Purpose: Computes the entropy of water vapor as a function of temperature and pressure; $\bar{s} = f(T, p_{H_2O})$

Form: S = SH2O(T,PH2O)

Restrictions: Limited to vapor region
$p_{H_2O} > 0$

Function DGH2O

Purpose: Computes the standard Gibbs free energy change of formation for water vapor as a function of temperature; $\Delta G_f^\circ = f(T)$

Form: DG = DGH2O(T)

Restrictions: Ideal gas
$80 < T < 5300$

4.5.1.4 Carbon Monoxide (CO)

Function HCO

Purpose: Computes the enthalpy of carbon monoxide as a function of temperature; $\bar{h} = f(T)$

Form: H = HCO(T)

Restrictions: Ideal gas

Function SCO

Purpose: Computes the entropy of carbon monoxide as a function of temperature and pressure; $\bar{s} = f(T, p_{CO})$

Form: S = SCO(T,PCO)

Restrictions: Ideal gas
$p_{CO} > 0$

Function DGCO

Purpose: Computes the standard Gibbs free energy change of formation for carbon monoxide as a function of temperature; $\Delta G_f^\circ = f(T)$

Form: DG = DGCO(T)

Restrictions: Ideal gas
$80 < T < 5300$

4.5.1.5 Nitrogen (N_2)

Function HN2

Purpose: Computes the enthalpy of nitrogen as a function of temperature; $\bar{h} = f(T)$

Form: H = HN2(T)

Restrictions: Ideal gas

Function SN2

Purpose: Computes the entropy of nitrogen as a function of temperature and pressure; $\bar{s} = f(T, p_{H_2})$

Form: S = SN2(T,PN2)

Restrictions: Ideal gas
$p_{N_2} > 0$

4.5.1.6 Oxygen (O_2)

Function HO2

Purpose: Computes the enthalpy of oxygen as a function of temperature; $\bar{h} = f(T)$

Form: H = HO2(T)

Restrictions: Ideal gas

Function SO2

Purpose: Computes the entropy of oxygen as a function of temperature and pressure; $\bar{s} = f(T,p_{O_2})$

Form: S = SO2(T)

Restrictions: Ideal gas
$P_{O_2} > 0$

4.5.1.7 Argon (Ar)

Function HAR

Purpose: Computes the enthalpy of argon as a function of temperature; $\bar{h} = f(T)$

Form: H = HAR(T)

Restrictions: Ideal gas

Function SAR

Purpose: Computes the entropy of argon as a function of temperatue and pressure; $\bar{s} = f(T,p_{Ar})$

Form: S = SAR(T,PAR)

Restrictions: Ideal gas
$P_{Ar} > 0$

4.5.1.8 Carbon Dioxide (CO_2)

Function HCO2

Purpose: Computes the enthalpy of carbon dioxide as a function of temperature and pressure; $\bar{h} = f(T,p_{CO_2})$

Form: H = HCO2(T,PCO2)

Restrictions: Limited to vapor region

Function SCO2

Purpose: Computes the entropy of carbon dioxide as a function of temperature and pressure; $\bar{s} = f(T, p_{CO_2})$

Form: S = SCO2(T,PCO2)

Restrictions: Limited to vapor region
$p_{CO_2} > 0$

Function DGCO2

Purpose: Computes the standard Gibbs free energy change of formation of carbon dioxide as a function of temperature; $\Delta G_f^\circ = f(T)$

Form: DG = DGCO2(T)

Restrictions: Ideal gas
$80 < T < 5300$

4.5.1.9 Hydrogen Sulfide (H_2S)

Function HH2S

Purpose: Computes the enthalpy of hydrogen sulfide as a function of temperature; $\bar{h} = f(T)$

Form: H = HH2S(T)

Restrictions: Ideal gas

Function SH2S

Purpose: Computes the entropy of hydrogen sulfide as a function of temperature and pressure; $\bar{s} = f(T, p_{H_2S})$

Form: S = SH2S(T,PH2S)

Restrictions: Ideal gas
$p_{H_2S} > 0$

Function DGH2S

Purpose: Computes the standard Gibbs free energy changes of formation for hydrogen sulfide as a function of temperature; $\Delta G_f^\circ = f(T)$

Form: DG = DGH2S(T)

Restrictions: Ideal Gas
80 < T < 5300

4.5.1.10 Carbonyl Sulfide (COS)

Function HCOS

Purpose: Computes the enthalpy of carbonyl sulfide as a function of temperature; $\bar{h} = f(T)$

Form: H = HCOS(T)

Restrictions: Ideal gas
80 < T < 5300

Function SCOS

Purpose: Computes the entropy of carbonyl sulfide as a function of temperature and pressure; $\bar{s} = f(T, p_{COS})$

Form: S = SCOS(T,PCOS)

Restrictions: Ideal gas
80 < T < 5300; $p_{COS} > 0$

Function DGCOS

Purpose: Computes the standard Gibbs free energy change of formation for carbonyl sulfide as a function of temperature; $\Delta G_f^\circ = f(T)$

Form: DG = DGCOS(T)

Restrictions: Ideal gas
80 < T < 5300

4.5.1.11 Nitric Oxide (NO)

Function HNO

Purpose: Computes the enthalpy of nitric oxide as a function of temperature; $\bar{h} = f(T)$

Form: H = HNO(T)

Restrictions: Ideal gas

Function SNO

Purpose: Computes the entropy of nitric oxide as a function of temperature and pressure; $\bar{s} = f(T, p_{NO})$

Form: S = SNO(T,PNO)

Restrictions: Ideal gas
$p_{NO} > 0$

Function DGNO

Purpose: Computes the standard Gibbs free energy change of formation for nitric oxide as a function of temperature; $\Delta G_f^\circ = f(T)$

Form: DG = DGNO(T)

Restrictions: Ideal gas
$80 < T < 5300$

Function AKPNO

Purpose: Computes the equilibrium constant of the NO formation reaction $1/2\ N_2 + 1/2\ O_2 \rightarrow NO$ as a function of temperature; $K_{p_{NO}} = f(T)$

Form: KPNO = AKPNO(T)

Restrictions: Ideal gas
$-280 < T < 5300$

4.5.1.12 Hydroxyl (OH)

Function HOH

Purpose: Computes the enthalpy of hydroxyl as a function of temperature; $\bar{h} = f(T)$

Form: H = HOH(T)

Restrictions: Ideal gas
$-280 < T < 5300$

Function SOH

Purpose: Computes the entropy of hydroxyl as a function of temperature and pressure; $\bar{s} = f(T,p_{OH})$

Form: S = SOH(T)

Restrictions: Ideal gas
$-280 < T < 5300$; $p_{CH} > 0$

Function DGOH

Purpose: Computes the standard Gibbs free energy change of formation for hydroxyl as a function of temperature; $\Delta G_f^\circ = f(T)$

Form: DG = DGOH(T)

Restrictions: Ideal gas
$80 < T < 5300$

4.5.1.13 Monatomic Hydrogen (H)

Function HH

Purpose: Computes the enthalpy of monatomic hydrogen as a function of temperature; $\bar{h} = f(T)$

Form: H = HH(T)

Restrictions: Ideal gas
$-280 < T < 5300$

Function SH

Purpose: Computes the entropy of monatomic hydrogen as a function of temperature and pressure; $\bar{s} = f(T,p_H)$

Form: S = SH(T,PH)

Restrictions: Ideal gas
$-280 < T < 5300$; $p_H > 0$

Function DGH

Purpose: Computes the standard Gibbs free energy change of formation for monatomic hydrogen as a function of temperature; $\Delta G_f^\circ = f(T)$

Form: DG = DGH(T)

Restrictions: Ideal gas
$80 < T < 5300$

4.5.1.14 Monatomic Oxygen (O)

Function HO

Purpose: Computes the enthalpy of monatomic oxygen as a function of temperature; $\bar{h} = f(T)$

Form: H = HO(T)

Restrictions: Ideal gas
$-280 < T < 5300$

Function SO

Purpose: Computes the entropy of monatomic oxygen as a function of temperature and pressure; $\bar{s} = f(T,p_O)$

Form: S = SO(T,PO)

Restrictions: Ideal gas
$-280 < T < 5300$; $p_O > 0$

Function DGO

Purpose: Computes the standard Gibbs free energy change of formation for monatomic oxygen as a function of temperature; $\Delta G_f^\circ = f(T)$

Form: DG = DGO(T)

Restrictions: Ideal gas
80 < T < 5300

4.5.1.15 Ammonia (NH_3)

Function HNH3

Purpose: Computes the enthalpy of ammonia as a function of temperature; $\bar{h} = f(T)$

Form: H = HNH3(T)

Restrictions: Ideal gas
-280 < T < 5300

Function SNH3

Purpose: Computes the entropy of ammonia as a function of temperature and pressure; $\bar{s} = f(T, p_{NH_3})$

Form: S = SNH3(T,PNH3)

Restrictions: Ideal gas
-280 < T < 5300; $p_{NH_3} > 0$

Function DGNH3

Purpose: Computes the standard Gibbs free energy change of formation for ammonia as a function of temperature; $\Delta G_f^\circ = f(T)$

Form: DG = DGNH3(T)

Restrictions: Ideal gas
-280 < T < 5300; $p_{NH_3} > 0$

4.5.1.16 Nitrogen Dioxide (NO_2)

Function HNO2

Purpose: Computes the enthalpy of nitrogen dioxide as a function of temperature; $\bar{h} = f(T)$

Form: H = HNO2(T)

Restrictions: Ideal gas

Function SNO2

Purpose: Computes the entropy of nitrogen dioxide as a function of temperature and pressure; $\bar{s} = f(T, p_{NO_2})$

Form: S = SNO2(T,PNO2)

Restrictions: Ideal gas
$p_{NO_2} > 0$

Function DGNO2

Purpose: Computes the standard Gibbs free energy change of formation for nitrogen dioxide as a function of temperature; $\Delta G_f^\circ = f(T)$

Form: DG = DGNO2(T)

Restrictions: Ideal gas
$-280 < T < 5300$

4.5.1.17 Sulfur Monoxide (SO)

Function HSO

Purpose: Computes the enthalpy of sulfur monoxide as a function of temperature; $\bar{h} = f(T)$

Form: H = HSO(T)

Restrictions: Ideal gas
$-280 < T < 5300$

Function SSO

Purpose: Computes the entropy of sulfur monoxide as a function of temperature and pressure; $\bar{s} = f(T, p_{SO})$

Form: S = SSO(T,PSO)

Restrictions: Ideal gas
$-280 < T < 5300$; $p_{SO} > 0$

Function DGSO

Purpose: Computes the standard Gibbs free energy change of formation for sulfur monoxide as a function of temperature; $\Delta G_f^\circ = f(T)$

Form: DG = DGSO(T)

Restrictions: Ideal gas
$-280 < T < 5300$; $p_{SO} > 0$

4.5.1.18 Sulfur Dioxide (SO_2)

Function HSO2

Purpose: Computes the enthalpy of sulfur dioxide as a function of temperature; $\bar{h} = f(T)$

Form: H = HSO2(T)

Restrictions: Ideal gas

Function SSO2

Purpose: Computes the entropy of sulfur dioxide as a function of temperature and pressure; $\bar{s} = f(T, p_{SO_2})$

Form: S = SSO2(T,PSO2)

Restrictions: Ideal gas
$p_{SO_2} > 0$

Function DGSO2

Purpose: Computes the standard Gibbs free energy change of formation for sulfur dioxide as a function of temperature; $\Delta G_f^\circ = f(T)$

Form: DG = DGSO2(T)

Restrictions: Ideal gas
$-280 < T < 5300$

4.5.1.19 Sulfur Trioxide (SO_3)

Function HSO3

Purpose: Computes the enthalpy of sulfur trioxide as a function of temperature; $\bar{h} = f(T)$

Form: H = HSO3(T)

Restrictions: Ideal gas

Function SSO3

Purpose: Computes the entropy of sulfur trioxide as a function of temperature and pressure; $\bar{s} = f(T, p_{SO_3})$

Form: S = SSO3(T)

Restrictions: Ideal gas
$p_{SO_3} > 0$

Function DGSO3

Purpose: Computes the standard Gibbs free energy change of formation for sulfur trioxide as a function of temperature; $\Delta G_f^\circ = f(T)$

Form: DG = DGSO3(T)

Restrictions: Ideal gas
$-280 < T < 5300$; $p_{SO_3} > 0$

4.5.1.20 Sulfur (S_2)

Function HS2

Purpose: Computes the enthalpy of gaseous sulfur as a function of temperature; $\bar{h} = f(T)$

Form: H = HS2(T)

Restrictions: Ideal gas

4.5.1.21 Carbon (C)

Function HC

Purpose: Computes the enthalpy of pure solid carbon as a function of temperature; $\bar{h} = f(T)$

Form: H = HC(T)

Restrictions: Solid carbon

4.5.2 Steam Table Subprograms

We saw in Chapter 3 that many of the components utilize subcooled water, saturated steam-water mixtures, or superheated steam as the working fluid. We also saw that we need the capability to obtain just about all the thermodynamic properties in each of these three fluid regions. For this purpose, a proprietary set of steam tables has been used which is called by a master steam table subroutine FINDER. This subroutine returns all the other thermodynamic properties given the pressure and one other property as input. The subroutine has the following calling sequence

```
CALL FINDER(P,K,T,H,Q,S,V,IPH)
```

where P is pressure (psia); T, temperature (°F); H, specific enthalpy (Btu/lbm); Q, quality (fraction); S, specific entropy (Btu/lbm°R); V, specific volume (ft^3/lbm); and IPH, the phase of the fluid according to the convention established in Table 4.5-1. As we have already mentioned, the pressure P is always one input. The second input depends on the integer value for K, according to Table 4.5-2. All other properties are

Table 4.5-1
Correlation between IPH and Fluid Condition

IPH	Fluid Condition
1	Subcooled Water
2	Saturation Region
3	Superheated Steam
4	Supercritical Fluid

Table 4.5-2
Correlation between K and Input Parameters

K	Input Parameters
+1	P,T
-1	P,H
-2	P,Q
0	P,S

subsequently returned. Obviously, when K = +1, the fluid state must be superheated, subcooled, or supercritical, and when K = -2, the fluid must be saturated.

Zero specific enthalpy and zero specific entropy are assigned to the saturated liquid states at the freezing point of water (32.02°F). Note that this reference state is different from that used in the gas table

property routines where we used zero absolute temperature as the base. The enthalpies with respect to the two bases are related by

$$\overline{h} = 18.016\ h - 118256.07 \qquad (4.5\text{-}1)$$

where h is the specific enthalpy (Btu/lbm) from the steam tables using subroutine FINDER and $\overline{h}$ is the molar enthalpy (Btu/lbmole) from the gas tables using function HH2O. The entropies are similarly related by

$$\overline{s} = 18.016(s + 0.5443) \qquad (4.5\text{-}2)$$

where s is the specific entropy (Btu/lbm°R) from the steam tables using subroutine FINDER and $\overline{s}$ is the molar entropy (Btu/lbmole°R) from the gas tables using the function SH2O. When using FINDER and HH2O or SH2O in the same calculation, we must use Equations (4.5-1) and/or (4.5-2) to ensure consistency in our calculations.

4.6 Auxiliary Subprograms

The auxiliary subprograms perform a wide range of duties. These particular subprograms do not fit into the other four main categories of subprograms which we have discussed thus far. Again each subprogram is listed in Appendix A.

4.6.1 Subroutine ATERP

This subroutine performs a modified linear interpolation based on the equation for a straight line

$$y = mz + b \qquad (4.6\text{-}1)$$

where z is the abscissa, m the slope, b the y-intercept, and y the ordinate. The real dependent variable, however, is x which related to z by

$$x = \frac{1}{z} . \qquad (4.6\text{-}2)$$

This type of interpolation is appropriate when one tries to determine the equilibrium constant K_p for a temperature T between two temperatures in a table, since a plot of $\ell n K_p$ versus 1/T is linear over a wide range of temperatures. The calling sequence is

```
CALL ATERP(X,Y,M,XX,YY)
```

where X is the array of abscissa values,
Y is the corresponding array of ordinate values,
M is the number of (X,Y) pairs (M<50),
XX is the abscissa of interest, and
YY is the interpolated ordinate corresponding to XX.

If XX is less than X(1) or if XX is greater than X(M), appropriate error messages are printed out.

4.6.2 Block Data BLDATA

This non-executable subprogram provides a convenient location for storing data which are transferred to other subprograms via COMMON blocks. The primary types of data which are stored here are default values for variables in namelist $MASTER, molecular weights of various species in the coal and in various gaseous mixtures, higher and lower heating values of combustible species in the coal and power gas, and other constants.

We shall summarize the numerical values used for some of these parameters by way of Table 4.6-1 to Table 4.6-8. For the default values of the variables in namelist $MASTER, Appendix B.2 should be consulted, where the meaning of each variable is also given.

From Chapter 3, it became apparent that the molecular weights of the various species in the coal (before and after application of the Dulong approximation) and in the various gaseous mixtures (air, power gas, and products of combustion) must be specified. The variables WTC(I), where I=1 to 6, are the molecular weights of the C, H, O, N, S, and H_2O (liquid) in the coal. The numerical values used are summarized in Table 4.6-1. Note that the need for the molecular weight of the ash

Table 4.6-1
Molecular Weights of Species in Coal
(Before Dulong Approximation)

I	Species	Molecular Weight WTC(I)
1	C(s)	12.011
2	H	1.008
3	O	16.000
4	N	14.006
5	S	32.064
6	$H_2O(\ell)$	18.016

in the coal never arose and, fortunately, no value for this needs to be specified. After application of the Dulong approximation, the species become C, H_2, H_2O (vapor), N_2, S_2, and H_2O (liquid), for which the molecular weights are assigned the values shown in Table 4.6-2 in the array WTCD(I), for i=1 to 6. Again, the molecular weight of the ash

is not needed. The molecular weights of the species in the air which we assumed to be composed of N_2, O_2, Ar, and $H_2O(g)$, are assigned to the variable WTA(I), for I=1 to 4, and are shown in Table 4.6-3. For completeness, we assign the molecular weight of steam to WTS, where WTS = 18.016, since we also have steam entering the gasifier.

Table 4.6-2
Molecular Weights of Species in Coal
(After Dulong Approximation)

I	Species	Molecular Weight WTCD(I)
1	$C(s)$	12.011
2	H_2	2.016
3	$H_2O(g)$	18.016
4	N_2	28.013
5	S_2	64.128
6	$H_2O(\ell)$	18.016

Table 4.6-3
Molecular Weights of Species in Air

I	Species	Molecular Weight WTA(I)
1	N_2	28.013
2	O_2	32.000
3	Ar	39.948
4	$H_2O(g)$	18.016

In the gasifier model in Chapter 3, we assumed the presence of ten gaseous species in the power gas which was formed. The molecular weight of each of these species is summarized in Table 4.6-4, where the variable

name WTGF(I), I=1 to 10, is used. Similarly in the combustor model we assumed the presence of fifteen species, whose molecular weights which

Table 4.6-4
Molecular Weights of Species in Power Gas

I	Species	Molecular Weights WTGF(I)
1	H_2	2.016
2	CO	28.010
3	CH_4	16.042
4	$H_2O(g)$	18.016
5	CO_2	44.010
6	N_2	28.016
7	Ar	39.950
8	H_2S	34.080
9	COS	60.075
10	NH_3	17.031

we denote by WTCM(I), I=1 to 15, are summarized in Table 4.6-5. Finally it is convenient to combine the nineteen species in Tables 4.6-4 and 4.6-5

Table 4.6-5
Molecular Weights of Species in Combustor Product Gas

I	Species	Molecular Weights WTCM(I)
1	CO_2	44.010
2	$H_2O(g)$	18.016
3	N_2	28.016
4	O_2	32.000
5	Ar	39.950
6	NO	30.008
7	CO	28.010
8	H	1.008
9	O	16.000
10	OH	17.008
11	H_2	2.016
12	NO_2	46.008
13	SO	48.066
14	SO_2	64.066
15	SO_3	80.066

into one array, with the molecular weights assigned to array WTGMIX(I), I=1 to 19, as shown in Table 4.6-6. The subscript-species correlation shown in Table 4.6-6 is used in all subprograms in which a gaseous mixture is present except the gasifier (GSFR) and combustor (CMBSTR) subroutines and their associated auxiliary subroutines (SYSTEM and NEWTON).

Table 4.6-6
Molecular Weights of Species in the Generalized Gaseous Mixture

I	Species	Molecular Weight WTGMIX(I)
1	H_2	2.016
2	CH_4	16.042
3	$H_2O(g)$	18.016
4	CO	28.010
5	N_2	28.016
6	O_2	32.000
7	Ar	39.950
8	CO_2	44.010
9	H_2S	34.080
10	COS	60.075
11	NO	30.008
12	OH	17.008
13	H	1.008
14	O	16.000
15	NH_3	17.031
16	NO_2	46.008
17	SO	48.066
18	SO_2	64.066
19	SO_3	80.066

The species for which we take credit for contributing to the heating value of the power gas are H_2, CO, and CH_4 and in the coal $C(s)$, H_2, and S_2. We use the values shown in Tables 4.6-7 and 4.6-8 to compute effective heating values for the power gas and coal, respectively. Note the

Table 4.6-7
Heating Values of Combustible Species in Power Gas

I	Species	Higher Heating Values HHVG(I) (Btu/lbmole)	Lower Heating Value LHVG(I) (Btu/lbmole)
1	H_2	122,971	104,040
2	CO	121,750	121,750
3	CH_4	383,027	345,170

Table 4.6-8
Heating Values of Combustible Species in Coal

I	Species	Higher Heating Value HHVC(I) (Btu/lbm)	Lower Heating Value LHVC(I) (Btu/lbm)
1	C(s)	14,095	14,095
2	H_2	60,997	51,605
3	S_2	4,848.4	4,848.4

difference in units. The resulting effective heating values for the power gas and coal are used only in the efficiency calculations which are described in Section 4.6.6 and in the pollution calculation described in Section 4.6.16. The actual calculation of the heating values for the power gas takes place in subroutine GSFR and for the coal in subroutine DULONG, which is described in Section 4.6.3.

We complete the description of the data stored in BLOCK DATA by assigning the universal gas constant the value 1.987 Btu/lbmole°R, the difference between the Rankine and Fahrenheit temperatures the value 460 (°R), and atmospheric pressure the value 14.696 psia. The data sorted in BLOCK DATA is used throughout the computer program.

4.6.3 Subroutine DULONG

The purpose of subroutine DULONG is two-fold: to obtain the coal composition for the purpose of enthalpy determination using the Dulong approximation described in Section 3.2 and to then compute the higher and lower heating values of the coal based on this approximation. Using the assumptions and nomenclature of Section 3.2.1, the relevant equations for the weight fractions of $C(s)$, H_2, $H_2O(g)$, N_2, S_2, $H_2O(\ell)$, and ash in the coal are the following.

$$\omega_{d1} = \omega_{c1} \tag{4.6-1}$$

$$\omega_{d2} = \omega_{c2} - \frac{\nu_{d2}}{\nu_{c3}} \omega_{c3} \tag{4.6-2}$$

$$\omega_{d3} = \omega_{c3} + \frac{\nu_{d2}}{\nu_{c3}} \omega_{c3} \tag{4.6-3}$$

$$\omega_{d4} = \omega_{c4} \tag{4.6-4}$$

$$\omega_{d5} = \omega_{c5} \tag{4.6-5}$$

$$\omega_{d6} = \omega_{c6} \tag{4.6-6}$$

$$\omega_{d7} = \omega_{c7} \tag{4.6-7}$$

Using these adjusted weight fraction compositions, the higher and lower heating values are easily calculated with the help of the values in Table 4.6-8. For completeness, the effective molecular weight ν_{afc} of the ash free coal is also calculated here using

$$\nu_{afc} = \frac{1}{\sum_{i=1}^{6} \frac{\omega_{ci}}{\nu_{ci}(1-\omega_{c7})}} \qquad (4.6\text{-}8)$$

The calling sequence is

```
      CALL DULONG(WFC,
     1    WFCD,LVCOAL,HVCOAL,WTAFC)
```

where WFC(I) corresponds to ω_{ci} above, WFCD(I) to ω_{di}, and WTAFC to ν_{afc}. LVCOAL and HVCOAL are the calculated lower and higher heating values (But/lbm of coal) of the coal, respectively.

4.6.4 Subroutine DUMCMB

Subroutine DUMCMB is a dummy subroutine which simply takes the values of the parameters in the argument list of subroutine CMBSTR and puts them into a common block (labeled CMBST1) for use in subroutine SYSTEM. The reason for this rather strange maneuver is to facilitate the use of the component subroutines by using parameter lists to transfer data between two subprograms. However, in SYSTEM it is more convenient to use labeled common. It is not permissible in FORTRAN to have the same variable in both a parameter list and common block in the same subroutine.

4.6.5 Subroutine DUMGAS

Like subroutine DUMCMB, subroutine DUMGAS is also a dummy subroutine. The values in the argument list of subroutine GSFR are put into common

blocks (labeled GASFY1 and GASFY2). The reason for doing this is similar to that given for subroutine DUMCMB.

4.6.6 Subroutine EFFICY

It is appropriate here to define the four kinds of efficiencies which we shall use to assess the cycle performance in Chapter 5. The first efficiency which we define is the gasification efficiency. As the name suggests, we define this to be the ratio of the heating value of the power gas to the sum of the heating value of the coal and the heat added to the gasifier, all in consistent units, of course. The steam cycle efficiency is defined as the ratio of the net work output from the steam cycle to the heat input to the steam cycle. This is the only efficiency which does not depend on whether the higher or lower heating values are used. We define the combined cycle efficiency as the ratio of the net work output for the entire system to the heating value of the power gas. Finally, we define the coal-pile-to-bus-bar or station efficiency as the product of the combined cycle and gasification efficiencies reduced by a specified percentage because of station requirements for power, such as lighting, heating, and so forth. With the exception of steam cycle efficiency, the use of higher or lower heating values gives different results. As we shall see in Chapter 5, we shall consistently and somewhat arbitrarily use the station efficiency based on lower heating values to assess the performance of each cycle.

4.6.7 Subroutine HGAS2

This simple subroutine calculates the molar enthalpy of a gas specified to have a certain pressure (psia), temperature (°F), and composition (mole fraction). The species assumed to be present (with corresponding subscripts) are those shown in Table 4.6-6. The mole fraction composition MFG(I) for I=1 to 19, of the gaseous mixture along with the pressure P and temperature T are used in the call statement

```
CALL HGAS2(P,T,MFG,HG)
```

to obtain the molar enthalpy HG(Btu/lbmole) of the gaseous mixture. As mentioned before, pressure effects on enthalpy are included only for CH_4, H_2O, and CO_2. All remaining species are assumed to behave like ideal gases, for which the enthalpy is a function of temperature only. The molar enthalpy of each individual species, of course, is provided by the appropriate property subprograms described in Section 4.5.

4.6.8 Subroutine SGAS2

Like HGAS2, subroutine SGAS2 calculates another important property of a gaseous mixture given its pressure (psia), temperature (°F), and composition (mole fraction). This property is the molar entropy (Btu/lbmole°R) which we represent by SG. The calling sequence becomes

```
CALL SGAS2(P,T,MFG,SG)
```

where P, T, and MFG have the same meaning as in subroutine HGAS2. It should be recalled that the entropy, even for an ideal gas, is a function

of pressure. The molar entropy of each individual species is provided by the appropriate property subprograms described in Section 4.5.

4.6.9 Subroutine INVDET

Subroutine INVDET[22] provides the matrix inversion required by the multi-dimensional Newton-Raphson iteration to obtain a solution to the gasifier and combustor models. Numerical round-off error is reduced by maximizing the pivitol elements in the algorithm.

4.6.10 Subroutine MAIR

Subroutine MAIR takes the air composition on a four-component weight fraction basis and converts it to a composition on a four-component mole fraction basis, and compositions on nineteen-component mole and weight fraction bases. In addition, the molecular weight of the air is calculated. This enables the air to be treated as a special gas for which we may use the other auxiliary subprograms like HGAS2 which facilitate the calculations. Table 3.2-2 and Table 4.6-6 must be used to establish the correlation between species and subscript designations for the four- and nineteen-component compositions respectively.

4.6.11 Subroutine MGAS1

Subroutine MGAS1 takes the gasifier power gas composition on the ten-component mole fraction basis as defined by Table 3.2-3 and converts it to mole and weight fraction compositions on the nineteen-component basis defined in Table 4.6-6. In addition, the molecular weight of the power gas is calculated.

4.6.12 Subroutine MGAS2

Subroutine MGAS2 takes the fifteen-component combustor product gas composition as defined by Table 3.2-6 and converts it to the nineteen-component composition as defined by Table 4.6-6 by mole and weight fractions. The molecular weight of the product gas is also calculated.

4.6.13 Subroutine MGAS3

Subroutine MGAS3 simply converts the gas composition by mole fraction on the nineteen-component basis as defined by Table 4.6-6 to one by weight fraction on the same basis. The molecular weight of the gas is also calculated.

4.6.14 Subroutine NEWTON

Subroutine NEWTON performs the multi-dimensional Newton-Raphson iterations on the two systems of equations which describe the gasifier and combustor. The initial guess for the solution vector was chosen to minimize the number of iterations required to obtain a solution and is, in fact, the solution to a representative case. The mathematics of this iteration scheme are described in Section 3.2.2 and is not repeated here. The implementation of this scheme on the computer is rather tedious but straightforward. Mole fractions are generally calculated to fifth-place accuracy.

4.6.15 Subroutine SYSTEM

Subroutine SYSTEM contains the equations which we developed in Sections 3.2.1.1 and 3.2.1.2 for the gasifier and combustor models,

respectively. Each of the governing equations in these sections was written so that zero appeared on one side and all the other terms on the other. Except for this trivial modification, the equations which are stored in SYSTEM are practically identical in form to the ones written in Sections 3.2.1.1 and 3.2.1.2.

4.6.16 Subroutine POLUTE

In subroutine POLUTE, we compute the amount of nitric oxides NO_x and sulfur oxides SO_x that go up the power plant stack and into the atmosphere. The subroutine requires as input the composition of the stack gas (by mole fraction μ_i and weight fraction ω_i), the mass flow $w_{\delta g}$ of the stack gas (per lbm of coal), the higher heating value of the coal H_{HVC} and the "freeze temperature" T_F for the NO producing reaction. We shall calculate the amount of pollutants in units of pounds of NO_x (or SO_x) per million Btu of heat input. The higher heating value of the fuel is used for the heat input based on federal regulations.

The NO producing reaction $1/2\ N_2 + 1/2\ O_2 \rightleftarrows NO$ appears to slow down significantly in the reverse direction when the temperature is below about 2400°F.[23] Consequently, we shall calculate two values for the amount of NO_x pollution: NO_{Equil} assuming equilibrium at the combustor outlet temperature and NO_{Freeze} assuming the NO producing reaction "freezes" at T_F. Rather than doing a full-blown equilibrium calculation for temperature T_F, we assume that the mole fractions of $N_2(\mu_{N_2})$ and $O_2(\mu_{O_2})$ will not change significantly for the two temperatures and calculate the mole fraction of $NO(\mu_{NO_{Freeze}})$ from

$$\mu_{NO_{Freeze}} \cong K_p\sqrt{\mu_{N_2}\mu_{O_2}}$$

which is the equilibrium equation for 1/2 N_2 + 1/2 $O_2 \rightleftarrows$ NO with equilibrium constant K_p, to be evaluated at temperature T_F. Function AKPNO, of course, is used to get K_p at T_F. We shall see in Chapter 5 that the mole fraction of NO(μ_{NO}) is practically numerically equal to the weight fraction of NO(ω_{NO}), so it is reasonable to assume that

$$\omega_{NO_{Freeze}} \cong \mu_{NO_{Freeze}}$$

We have two weight fractions for NO: ω_{NO} from the original stack gas composition and $\omega_{NO_{Freeze}}$ from the NO producing reaction frozen at T_F. The expression for NO_{Equil} is given by

$$NO_{Equil} = 10^6\frac{(\omega_{NO} + \omega_{NO_2})w_{\delta g}}{H_{HVC}}$$

For NO_{Freeze}, we neglect the contribution by NO_2, since it turns out to be much smaller than that due to NO, and get

$$NO_{Freeze} \cong 10^6\frac{\mu_{NO_{Freeze}}w_{\delta g}}{H_{HVC}}$$

The amount of SO_x produced, SO_{Equil}, is similarly calculated by

$$SO_{Equil} = \frac{10^6(\omega_{SO} + \omega_{SO_2} + \omega_{SO_3})w_{\delta g}}{H_{HVC}}$$

Freezing of the SO_x producing reactions apparently does not occur physically and, therefore, is not modeled.

4.6.17 Subroutine TERP

This subroutine performs a linear interpolation based on the equation for a straight line

$$y = mx + b$$

where x is the abscissa, m the slope, b the y-intercept, and y the ordinate. The calling sequence is

```
CALL TERP(X,Y,M,XX,YY)
```

where X is the array of abscissa values,
Y is the corresponding array of ordinates,
M is the number of (X,Y) pairs (M<50),
XX is the abscissa of interest, and
YY is the interpolated ordinate corresponding to XX.

As in ATERP, appropriate error messages are printed out if interpolation is attemped outside the domain of X values.

4.6.18 Subroutine TGASH

Subroutine TGASH performs the inverse function of subroutine HGAS2. It was frequently necessary in the component models to determine the gas temperature TG(°F) given its pressure P (psia), molar enthalpy H (Btu/lbmole), and gas composition MFG(I) on the nineteen component mole fraction basis. Subroutine HGAS2 is used in a simple one-dimensional

Newton-Raphson iteration to accomplish this task. If convergence to a relative error of 10^{-5} does not occur in 15 iterations, an appropriate error message is printed. The calling sequence is

```
CALL TGASH(P,H,MFG,TG)
```

where P, H, and MFG are inputs and the gas temperature TG is the output.

4.6.19 Subroutine TGASS

Subroutine TGASS is completely analogous to subroutine TGASH. Now the gas temperature TG(°F) is to be found given the gas pressure P (psia), molar entropy S (Btu/lbm°R), and gas composition MFG(I) on the nineteen-component mole fraction basis. Again a simple Newton-Raphson iteration is used and an appropriate error message is printed if convergence does not occur in 15 iterations. The calling sequence is

```
CALL TGASS(P,S,MFG,TG)
```

where P, S, and MFG are the inputs and the gas temperature TG is the output.

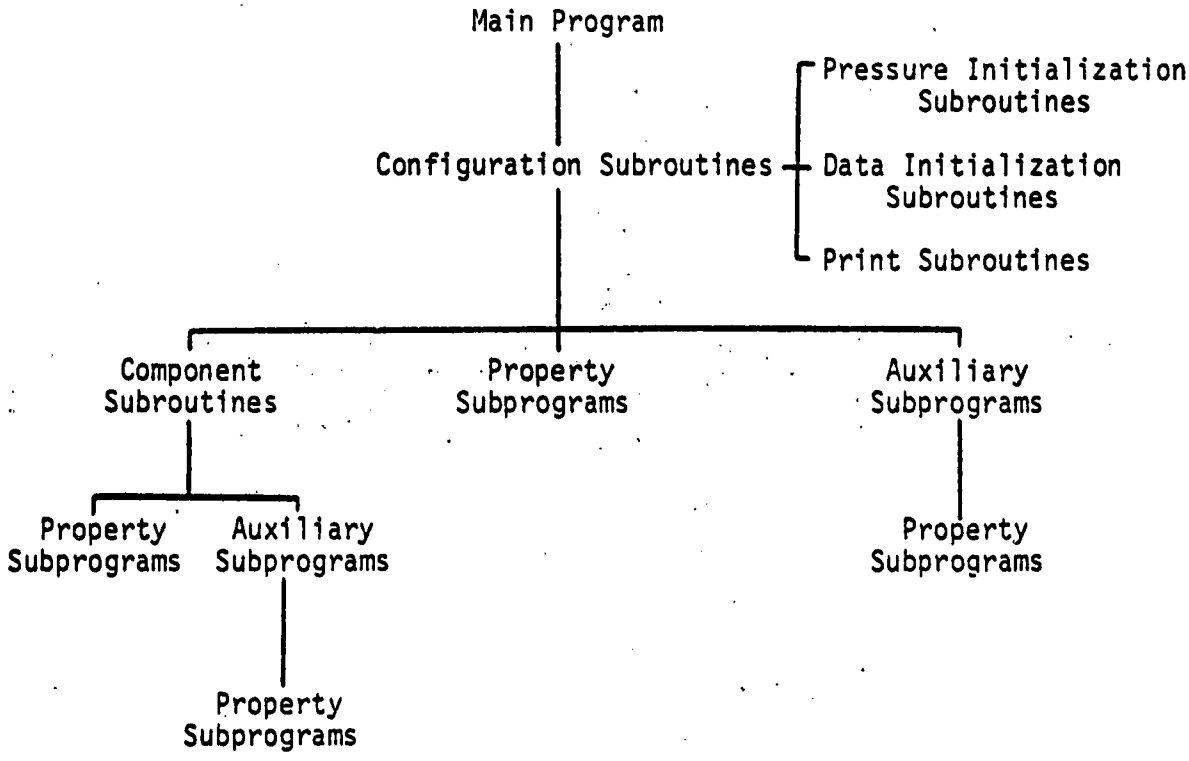

Figure 4.1-1 Program Hierarchy

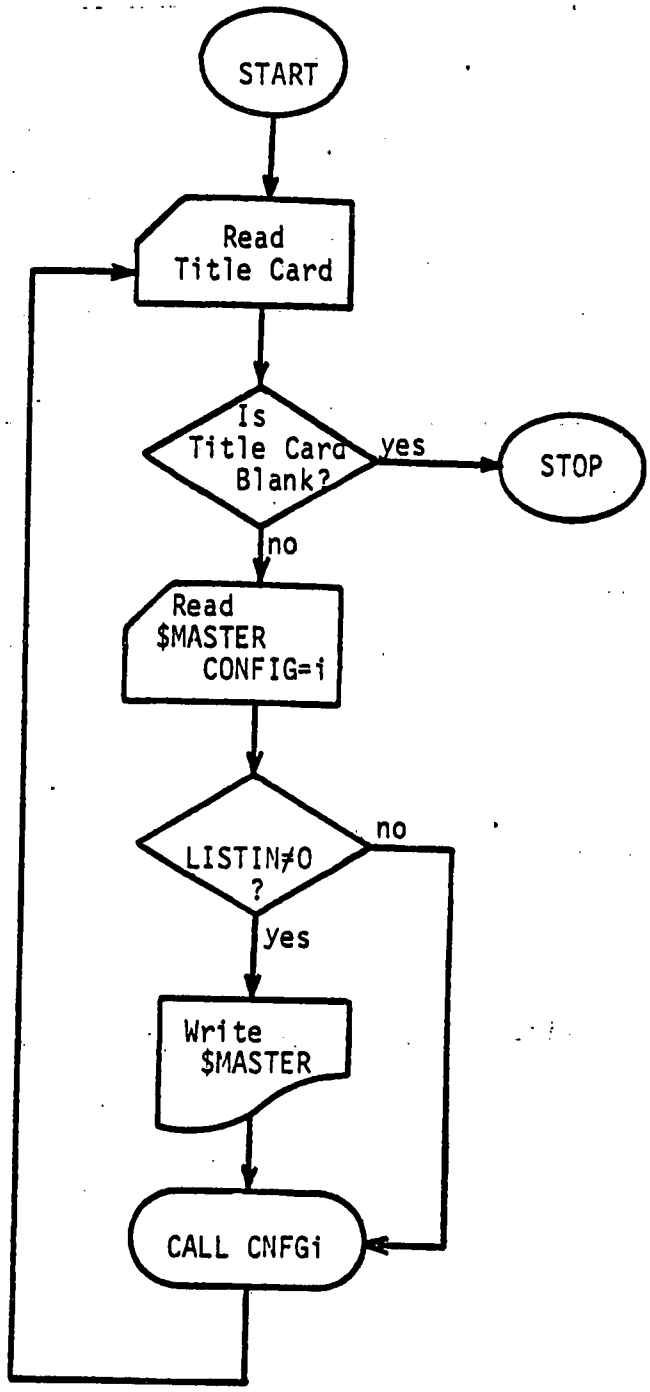

Figure 4.2-1 Flow Chart of Main Program CGACC

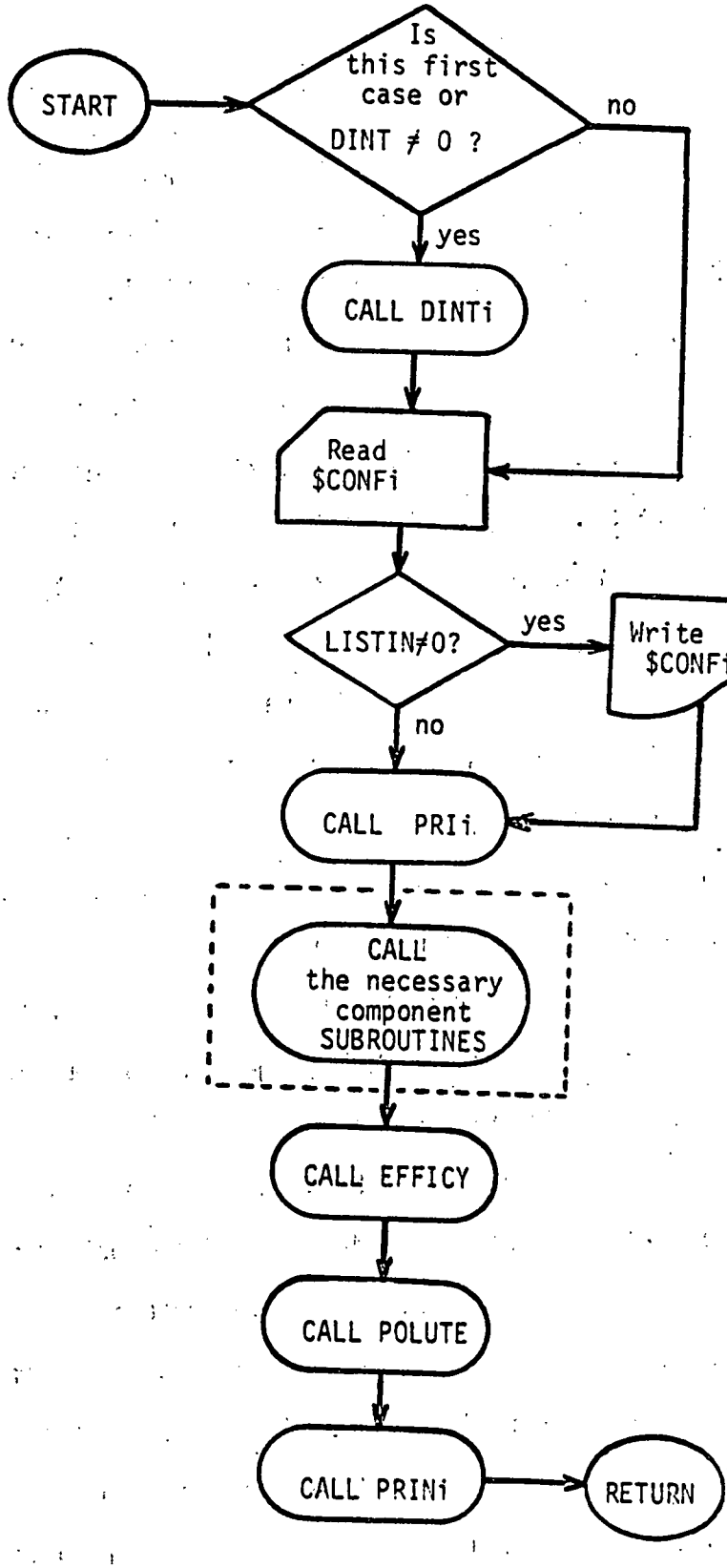

Figure 4.3-1 Simplified Flow Chart of Configuration Subroutines--CNFGi

CHAPTER 5

RESULTS

5.1 Introduction

In this chapter the computer program described in Chapter 4 is used to obtain the results which are needed to improve each basic configuration as well as to perform some parametric studies. It should be emphasized that the primary objective is to improve the performance of each integrated combined cycle within certain constraints. For example, the designs must meet federal gaseous emission criteria on SO_x and NO_x. Water and heat rejection requirements will be inherently determined from these analyses.

In Section 5.2, reasonable values are assigned to all specifiable cycle point parameters for the systems shown in Figures 2.3-1 to 2.3-4 followed by the calculation of the resulting station efficiency for each of these four base cases. The computer program, of course, provides this result as well as all other results to follow. Then in Section 5.3, the effect on station efficiency of adding regenerative feedwater heaters, gas-to-gas regenerators, and intercooled compressors to each configuration will be examined. As each effect is determined, a judgement will be made as to whether that particular addition remains in each cycle or not. Each configuration will subsequently be optimized in Section 5.4 by varying certain key cycle point parameters without consideration of the pollution criteria. Then in Section 5.5 each configuration will be reviewed to determine if the designs meet the criteria on gaseous effluents. Any of the configurations which will require modifications will be re-optimized. Following this, each optimized configuration will be summarized in Section 5.6 by way of presenting new cycle schematics and discussing the resulting

water and heat rejection requirements. Then in Section 5.7, a limited number of parametric studies will be presented. Finally in Section 5.8, some of the assumptions that have been made during the course of these analyses will be discussed.

It is important to note that the computer program was not written to provide an automatic optimization. The purpose of the program is to perform all the tedious calculations which are necessary to obtain the kind of results to be presented in this chapter. We shall soon see that a careful examination of the results printed in the computer output will enable us to make certain observations that may otherwise be overlooked. This approach is also helpful in trying to explain some of the sometimes surprising results to be presented shortly. For obvious reasons it is not possible to include the computer printout for every case which is analyzed; rather, only results which are germane to the discussion at hand or possibly a subsequent discussion will be presented, usually in tabular form.

5.2 Specification of Parameters and Calculation of Base Case Station Efficiencies

In Section 2.3 cycle component layouts for each of the four configurations were developed, with the resulting cycle schematics shown in Figures 2.3-1 to 2.3-4. In this section it is now necessary to assign values to each of the specifiable parameters for these cycles. While this may seem somewhat arbitrary, it is justified since many of these assigned values will be varied later during either the optimization or the parametric studies. The goal for now is simply to obtain four bases cases, one for each configruation, from which this study may begin. Let us first restrict our attention to

Configuration 1, the case of an adiabatic gasifier integrated with a waste heat combined cycle. For the other configurations, it will be necessary only to indicate the pertinent changes from the input to Configuration 1.

First, let us fix the coal and air compositions and the specific heat of the ash. Table 5.2-1 gives the ultimate analysis of the coal, which is

Table 5.2-1
Ultimate Analysis of Coal
(Weight Fraction)

Carbon	0.7304
Hydrogen	0.0528
Oxygen	0.0616
Nitrogen	0.0088
Sulfur	0.0264
Moisture	0.0300
Ash	0.0900

assumed to be Pennsylvania high volatile bituminous[17], the composition of which has been adjusted for 3 percent moisture and 9 percent ash. Note that the weight fraction of *liquid* water is included in the ultimate analysis and recall that the Dulong approximation assumed that all the oxygen combines with the necessary hydrogen to form water *vapor*; this distinction is necessary when the entahlpy of the coal is later determined in the gasifier model. It should be noted that the ash will leave the gasifier at an elevated temperature representing a sensible heat loss and that most of the sulfur will be converted to hydrogen sulfide of which most is removed representing a chemical energy loss. The air composition is given in Table 5.2-2. Note that dry air is assumed for these and all remaining calculations. Raznjevic[24] gives the specific heat of ash as 0.19 Btu/lbm-°F, and in the interest of being slightly conservative

let us use 0.20 Btu/lbm-°F. The effect of coal composition on the cycle performance of only Configuration 1 will be examined in Section 5.7 by using three other types of coal.

Table 5.2-2
Composition of Air
(Weight Fraction)

N_2	0.7546
O_2	0.2319
Ar	0.0135
$H_2O(g)$	0.0000

Next, it is convenient to specify all the pressure-related data including any assumed pressure drops. The gasifier is assumed to be operated at 11 atm, the combustor at 10 atm, the steam-side of the boiler at 1600 psia, and the condenser at 1.75 psia (or approximately 3.5 inches of mercury). Ambient pressure is taken to be 14.7 psia. The following pressure drops are assumed in the gas cycle portion: none through the gasifier and combustor, a 10 psi drop through the steam-side of the steam generator with a total of 0.7 psi through the gas-side, a 0.1 psi drop through the gas cooler, and a 0.1 psi drop through the gas cleanup system. Note that there is an implied pressure drop of more than 10 psi through the gas throttle valve, representing additional conservatism in the analysis. In the steam-cycle portion the following pressure drops are assumed: 0.0362, 0.2569, and 0.3974 psi through the gas-side of the superheater, evaporator, and economizer sections of the boiler, respectively (see Appendix B), and 10, 0, and 0.1 psi through the same sections on the steam-side; a 400 psi drop through the steam throttle valve; and none in the condenser.

Now the temperature-related input is specified. Ambient conditions are assumed for each air, coal, and water inlet to the system, with

ambient temperature taken to be 77°F. The gasifier is assumed to operate at 2000°F with the same ash discharge temperature. Superheated steam is assumed to enter the gasifier at 620°F. The gas is assumed to be cooled to 200°F by the gas cooler. The combustor is assumed to operate at 2000°F, the practical limit for a conventional land-based gas turbine. Superheated steam at a temperature of 960°F is generated in the boiler with 7°F of subcooling assumed at the evaporator inlet. The cooling water to the condenser is at 70°F and is assumed to undergo a 5°F temperature rise. Finally, the pinch point temperature differences within the steam generator and boiler is specified to be greater than or equal to 40°F.

The various efficiencies may now be assigned representative values. The following component efficiencies are assumed: 0.90 for the air compressors, 0.75 for the pump serving the steam generator, 0.85 for the gas turbine, 0.90 for the steam turbine, and 0.85 for the feedwater pump. According to Section 3.14, the capability exists to remove H_2S, COS, CO_2, and NH_3 from the power gas. It is conservatively assumed that only 90 percent by weight of the H_2S is removed; all the remaining gas is eventually burned in the combustor, since this would result in economical operation of the gas cleanup system. This completes the input specifications for Configuration 1.

In the other three configurations, the cycle point input is chosen deliberately to be identical to that of Configuration 1 where possible. This will enable us to make a more straightforward comparison of the results for the four base cases. In Configurations 2 and 4, the combustor exit temperature is no longer assumed to be 2000°F; instead combustion

with 10 percent excess air is required, since these configurations use a supercharged boiler. It is also assumed for these two configurations that the water which enters the evaporator section of the boiler is at least 7°F subcooled. Refer to Section 3.4 for a description of the subtle distinction between the models for the two different types of boilers. In Configurations 3 and 4, there is no air compressor serving the gasifier, and so the corresponding input conditions are no longer relevant. All other input for these configurations remains the same. One other point should be made. In Configuration 3, the heat source for the endothermic gasifier is the combustor, and both of these components operate at 2000°F which implies heat transfer through a zero temperature difference and an infinite heat transfer area. For now, let us accept this and reexamine this issue after the optimization is completed.

Recall that in Section 4.6, for the description of subroutine EFFICY, four different efficiencies were defined: the station, the combined cycle, the steam cycle, and the gasification efficiencies. In all of these, low heating values will be used consistently. Furthermore, let us agree to use the station efficiency to assess cycle performance. Included in this will be an assumed 10 percent station load, which includes station auxiliaries, lighting, generation losses, and so forth. Table 5.2-3 summarizes the resulting efficiencies for each configuration.

Table 5.2-3
Summary of Efficiencies for Base Cases

	Efficiency (%) of Configuration			
	1	2	3	4
Station	34.57	29.87	38.63	32.72
Combined Cycle	44.36	38.34	45.48	38.52
Steam Cycle	35.02	35.02	35.02	35.02
Gasification	86.58	86.58	94.38	94.38

By examining the station efficiencies, we note that the waste heat configurations perform better than those using a supercharged boiler, and that the configurations incorporating an endothermic gasifier perform better than those with an adiabatic gasifier. To help explain these trends, let us summarize from the computer output the flow, heat, and work quantities for each configuration as well as other pertinent miscellaneous information as shown in Table 5.2-4. It should be noted at this point that all flows, heat, and work quantities are always given with respect to a pound of coal. Furthermore, the lower heating value of the coal described earlier is 12747 Btu (per pound of coal). This provides a convenient reference value to which all work and heat quantities may be compared. For example, we see that approximately 20 percent of the heating value of the coal is thrown away in the gas cooler for Configurations 1 and 2, but only 5 percent for Configurations 3 and 4. For completeness, the lower heating values of the power gas are also given in this table. These values are qualitatively consistent with those obtained in Section 2.2, where coal gasification is first discussed.

Table 5.2-4
Summary of Miscellaneous Results for Base Cases

	Configuration			
	1	2	3	4
Flows (lbm)				
Gasifier				
Coal	1.000	1.000	1.000	1.000
Steam	0.022	0.022	0.997	0.997
Air	3.783	3.783	--	--
Dirty Gas	4.715	4.715	1.907	1.907
Ash	0.090	0.090	0.090	0.090

Table 5.2-4 (Continued)

	Configuration 1	2	3	4
Flows (lbm) (continued)				
Gas Cleanup				
Dirty Gas	4.715	4.715	1.907	1.907
Water	0.285	0.285	0.179	0.179
Clean Gas	4.977	4.977	2.061	2.061
Waste	0.023	0.023	0.025	0.025
Combustor				
Fuel	4.977	4.977	2.061	2.061
Air	19.845	6.732	23.764	10.887
Products	24.822	11.709	25.825	12.948
Boiler				
Gas-side	24.822	11.709	25.825	12.948
Steam-side	3.920	5.649	4.258	5.568
Net Work (Btu)				
Gas Cycle	3018	1525	3432	1967
Steam Cycle	1878	2706	2039	2667
Total	4896	4231	5471	4634
Low Heating Values				
Coal (Btu/lbm)	12747	12747	12747	12747
Gas (Btu/SCF)	135	135	288	288
Heat Transfer (Btu)				
To Gasifier from Combustor	0	0	5041	5041
To Steam Cycle	5362	7727	5823	7615
Gas Cycle Loss	4367	3495	3492	3165
From Steam Cycle	3484	5021	3784	4948
Excess Air to Combustor (%)	224	10	140	10
Combustor Exit Temp. (°F)	2000	3250	2000	3057
Stack Gas Temp. (°F)	324	263	319	423
Gas Cooler Heat Loss (Btu)	2606	2606	623	623
Minimum Temp. Differences (°F)				
Steam Generator	1380	1380	733	733
Boiler	40	140	40	300

Let us first restrict our attention to Configurations 1 and 2. From the flows given in Table 5.2-4 it may be seen that these two configurations basically differ in the amount of gas flow through the boilers. The reason for this, of course, is that the fuel is burned by design with a large amount of excess air for Configuration 1 compared to the specified 10 percent for Configuration 2. The net effect of this and the larger amount of heat transfer to the steam cycle for the supercharged boiler cases is to de-emphasize the gas cycle. Recall from Section 2.1 that an alternate expression for the combined cycle efficiency was given as

$$\eta_{cc} = 1 - \left(\frac{Q_\ell + Q_2}{Q_1}\right) + \frac{Q_2}{Q_1}\eta_2 \qquad (2.1\text{-}10)$$

Actually calling η_{cc} the combined cycle efficiency is a misnomer here since it is convenient to interpret Q_1 as the heating value of the coal, not of the gas, actually resulting in an effective station efficiency without the usual 10 percent station load included. Note further that η_2 represents the steam cycle efficiency and Q_2 the amount of heat transferred to the steam cycle from the gas cycle. The sum of Q_ℓ and Q_2 must be less than Q_1 in order to have work produced by the first cycle. Table 5.2-4 clearly shows that the sum of Q_ℓ and Q_2 is higher for Configuration 2 compared to Configuration 1, while η_2 is identical. Note that Q_ℓ is lower for Configuration 2 but Q_2 is much higher, resulting in lower performance for Configuration 2. The same line of reasoning applies to the comparison between Configurations 3 and 4. When Configuration 3 is compared to Configuration 1, it is seen that the former is superior primarily because of the much lower gas cycle heat loss which more than makes up for the higher heat transfer to the steam cycle. In Configuration 4, both the

heat loss and heat transfer to the steam cycle are lower than in Configuration 2 with both having the same steam cycle efficiency. Equation (2.1-10) clearly shows that the efficiency of Configuration 4 should be greater than that of Configuration 2. When all the above considerations are taken into account, Configuration 3 should be expected to have the best performance and does.

Let us briefly discuss some of the other efficiencies shown in Table 5.2-3. Note that the gasification efficiencies for the same gasifier type are identical, and that those for the endothermic configurations are higher than those for the adiabatic. We must be cautious, however, and not read too much into this. If the latent heat of vaporization of the steam required by the gasification process were included in the denominator of the definition of the gasification efficiency, then all such efficiencies would have practically the same value. This is of no real concern since the station efficiency is independent of the definition of gasification efficiency. Note that the combined cycle efficiencies, as they have been defined, are significantly higher than the station efficiencies, since the later include gasification system losses and the assumed 10 percent station load. Also, as has been already noted, the steam cycle efficiency is identical for all four configurations, since the steam cycle operating conditions are identical. For completeness, let us define gas cycle efficiency as the ratio of the net work produced by the gas cycle including the gasification system to the heating value of the gaseous fuel, in consistent units of course. For Configurations 1 to 4 respectively, these are 27.35, 13.83, 28.52, and 16.35 percent. It is seen that the

gas cycle in the configurations employing a supercharged boiler is definitely de-emphasized. The result, as we have seen, has been poorer performance for these configurations. Clearly by increasing the work produced in the gas cycle compared to that of the steam cycle, better performance can be expected.

Let us verify that the minimum temperature differences within the steam generator and boilers are equal to or greater than the specified minimum of 40°F. Table 5.2-4 shows that this condition is easily met in the steam generator for each configuration. This clearly shows that there is sufficient sensible heat in the power gas to raise the required amount of steam needed for the gasification process. Since endothermic gasification requires more steam, the minimum temperature difference is lower for Configurations 3 and 4 compared to Configurations 1 and 2. The minimum temperature difference within the waste heat boilers of Configurations 1 and 3 is seen to be exactly 40°F, but must be greater than this in the supercharged boilers to ensure the presence of subcooled water in the economizer section. In Figures 5.2-1 and 5.2-2, the T-Q diagrams are shown for the boilers of Configurations 1 and 2, respectively. These temperatures are representative of each type of boiler. Note that the heat transfer within each boiler section is also given on each figure. Note also the locations of the pinch points. In Chapter 3 it was claimed that the pinch point for the supercharged boiler must occur between the economizer and stack. This is indeed the case here. Finally note the much larger temperature clearance throughout the supercharged boiler compared to the waste heat boiler; this results in greater irreversibilities

and explains qualitatively why the configurations employing a supercharged boiler do not perform as well as those incorporating a waste heat boiler.

5.3 Effect of Additional Components

5.3.1 Regenerative Feedwater Heaters

The purpose of this section is to show how the station efficiency is affected by regenerative feedwater heating. As we shall soon see, this change will increase the steam cycle efficiency. It is the station efficiency, however, that is to be improved. Improving the gas cycle, steam cycle, or gasification efficiencies in and of themselves will not necessarily improve the overall performance.

In order to keep the steam cycle simple and so as not to obscure the basic effect of feedwater heating, let us use only one closed feedwater heater and one open feedwater heater, the latter of which can also serve as a deaerator. Following the usual practice of placing the deaerator last in the feedwater train, the steam cycle is modified as shown in Figure 5.3-1. Note that the "condensate" on the shell-side of the closed feedwater heater is flashed into the shell-side of the condenser through a throttle valve. The heating of the feedwater is accomplished by extracting a small portion of the turbine flow. The first extraction occurs at a higher pressure, of course, than the second. The lowest pressure in the steam cycle occurs at the turbine exit, where the exhaust flow enters the condenser. Note that it is necessary to add a condensate pump to the feedwater train for two reasons. The first is that two-phase flow through the tube-side of the closed feedwater heater is undesirable and adding heat to the saturated liquid from

the condenser at the condenser shell-side pressure would tend to form vapor. The pump serves to subcool the fluid by increasing the pressure. The second reason for the condensate pump is that the deaerator is an open heater at a pressure above the shell-side condenser pressure. Obviously a pump is needed to take the condensate at the condenser pressure and deliver it to the deaerator at a higher pressure. Figure 5.3-1 is applicable to the steam cycle of all four configurations. Reasonable values for the new specifiable parameters will now be assigned.

The pressure related data are given first followed by the other data. Let us assume that the first extraction flow occurs at a pressure of 30 psia and the second at 6 psia. The shell-side condenser pressure remains the same as before. Let us assume no additional pressure drops, since a lumped loss of 400 psi is already used. The only temperature-related data that needs to be specified is the terminal temperature difference in the closed feedwater heater which is taken to be 3°F. The efficiency of each turbine stage is taken to be 0.90 and that of the condensate pump also 0.90. The feedwater pump efficiency is unchanged from before. In Section 5.4, more realistic values for the low-pressure steam turbine efficiencies will be used.

When the steam cycles of each of the basic cycles of Section 5.2 are modified according to Figure 5.3-1 using the above data, the somewhat surprising results shown in Table 5.3-1 are obtained. The station efficiency for each configuration decreased slightly. As expected, the regenerative feedwater heating, however, did increase the steam cycle efficiency from 35.02 percent to 37.88 percent. The deterioration in in station efficiency may be explained by comparing the heat rejected

from the steam cycle in the condenser to the heat loss through the stack gas. Feedwater heating tends to increase the stack gas temperature, since hotter

Table 5.3-1
Results with Feedwater Heating

	Configuration 1	2	3	4
Station Efficiency (%)				
Without	34.57	29.87	38.63	32.72
With	34.29	29.47	38.32	32.32
Steam Cycle Efficiency (%)				
Without	35.02	35.02	35.02	35.02
With	37.88	37.88	37.88	37.88
Increase in Stack Gas Heat Loss over Base Case (Btu)	510	732	553	724
Decrease in Steam Cycle Heat Rejected over Base Case (Btu)	470	676	510	669
Final Feedwater Temp. (°F)				
Without	122.8	122.8	122.8	122.8
With	252.9	252.9	252.9	252.9
Stack Gas Temp. (°F)				
Without	324.1	262.8	319.1	422.8
With	405.7	502.9	402.0	622.9
Dew Point Temp. (°F)	93	119	116	141

water enters the economizer. Let us refer to the temperature of the feedwater into the economizer as the final feedwater temperature. From Table 5.3-1, it is seen that for all configurations, this temperature has increased from 122.8°F to 252.9°F. The stack gas temperature is seen to be correspondingly higher. In each case, the increase in heat loss through the stack is greater than the savings in heat rejected from the steam cycle. Although the steam cycle efficiency is improved,

this improvement is not enough to improve the station efficiency. However, this could not be known a priori because of the two competing effects.

Although the above trend indicates that cycle performance deteriorates slightly when feedwater heating is employed, the heaters will be kept in the cycle for the reasons which follow. In Table 5.3-1, the dew point temperatures are given for each configuration. Without feedwater heating, the final feedwater temperature is 122.8°F, and Configuration 4 would probably begin to condense some of the water vapor locally within the economizer. Furthermore, this final feedwater temperature is a direct result of the 1.75 psia assumed condenser pressure. If a pressure of 0.75 psia were assumed, the final feedwater temperature without heating would be about 93°F. Clearly, all four configurations would probably have local consensation in the stack gas. This is to be avoided because of the corrosive nature of the acid which would form. Another reason for keeping the feedwater heaters in the cycle is to provide a convenient location to deaerate the water, namely the open feedwater heater. Finally, a higher stack gas temperature increases the so-called stack effect, and a smaller diameter stack may be used. For these reasons, the two feedwater heaters will be kept in each configuration, and the loss of less than 0.5 percentage points in station efficiency will be accepted. Unless otherwise stated, all subsequent results are presented with the regenerative feedwaters heaters in the steam cycle.

5.3.2 Intercooled Compressor Serving the Combustor

Next the air compressor serving the combustor is replaced with a two-stage intercooled compressor on each configuration. The schematic

of this modified portion of the gas cycle is shown in Figure 5.3-2 and applies to all four configurations. The intercooler serves to reduce the effective temperature of the gas during compression, tending to make the process more nearly isothermal, which requires much less work than adiabatic compression. It is for this reason that the effect of an intercooled compressor on each of the four configurationsis examined. As always, it is the station efficiency that must be used as a basis for comparison.

The new data applicable to the modified portion of the cycles must first be specified. It is easily shown that the optimum pressure ratio for each stage of the two-stage compression is equal to the square root of the product of the initial and final pressures. This results in the minimum amount of total compressor work being required. Since the combustor is assumed to operate at 10 atmospheres, the first-stage outlet pressure is taken to be 3.162 atmospheres. A 0.1 psi drop through the intercooler is further assumed. The temperature to which the air is cooled in the intercooler must be specified. It is arbitrarily assumed that the air may be cooled to within 50°F of ambient or to 127°F. Each stage of compression is assumed to have an efficiency of 0.9.

With these modifications to each configuration and with the regenerative feedwater heaters now in the system, the results summarized in Table 5.3-2 are obtained. It should first be noted that this modification does not improve station efficiency for any configuration. The most immediate effect of intercooling is seen in the reduction of the temperature of the air to the combustor. In Configurations 1 and 3, this results in less air flow to the combustor since the lower air temperature is a more effective diluent. However, in Configurations 2 and

4, the amount of air to the combustor is fixed since 10 percent excess air is stipulated. Now the lower air inlet temperature serves to reduce the combustor outlet temperature.

Table 5.3-2
Results with Intercooled Compressor
Serving the Combustor

	Configuration 1	2	3	4
Station Efficiency (%)				
Without	34.29	29.47	38.32	32.32
With	32.75	28.74	36.48	31.19
Air Temp. to Combustor (°F)				
Without	622.1	622.1	622.1	622.1
With	378.7	378.7	378.7	378.1
Air Flow To Combustor (lbm)				
Without	19.84	6.73	23.76	10.89
With	17.06	6.73	20.46	10.89
Combustor Outlet Temp. (°F)				
Without	2000.	3250.	2000.	3057.
With	2000.	3154.	2000.	2920.
Gas Cycle Heat Loss (Btu)				
Without	4877.	4228.	4045.	3889.
With	5391.	4681.	4661.	4601.
Heat to Steam Cycle (Btu)				
Without	4852.	6994.	5270.	6891.
With	4375.	6430.	4699.	6001.
Gas Cycle Net Work (Btu)				
Without	4856.	4175.	3432.	1967.
With	4638.	4071.	3387.	2145.

From the tabulation of results, it can further be seen for Configurations 1 and 3 that the gas cycle heat loss increases substantially while the heat transfer to the steam cycle decreases by a smaller amount. The intercooling is the primary reason for the additional heat loss. Since the steam cycle

efficiency is unchanged (for all configurations), the station efficiency must decrease. Less heat is transferred to the steam cycle primarily because there is less gas flow. It is further shown for Configurations 1 and 3 that the net amount of work produced in the gas cycle has decreased; the work of compression decreased but the work of expansion decreased by a greater amount, a direct result of the lower gas flow due to the lower air flow. Clearly, for Configurations 1 and 3, intercooled compressors serving the combustor do not improve performance.

Let us now examine Configuration 2. Again the gas cycle heat loss increases but the heat transfer to the steam cycle decreases by an amount greater than this. Recall from Equation (2.1-10) that this heat transfer to the steam cycle is multiplied by n_2. The decrease in $(Q_\ell + Q_2)/Q_1$ is seen to be smaller than the decrease in $\frac{Q_2}{Q_1} n_2$, resulting in poorer performance. Again intercooling causes the effective gas cycle heat loss to increase, and the lower heat transfer to the steam cycle is caused by the lower combustor exit temperature. To make matters worse, the stack gas temperature increased about 60°F (not shown). As before, the net gas cycle work has decreased, although some work of compression is saved. Intercooling is not desirable, therefore, in Configuration 2.

A similar line of reasoning applies to Configuration 4 except that now the net gas cycle work has increased. However, the decrease in total heat rejected from the gas cycle compared to the decrease in the weighted heat transfer to the steam cycle, results in overall deteriorated performance.

In summarizing, the addition of an intercooled compressor serving the combustor is not warranted. Unless otherwise stated, all subsequent

results are presented without intercooled air compressors serving the combustor.

5.3.3 Regenerator within Gas Clean-up System

Let us examine the temperature of gas leaving the steam generator for the new base cases, which include feedwater heating but not intercooled compression. For Configurations 1 and 2 the steam generator gas exit temperature is 1982°F and for Configurations 3 and 4 only 820°F. Note that the exit temperature of the adiabatic gasification type of configurations is much higher than that of the endothermic type. This is caused by the much higher steam demand to the gasifier for the latter, which is a characteristic of endothermic gasification as seen in Section 5.2. Generating significantly more steam for the gasifier removes more sensible heat from the power gas, thus lowering its temperature substantially. Since the gas must be cooled for the gas cleanup operation, a great amount of sensible heat is lost in the gas cooler when the gas temperature is excessively high. In fact, this is the chief reason why the endothermic configurations perform better than the adiabatic. Clearly, if these heat losses could be reduced, then the cycle performance would be improved.

A gas-to-gas counterflow heat exchanger between the "dirty" power gas entering the gas cleanup system and the "clean" gas leaving this system will reduce these losses. We may also refer to this device as a regenerator, since heat is being transferred from one fluid stream in the cycle to another. Figure 5.3-3 shows how each cycle must now be modified to include this new component. As noted in Section 3.11, the the regenerator effectiveness must be specified, which shall be taken

to be 0.80 for now. Later in Section 5.7 a parametric study on this parameter will be done. The pressure drop on each side of the regenerator will be taken to be 0.1 psi.

When this modification is made to the cycles, the results summarized in Table 5.3-3 are obtained. The improvement in cycle performance is dramatic, especially for the first two configurations. Without the regenerator in service, the configurations with an endothermic gasifier performed better than those with an adiabatic gasifier. This is not surprising since the higher steam demand for endothermic gasification results in less heat being lost in the gas cooler, as shown in Table 5.3-3 for the results

Table 5.3-3
Results with 80% Effective Regenerator
within Gas Cleanup System

	Configuration			
	1	2	3	4
Station Efficiency (%)				
Without	34.29	29.47	38.32	32.32
With	41.53	36.04	40.04	34.17
Heat Loss in Gas Cooler (Btu)				
Without	2606.	2606.	623.	623.
With	485.	485.	122.	122.

without regeneration. But with the regenerators in service, the adiabatic configurations are superior to the endothermic. Generating steam from 77°F water with 2000°F gas represents a large irreversibility compared to that associated with 80% effective gas-to-gas regeneration. Since endothermic gasification requires much more steam than adiabatic, the former contribution to the total irreversibility is emphasized, thus de-emphasizing the contribution from the latter. Configuration 1 now

becomes the best performer. Note however that the two configurations utilizing a waste heat system are still superior to the two incorporating a supercharged boiler system.

Unless otherwise stated, all subsequent results are presented with the regenerator in the gas cleanup system.

5.3.4 Regenerator between Air Stream to Gasifier and Power Gas Stream

Next let us examine the temperatures of the air entering the gasifier and of the power gas leaving the gasifier on Configurations 1 and 2. Since there is no air flow to the gasifier for Configurations 3 and 4, these two cycles are dismissed from further consideration in this section. The air inlet temperatures are shown in Table 5.3-4 to be 651.9°F for Configurations 1 and 2 while the gasifier gas exit temperature is 2000°F. The large temperature clearance between these two fluid streams suggests that a regenerator could be incorporated into these configurations as shown in Figure 5.3-4.

Again the regenerator effectiveness is assumed to be 0.80. The pressure drops on each side of regenerator are assumed to be 0.1 psi. With this modification, the results shown in Table 5.3-4 are obtained.

Table 5.3-4
Results with 80% Effective Regenerator between Gasifier Air and Gas Streams

	Configuration 1	Configuration 2
Station Efficiency (%)		
Without	41.53	36.04
With	41.80	36.62

Table 5.3-4 (Continued)

	Configuration 1	Configuration 2
Temp. of Air to Gasifier (°F)		
Without	651.9	651.9
With	1730.4	1730.4
Heat Transfer in Regenerator within Gas Cleanup System (Btu)		
Without	2121.	2121.
With	1096.	1096.
Heat Transfer in Present Regenerator (Btu)		
Without	0.	0.
With	902.	902.
Steam Flow to Gasifier (lbm)		
Without	0.022	0.022
With	0.195	0.195
Heat Transfer in Steam Generator (Btu)		
Without	28.	28.
With	252.	252.
Gas Cycle Heat Loss (Btu)		
Without	3240.	1782.
With	3192.	1695.
Air Flow to Gasifier (lbm)		
Without	3.783	3.783
With	3.121	3.121
Enthalpy of Air to Gasifier (Btu)		
Without	1017.	1017.
With	1740.	1740.
Heating Value of Gas (Btu/SCF)		
Without	135.	135.
With	155.	155.

Note that the station efficiency improves only slightly. The reason for this, of course, is that the other regenerator is already effectively reducing the heat loss from the power gas flow stream. Note also that

the required steam flow to the gasifier has increased from 0.022 to 0.195 lbm. This results in more heat transfer in the steam generator helping to reduce the total gas cycle heat loss slightly. Note that the hotter air into the gasifier results in less air demand but more total sensible heat is being added to the gasification process from the air. Furthermore, the lower heating value of the power gas is improved from 135 to 155 Btu/SCF. All of these observations are consistent with the conclusions in Chapter 2, concerning the effect of adding heat to the gasification process.

Admittedly, this regenerator improves the performance very little. As implied above, the gasification efficiency is significantly improved (from 86.58 to 94.75 percent). Improving the gasification efficiency significantly does not necessarily result in a significant improvement in station efficiency. Although the incremental improvement in performance is small, this regenerator shall be kept in Configurations 1 and 2 for all subsequent calculations unless otherwise stated. In Section 5.7, the relative importance of the two regenerators in the adiabatic configurations will be determined.

5.3.5 Intercooled Compressor Serving the Gasifier

Finally, an intercooler is added to the compressor serving the gasifier on Configurations 1 and 2 with the hope that the station efficiency may be increased by reducing the work of compression. The cycles must be modified according to Figure 5.3-5 where only the affected portion of the cycle is shown. Note that this modification applies only to the two configurations incorporating an adiabatic gasifier.

As before, the first-stage pressure ratio is taken to be equal to the square root of the product of the inlet pressure of the first stage and outlet pressure of the second stage; therefore the pressure at the outlet of the first stage is 3.317 atmospheres. Again it is assumed that a 0.1 psi pressure drop occurs through the gas cooler, that the gas is cooled to within 50°F of ambient or to 127°F, and that each compressor stage has an efficiency of 0.90.

With this modification, the results shown in Table 5.3-5 are obtained. Note that the station efficiency of Configuration 1 has decreased, but that of Configuration 2 has just about remained the same. In Configuration 1 the small increase in the net gas cycle work is not enough to offset the even greater increase in the gas cycle heat loss. In Configuration 2 the larger amount of net gas cycle work is just about cancelled by the effect due to the greater gas cycle heat loss.

Table 5.3-5
Results with Intercooled Compressor
Serving the Gasifier

	Configuration 1	Configuration 2
Station Efficiency (%)		
Without	41.80	36.62
With	41.62	36.63
Gas Cycle Net Work (Btu)		
Without	3705.	1609.
With	3709.	1662.
Gas Cycle Heat Loss (Btu)		
Without	3192.	1694.
With	3265.	1774.

In summarizing, the addition of an intercooled compressor serving the gasifier is not warranted. Unless otherwise stated, all subsequent results are presented without an intercooled air compressor serving the gasifier.

5.4 Optimization

The purpose of this section is to optimize each configuration by determining those operating conditions which maximize the station efficiency. It can be argued that the optimization needs to be done with respect to only three variables: the gasifier exit temperature, the combustor pressure, and the gasifier steam temperature. Increasing the steam cycle peak pressure would improve performance but the steam turbine exit quality is already near the practical lower limit of 88 percent and increasing the steam pressure would make the turbine exhaust even wetter. It has already been shown that feedwater heating is not really desirable in a combined cycle. Clearly the optimum steam extraction pressures would be the limiting low pressure in the steam cycle, namely the condenser pressure. It is not necessary, therefore, to optimize with respect to these pressures. Obviously, increasing the gas turbine inlet temperature would result in improved station efficiency, but this parameter is fixed by present-day gas-turbine technology at 2000°F, similarly for the peak steam-cycle temperature of 960°F. For the supercharged boiler configurations, the excess air fraction is a specifiable parameter. However, when the excess air was increased from the current value of 10 percent, performance did not improve. Consequently this parameter too does not need to be considered in the optimization. All other variables have obvious optimum values (like zero pressure drops) and are dismissed.

The effect on performance of some of these parameters is considered in the parametric studies of Section 5.7.

Before the optimization procedure is described let us adjust the steam turbine second- and third-stage efficiencies to be more realistic, namely 0.825 and 0.750 respectively. The new base case station efficiencies become 41.26, 35.74, 39.52, and 33.47 percent for Configurations 1 to 4 respectively. The steam turbine exit quality is calculated to be 87.9 percent for each configuration and is marginally acceptable.

For each configuration, the following optimization procedure is suggested. Let us use the data for each cycle as already described up to this point. Then, varying only the temperature of the gas leaving the gasifier, let us note the value which results in the highest station efficiency. With this optimum value for the gasifier exit gas temperature, the peak gas cycle or combustor pressure will then be varied and the station efficiency calculated. The optimum value will be noted. Finally, with the above two optimum values being used, the temperature of the superheated steam entering the gasifier will be varied, and the effect on station efficiency noted. Depending on the outcome, this procedure may have to be repeated until no further changes in the optimum conditions occur. In the next four subsections, each configuration is optimized in turn. It should be emphasized that the results of our effort in Section 5.3 are incorporated into all subsequent calculations, unless otherwise stated.

5.4.1 Configuration 1

As already outlined, the optimization begins with the waste heat combined cycle integrated with an adiabatic gasifier. All other

parameters have the previously specified values. Table 5.4-1 shows the resulting station efficiencies as this temperature is varied from 1600°F to 2600°F in 200°F increments. Note that the station efficiency is not

Table 5.4-1
Configuration 1 - Optimum Gasifier Temperature

Gas Temperature (°F)	Station Efficiency (%)
1600	40.75
1800	41.17
2000	41.26
2200	41.25
2400	41.22
2600	41.19

a strong function of gasifier exit gas temperature. This shows that if it is desirable to operate the gasifier at higher temperatures, then the station efficiency will not be unduly compromised. For example, the steam flow to the gasifier is 0.457 lbm for gasification at 1600°F but only 0.105 lbm at 2600°F. Furthermore the gasification reactions would proceed faster at the higher temperature. This could result qualitatively in a smaller gasifier design, since the residence time of the species in the gasifier could be reduced. In any event, the optimum value is taken to be 2000°F, which, incidentally, is the value used prior to this phase of the calculations.

With this value for gasification temperature, the gas cycle pressure is now varied. It should be noted, however, that the optimum pressure for the gasification system is not independent of that for the gas turbine cycle. Clearly, these two pressure levels should be as nearly the same as possible, since any difference between them tends to act as an effective

gas cycle pressure drop in the throttle valve. In reality, the gasification pressure must be slightly higher than the gas turbine cycle pressure because there will be losses in the real system. Let us use a difference of 1 atmosphere between the two systems. Considering the other pressure drops which have previously been specified, this is equivalent to assuming a 13.5 psi drop through the throttle valve after the steam generator. The resulting station efficiencies are shown in Table 5.4-2, where the combustor pressure is the independent variable. Note that the optimum

Table 5.4-2
Configuration 1 - Optimum Gas Cycle Pressure

Combustor Pressure (atm)	Station Efficiency (%)
5	40.58
10	41.26
15	40.62
20	39.54
25	38.28
30	36.83

pressure occurs at the value that has been used all along, that is, 10 atm. It should be noted that the calculated gasifier steam flow varies only slightly from 0.181 to 0.238 lbm as the pressure is increased from 5 to 30 atm. For pressures above 15 atm, the calculated results indicate that it is not possible to raise the 960°F superheated steam in the waste heat boiler. In fact, at 30 atm, only 792°F steam could be produced. This partly accounts for the poorer performance at increased pressure.

Finally, the temperature of the steam entering the gasifier is varied from 400°F to 1000°F in 100°F increments. The results, shown in Table 5.4-3, clearly show that there is no measurable effect of

this parameter on station efficiency. Let us take the "optimum" value to be 600°F, since this will result in a smaller superheat section in the steam generator compared to raising 1000°F steam. One reason for the insensitivity

Table 5.4-3
Configuration 1 - Optimum Temperature of Steam to Gasifier

Steam Temperature (°F)	Station Efficiency (%)
400	41.25
500	41.25
600	41.26
700	41.26
800	41.26
900	41.26
1000	41.27

of the results to this parameter is that very little steam is required by the gasifier; recall that only about 0.2 lbm of steam is needed. The extra sensible heat transferred from the power gas to effect additional superheating is minimal. In fact, only about 50 Btu of additional heat are required as the steam temperature is increased from 600 to 1000°F. Later, for the configurations incorporating an endothermic gasifier, it will be seen that this is no longer the case.

Clearly, the optimization procedure does not need to be repeated. The optimum gasifier gas temperature of 2000°F and the optimum gas cycle pressure of 10 atm were used from the outset. The somewhat arbitrary gasifier steam temperature of 600°F is sufficiently close to the original value of 620°F that a new iteration is not necessary. Furthermore, station efficiency hardly depends on this steam temperature anyway.

We conclude, therefore, that the optimized cycle has a station efficiency of 41.26 percent. It should be emphasized that this includes

the 10 percent station load factor. Pressure drops and component inefficiencies are also included. Without this 10 percent factor, the station efficiency would be 45.84 percent. It should be pointed out, however, that we have yet to consider the impact of meeting the federal gaseous emission requirements on nitric oxides. These are considered in Section 5.5.

5.4.2 Configuration 2

Now the indicated optimization procedure is applied to the supercharged boiler combined cycle integrated with an adiabatic gasifier. From Table 5.4-4, the optimum gasification temperature is seen to be 1800°F, giving a station efficiency which is only slightly better than the new base case value of 35.74 percent. The steam flow required by the gasifier is 0.264 lbm at the optimum gasification temperature. As in Configuration 1, the

Table 5.4-4
Configuration 2 - Optimum Gasifier Temperature

Gas Temperature (°F)	Station Efficiency (%)
1600	35.42
1800	35.79
2000	35.74
2200	35.67
2400	35.59
2600	35.51

station efficiency is not drastically affected by the gasification temperature. Again consideration of other factors such as reduced steam flow and smaller gasifier designs at higher temperatures may dictate actual operation off optimal conditions. The above results again indicate that the sacrifice in station efficiency would be minimal.

The gas cycle pressure is varied next. As before, the value of the gasification temperature which proved to be optimal is now used. The resulting station efficiencies are shown in Table 5.4-5. The optimum pressure is seen to be 10 atm, which is the value that has been used thus

Table 5.4-5
Configuration 2 - Optimum Gas Cycle Pressure

Combustor Pressure (atm)	Station Efficiency (%)
5	32.20
10	35.79
15	35.60
20	35.28
25	34.89
30	34.50

far. The decrease in station efficiency for pressures above 10 atm is primarily due to the reduction in net work (134 Btu for 30 atm) produced in the gas cycle, although there is a small decrease in net work (49 Btu) produced in the steam cycle. As expected, for this configuration it is always possible to raise the 960°F steam in the boiler, since a supercharged boiler is now in the cycle.

Finally, the temperature of the steam to the gasifier is varied, with the results shown in Table 5.4-6. It is emphasized that the gasification

Table 5.4-6
Configuration 2 - Optimum Temperature of Steam to Gasifier

Steam Temperature (°F)	Station Efficiency (%)
400	35.77
500	35.78
600	35.79
700	35.79
800	35.80
900	35.81
1000	35.82

temperature of 1800°F and gas cycle pressure of 10 atm obtained above are used to obtain the results of Table 5.4-6. Again the "optimum" steam temperature will be taken to be 600°F, since a smaller superheat section in the steam generator will be needed compared to raising 1000°F steam. Also, as in the results of Configuration 1, the entire cycle is practically independent of this parameter.

When the above optimization procedure is repeated using the latest optimum values, the same results are obtained. It is concluded that for Configuration 2 the optimum operating conditions are as follows: 1800°F gasification temperature, 10 atm gas cycle pressure, and 600°F gasifier steam temperature. While the last specification is not really optimal, the decrease in station efficiency from that at 1000°F is almost undetectable. It appears that the station efficiency for the optimized cycle is only 35.79 percent, which is significantly below that of Configuration 1. Again it is pointed out, however, that consideration of the pollution criteria may reduce this gap.

5.4.3 Configuration 3

The same optimization procedure is now applied to the waste heat combined cycle integrated with an endothermic gasifier. As before, the gasification temperature is varied first. The results are shown in Table 5.4-7. The optimum gasification temperature is seen to be between 1800°F and 2000°F. The lower temperature is chosen as optimum even though slightly more steam is required in the gasification process (1.038 lbm at 1800°F compared to 0.997 lbm at 2000°F). The reason for this is

that the heat source for the endothermic gasifier is the combustor, which, it should be recalled, has a product gas exit temperature of 2000°F in order to be compatible with the turbine inlet temperature. The effective temperature of the heat source for the gasifier must be higher than the gasification temperature because of the second law of thermodynamics, since it is impossible to transfer heat from one temperature to a higher temperature in a cycle without expending work. It is indeed fortuitous that the optimum gasification temperature turned out to be significantly below the 2000°F temperature of the heat source. Unlike Configurations 1 and 2, Configuration 3 cannot be operated at gasification temperatures above this limiting value. For completeness, it is also seen from the program

Table 5.4-7
Configuration 3 - Optimum Gasifier Temperature

Gas Temperature (°F)	Station Efficiency (%)
1600	39.18
1800	39.52
2000	39.52
2200	39.41
2400	39.27
2600	39.12

output that 4627 Btu are required by the gasifier. Of course, the same amount of heat is removed from the combustor, since no losses are assumed.

Next the combustor pressure is varied with the above optimum value being used and the resulting station efficiencies are shown in Table 5.4-8, where the optimum again is the value that has been used all along, namely 10 atm. As in the other waste heat system configuration, it is not possible to raise 960°F steam for combustor pressures above 15 atm.

At 30 atm, the temperature of the steam to the turbine is only 801°F. As before, this accounts in part for the reduced performance at higher combustor pressures.

Table 5.4-8
Configuration 3 - Optimum Gas Cycle Pressure

Combustor Pressure (atm)	Station Efficiency (%)
5	38.53
10	39.52
15	39.12
20	38.26
25	37.20
30	36.00

Finally, the gasifier steam temperature is varied with the above two optimum values now being used. The resulting station efficiencies are shown in Table 5.4-9. It should be noted that there is a larger effect on station efficiency now compared to that of the adiabatic configurations.

Table 5.4-9
Configuration 3 - Optimum Temperature of Steam to Gasifier

Steam Temperature (°F)	Station Efficiency (%)
400	39.44
500	39.48
600	39.52
700	39.55
800	39.59
900	39.62
1000	39.66

Not shown in Table 5.4-9 is the effect of increasing this steam temperature on the steam generator gas-side exit temperature. For a steam temperature of 1000°F, the power gas is cooled to 367°F from the base case value of

568°F. In Section 5.6, it will be shown how the regenerator and possibly the gas cooler may be eliminated by taking advantage of this.

When the above procedure is repeated starting with a steam temperature of 1000°F, a combustor pressure of 10 atm, and a gasifier gas exit temperature of 1800°F, the optimum conditions do not shift. For the time being, these are accepted as optimal. The optimum station efficiency is 39.66 percent without consideration of the pollution criteria.

5.4.4 Configuration 4

Finally, the optimization procedure is applied to the supercharged boiler combined cycle integrated with an endothermic gasifier. As usual, the gasification temperature is varied first with the resulting station efficiencies shown in Table 5.4-10. The optimum gasification temperature is seen to be 1800°F. Unlike Configuration 3, the combustor outlet temperature is well above all feasible gasification temperatures; at the optimum the combustor outlet temperature is 3166°F. Again it would be

Table 5.4-10
Configuration 4 - Optimum Gasifier Temperature

Gas Temperature (°F)	Station Efficiency (%)
1600	33.12
1800	33.55
2000	33.47
2200	33.40
2400	33.21
2600	33.02

possible to operate the gasifier at a higher than optimal temperature if this became desirable for other reasons. For completeness, the amount of

heat required by the gasifier is 4627 Btu and, again, must be equal to that supplied by the combustor.

Using the above 1800°F gasification temperature, the combustor pressure is now varied with the resulting effect on station efficiency shown in Table 5.4-11. For the first time the optimum gas cycle pressure is no longer the value that has been assumed all along, but rather 20 atm. Doubling the gas cycle pressure has added more than 2 percentage points to the previous highest station efficiency.

Finally with these two optimum values fixed, the temperature of the steam to the gasifier is varied with the resulting station efficiencies

Table 5.4-11
Configuration 4 - Optimum Gas Cycle Pressure

Combustor Pressure (atm)	Station Efficiency (%)
5	29.00
10	33.55
15	35.29
20	35.81
25	35.54
30	35.23

shown in Table 5.4-12. Note that it is not possible to have a superheated steam temperature of 400°F since this is below the saturation temperature of the water-side of the steam generator. As in the other endothermic configuration, the temperature of the gas leaving the steam generator is reduced substantially as the steam temperature is increased; from 553°F for the new base case to 339°F for the 1000°F steam temperature. More will be said about this in Section 5.6.

When the above procedure is repeated starting with a steam temperature of 1000°F, a combustor pressure of 20 atm, and a gasifier gas exit temperature of 1800°F, the optimum conditions remain the same. Therefore, for

Table 5.4-12
Configuration 4 - Optimum Temperature of Steam to Gasifier

Steam Temperature (°F)	Station Efficiency (%)
500	35.77
600	35.81
700	35.84
800	35.87
900	35.90
1000	35.93

now these conditions are accepted as optimal. The optimum station efficiency for Configuration 4 is only 35.93 percent, without consideration of the pollution critera.

5.5 Consideration of the Gaseous Pollution Criteria

The model that has been used so far is capable of predicting the amount of sulfur oxides (SO_x) and nitrogen oxides (NO_x) that enter the atmosphere from the stack. Recall that the combustor model, in particular, provides the composition of the product gas; that is, the mole (and weight) fraction of each constituent in the product gas, and hence stack gas, is known. Recall also that the amount of gas that the enters the atmosphere through the stack is calculated.

Through the EPA, the federal government has set limits on these two types of pollutants from power plants. These limits are summarized in

Table 5.5-1 for the various fuel types. Note that the units used in this table are lbm (of pollutant) per million Btu (of fuel input based on the

Table 5.5-1
Federal Emission Limits[31,25]

Type of Fuel	Limit (lbm per 10^6 Btu) SO_x	NO_x
Coal	1.2	0.7
Oil	0.8	0.3
Gas	0.2	0.2

higher heating value of the fuel). Note further that the limit varies with fuel type, the limits for gaseous fuels being the most stringent. Let us use the limits for a coal-fired plant, since this is in fact our primary fuel. It obviously would be much more difficult to meet the limits for a gaseous fuel.

As alluded to in Chapter 4 during the discussion of subroutine POLUTE, the NO producing reaction is reported[23] to freeze at a temperature of about 2400°F. In other words, the NO producing reaction slows down markedly in the reverse direction for temperatures below 2400°F. So it may be argued that even though combustion takes place at temperatures over 3000°F which produces a larger amount of NO, the concentration of NO will decrease as the stack gas temperature is approached. However, because of the above mentioned freeze phenomenon, the concentration of NO never goes below its equilibrium value at 2400°F.

It should be noted that provisions have been made already for reducing SO_x emissions via the gas cleanup system. Recall that it was assumed that 90 percent of the H_2S is removed from the power gas before it is burned

in the combustor. Since there is much free oxygen in the combustor, the sulfur in the remaining H_2S and all the COS ends up mostly in the form of SO_2 with smaller amounts in the form of SO and SO_3.

Although more complete results on the gas composition are presented in the next section, let us present some of these now in order to see the relative magnitudes. These abridged results are shown in Table 5.5-2 and are from the calculations which yield the optimum operating conditions discussed in the previous section. For the values given, it is assumed

Table 5.5-2
Abridged Results on Combustor Product Gas Composition
(PPM by Weight)

Effluent	Configuration 1	2	3	4
SO	0	0	0	0
SO_2	230	620	220	500
SO_3	30	0	20	0
NO	520	3420	480	2810
NO_2	20	0	10	10

that equilibrium exists at the combustor exit temperature, namely 2000, 3610, 2000, and 3354°F respectively for Configurations 1 to 4.

When the amount of SO_x and NO_x are calculated according to the method given in Section 4.6, the results shown in Table 5.5-3 are obtained assuming equilibrium at the just stated combustor exit temperatures. Note that even for equilibrium at 2000°F, Configurations 1 and 3 are unacceptable with respect to NO_x. Configurations 2 and 4 are also unacceptable with respect to NO_x at this point, but it is important to remember that these values correspond to equilibrium at temperatures of 3610 and 3354°F

respectively, which are above the 2400°F freeze temperature. All configurations meet the 1.2 lbm/10^6 Btu limit on SO_x; it is concluded that at least

Table 5.5-3
Gaseous Emissions Assuming Equilibrium
at the Combustor Exit Temperature
(lbm/10^6 Btu)

Effluent	Configuration 1	2	3	4
SO_x	0.60	0.57	0.50	0.49
NO_x	1.24	3.21	1.03	2.74

for the coal which is assumed thus far, that 90 percent H_2S removal is effective. In fact, this leaves plenty of margin in the tail gas effluents from the sulfur recovery operation in the Claus plant.

Now let us modify the calculation of the NO_x emissions by the method discussed in Section 4.6, namely by assuming that NO producing reaction freezes at 2400°F. These results are shown in Table 5.5-4. The NO_x for Configurations 1 and 3 must obviously increase while that for Configurations 2 and 4 must decrease. Now the supercharged boiler configurations are

Table 5.5-4
NO_x Emission Assuming NO Producing
Reaction Freezes at 2400°F
(lbm/10^6 Btu)

Effluent	Configuration 1	2	3	4
NO_x	3.54	0.41	2.93	0.47

acceptable with respect to both NO_x and SO_x emissions. The waste heat boiler configurations, however, exceed the limit on NO_x by more than a

factor of 4. As mentioned during the development of the combustor model, flue gas recirculation is sometimes used as a means to reduce the NO_x. In essence some of the relatively cool flue gas is recirculated back into the combustor thus replacing some of the excess air as the diluent. This serves two purposes: one is to reduce the amount of gas that actually goes to the atmosphere and the other is to reduce the amount of NO produced in the first place.

Let us incorporate flue gas recirculation and modify the waste heat configurations as shown in Figure 5.5-1, where only the affected portion of the cycle is shown. Recall from the development of the combustor model in Section 3.2 that unless the flue gas enters the combustor at a reduced temperature the benefit of flue recirculation is lost. Also gas compressors are needed, since the flue gas is at atmospheric pressure and the combustor operates at elevated pressures. The first gas cooler is added to reduce the work required by the first stage of compression. The intercooler helps to reduce the work required by the second stage of compression. Finally the second gas cooler is utilized to lower the temperature of the compressed flue gas before entering the combustor to maximize the effect of the flue gas recirculation.

Additional data need to be specified before the NO_x emission can be calculated. Let us assume that each of compressor stages has an efficiency of 0.9 and that the first gas cooler reduces the flue gas temperature to 250°F, the second to 300°F, and the third to 350°F. Note that is is not possible to reduce these temperatures to within 50°F of ambient as before because the flue gas has a high volume fraction of water vapor. As the pressure increases, the dew point temperature

increases. Condensation in the flue gas recirculation system is to be avoided for the same reasons it is to be avoided elsewhere in the system. A pressure drop of 0.1 psi is assumed in each gas cooler.

With this modification to only Configurations 1 and 3, the results shown in Table 5.5-5 are obtined. Note the decrease in performance as the fraction of flue gas recirculation is increased. In order to ensure some margin, it appears that about 53 percent recirculation is necessary for

Table 5.5-5
Effect of Flue Gas Recirculation
on Configurations 1 and 3

Configuration 1

Fraction of Flue Gas Recirculated	Station Efficiency (%)	NO_x (lbm/10^6 Btu)
0.30	38.36	1.89
0.35	37.95	1.62
0.40	37.55	1.34
0.45	37.19	1.05
0.50	36.85	0.74
0.55	36.56	0.33

Configuration 3

Fraction of Flue Gas Recirculated	Station Efficiency (%)	NO_x (lbm/10^6 Btu)
0.30	37.08	1.37
0.35	36.71	1.10
0.40	36.38	0.82
0.45	36.07	0.49

Configuration 1, while for Configuration 2 only 45 percent is needed. Unless otherwise stated, the fraction of recirculated flue gas is fixed at these values for all subsequent calculations. The NO_x shown in Table 5.5-5 has been calculated assuming the 2400°F freeze temperature.

When Configurations 1 and 3 are checked to determine how flue gas recirculation might effect the previously calculated optimum conditions, no shift in these parameters occurs. That is, the two configurations are still optimum for the previously determined operating conditions..

Finally, let us verify one of the assumptions made in Section 4.6 concerning the numerical equivalence of the mole and weight fraction of NO. For each configuration, these are shown in Table 5.5-6, assuming 53 and 45 percent recirculation for Configurations 1 and 3 and no recirculation,

Table 5.5-6
Numerical Equivalence of Mole and Weight Fraction of NO

	Configuration 1	2	3	4
Mole Fraction	.00018	.00342	.00016	.00263
Weight Fraction	.00019	.00353	.00017	.00277

of course, for Configurations 2 and 4. Clearly, the approximation made in Section 4.6.16 is justified since ample margin exists in the calculated NO_x emissions compared to the limiting value.

5.6 Review of Results

The main purpose of this section is to summarize some of the more important results. After modifying Configurations 3 and 4 still further, new cycle schematics for each optimized configuration will be presented. In addition, the water and heat rejection requirements will be given for each optimized configuration.

Before summarizing the results, let us review the results for the optimization of Configurations 3 and 4 with respect to the gasifier steam temperature. Recall that as this temperature was increased the temperature of the power gas leaving the steam generator decreased a few hundred degrees. By increasing the steam temperature even further, the gas temperature at the steam generator exit could be decreased to within the temperature range of the gas cleanup system, which is 200 to 260°F. This suggests that the regenerator can be removed from these endothermic configurations at the expense of making the steam generator superheater larger. When this regenerator is removed from these configurations and the temperature of the steam to the gasifier is increased, the results shown in Table 5.6-1 are obtained. Only the results for the steam temperature which gives a steam generator gas exit temperature near 200°F are presented. Clearly, the gas

Table 5.6-1
Results without Regenerator
in Service and Elevated Gasifier
Steam Temperatures

	Configuration 3	Configuration 4
Gasifier Steam Temp. (°F)	1280	1200
Station Efficiency (%)		
Previous Optimum	36.07	35.93
Without Modifications	36.14	35.95
Steam Generator Gas Exit Temperature (°F)	211.	222.
Heat Removed by Gas Cooler (Btu)	11.	22.

cooler before the gas cleanup system could also be removed, since cleanup at both 211 and 222°F is acceptable. This would result in even higher performance, but the improvement would be small.

It should be noted that the purpose of this modification is to eliminate the use of expensive equipment and not to improve the station efficiency by less than a tenth of a percentage point. By taking advantage of using a higher gasifier steam temperature, it is possible to eliminate an expensive piece of equipment, namely the regenerator, from Configurations 3 and 4. The gas cooler, however, will be left in the cycles, but it should be kept in mind that these too could be eliminated if an actual plant were to be built.

An obvious question arises. Why is it possible to allow steam temperatures in excess of 960°F in the steam generator but not in the boilers? A careful examination of the differences between the two provides the answer. The primary reason for limiting the steam temperature to about 1000°F in the supercharged and waste heat boilers is that stress problems arise at elevated temperatures because of the large pressure differential between the two sides. In the waste heat boiler, the steam-side operates at 1600 psia but the gas-side at atmospheric pressure. In the supercharged boiler, the steam-side again operates at 1600 psia but the gas-side at ten or twenty atmospheres. In any event, at elevated temperatures stress problems arise with these kinds of pressure differentials. This is not the case in the steam generator, however, because both sides are necessarily at approximately the same pressure. Consequently, it is probably no problem to raise the higher temperature steam in the steam generator. Unless otherwise stated the regenerator in Configurations 3 and 4 is removed from the respective cycles for all subsequent calculations. When Configurations 3 and 4 are re-optimized, no changes from the previous optimum conditions result.

We are in a position now to modify Figures 2.3-1 to 2.3-4 based on the results up to this point. The modified configurations are shown schematically in Figures 5.6-1 to 5.6-4 for Configurations 1 to 4 respectively. Configuration 1 now has regenerative feedwater heating, single stage air compressors, two regenerators, and flue gas recirculation. Configuration 2 similarly has regenerative feedwater heating, single stage air compressors, and one regenerator, but no flue gas recirculation. Configuration 3 has regenerative feedwater heating, a single stage air compressor, flue gas recirculation, but no regenerators at all. Finally, Configuration 4 is unmodified from original cycle presented in Chapter 2 except for the addition of the regenerative feedwater heating. The new cycle schematics represent the final versions of the original cycles presented in Chapter 2 with gaseous emission criteria now considered.

Let us now summarize some of the key results for each optimized configuration as shown in Table 5.6-2. These results apply to the cycles shown in Figures 5.6-1 to 5.6-4. From this table it is seen that all four configurations have practically the same station efficiency, although Configuration 1 is marginally the best. More importantly, Configuration 1 requires less total steam than the other configurations. As expected, the endothermic configurations require much more steam than the adiabatic ones. Note that the amount of heat rejected through the condenser for the waste heat configurations is significantly below that for the supercharged boiler configurations. For Configuration 1, only about 29 percent of the heat input to the cycle is actually rejected to the heat sink, probably a river, compared to about 63 percent for an equally efficient conventional fossil-fueled plant. This difference could be significant

enough to eliminate the need for expensive cooling towers, which seem today to be almost standard equipment on new power plants. This benefit practically disappears for the supercharged boiler configurations. Another interesting trend is the ratio of gas cycle work to steam cycle work. Once again the indication is that de-emphasizing the gas cycle is undesirable. If flue gas recirculation were not needed, then the configurations

Table 5.6-2
Summary of Results for
Final Version of Each Configuration

	Configuration 1	2	3	4
Station Efficiency (%)	36.67	35.79	36.14	35.95
Combined Cycle Efficiency (%)	43.01	41.83	42.08	44.86
Heating Value of Gas (Btu/SCF)	155.	157.	288.	290.
Water Requirement (lbm)				
Gasification	0.195	0.264	1.038	1.068
Gas Cleanup	0.268	0.243	0.123	0.000
Total	0.463	0.507	1.161	1.068
Heat Rejected (Btu)				
Gas Cycle	3861.	1710.	4114.	2243.
Steam Cycle	3692.	5968.	3515.	5412.
Ratio of Gas Cycle Work to Steam Cycle Work	1.44	0.47	1.53	0.63
Fraction of Flue Gas Recirculated	0.53	--	0.45	--
Pollution (lbm/10^6 Btu)				
NOx	0.52	0.41	0.50	0.47
SOx	0.59	0.57	0.49	0.49
Station Efficiency (%) without Pollution Control	41.26	35.79	39.66	35.93

with high gas cycle work to steam cycle work ratios would be superior to those with low such ratios. Flue gas recirculation takes its toll on station efficiency, somewhat masking the correlation between this ratio and cycle performance. For added proof of this, refer to the results

presented in Tables 5.2-3 and 5.2-4. For completeness, the amount of flue gas recirculation as well as the amount of NO_x and SO_x emissions are also given in Table 5.6-2.

It is convenient at this point to present typical equilibrium compositions of the clean fuel gas and the combustor product gas. The former are summarized in Table 5.6-3 and the latter in Table 5.6-4. Note that the composition is given by mole fraction (or volume fraction).

Table 5.6-3 shows that the fuel gas for Configurations 1 and 2 is composed mostly of N_2, CO, and H_2. Recall that these configurations incorporate adiabatic gasifiers and that a large amount of air is required. Consequently, a high fraction of the fuel gas is composed of N_2, which

Table 5.6-3
Composition of Clean Fuel Gas
for Final Version of Each Configuration
(Mole Fraction)

Species	Configuration 1	2	3	4
H_2	0.1835	0.1933	0.4968	0.4950
CH_4	0.0021	0.0046	0.0299	0.0530
H_2O	0.0784	0.0784	0.0784	0.0392
CO	0.3017	0.2954	0.3771	0.3822
N_2	0.4256	0.4130	0.0022	0.0024
Ar	0.0053	0.0052	0.0000	0.0000
CO_2	0.0027	0.0094	0.0149	0.0274
H_2S	0.0004	0.0004	0.0006	0.0006
COS	0.0002	0.0002	0.0001	0.0002
NH_3	0.0001	0.0001	0.0000	0.0000

serves to lower the effective heating value of the gas, thus giving a low-Btu fuel gas. For Configurations 3 and 4, the nitrogen in the fuel gas is due only to that in the coal, since endothermic gasification

requires no air. For these configurations, the fuel gas is composed mostly of H_2 and CO, thus yielding a higher effective heating value for the fuel gas. These results agree with the general trends indicated in Section 2.2. It should also be noted that the amount of CH_4 produced is insignificant for all configurations, although more is produced in the endothermic gasifiers. This is unfortunate since CH_4 has a heating value of about 1000 Btu/SCF and is the primary component in natural gas. Clearly the gasification processes would have to be modified substantially to produce a synthetic natural gas (mostly CH_4). This is, of course, outside the scope of this dissertation.

Table 5.6-4 shows that the combustor product gas is composed mostly of N_2, which is not surprising since air is necessary to the combustion process.

Table 5.6-4
Composition of Combustor Product Gas
for Final Version of Each Configuration
(Mole Fraction)

Species	Configuration 1	2	3	4
H_2	0.0000	0.0006	0.0000	0.0002
H_2O	0.1254	0.1327	0.1995	0.1865
CO	0.0000	0.0037	0.0000	0.0008
N_2	0.7025	0.6922	0.6430	0.6511
O_2	0.0185	0.0121	0.0165	0.0148
Ar	0.0088	0.0087	0.0081	0.0082
CO_2	0.1443	0.1441	0.1325	0.1343
NO	0.0002	0.0034	0.0002	0.0027
OH	0.0000	0.0020	0.0000	0.0012
H	0.0000	0.0001	0.0000	0.0000
O	0.0000	0.0001	0.0000	0.0000
NO_2	0.0000	0.0000	0.0000	0.0000
SO	0.0000	0.0000	0.0000	0.0000
SO_2	0.0003	0.0003	0.0002	0.0002
SO_3	0.0000	0.0000	0.0000	0.0000

The main products of combustion are H_2O and CO_2 as expected. Practically no CO is produced by Configurations 1 and 3 with a significant amount produced by Configuration 2 and a moderate amount by Configuration 4. Note that in Configurations 1 and 3, the amount of NO is quite low because of the flue gas recirculation. Note that practically no NO_2, no SO, and no SO_3 are produced.

5.7 Parametric Studies

Let us determine the sensitivity of station efficiency to variations in some of the parameters, the values of which have been assigned somewhat arbitrarily in Section 5.2. Among the parameters that will be varied are coal composition, regenerator effectiveness, pressure drops and component efficiencies, boiler pinch points, and gas turbine inlet temperature.

5.7.1 Coal Composition

As mentioned before, the coal which has been assumed in all the previous calculations is a Pennsylvania high volatile bituminous coal. Let us now use three other coals, the compositions of which are given in Table 5.7-1. For convenience, the composition of the Pennsylvania coal is listed in this table also. Note that a typical eastern coal[26], a Wyoming coal[27], and an Illinois coal[13] are used. It should be noted that the Illinois coal is the same one used in ECAS[14] and is actually referred to as Illinois No. 6. The effect on the station efficiency for only Configuration 1 will be shown since similar results are obtained for the other configurations. For each of these three other coals, the station efficiency is improved slightly

Table 5.7-1
Coal Compositions for Parametric Study
(Weight Fractions)

	Reference Coal	Typical Eastern Coal	Wyoming Coal	Illinois No. 6
C	0.7304	0.786	0.730	0.596
H	0.0528	0.049	0.056	0.059
O	0.0616	0.020	0.151	0.200
N	0.0088	0.005	0.012	0.010
S	0.0264	0.010	0.005	0.039
$H_2O(\ell)$	0.0300	0.020	0.000	0.000
Ash	0.0900	0.110	0.046	0.096

with the change in station efficiency being less than one percentage point as shown in Table 5.7-2. As expected, the amount of SO_x produced varies directly with the weight fraction of sulfur in the coal. Note that even for the higher sulfur Illinois No. 6 the amount of SO_x produced is still below the 1.2 lbm/10^6 Btu limit. For completeness, the lower heating values of each coal, calculated from the Dulong approximation, are also tabulated.

Table 5.7-2
Results of Parametric Study on Coal Composition
(Configuration 1)

	Reference Coal	Typical Eastern Coal	Wyoming Coal	Illinois No. 6
Station Efficiency (%)	36.67	36.84	37.33	36.76
SO_x (lbm/10^6 Btu)	0.59	0.21	0.12	1.10
Lower Heating Values (Btu/lbm)	12,747	13,526	12,222	10,334

From this brief parametric study, it can be seen that the cycle performance is fortunately not a strong function of coal composition.

5.7.2 Relative Importance of Regenerators in Configurations 1 and 2

Next let us try to determine the relative importance of the two regenerators incorporated in the adiabatic configurations. This is most easily done by varying the effectiveness of one regenerator while keeping the other one fixed at its nominal value of 0.80. Let us refer to the regenerator in the gas cleanup system as RG2 and that adjacent to the gasifier as RG1.

Let us hold the effectiveness of RG2 at 0.80 and vary the effectiveness of RG1 as shown in Table 5.7-3, where the resulting station efficiencies are

Table 5.7-3
Results of Parametric Study on the Effectiveness of RG1 with that of RG2 Held at 0.80

Effectiveness of RG1	Station Efficiency (%) Configuration 1	2
0.80	36.67	35.79
0.60	36.60	35.68
0.40	36.52	35.58
0.20	36.44	35.46
0.00	36.35	35.34

also shown. It is noted that the decrease in station efficiency is not significant as the effectiveness of RG1 is decreased. In fact, if RG1 were removed completely, the station efficiency would drop less than 0.5 percentage points from its nominal value.

Next let us hold the effectiveness of RG1 at 0.80 and vary the effectiveness of RG2 as shown in Table 5.7-4, where the resulting station efficiencies are also shown. Now the deterioration in performance is dramatic. In fact, for both Configurations 1 and 2, the station efficiency would drop about 3 percentage points if RG2 were removed from the cycle. Clearly the

the regenerator in the gas cleanup system is the more important one. The effect of this trend on economic decisions concerning these regenerators is obvious.

Table 5.7-4
Results of Parametric Study on the Effectiveness of RG2 with that of RG1 Held at 0.80

Effectiveness of RG1	Station Efficiency (%) Configuration 1	2
0.80	36.67	35.79
0.60	35.90	35.14
0.40	35.11	34.40
0.20	34.31	33.63
0.00	33.51	32.85

5.7.3 Pressure Drops and Component Efficiencies

In order to see the effect of the assumed pressure drops and component efficiencies on station efficiency let us first make all the pressure drops zero and note the results. Then with zero pressure drops, let us calculate the station efficiencies assuming all the compressors, pumps, and turbines are 100 percent efficient. The effect of the assumed pressure drops is shown in Table 5.7-5. Note that the station efficiency increases

Table 5.7-5
Results of Parametric Study on Pressure Drops

	Station Efficiency (%) Configuration 1	2	3	4
With Pressure Drops	36.67	35.79	36.14	35.95
Without Pressure Drops	37.53	36.78	36.95	36.85

by about 1 percentage point for all configurations. The improvement in performance by assuming ideal components is much more dramatic as shown in Table 5.7-6. In fact, more than 6 percentage points are lost because of

Table 5.7-6
Results of Parametric Study on Efficiencies
of Compressors, Pumps, and Turbines
(Without Pressure Drops)

	Station Efficiency (%)			
	Configuration			
	1	2	3	4
Non-ideal Components	37.53	36.78	36.95	36.85
Ideal Components	44.73	43.04	43.49	43.74

the inefficiencies associated with the pumps, compressors, and turbines compared to the zero pressure drop cases. Marked improvement in overall performance can be expected by decreasing the irreversibilities associated with these components, although significant improvements in these component efficiencies are unlikely.

5.7.4 Boiler Pinch Point Temperature Differences

Let us now decrease the pinch point temperature differences in the boiler of each configuration from 40 to 20°F. This would require a large boiler, since more heat transfer area would be needed. As shown in Table 5.7-7, the improvement in performance is not great. In fact, for Configuration 2 the performance is unchanged since a 20°F pinch point temperature difference is not possible. For this case, the computer output indicates that the pinch point temperature difference has to be 40°F to ensure 7°F

subcooled water in the economizer. Based on these results, it is unlikely that decreasing the pinch point temperature difference in the boilers from 40°F to 20°F could be economically justified.

Table 5.7-7
Results of Parametric Study on
Boiler Pinch Point Temperature Differences

	Station Efficiency (%)			
	Configuration			
	1	2	3	4
With 40°F	36.67	35.79	36.14	35.95
With 20°F	37.21	35.79	36.64	36.13

5.7.5 Gas Turbine Inlet Temperature of 2400°F

Finally, let us determine how much the station efficiency could be improved by increasing the turbine inlet temperature to 2400°F. Because Configuration 1 has resulted in the best performance, let us now restrict our attention only to this configuration. It is reasonable to expect that similar improvements in station efficiency for each of the other configurations would result for a similar increase in gas turbine inlet temperature. For the remainder of this subsection, therefore, we restrict our attention to Configuration 1 only.

The higher gas turbine inlet temperature will require a different amount of flue gas recirculation. Let us vary the fraction of flue gas recirculated for the new turbine inlet temperature of 2400°F as shown in Table 5.7-8. Also shown in this table are the resulting station efficiencies and the amounts of NO_x that enter the atmosphere. It should be emphasized that since the "freeze" and "equilibrium" temperatures are

both 2400°F, the calculated amounts of NO_x are essentially identical for the two methods of computation. Note that about 40 percent flue gas recirculation is sufficient to reduce the NO_x to below the 0.7 lbm/10^6 Btu limit with ample

Table 5.7-8
Parametric Study on Flue Gas Recirculation
at Gas Turbine Inlet Temperature of 2400°F
for Configuration 1

Fraction of Flue Gas Recirculated	Station Efficiency (%)	NO_x (lbm/10^6 Btu)
0.00	44.93	2.36
0.10	44.07	1.94
0.20	43.23	1.51
0.30	42.43	1.06
0.40	41.66	0.54

margin. It may be recalled from Section 5.5 that with a turbine inlet temperature of 2000°F, Configuration 1 required 53 percent flue gas recirculation reducing the amount of NO_x to 0.52 lbm/10^6 Btu.

From Table 5.7-8 it is easily seen that increasing the gas turbine inlet temperature to 2400°F from 2000°F would result in a substantial improvement in overall performance. A 400°F increase in this parameter causes the station efficiency to increase almost exactly 5 percentage points. Furthermore, Table 5.7-8 shows the price that must be paid to meet the current pollution criteria with respect to NO_x emissions. Meeting the criterion on NO_x by using flue gas recirculation results in lowering the station efficiency by more than 3 percentage points.

5.8 Discussion of Assumptions

In this section, some of the assumptions that have been explicitly made or implied are now discussed in light of the results which have been

obtained. There are two basic kinds of results which have been presented: one type is relative and the other absolute. When each configuration was compared with the others, the results which were used in this comparison were all relative. Because consistent assumptions were always made among the four configurations, this comparison was not only valid but also quite instructive. Obviously, these kinds of relative results cannot be that sensitive to the assumptions that have been made. Each configuration was modeled in parallel to ensure this consistency throughout. The second kind of result is necessarily more sensitive to the assumptions. If we were to build the type of plant which has been referred to as Configuration 1, how close could we expect to come to the calculated station efficiency of 36.67 percent or a heat rate of 9307 Btu/kwhr? It is believed that the calculated results are a best estimate of the results which would be obtained from an actual plant.

5.8.1 Dulong Approximation

Several sources[18,26] give the accuracy of the Dulong approximation to be within 2 to 3 percent. That is to say, the heating value of the coal based on measurements from a bomb calorimeter agree to within 2 or 3 percent of that obtained from application of the Dulong approximation. While this error may seem to be substantial, it is well within usual engineering accuracy. Furthermore, to determine the actual enthalpy for for a wide variety of coals and conditions would be an impossible task. The Dulong approximation provides a practical means of obtaining the heating value and enthalpy of the coal for analytical purposes.

5.8.2 Chemical Equilibrium

It is generally agreed that thermodynamic equilibrium would exist in the gasifier for temperatures above 1700°F[28]. Since the optimum value of gasification temperature is well above this for each configuration, the assumption of thermodynamic equilibrium appears to be justified. This is indeed fortuitous since the kinetics for reactions involving coal are extremely unpredictable and are highly dependent on coal type[29]. Also, as pointed out in Section 2.4, a high gasification temperature is advantageous from the standpoint of not producing problemsome tars, phenols, mercaptans, and so forth.

As mentioned in Chapter 3, the equilibrium composition of the product gas leaving the combustor is also calculated. Again equilibrium is assumed at the existing flame temperature. With the exception of the computation of frozen NO for pollution purposes, the composition of the fuel gas is assumed to be frozen at the gasifier exit conditions and composition of the products of combustion is assumed to be frozen at the combustor exit conditions. Although an equilibrium composition could have been calculated at each cycle point, this was not deemed practical for two reasons. First, many reactions slow down considerably as temperature is reduced and it is unlikely that equilibrium is achieved for reasonable time periods. Second, much more computational time would be required. Since it is believed that this would have a very small effect on results, this refinement is not justified.

5.8.3 Feasibility of an Endothermic Gasifier

There are many possible ways to deliver heat to the gasifier. Among these are gases, pebbles, molten salts, and slag. For each of these, heat could be removed from a high temperature heat source, presumably the combustor, and transferred to the gasifier by one of these heat transfer media. The high-temperature gas-cooled reactor provides an immediate example of how a gas may be used. The Mayland Pebble-Bed Gasifier[29] uses pebbles to effect the necessary heat transfer. Molten salts are used in the Kellogg gasification processes[29]. Finally, the Rummel Double-Shaft Gasifier[29] utilizes the coal slag to provide the necessary heat transfer. As noted in Section 2.4, Texaco is reporting progress on material problems associated with coal slag. Although the reason for heat transfer to the gasification process in each of these cases may be different, the basic ideas should be applicable to Configurations 3 and 4.

5.8.4 Limits on NO_x and SO_2 Effluents

It appears that the appropriate limits on NO_x and SO_2 emissions will be changed in the very near future: probably from 0.7 lbm/10^6 Btu to 0.6 lbm/10^6 Btu for NO_x and from 1.2 lbm/10^6 Btu to 99 percent removal for SO_2. From the results presented in this chapter, the projected limit on NO_x is already met. The more stringent limit on SO_2 will cause only a slight decrease in station efficiency, but the capital cost of the sulfur removal system will more than double[1]. Also, new combustor designs are now emerging which are effective in reducing the NO_x emissions; if flue gas recirculation could be eliminated on the waste heat configurations, the station efficiency could be significantly improved.

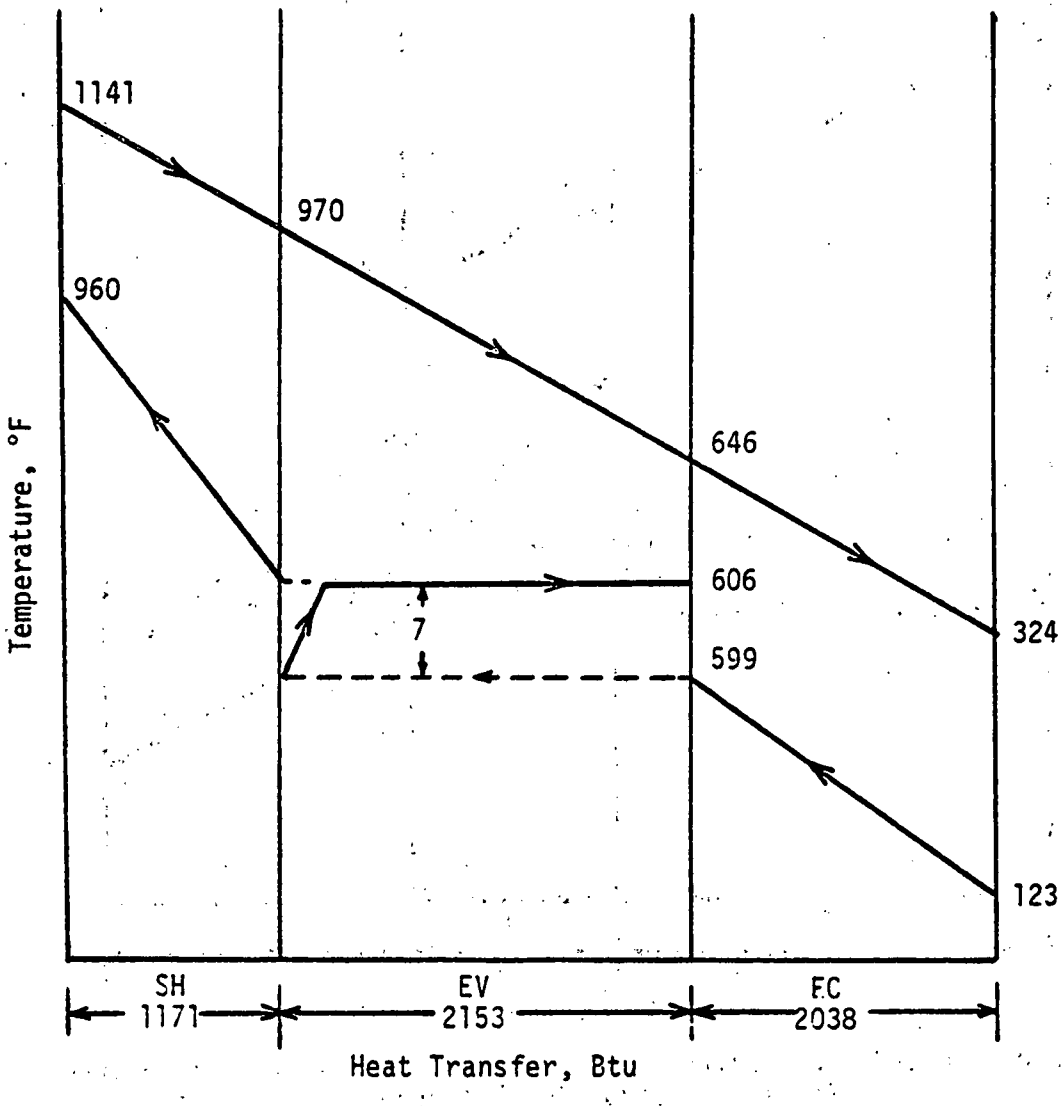

Figure 5.2-1 Temperature-Heat Transfer Diagram for Waste Heat Boiler (Typical Results from Configuration 1)

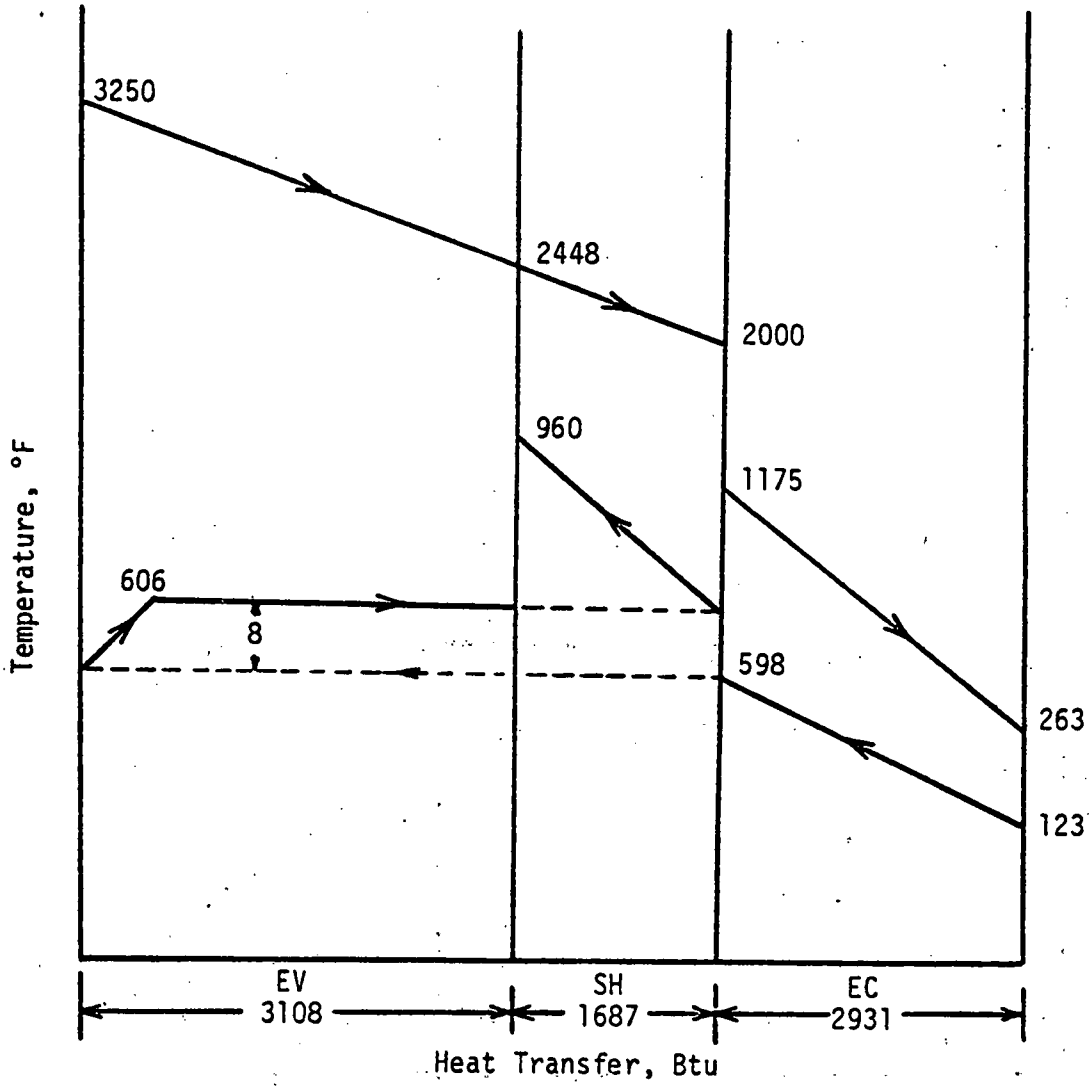

Figure 5.2-2 Temperature-Heat Transfer Diagram for Supercharged Boiler (Typical Results from Configuration 2)

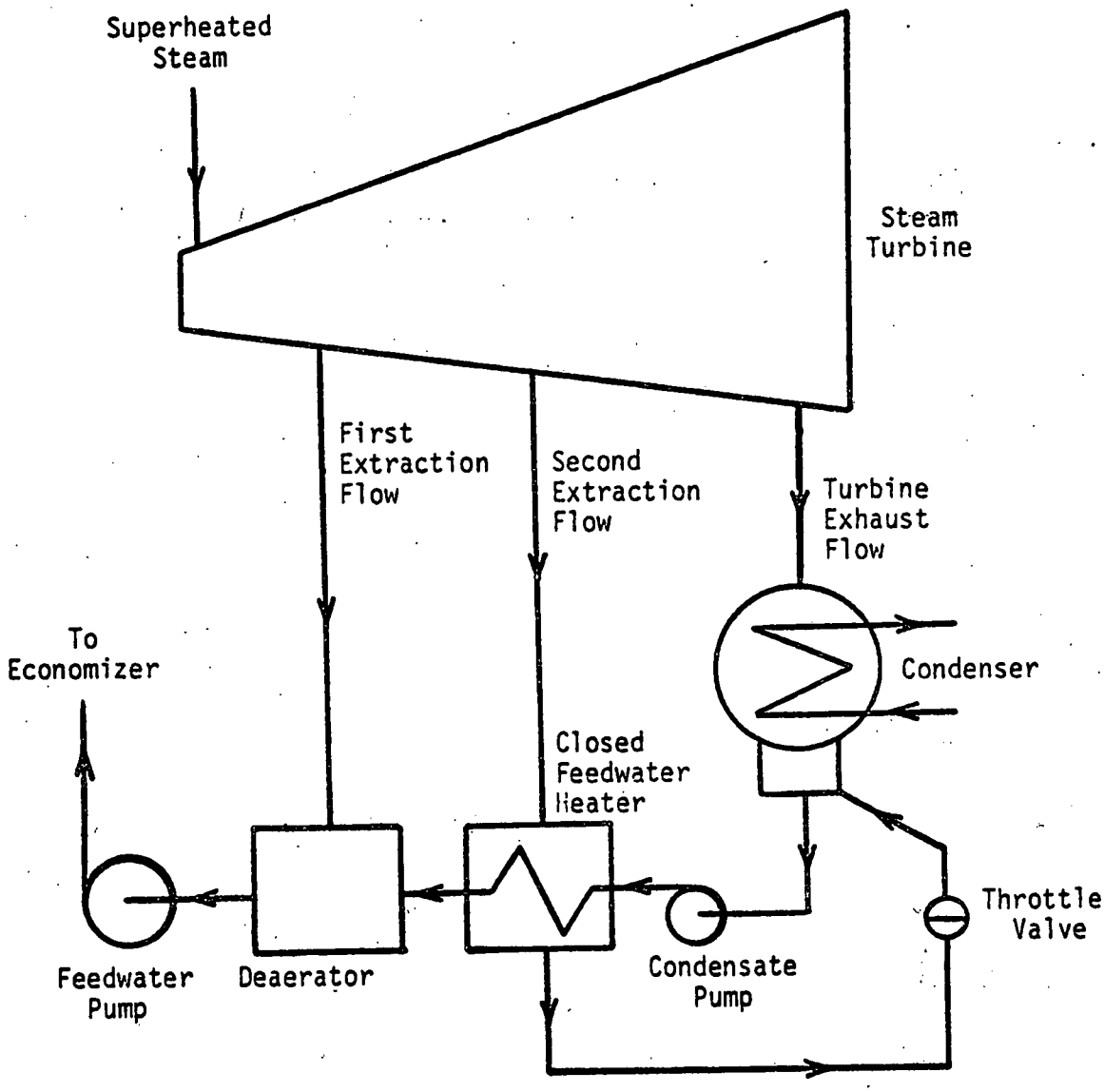

Figure 5.3-1 Steam Cycle Schematic with Regenerative Feedwater Heaters

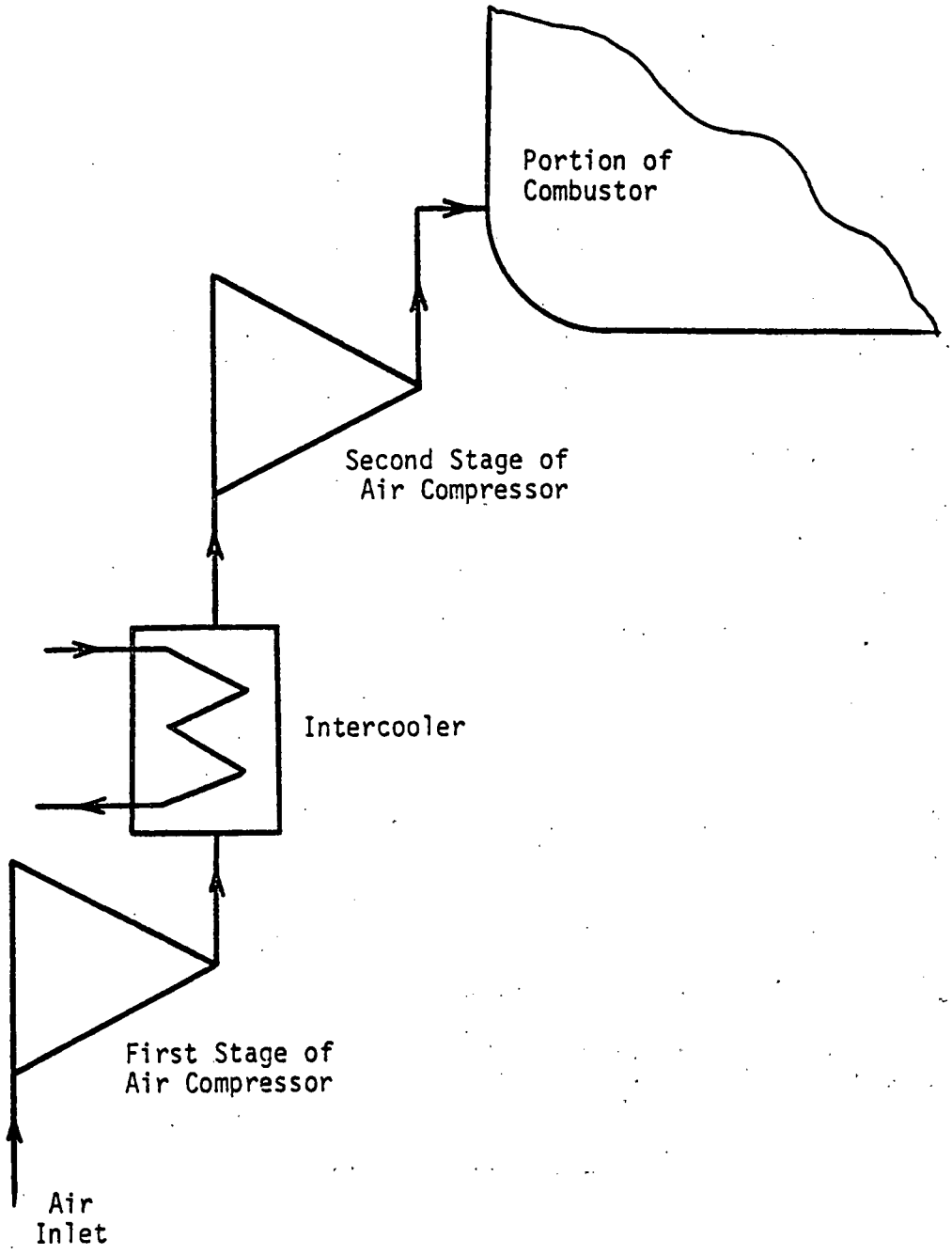

Figure 5.3-2 Schematic of Two-Stage Intercooled Air Compressor Serving Combustor

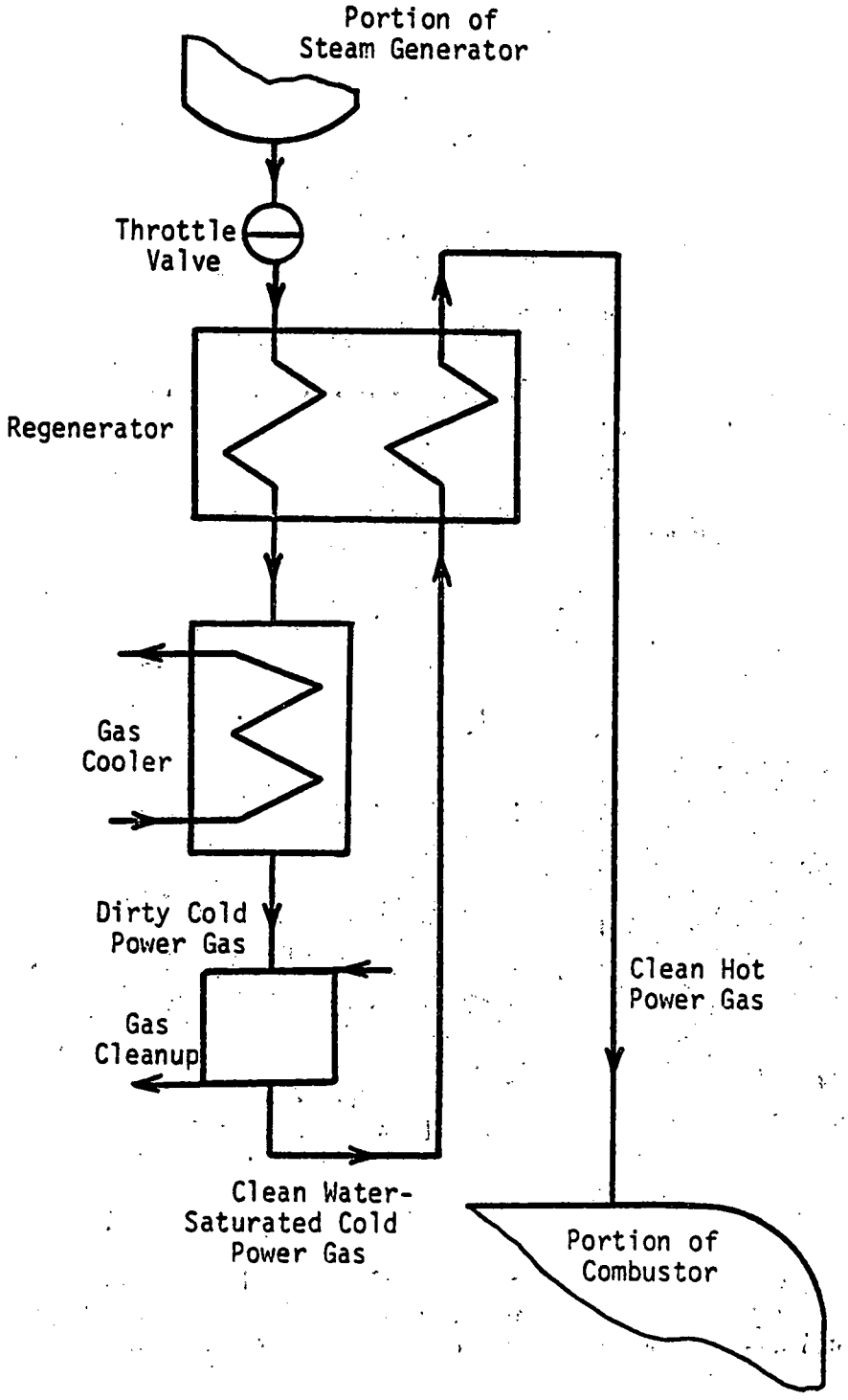

Figure 5.3-3 Schematic of Portion of System from Steam Generator to Combustor with Regenerator within Gas Cleanup System

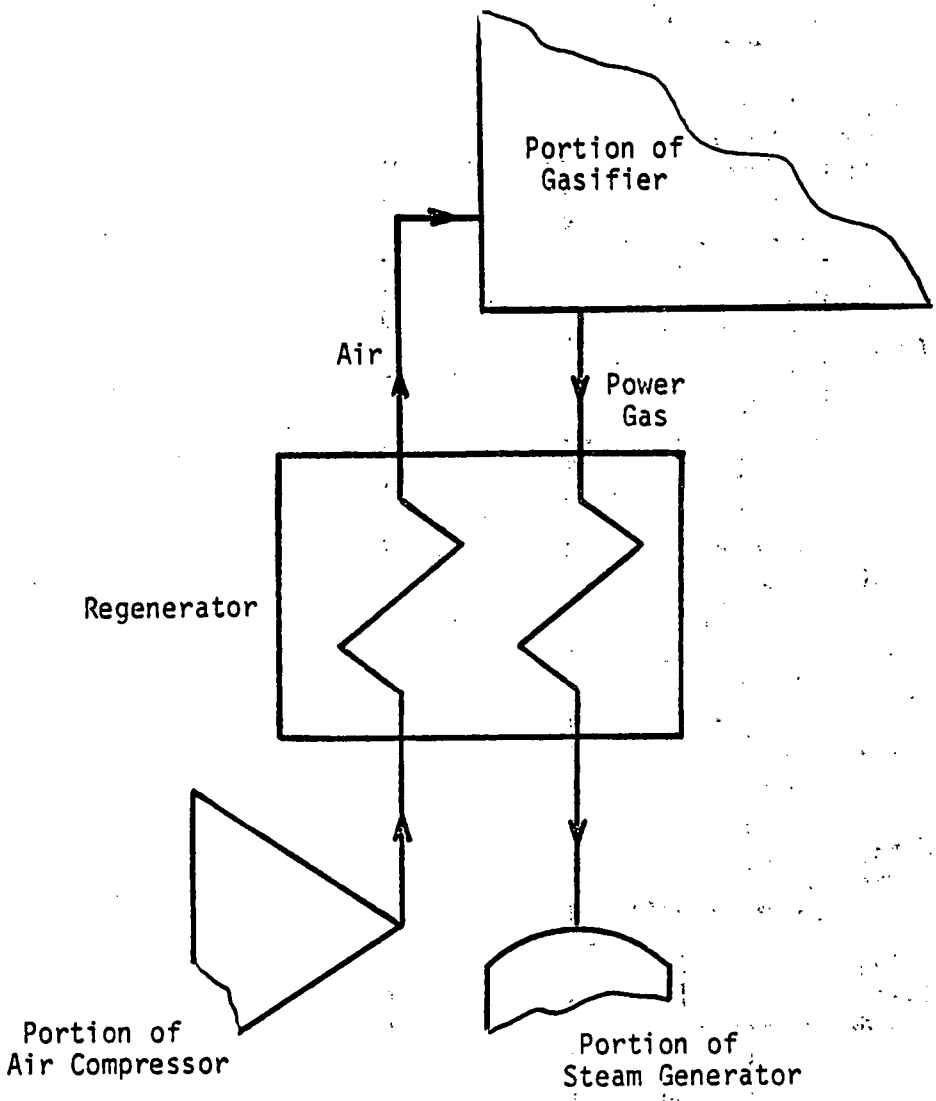

Figure 5.3-4 Schematic of Portion of System from Air Compressor Serving Gasifier to Steam Generator with Regenerator Included in System (Applicable to Configurations 1 and 2 Only)

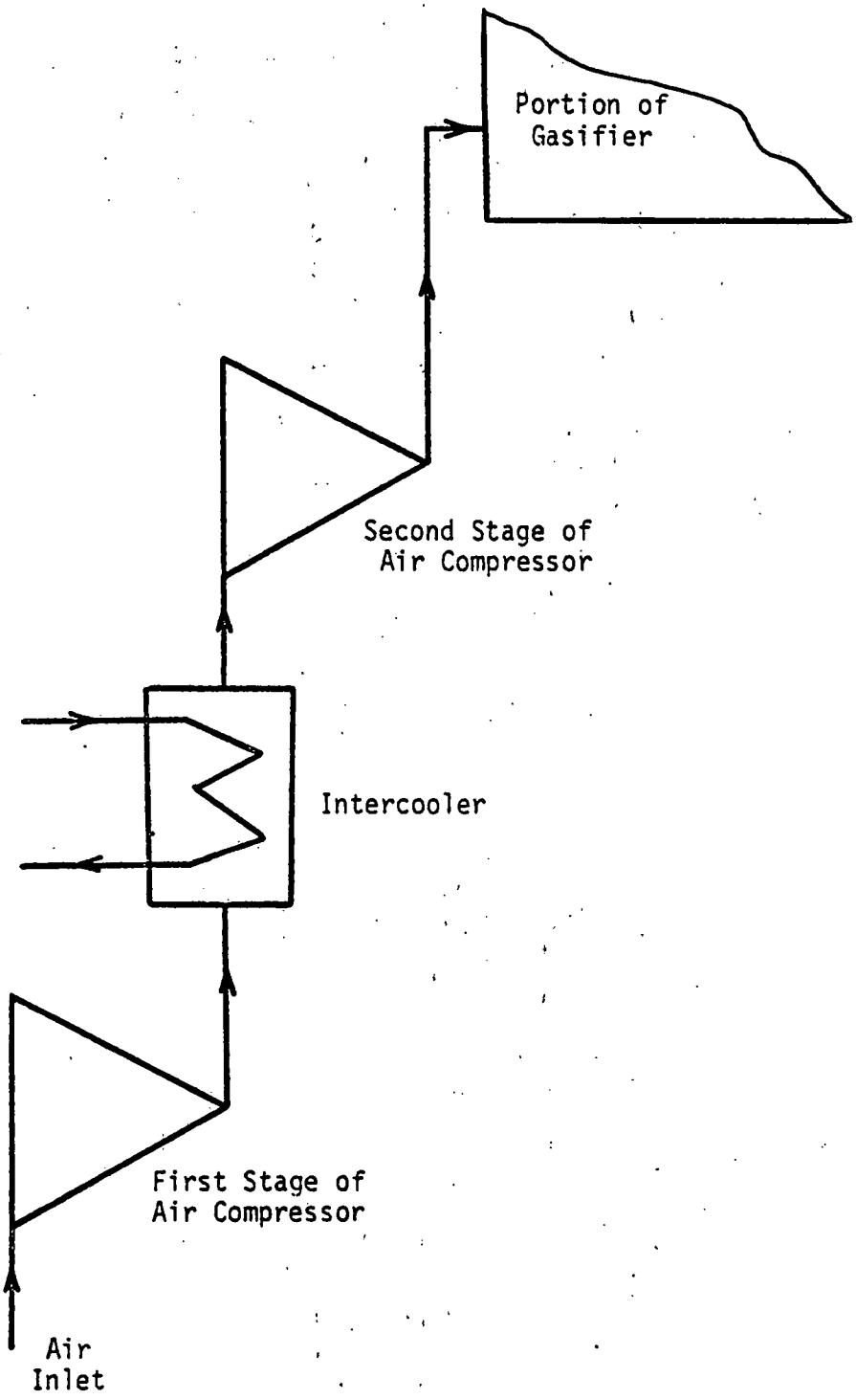

Figure 5.3-5 Schematic of Two-Stage Intercooled Air Compressor Serving Gasifier (Applicable to Configurations 1 and 2 Only)

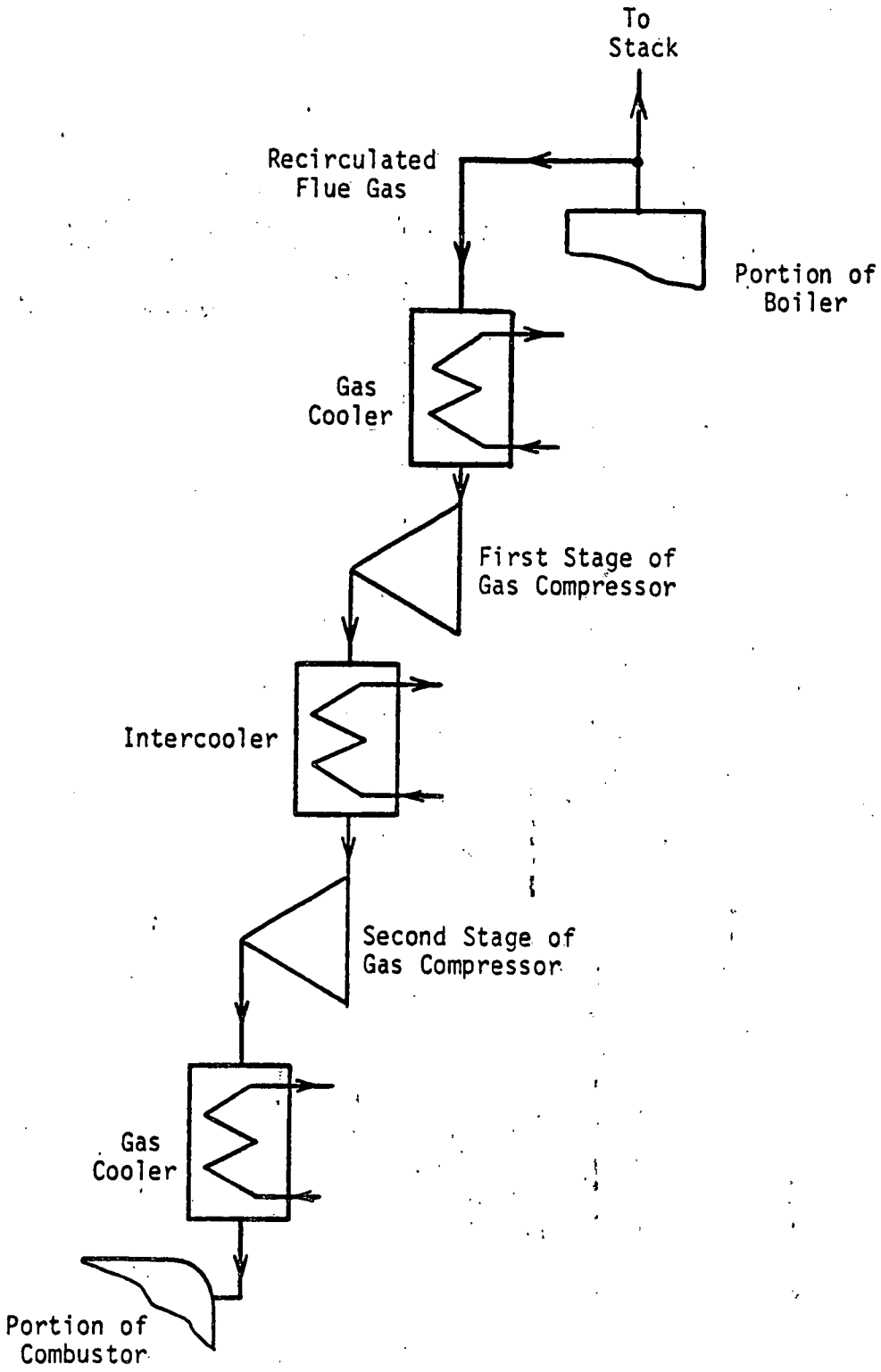

Figure 5.5-1 Schematic of Portion of System from Stack to Combustor Showing Flue Gas Recirculation Train

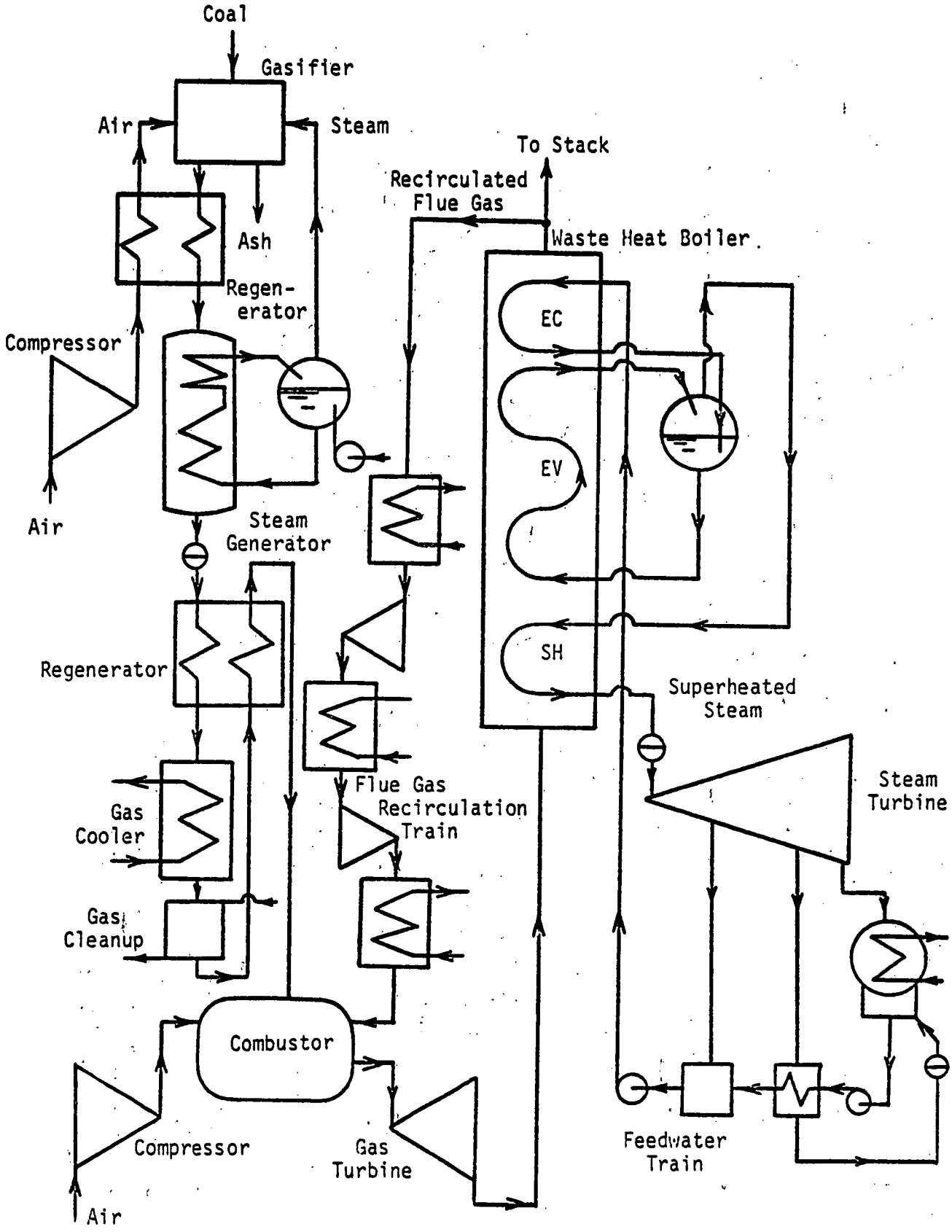

Figure 5.6-1 Schematic of Final Version of Configuration 1

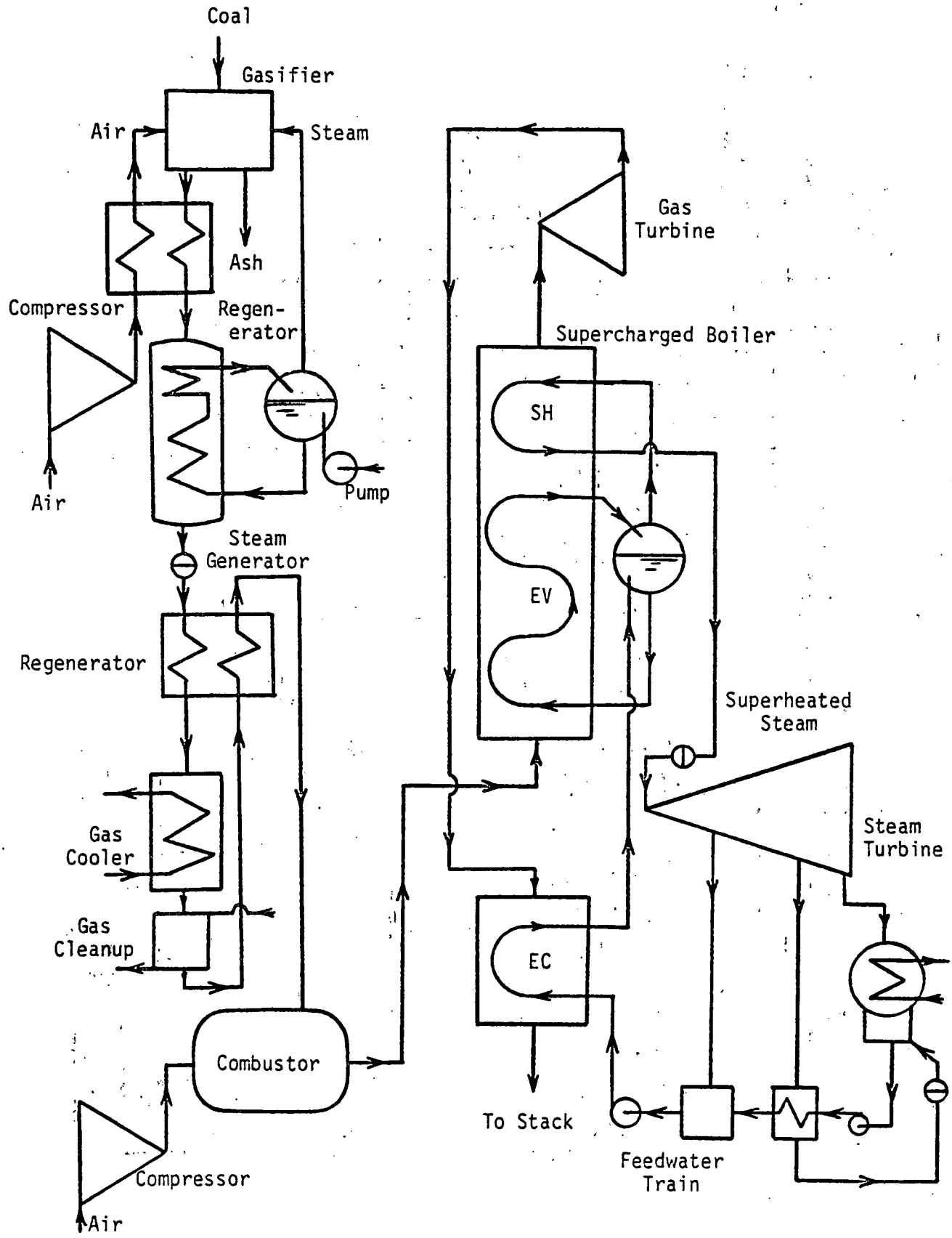

Figure 5.6-2 Schematic of Final Version of Configuration 2

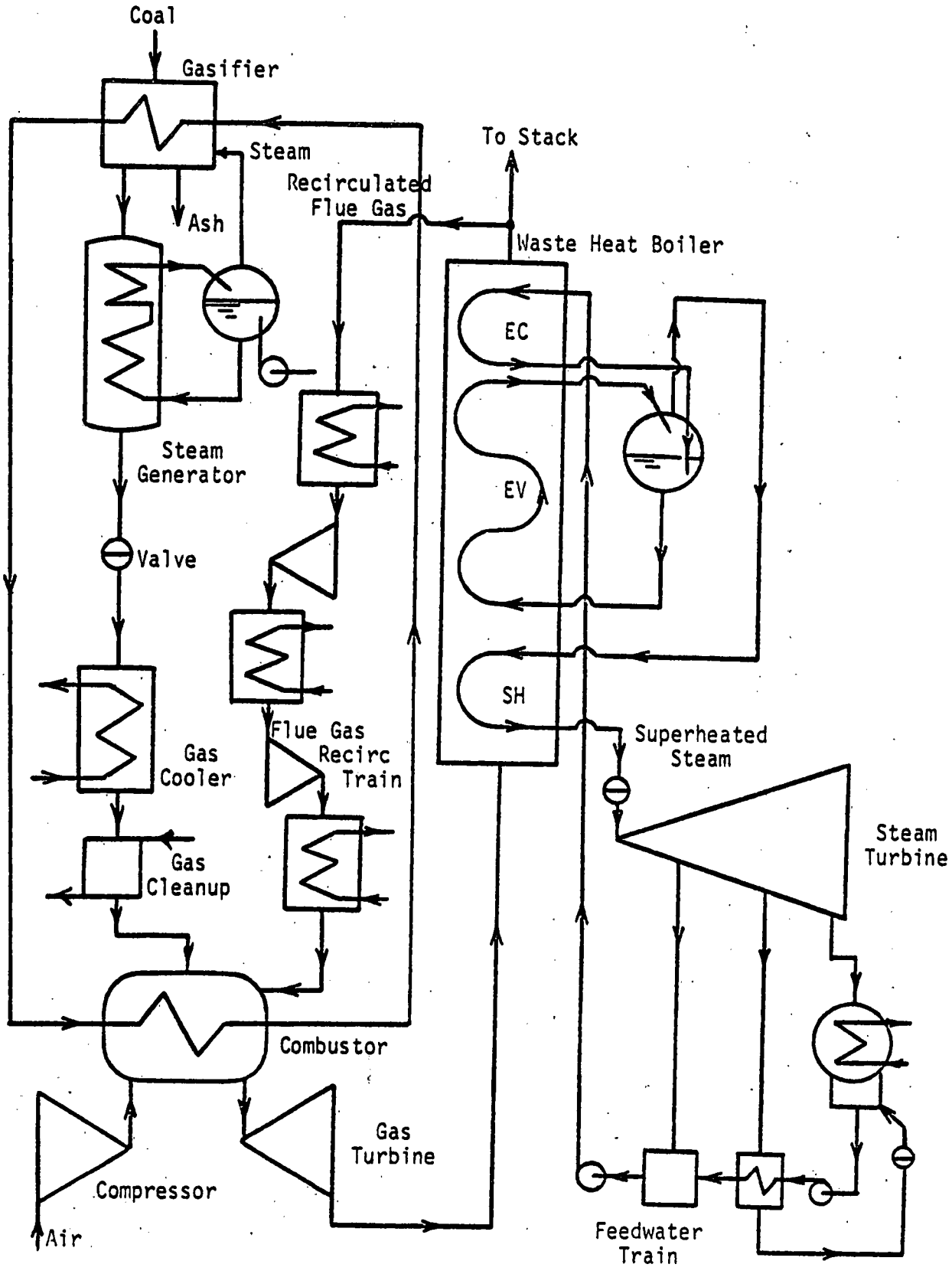

Figure 5.6-3 Schematic of Final Version of Configuration 3

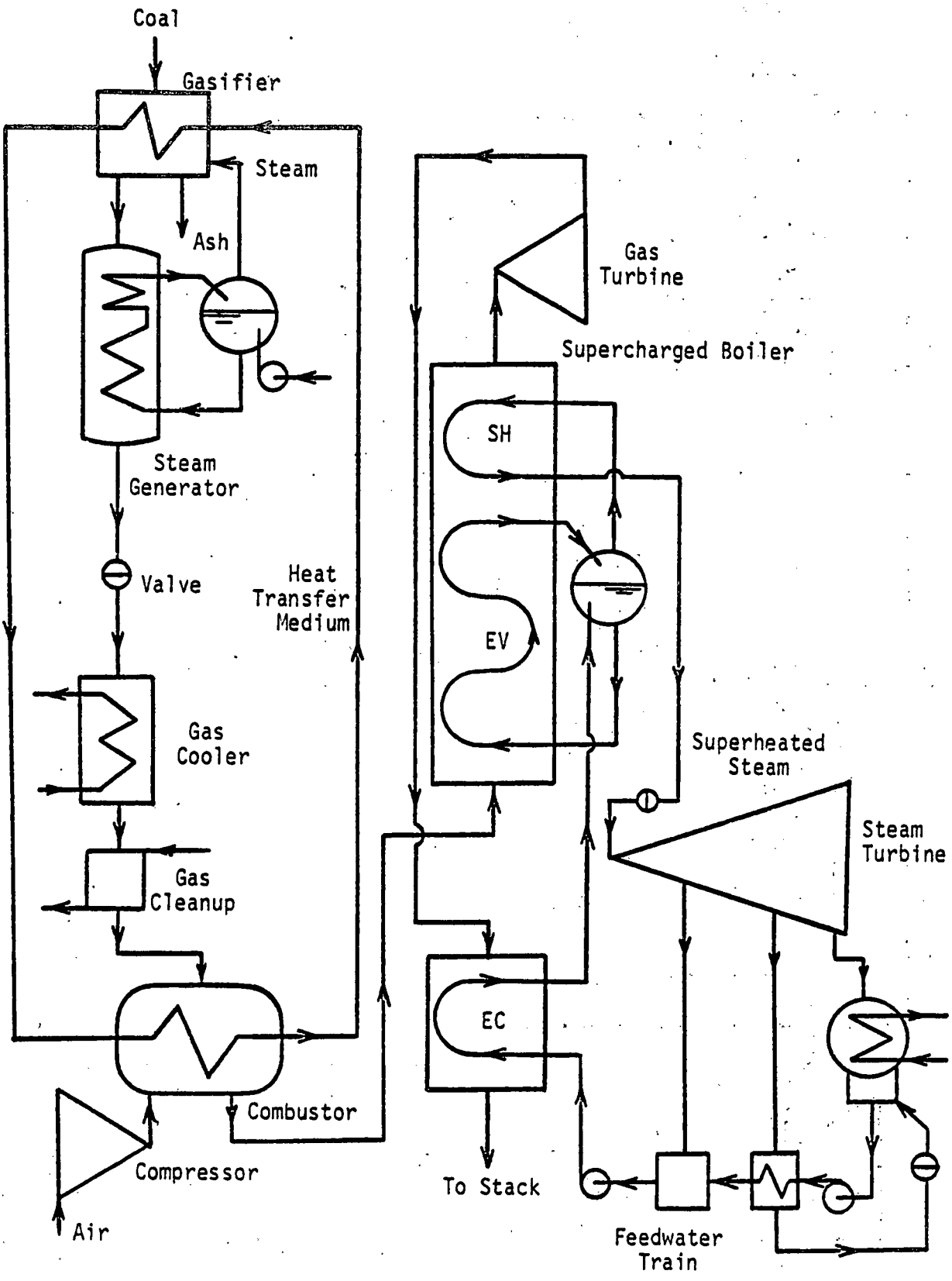

Figure 5.6-4 Schematic of Final Version of Configuration 4

CHAPTER 6

CONCLUSIONS AND RECOMMENDATIONS FOR FURTHER STUDY

Several conclusions may be drawn from the results presented in the previous chapter. First and foremost is the result of the optimization with respect to both components and operating conditions with consideration of the emission criterion on nitric oxides. As summarized in Table 5.6-2, Configuration 1 results in the best station efficiency but only by a marginal amount. In fact, the difference between the highest and lowest station efficiencies is less than 1 percentage point. If the nitric oxide problem that exists on the configurations which utilize waste heat boilers could be solved without the use of flue gas recirculation, then these configurations could have higher station efficiencies by as much as five percentage points over those incorporating supercharged boilers. All of these comments depend, of course, on the validity of the 2400°F freeze temperature for the NO producing reaction.

While Configuration 1 is marginally the best performer, it does require the most equipment. Further complicating the trade-offs which must be made concerning the search for the best configuration is the relatively small consumable water requirement for Configuration 1. In general, the configurations employing endothermic gasifiers require about twice as much total water as those incorporating adiabatic gasifiers. Finally, the waste heat configurations reject a much smaller amount of heat from the steam cycle compared to that of the supercharged boiler configurations. This could result in substantial capital cost savings if cooling towers could be eliminated on the waste heat configurations.

It is instructive to compare these results with the station efficiency of a conventional coal-fired plant with stack gas scrubbers. Osterle, Impink, et al.[17] calculate the station efficiency of a coal-fired plant under assumptions very similar to those made in this work to be 37.5 percent, without consideration of the penalty from the stack gas scrubbers. Rubin[30] presents data which shows that about 2 1/2 percentage points should be subtracted from the above station efficiency to include the energy requirements of the scrubbers. Therefore, the station efficiency of 36.67 percent for Configuration 1 is slightly better than that of 35.0 percent for a conventional coal-fired plant. Configuration 1 appears to be significantly better than a nuclear plant, the station efficiency of which is usually given as 33 percent. In terms of heat rates, these station efficiencies correspond to 9307, 9750, and 10,300 But/kwhr for Configuration 1, the coal-fired plant, and the nuclear plant respectively.

As already mentioned, it appears that better performance can be expected when the amount of work produced by the gas cycle is a high fraction of the total work. This is a characteristic of the configurations employing a waste heat boiler. Unfortunately, these same configurations are unacceptable with respect to nitric oxide emissions. When flue gas recirculation is used as a means to reduce the amount of this effluent, the station efficiency decreases substantially to very nearly the values of station efficiency for the supercharged boiler configurations.

Regenerative feedwater heating in the steam cycle portion of a combined cycle results in a deterioration of plant performance. While

the steam cycle efficiency improves, the station efficiency does not. As seen in Section 5.3, the decrease in heat rejection from the steam cycle through the condenser is smaller than the increase in the gas cycle heat loss through the stack. Feedwater heating raises the final feedwater temperature. A higher stack gas temperature, of course, results in a higher sensible heat loss through the stack. It should be noted that this conclusion is a result of the concept of a combined cycle and does not apply to a conventional fossil-fueled power plant. In the latter, feedwater heating does improve the plant performance significantly. Several reasons have been identified, however, which make some feedwater heating desirable. In a combined cycle only a minimum number of feedwater heaters should be used.

For the configurations employing an adiabatic gasifier it appears that some kind of heat recovery system is necessary beyond that of the steam generator. A gas-to-gas counterflow heat exchanger between the gas streams to and from the cleanup process is seen to improve station efficiency more than 3 percentage points if the device is 80 percent effective. Increasing the temperature of the steam to the gasifier in the endothermic configurations allows the elimination of this regenerator. In these configurations the steam generator is capable of reducing the gas temperature to the proper level required by the cleanup process. It should also be noted for the adiabatic configurations that the regenerator near the gas cleanup system is much more important than the one between the air and gas streams to and from the gasifier respectively. In fact, with the former in service at an effectiveness of 0.80, the latter may be removed completely with the station efficiency decreasing less than 1/2 percentage point.

With the exception of Configuration 3, the effective gasification temperature may be chosen to be higher than that which results in the optimum station efficiency. The advantages of this are faster reaction rates, a lower steam requirement, and conditions which are more conducive to attaining chemical equilibrium. Since the heat source for the endothermic gasification required by Configuraion 3 is at 2000°F, the effective gasification temperature must necessarily be below this. The effect of gas cycle pressure on station efficiency is much larger than that of the effective gasification temperature. Although the temperature of the steam to the gasifier hardly affects the plant performance, proper specification of this parameter for the endothermic configurations does result in the saving of expensive equipment, namely a regenerator.

In all cases, the use of intercooled air compressors does not appear to be justified. The station efficiencies either dropped slightly or remained the same when this modification was made to each configuration.

Fortunately, each configuration is fairly insensitive to different types of coal. When three other types of coal were used in the analysis, the station efficiency hardly changed. Although this study was shown for Configuration 1 only, similar results are obtained for the other configurations. Boiler pinch point temperature differences, too, are unimportant. Halving the 40°F minimum pinch point temperature difference results in a relatively small improvement in station efficiency with the largest increase of slightly more than 1/2 percentage point occurring on Configuration 1.

The inefficiencies associated with the cycle components, particularly the turbines and compressors, play a major role in reducing plant performance. For the hypothetical case of ideal components, the station efficiency would increase more than 6 percentage points. The pressure drops apparently play a much smaller role in determining station efficiency.

Finally, it was seen that the real success of the combined cycle concept integrated with a coal gasifier depends on the attainment of the 2400°F gas turbine inlet temperature. It was shown for Configuration 1 that an increase of almost exactly 5 percentage points would result, after consideration of the pollution criteria. The use of flue gas recirculation to control the production of NO on the waste heat configurations results in decreasing the station efficiency about 3 percentage points.

One obvious extension to the above work is the task of sizing the equipment necessary to obtain a specified electrical power output, say 500 MWe. The results of this could be used for two further studies: an economic study where the trade-offs could be assessed quantitatively between reduced station efficiency on one hand and reduced capital, operating, and maintenance costs on the other; and a transient study where the controls for the best configuration with respect to both performance and economics could be developed. The question of load follow capability could be addressed more appropriately during the course of the design of the control systems. The economic and technical feasibility of gas storage for later use either as a fuel for a combined cycle or as a chemical feedstock for some other process could also be determined.

REFERENCES

1. Ad Hoc Panel on Low-Btu Gasification of Coal of the Committee on Processing and Utilization of Fossil Fuels, "Assessment of Low- and Intermediate-Btu Gasification of Coal," Commission on Sociotechnical Systems of the National Research Council for the National Academy of Sciences, Washington, 1977.

2. P. F. H. Rudolph, "The Lurgi Process for Coal Gasification," Energy Technology Handbook, D. M. Considine (ed.), McGraw-Hill Book Company, New York, 1977, pp. 1-188 to 1-200.

3. W. W. Bodle and K. C. Vyas, "Clean Fuels from Coal," The Oil and Gas Journal, pp. 73 to 88, August, 1974.

4. R. T. Haslan and R. P. Russel, Fuels and Their Combustion, McGraw-Hill Book Company, New York, 1926.

5. Ad Hoc Panel on the Evaluation of Coal Gasification Technology, "Evaluation of Coal Gasification Technology: Part II--Low- and Intermediate-Btu Fuel Gases," National Research Council for National Academy of Sciences, Washington, 1973.

6. W. W. Bodle and K. C. Vyas, "Clean Fuels from Coal--Introduction to Modern Processes," Clean Fuels from Coal Symposium, Vol. II, Institute of Gas Technology, Chicago, pp. 11 to 25, 1975.

7. E. H. Hall et al., Fuel Technology: A State-of-the-Art Review, U.S. Environmental Protection Agency, Publication NTIS PB-242-535, National Technical Information Service, Springfield, Virginia, 1975.

8. D. Hebden, "High Pressure Gasification under Slagging Conditions," Paper presented at the Seventh Synthetic Pipeline Gas Symposium of the AGA, ERDA, and IGU, Chicago, 1975.

9. C. G. Von Fredersdorff and M. A. Elliott, "Coal Gasification," Chemistry of Coal Utilization--Supplementary Volume, H. H. Lowry (ed.), John Wiley & Sons, Inc., New York, 1963.

10. R. T. Grace, "Bi-Gas Process for Production of High-Btu Pipeline Gas from Coal," Energy Technology Handbook, D. M. Considine (ed.), McGraw-Hill Book Company, New York, 1977, pp. 1-212 to 1-218.

11. K. Traenckner, "Pulverized-Coal Gasification Ruhrgas Processes," Transactions of the ASME, 1953.

12. D. T. Beecher et al., Energy Conversion Alternatives Study (ECAS), Westinghouse Phase II Final Report, NASA CR-134942, Vol. I to III, Cleveland, November, 1976.

13. J. C. Corman et al., Energy Conversion Alternatives Study (ECAS), General Electric Phase II Final Report, NASA-CR 134949, Vol. I to III, Cleveland, December, 1976.

14. Evaluation of Phase 2 Conceptual Designs and Implementation Assessment Resulting from the Energy Conversion Alternatives Study (ECAS), NASA Lewis Research Center, NASA TX-73515, Cleveland, April, 1977.

15. D. J. Ahner et al., "Economics of Power Generation from Coal Gasification for Combined-Cycle Power Plants," Combustion, Vol. 47, pp. 26 to 35, April, 1976.

16. J. F. Osterle, "Thermodynamic Considerations in the Use of Gasified Coal as a Fuel for Power Conversion Systems," Proceedings of the Frontiers of Power Technology Conference at Oklahoma State University, Carnegie-Mellon University, Pittsburgh, October, 1974.

17. J. F. Osterle, A. J. Impink, Jr., M. H. Lipner, and A. Candris, "Pressurized Gasification Systems Coupled to Combined Steam-Gas Power Cycles for the Generation of Clean Electric Power from Pennsylvania Coal," Final Report Prepared for the Pennsylvania Science and Engineering Foundation under Agreement Number 241, Carnegie-Mellon University, Pittsburgh, July, 1975

18. Steam/Its Generation and Use, Babcock and Wilcox Company, New York, 1972.

19. J. M. Smith and H. C. Van Ness, Introduction to Chemical Engineering Thermodynamics, 3d. ed., McGraw-Hill Book Company, New York, 1975.

20. F. Kreith, Principles of Heat Transfer, 2d. ed., International Textbook Company, Scranton, Pa., 1965.

21. D. R. Stull and H. Prophet (Proj. Dir.), JANAF Thermochemical Tables, 2d. ed., Office of Standard Reference Data, National Bureau of Standards, Washington, June, 1971.

22. Robert W. Hornbeck, Numerical Methods, Quantum Publishers, Inc., New York, 1975.

23. H. C. Hottel et al., Thermodynamic Charts for Combustion Processes, John Wiley & Sons, Inc., New York, 1949.

24. Kuzman Raznjevic, Handbook of Thermodynamic Tables and Charts, McGraw-Hill Book Company, New York, 1976.

25. James R. Small and James A. Williamson, "Source Monitoring of NO_x and SO_2," Energy Technology Handbook, D. M. Considine (ed.), McGraw-Hill Book Company, New York, 1977, p. 9-374.

26. David Pasquinelli, "Investigation of the Accuracy of the Dulong Approximation," unpublished master's project, Carnegie-Mellon University, Pittsburgh, 1976.

27. G. J. Van Wylen, Thermodynamics, John Wiley & Sons, Inc., New York, 1966, p. 443.

28. A. K. Mehta, "Mathematical Modeling of Chemical Processes for Low Btu/Gasification of Coal for Electric Power Generation," Final Report of work performed under contract no. E(49-18)-1415 for ERDA, Combustion Engineering, Inc., Windsor, Conn., August, 1976.

29. "Optimization of Coal Gasification Processes," Interium Report No. 1, Vol. 1 prepared for Office of Coal Research under contract no. 14-01-0001-497, U.S. Department of the Interior, Washington.

30. E. S. Rubin (Proj. Dir.), "Comparative Environmental Assessments of Coal Utilization Systems: Vol. I: Overview and Summary," Final Report prepared for Brookhaven National Lab (D.O.E.), Middle Atlantic Power Research Committee, and Pennsylvania Science and Engineering Foundation by the Center for Energy and Environmental Studies, Carnegie-Mellon University, Pittsburgh, March, 1978.

31. "Standards of Performance for New Stationary Sources," Federal Register, Vol. 36, No. 247, December 23, 1971.

COO-EY77S024196-2

2 ENERGY CONSERVATION IN COAL CONVERSION

1 Energy Conservation Potential in Shaft Power Generation and Distribution

R. G. McMillin

Carnegie-Mellon University
Pittsburgh, PA 15213

June, 1978

Prepared for

THE U.S. DEPARTMENT OF ENERGY
Pittsburgh Energy Technology Center
UNDER CONTRACT NO. EY77S024196

ABSTRACT

A criteria for determining the most energy efficient horsepower break-point for using electric motors or steam turbines is developed and applied to the prime movers in the Ralph M. Parsons Co. Oil/Gas Complex. No significant amount of energy can be saved, since the electric motor turbine break-point established by Ralph M. Parsons Co. coincides with the criteria developed in this study.

TABLE OF CONTENTS

LIST OF FIGURES

INTRODUCTION

In accordance with the commercial concept design of the Oil/Gas complex as described in Reference 1,524,000 HP of shaft work is provided by prime movers. These prime movers are either turbines or motors. The turbines utilize steam directly. The motors are supplied with electricity from a turbine-dirven generator. Reference 2 indicates that the drivers correspond to the following HP ranges:

Range	Driver
0 - 10,000 HP	Motor
10,000 - 15,000	Variable
> 15,000	Turbine

This report will determine whether energy can be saved by replacing a motor with a turbine or vice-versa.

METHOD OF APPROACH

The first task was to determine the efficiency of the two 110.0 MW turbine drivers used in the power generation unit of Reference 1. The efficiency of either of these multi-stage extraction turbines is 86% (Appendix A).

Reference 3 indicates a 110.0 MW generator efficiency of 97%.

The motor efficiencies (References 4 and 5) range from 80% @ 1 HP to 96.4% @ 10,000 HP.

The overall system efficiency is desribed by the following equation:

$$\eta \text{ system} = \eta \text{ turbine} \times \eta \text{ generator} \times \eta \text{ motor}$$

where the turbine and generator efficiencies are fixed for the 110 mw turbine-generator sets, and the motor efficiency varies with HP (see Appendix B for sample calculation). The curve constructed from this equation is seen in Figure 1. Also present are the efficiency curves of multi-stage condensing turbines and single stage turbines.

Figure 2 allows for accurate resolution of the "Average Efficiency of Multi-Stage Condensing Turbine" curves of Figure 1. It is imperative to note the high sensitivity of the turbine efficiency curves to the superheat and vacuum correction factors.

To demonstrate the sensitivity of the turbine efficiency to these correction factors, consider a 10,000 HP turbine utilizing 900 psi steam. From Figure 1, the average efficiency is 76%. If the incoming steam is superheated by 300°F, however, and exits to a 26 in. Hg. vacuum, the "corrected" efficiency is 79.4%. (1.035 x 1.01 x 76% = 79.4%).

Although the turbine-generator-motor curve of Figure 1 is slightly above the average multi-stage condensing turbines, it is by an insignificant amount when the effect of correction factors and the precision of information concerning the various efficiencies is properly evaluated.

CONCLUSION

Figure 1 indicates that below 10,000 Hp, an electric motor driver is the more efficient choice, between 10,000 Hp and 15,000 Hp depending on superheat temperature and condenser vacuum, either motor or turbine driver could be used, and for drivers above 15,000 Hp, turbines would be more efficient. With respect to Reference 2, no significant amount of energy can be saved by replacing a motor with a turbine, or a turbine with a motor.

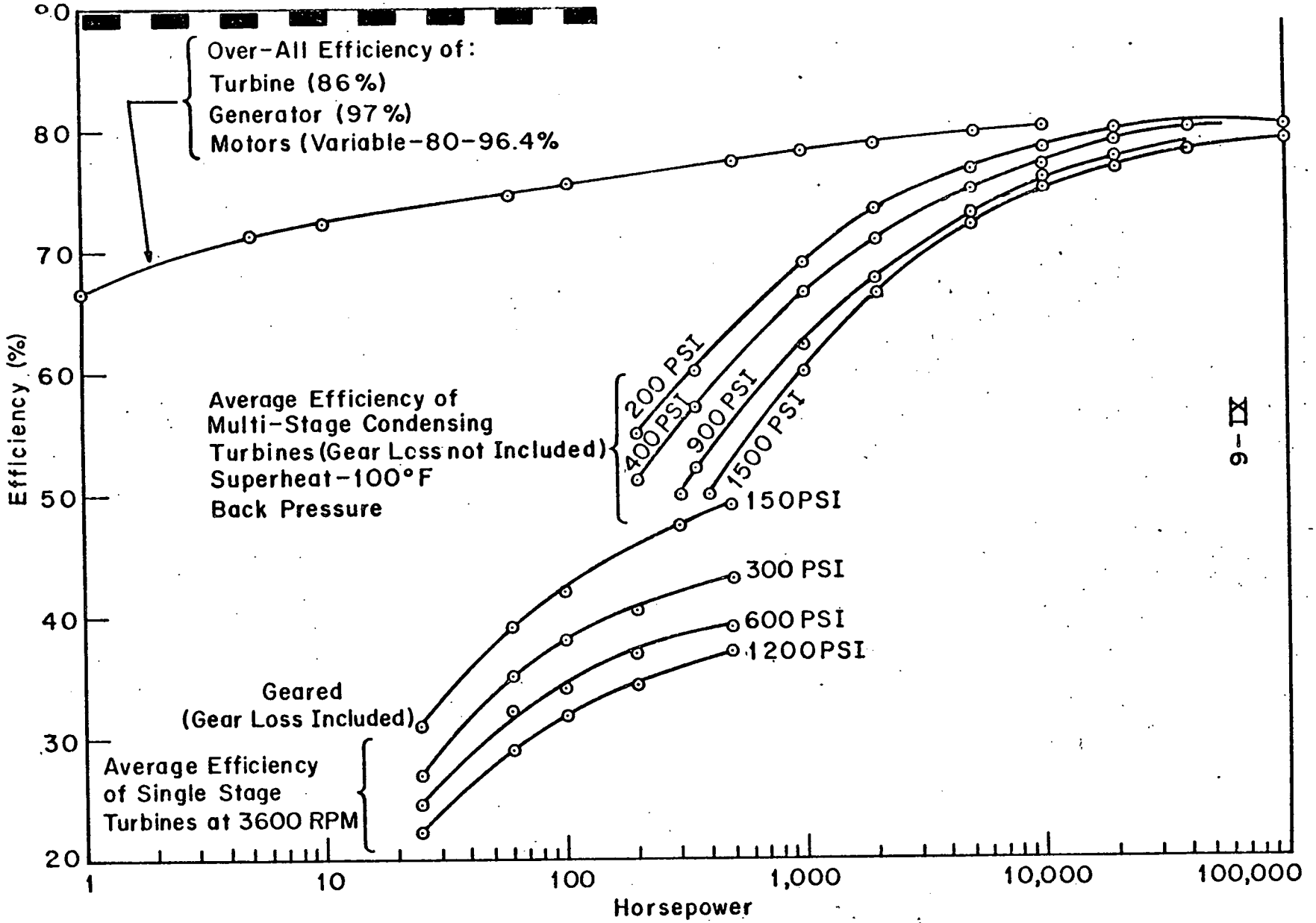
Over-All Efficiency of:
Turbine (86%)
Generator (97%)
Motors (Variable-80-96.4%
Average Efficiency of
Multi-Stage Condensing
Turbines (Gear Loss not Included)
Superheat-100°F
Back Pressure
200 PSI
400 PSI
900 PSI
1500 PSI
150 PSI
300 PSI
600 PSI
1200 PSI
Geared
(Gear Loss Included)
Average Efficiency
of Single Stage
Turbines at 3600 RPM
Efficiency (%)
90
80
70
60
50
40
30
20
1
10
100
1,000
10,000
100,000
Horsepower
9-IX

FIG. 1

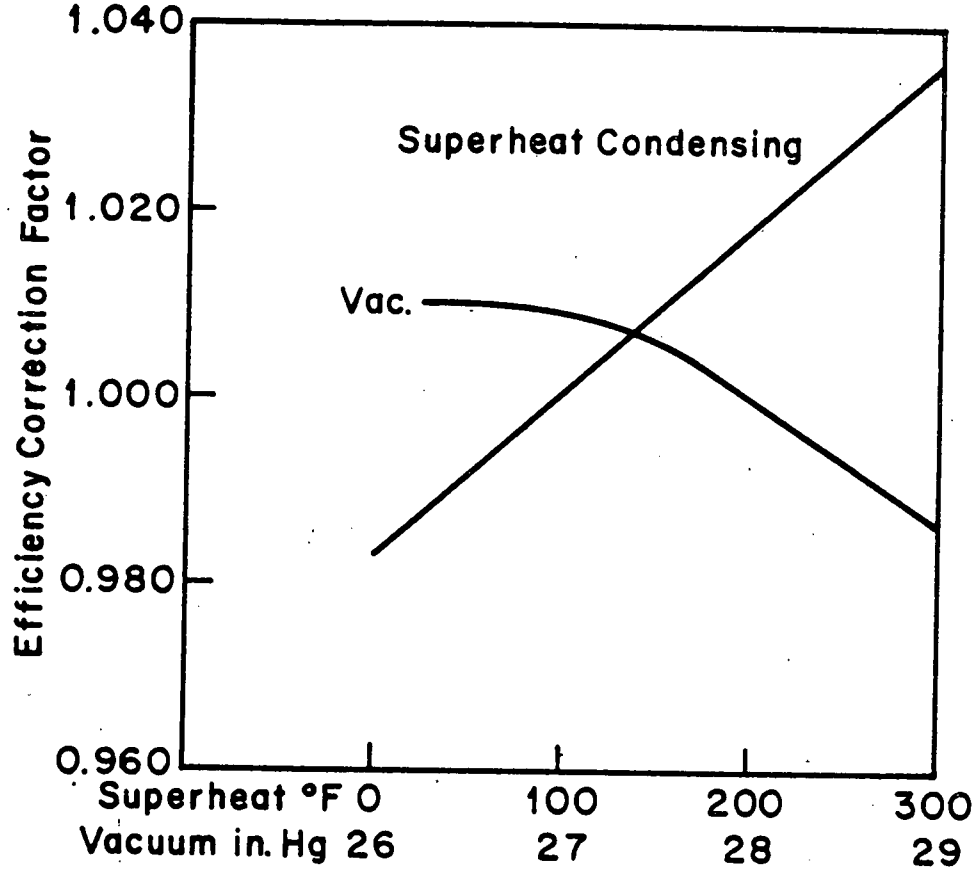
1.040
1.020
1.000
0.980
0.960
Efficiency Correction Factor
Superheat Condensing
Vac.
Superheat °F 0
Vacuum in. Hg 26
100
27
200
28
300
29

FIG. 2

REFERENCES

1. Oil/Gas Complex, Conceptual Design/Economic Analysis R&D Report No. 114, Contract No. E (49-18)-1775 March 1977.

2. Conversation with Andrew BeLa Ralph M. Parsons Company, Pasadena, California.

3. Conversation with W. G. Steltz, Westinghouse, Lester, Pennsylvania.

4. Converstion with Frank Konechi, U. S. Electric Motors, Milford, Conneticut.

5. Conversation with Bill Joseph, General Electric, Schenectady, New York.

6. Conversation with Dave Laser, Elliott Company, Jeanette, Pennsylvania.

7. Conversation with Professor W. T. Rouleau, Carnegie-Mellon University, Pittsburgh, Pennsylvania.

It is of interest to find the external turbine efficiency of the induction turbine operating under the constraints shown:

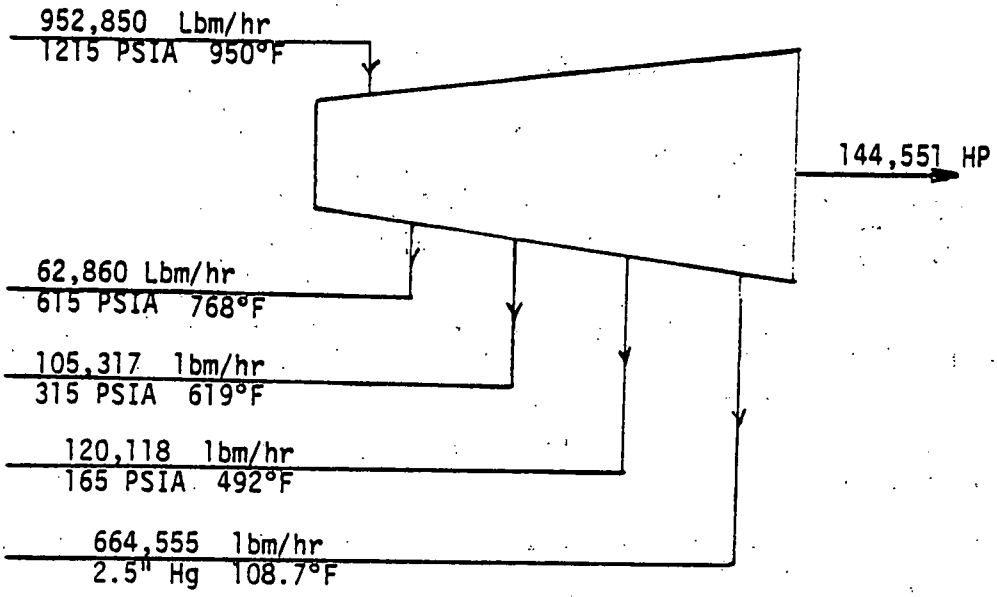

To do so, the inlet and exit states are examined:

S1 @ 1215 PSIA 950°F; S1 = State at point 1; $h_1 = 1469.7 \frac{Btu}{lbm}$

S2 @ 615 PSIA 768°F; $_1h_{2s} = 1377 \frac{Btu}{lbm}$; $\Delta_1 h_{2s} = 92.7 \frac{Btu}{lbm}$

S3 @ 315 PSIA 619°F; $_1h_{3s} = 1297 \frac{Btu}{lbm}$; $\Delta_1 h_{3s} = 172.7 \frac{Btu}{lbm}$

S4 @ 165 PSIA 492°F; $_1h_{4s} = 1234 \frac{Btu}{lbm}$; $\Delta_1 h_{4s} = 235.7 \frac{Btu}{lbm}$

S5 @ 2.5" Hg 108.7°F; $_1h_{5s} = 907 \frac{Btu}{lbm}$; $\Delta_1 h_{5s} = 562.7 \frac{Btu}{lbm}$

where h refers to the enthalpy at the specified inlet state and $_1h_{nS}$ refers to the isentropic enthalpy drop from that state to the outlet conditions found from Mollier diagrams.

A standard method for calculating the efficiency was employed.[6,7] First, the Rankine cycle steam rate (RCSR), described by:

$$RCSR \left(\frac{lbm}{HP\text{-}hr}\right) = \frac{2544 \text{ Btu/HP-hr}}{(h_1 - {}_1h_2) \text{ Btu/lbm}}$$

was found by using a "weighted average" of the available energy described by the isentropic enthalpy drop. This result in:

$$RCSR = \frac{2544 \text{ Btu/HP-hr}}{0.066\ (92.7) + 0.111\ (172.7) + 0.126\ (235.7) + 0.697\ (562.7)} = 5.689 \frac{lbm}{HP\text{-}h}$$

This is compared to the actual steam rate (ASR) of:

$$ASR = \frac{1{,}905{,}700 \text{ lbm/hr}}{\left(\frac{209.2 \text{ MW}}{.97}\right)\left(\frac{\text{HP}}{0.000746 \text{ MW}}\right)} = 6.592 \frac{\text{lbm}}{\text{HP-hr}}$$

This means the external efficiency is:

$$\frac{RCSR}{ASR} = \frac{5.689}{6.592} \times 100\% = 86.3\%$$

APPENDIX B

The overall system efficiency is described by the following equation:

$$\eta_{system} = \eta_{turbine} \times \eta_{generator} \times \eta_{motor}$$

Thus, the system efficiency at 10,000 HP, for example, was found to be:

$$\eta_{system} = 0.863 \times 0.97 \times 0.964 = 0.807$$

2 ENERGY CONSERVATION IN COAL CONVERSION

1 Basis for Fuel and Utility Costs

R. Kramek

Carnegie-Mellon University
Pittsburgh, PA 15213

June, 1978

Prepared for

THE U.S. DEPARTMENT OF ENERGY
Pittsburgh Energy Technology Center
UNDER CONTRACT NO. EY77S024196

TABLE OF CONTENTS

DISCUSSION OF TABLE 1

The reports in this study use a common basis for fuel and utility costs presented in Table 1. The costs for electricity, natural gas, distillate fuel oil, residual fuel oil, LPG, and coal have been excerpted from the FEA energy price projections[1], and are for FEA region V, which encompasses the design location of the Oil/Gas Complex designed by Ralph M. Parsons Co. The costs for cooling water and steam are averaged figures quoted in reference 2. The distillate fuels in Table 1 comprise light and middle fuel oil derivatives such as kerosene, and deisel fuel, and include No's 1,2,3,4, fuel oil. The residual fuels are No's 5,6, Bunker C and all other petroleum fuels which have a fifty per cent boiling point over 700°F. All costs are in 1977 dollars.

TABLE 1

ENERGY COSTS IN 1977 DOLLARS

Fuel	1978	1981	1984	1987	1990
Electricity $/kwhr	.0245	.0271	.03	.0327	.0353
Natural Gas $/MMBtu	1.45	1.77	2.19	2.60	3.01
Distillate Fuel Oil, $/MMBtu	2.94	3.12	3.27	3.42	3.57
Residual Fuel Oil, $/MMBtu	2.73	2.94	2.96	3.07	3.23
LPG, $/MMBtu	2.96	3.36	3.55	3.70	3.84
Coal, $/MMBtu	1.30	1.54	1.57	1.61	1.64
Steam, $/1000 lb					
High Pressure Superheated	3.60	--	--	--	--
Medium Pressure Saturated	3.10	--	--	--	--
Low Pressure Saturated	2.50	--	--	--	--
Cooling Water, ¢/1000 gal.	4.0	--	--	--	--

REFERENCES

1. "Energy Users Report Reference File", Section 41, Published by the Bureau of National Affairs, Inc., Wash., D.C. 1978.

2. Considine, D. M., Editor, Energy Technology Handbook, McGraw Hill Book Co., New York, 1977.

2 ENERGY CONSERVATION IN COAL CONVERSION

Using Second Law Analysis to Pinpoint Inefficiencies in Coal Conversion Processes

E. J. Mueller
L. Fucich

Carnegie-Mellon University
Pittsburgh, PA 15213

August, 1978

Prepared for

THE U.S. DEPARTMENT OF ENERGY
Pittsburgh Energy Technology Center
UNDER CONTRACT NO. EY77S024196

ABSTRACT

This study performs a second law analysis on the Fischer-Tropsch complex proposed by the Ralph M. Parsons Company. The second law efficiency of each process unit making up the complex was computed in order to determine areas where process improvements could be made.

The complex as a whole has a first law efficiency of 70% and a second law efficiency of 68.7%. Two areas where efficiencies could be improved are: unit 14, acid gas removal with a second law efficiency of 80.2%, and unit 21, sulfur recovery, which has a second law efficiency of 66.4%. Other areas had efficiencies greater than 87% which indicates energy recovery and conservation techniques had been implemented in the design of the complex.

ACKNOWLEDGEMENT

I would like to thank T. Ruppel of The Pittsburgh Energy Technology Center for his contributions to this study.

TABLE OF CONTENTS

LIST OF TABLES

LIST OF FIGURES

INTRODUCTION

Purpose

This report performs a second law analysis on the Fischer-Tropsch Complex of the Ralph M. Parson Company. A second law analysis, based on the concept of availability, is used to pinpoint and evaluate the dissipations in the F-T complex, and also to determine the efficiency of the complex. The analysis is performed on the entire complex to determine an over-all efficiency, and also on the individual process units to reveal areas for improvement. A second law analysis is used instead of a first law (energy) analysis because the results are measured with availability or useful energy and thus are the true efficiencies.

Second Law Analysis

Second Law Analysis is based on the concept of availability sometimes referred to as useful energy, potential energy, exergy and other names. This concept can seem abstract and difficult to understand but availability can be considered as the measure of a material to cause a desired change. Therefore, any material which is not in equilibrium with its surroundings has the potential of doing useful work as it approaches equilibrium with its surroundings, and this is the definition of availability.[1,12]

Description of Fischer-Tropsch Complex

The Ralph M. Parsons Fischer-Tropsch Complex is a coal conversion facility designed to use high-sulfur coal and convert it to SNG (substitute natural gas), LPGs (liquified petroleum gases), light and heavy naphthas, diesel fuel, fuel oil, oxygenates (primarily alcohols), and

electrical power for in-plant use and export. Using the Fischer-Tropsch process, the coal is gasified, the gases purified, and reacted to produce the above products. The industrial complex consists of a large mine that produces 40,000 tons per day (TPD) of run-of-mine coal which is supplied to a coal preparation plant, which in turn supplies 30,000 TPD of clean, sized coal with a heating value of 12,550 Btu/lb to the Fischer-Tropsch plant. All electricity and steam required for the Fischer-Tropsch complex are generated within the plant; therefore, the input to the plant is coal, air, and water. The overall material balance is shown on Figure 1 and the energy balance is shown on Figure 2. The estimated fixed capital investment is $1.5 billion based on fourth quarter 1975 dollars.

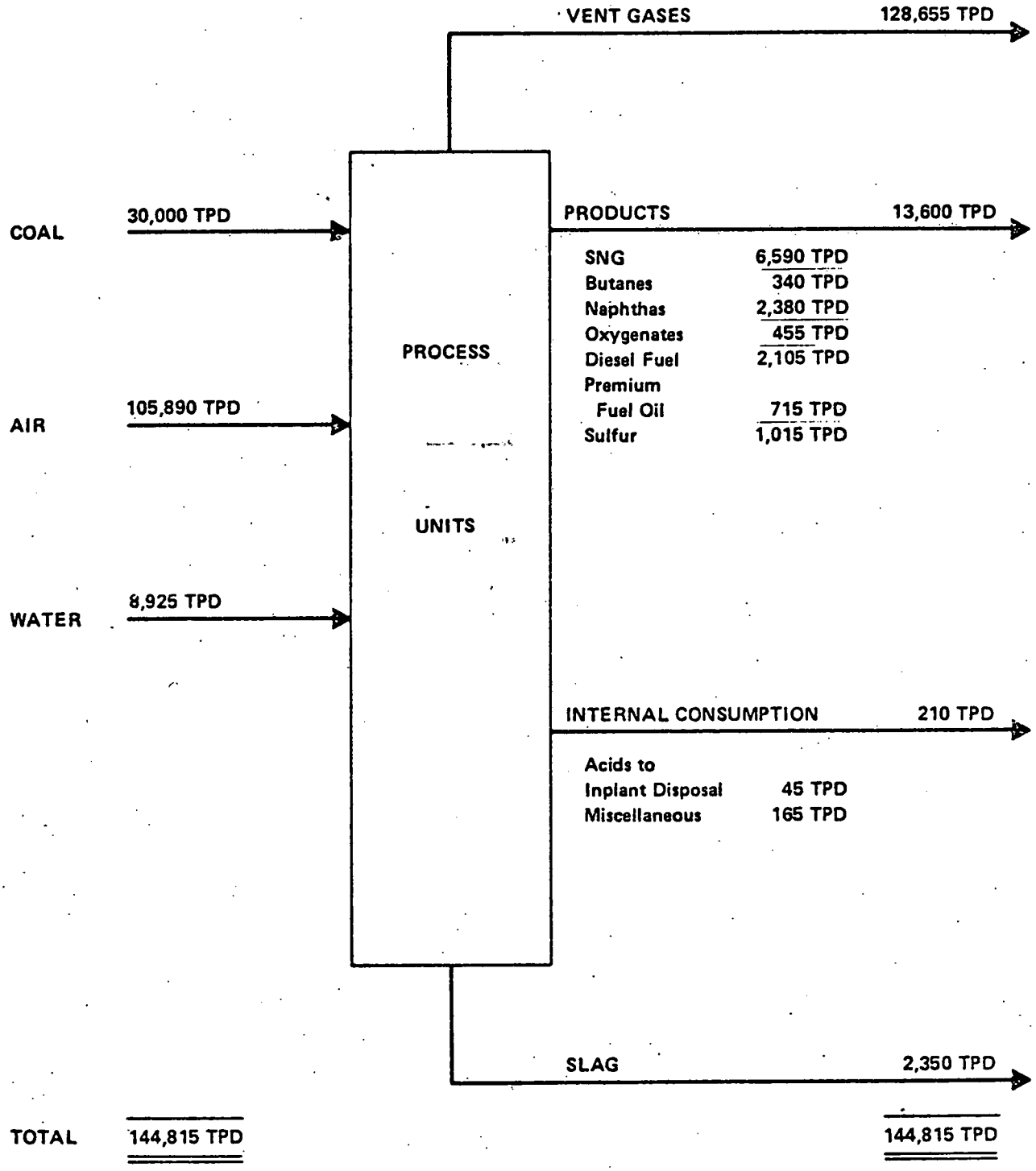

FIGURE 1

Overall Material Balance

Reproduced from R&D Report No. 114 - Interim Report No. 3 by the Ralph M. Parsons Company.

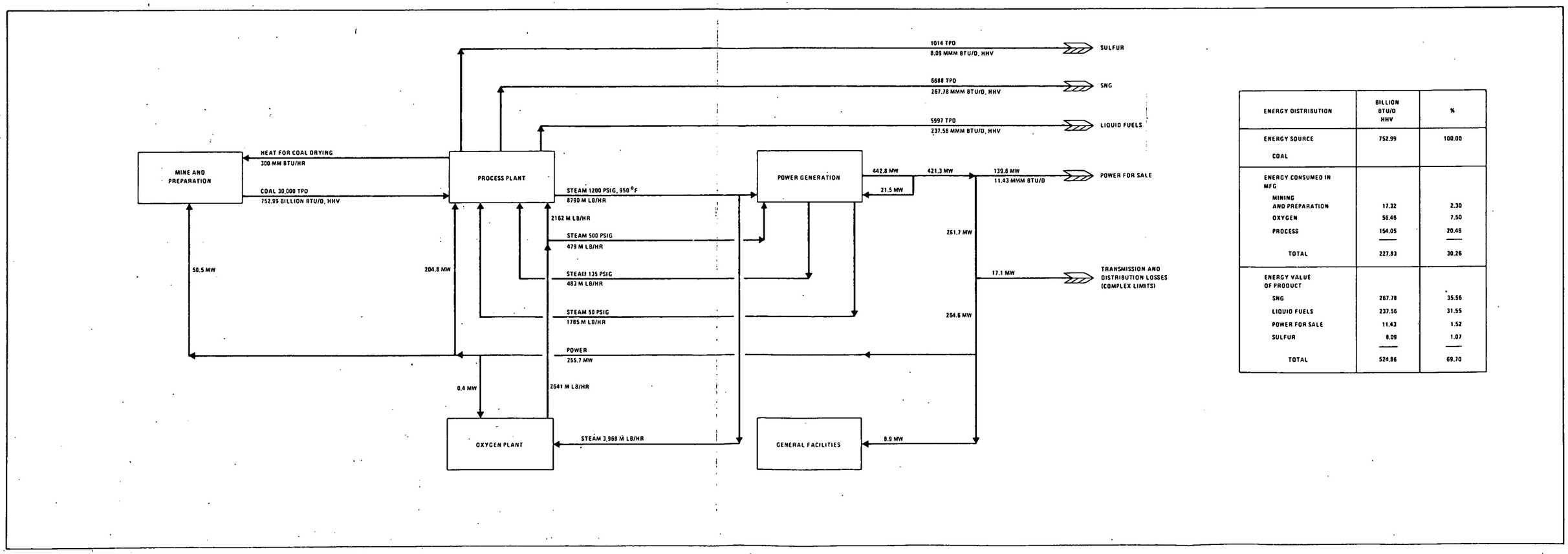

ENERGY DISTRIBUTION	BILLION BTU/D HHV	%
ENERGY SOURCE	752.99	100.00
COAL		
ENERGY CONSUMED IN MFG		
MINING AND PREPARATION	17.32	2.30
OXYGEN	56.46	7.50
PROCESS	154.05	20.46
TOTAL	227.83	30.26
ENERGY VALUE OF PRODUCT		
SNG	267.78	35.56
LIQUID FUELS	237.56	31.55
POWER FOR SALE	11.43	1.52
SULFUR	8.09	1.07
TOTAL	524.86	69.70

FIGURE 2

Energy Balance

Reproduced from R&D Report No. 114 - Interim Report No. 3
by the Ralph M. Parsons Company.

Procedure for Calculating Second Law Efficiencies

A second law analysis of the Parsons Fischer-Tropsch Complex was performed by first considering the entire plant, its inputs and outputs and then considering each separate process unit in order to pinpoint the process units which were the most energy inefficient.

The basis of the second law analysis is the concept of available energy or availability. Availabilities were calculated using equation (1)

$$(1)\quad A = \dot{m}\left[\left((Cp\ (T-To)) + Hc + Hv\right) - To\left((Cp\ \ell n\ (\frac{T}{To})) + \frac{Hv}{To} - \frac{R}{M}\ In\ (\frac{P}{Po}) + S°comb\right)\frac{RTo}{M} - \ell n\ Xo\right]$$

A = availability, Btu/HR

$\dot{m}$ = mass flow of the stream, lb_m/HR

Cp = constant pressure specific heat of the stream, Btu/lb_m-°R

T = temperature of the stream °R

To = dead state temperature = 537°F = 77°F

Hc = heat of combustion of the stream, Btu/lb_m

HV = heat of vaporization of the stream, Btu/lb_m

R = universal gas constant 1545 $\frac{ft\text{-}lb_f}{lb_m\text{-}°R}$

M = molecular weight

P = pressure of the stream, psia

Po = dead state pressure 14.7 psia

S°comb = entropy of combustion, Btu/lb_m-°R

Xo = mole fraction of substance in stream that occurs in nature.

Once the availabilities of all the inlet and outlet streams were determined, the second law efficiency was found as shown in equation 2:

(2) $E_{2L} = \frac{\Sigma Ao}{\Sigma Ai}$ (9)

E_{2L} = second law efficiency

Ao = availability out of unit

Ai = availability into unit

The availability loss through the unit is expressed as the sum of the availabilities in minus the sum of the availabilities out; this loss, then, is a measure of the inreversibility of the process.(7)

Using the relationships presented above, the second law efficiencies and the availability losses through the entire complex and each separate process unit were found and are shown on Tables 1 and 2 along with availabilities in and out.

Some examples of availability calculations follow.

The availability of coal was not determined using equation (1) but was determined from an equation presented in reference 12:

$$a_{coal} = hc_{coal} \times \frac{a_{carbon}}{hc_{carbon}}$$

a_{coal} = availability of coal $\frac{Btu}{lb_m}$

hc_{coal} = heat of combustion of coal, Btu/lb

a_{carbon} = availability of carbon, Btu/lb

hc_{carbon} = heat of combustion of carbon, 14,067 Btu/lb.

Therefore,

$$a_{coal} = 12{,}550 \frac{Btu}{lb} \times \frac{14760}{14067}$$

or,

a_{coal} = 13,168 Btu/lb

The availability of steam was calculated using a simplified version of equation (1):

$$a_{steam} = ((h_{t,p} - h_{to,po})) - To\ (S_{t,p} - S_{to,po}))$$

Using the steam tables for steam at 510 psia and 670°F:

$$a_{steam} = ((1340-49.5) - 537(1.592-.093))\ \frac{Btu}{lb_m}$$

$$a_{steam} = 485.5\ \frac{Btu}{lb_m}$$

Where,

$h_{t,p}$ = enthalpy of steam at pressure P and temperature T

$h_{to,po}$ = enthalpy of steam at pressure Po and temperature To

$S_{t,p}$ = entropy of steam at pressure P and temperature T

$S_{to,po}$ = entropy of steam at pressure Po and temperature To

An availability using equation 1 is shown here for an oxygen - nitrogen stream:

Oxygen	Nitrogen		
24,947 mph	509 mph	$\dot{m}$	mph = moles per hour
449,046 lb/hr	14252 lb/hr		
.245 $\frac{Btu}{lb°R}$	.258 $\frac{Btu}{lb°R}$	Cp	
650°	650°	T	
485 psia	485 psia	P	
.2035	.7567	Xo	

$$A_{N2} = 14,252\ [((.258\ (650-77)) - 537\ (.258\ \ln(\frac{1110}{537})) - (\frac{1545}{778}(28.01)\ln(\frac{485}{14.7}))) - (\frac{1545\ (537)}{778\ (28.01)}\ \ln(.7567)))]$$

$$A_{N2} = 2.72 \times 10^6\ \frac{Btu}{hr}$$

$$A_{O2} = 449046\ [((.245\ (650-77)) - 537\ ((.245\ \ln(\tfrac{1110}{537})) - (\tfrac{1545}{778}(32)\ \ln\ (\tfrac{485}{14.7}))) - (\tfrac{1545\ (537)}{778\ (32)}\ \ln(.2035)))]$$

$$A_{O2} = 96.3 \times 10^6 \text{ Btu/hr}$$

$$A_{O2N2} = A_{O2} + A_{N2} = 2.72 \times 10^6 \frac{\text{Btu}}{\text{hr}} + 96.3 \times 10^6 \frac{\text{Btu}}{\text{hr}}$$

$$A_{O2N2} = 99 \times 10^6 \frac{\text{Btu}}{\text{hr}}$$

Availabilities for flows in and out of various process units are shown in Figure 3.

TABLE I

Overall Availabilities of the Fischer-Tropsch Complex
Inlet and Outlet Streams

Inlet Streams

Stream Name	A, Availability, Btu/day	$\dot{m}$, Flow Rate, TPD
1. Coal Feed	790.09×10^9	30,000
2. Water	0	105,890
3. Air	0	8,925
Total	790.09×10^9	144,815

Outlet Streams

Stream Name	A, Availability, $\frac{\text{Btu}}{\text{day}}$	$\dot{m}$, Flow Rate, TPD
1. SNG	289.51×10^9	6,590
2. Oxygenates (Alcohols)	11.71×10^9	455
3. Diesel Fuel	83.83×10^9	2,105
4. Sulfur	9.13×10^9	1,015

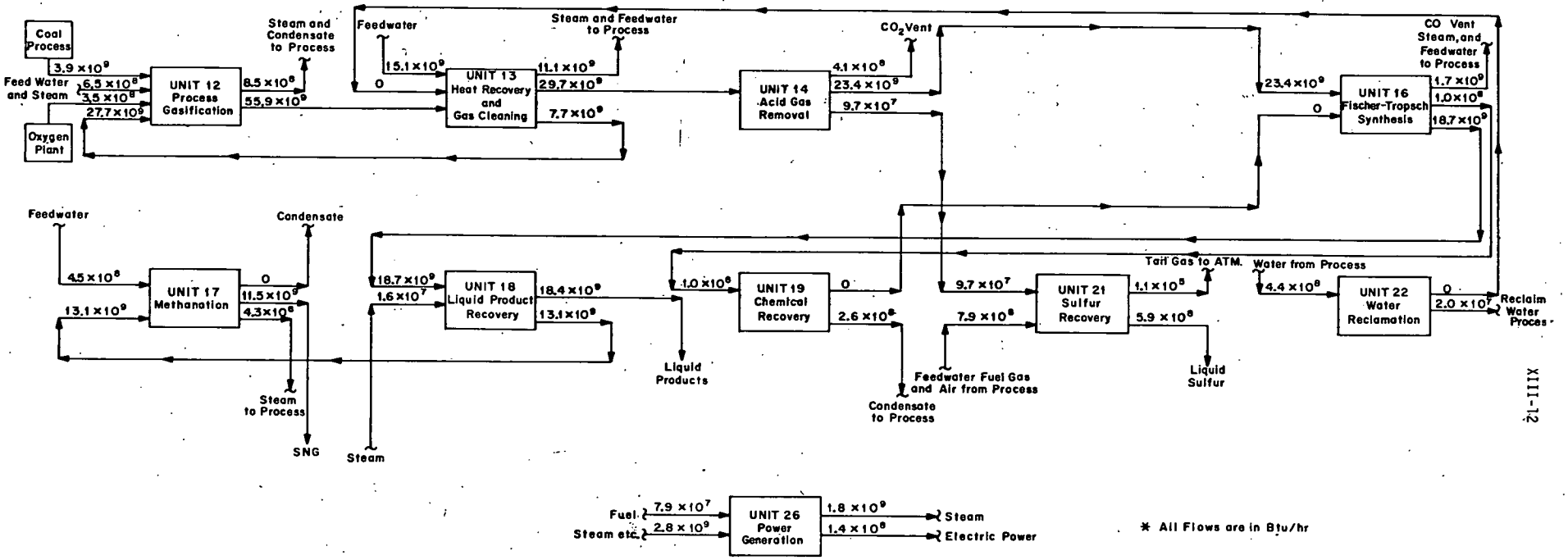

FIGURE 3
AVAILABLE ENERGY FLOW DIAGRAM OF FISCHER-TROPSCH COMPLEX

Outlet Streams (cont)

Stream Name	A, Availability, $\frac{Btu}{day}$	$\dot{m}$, Flow Rate, TPD
5. Naphthas	94.93×10^9	2,380
6. Fuel Oil	27.87×10^9	715
7. LPG (Butanes)	14.24×10^9	340
8. Electricity	11.43×10^9	--
TOTAL	542.64×10^9	13,600

$$\varepsilon = \text{second law efficiency} = \frac{\text{Outlet Availability}}{\text{Inlet Availability}} = \frac{542.64 \times 10^9}{790.09 \times 10^9} = 68.7\%$$

Net Availability Loss = $A_{inlet} - A_{outlet}$ =

$$790.09 \times 10^9 - 542.64 \times 10^9 = 247.45 \times 10^9 \text{ Btu/day}$$

TABLE 2

Availabilities of Inlet and Outlet Streams, Net Availability Loss, and the Second Law Efficiency of Each Process Unit

Unit #	Inlet Availability, A_i, Btu/hr	Outlet Availability, A_o, Btu/hr	$A_i - A_o$	2nd Law Efficiency E, A_o/A_i
12	61.64×10^9	56.73×10^9	4.91×10^9	.920
13	70.83×10^9	68.58×10^9	2.25×10^9	.968
14	29.74×10^9	23.86×10^9	5.88×10^9	.802
16	23.50×10^9	20.54×10^9	2.96×10^9	.874
17	13.57×10^9	11.97×10^9	1.60×10^9	.882
18	18.74×10^9	29.50×10^9		
19	26.96×10^7	25.61×10^7	1.35×10^7	.950
21	88.45×10^7	58.73×10^7	29.72×10^7	.664
22	44.37×10^7	2.01×10^7	42.36×10^7	.045
26	3.64×10^9	1.96×10^9	1.68×10^9	.538

Conclusions:

The Fischer-Tropsch Complex with a first law or energy efficiency of 70% for the overall has a second law of 68.7%. Individual process unit second law efficiencies are listed in Table 2. From this table, Units 12 and 13 have the highest efficiencies, 92% and 96.8% respectively; therefore, there is little improvement to be made in these units. The power generation system, Unit 26, has a second law efficiency of 53.7%; however, this unit consists only of a turbine and generator and uses steam generated in Units 16 and 17. The second law analysis also pinpointed process units with low second law efficiencies thus revealing areas for possible improvement. Unit 14, Acid Gas Removal, which uses a Selexol solution process, has a second law efficiency of 80.2%. Perhaps the present Selexol Acid Gas Removal System can be replaced by a DEA system to become more efficient. A study such as Section IX, Alternate Acid Gas Removals System Study, of this report can be performed on the Acid Gas Removal Unit of the Fischer-Tropsch Complex. Sulfur Recovery, Unit 21, with a second law efficiency of 66.4%, is another area where possible improvements should be analyzed to achiever higher efficiencies. Unit 22, Water Reclamation, has an extremely low second law efficiency of 4.5% which seems to suggest an area for large improvements. This is misleading due to the fact that most of the outlet streams consist of water at ambient temperatures and pressures resulting in a low outlet availability.

As demonstrated in this study, a second law analysis is a very useful method by which to evaluate industrial plants and processes in order to pinpoint areas for improvement. The methodology used on the Fischer-Tropsch Complex can be applied to other industrial plants and processes.

REFERENCES

1. R.A. Gaggioli and P.J. Petit, "Second Law Analysis for Pinpointing the True Inefficiencies in Fuel Conversion Systems", Marquette University, 1975.

2. J. Yoon, "Design of Thermal Energy Systems by Employing Availability Concepts", M.S. Thesis, Marquette University, 1974.

3. T.C. Ruppel,W.C.Peters,and D.L. Schwartz,"The Role of Thermodynami Effectiveness in Evaluating Coal Conversion RD&D,Pergamon Press,N. 1977

4. "Fischer-Tropsch Complex Conceptual Design/Economic Analysis", R&D Report No. 114-Interim Report No. 3, The Ralph M. Parsons Company, January, 1973.

5. Conversation with R.A. Gaggiolo, Marquette University, Milwaukee, Wisconsin.

6. Conversation with T.C. Ruppel, Pittsburgh Energy Technology Center, Pittsburgh, Pennsylvania.

7. J. Coull and E.B. Stuart, "Equilibrium Thermodynamics", John Wiley and Sons, Inc., New York, 1964.

8. Keenan and Kayes, "Gas Tables", John Wiley and Sons, Inc., New York, 1948.

9. Van Wylen and Sonntagg, "Fundamentals of Classical Thermodynamics", John Wiley and Sons, Inc., New York, 1973.

10. ASHRAE, "Thermodynamic Properties of Refrigerants", New York, 1969.

11. D.R. Stull and N. Prophet, "JANAF Thermochemical Tables", Second Edition, Washington, D.C., 1971.

12. R.A. Gaggioli, J. Yoon, S.A. Patulski, A.J. Latus, and E.F. Obert, "Pinpointing the Real Inefficiencies in Power Plants and Energy Systems", April, 1975.

13. T. Baumeister and L.S. Marks, "Standard Handbook for Mechanical Engineers", Seventh Edition, McGraw-Hill Book Company, 1967.

14. G.R. Fryling, "Combustion Engineering", Revised Edition, Combustion Engineering, Inc., New York, 1966.